Les liquides ioniques, leur utilisation et leur role comme solvants de réaction catalytique

Thibaut Gutel

N° d'ordre : 173 - 2007 Année 2007

THESE

présentée

devant l'UNIVERSITE CLAUDE BERNARD - LYON 1

ECOLE DOCTORALE DE CHIMIE, PROCEDES, ENVIRONNEMENT

Pour l'obtention

du DIPLOME DE DOCTORAT

Spécialité CHIMIE

(arrêté du 25 avril 2002)

présentée et soutenue publiquement le 12 octobre 2007

par

Thibaut Gutel

Ingénieur ESCOM

LES LIQUIDES IONIQUES, LEUR UTILISATION ET LEUR ROLE COMME SOLVANTS DE REACTION CATALYTIQUE

Directeurs de thèse :

Catherine SANTINI et Yves CHAUVIN

Jury : M. BASSET, Président

M. COLE-HAMILTON, Rapporteur

M. SIMONATO, Rapporteur

M. CHAUDRET

M. LEMAIRE

Mme OLIVIER-BOURBIGOU

UNIVERSITE CLAUDE BERNARD – LYON I

Président de l'Université	**M. le Professeur L.COLLET**
Vice-Président du Conseil Scientifique	M. le Professeur J.F. MORNEX
Vice-Président du Conseil d'Administration	M. le Professeur J. LIETO
Vice-Président du Conseil des Etudes et de la Vie Universitaire	M. le Professeur D. SIMON
Secrétaire Général	M. G. GAY

SECTEUR SANTE

Composantes :

UFR Médecine Lyon R.T.H Laënnec	Directeur : M. le Professeur D.VITAL-DURANI
UFR Médecine Lyon Grange-Blanche	Directeur : M . le Professeur X. MARTIN
UFR Médecine Lyon-Nord	Directeur : M. le Professeur F. MAUGUIERE
UFR Médecine Lyon-Sud	Directeur : M. le Professeur F.N. GILLY
UFR d'Odontologie	Directeur : M. O. ROBIN
Institut des Sciences Pharmaceutiques et Biologiques	Directeur : M. le Professeur F.LOCHER
Institut Techniques de Réadaptation	Directeur : M. le Professeur MATILLON
Département de Formation et Centre de Recherche en Biologie Humaine	Directeur : M. le Professeur P.FARGE

SECTEUR SCIENCES

Composantes :

UFR de Physique	Directeur : M. le Professeur A.HOAREAU
UFR de Biologie	Directeur : M. le Professeur H.PINON
UFR de Mécanique	Directeur : M. le Professeur H. BEN HADID
UFR de Génie Electrique et des Procédés	Directeur : M. le Professeur A.BRIGUET
UFR Sciences de la Terre	Directeur : M. le Professeur P.HANTZPERGUE
UFR de Mathématiques	Directeur : M. le Professeur M.CHAMARIE
UFR d'Informatique	Directeur : M. le Professeur M. EGEA
UFR de Chimie Biochimie	Directeur : M. le Professeur H. PARROT
UFR STAPS	Directeur : M. le Professeur R.MASSARELLI
Observatoire de Lyon	Directeur : M. le Professeur R.BACON
Institut des Sciences et des Techniques de l'ingénieur de Lyon	Directeur : M. le Professeur J. LIETO
IUT A	Directeur : M. le Professeur M.C. COULET
IUT B	Directeur : M. le Professeur R.LAMARTINE
Institut de Science Financière et d'Assurance	Directeur : M. le Professeur J.C AUGROS

A mon grand-père,

Les travaux exposés dans ce mémoire ont été réalisés entre septembre 2004 et octobre 2007 au Laboratoire de Chimie, Catalyse, Polymérisation et Procédés dans l'équipe de Chimie OrganoMétallique de Surface, unité mixte CNRS-CPE Lyon. Je suis reconnaissant envers Monsieur Gérard Pignault, directeur de CPE Lyon, pour m'avoir accueilli dans ses locaux.

Mes remerciements vont tout d'abord à Monsieur Jean-Marie Basset, Directeur de Recherche au CNRS, qui a bien voulu m'accueillir au sein de son laboratoire.

J'adresse mes plus vifs remerciements à Monsieur Yves Chauvin, Directeur de Recherche honoraire à l'Institut Français du Pétrole, agissant en qualité de co-directeur. En dépit de son éloignement, il a fait preuve d'une grande disponibilité et a été une source constante de conseils et de réflexions. Je lui suis très reconnaissant de sa contribution au développement de ce projet et de m'avoir fait profiter de ses connaissances et de sa grande expérience en chimie.

Je tiens à remercier Madame Catherine Santini, Directeur de Recherche au CNRS, qui a encadré mes travaux de thèse. Je la remercie tout particulièrement pour l'aide et le soutien qu'elle m'a apportés durant ces trois années.

Que Madame Olivier-Bourbigou, chercheur à l'Institut Français du pétrole et Messieurs Marc Lemaire, Professeur à l'Université Lyon 1, Bruno Chaudret, Directeur de Recherche au CNRS, Jean-Pierre Simonato, chercheur au Commissariat à l'Energie Atomique et David Cole-Hamilton, Professeur à l'Université de St Andrews, soient vivement remerciés de l'honneur qu'ils m'ont fait en acceptant de juger ce mémoire.

Ce travail a été effectué en collaboration avec le Commissariat à l'Energie Atomique, l'Institut Français du pétrole et la société Rhodia. Je tiens à remercier ces partenaires pour l'aide qu'ils ont portée à la progression de cette recherche.

Je tiens également à remercier Monsieur Bernard Fenet, le professeur Denis Bouchu, le professeur Agilio Padua pour leur aide .

Que tous les membres du laboratoire trouvent dans ces quelques lignes l'expression de ma plus profonde gratitude. Je pense en particulier aux étudiants en thèse ou en DEA avec lesquels j'ai partagé tout ou une partie de ces trois années.

Abbreviations and acronyms

Unity

eq. : equivalents	h : hour	g : gram
mL : milliliter	mn. : minute	mg : milligram
mol : mole	°C : degree Celsius	Hz : Hertz
mmol : millimole	K : degree Kelvin	ppm : part per million
µmol : micromole		

Techniques

b.p. :	boiling point
m.p. :	melting point
ESI :	ElectroSpray Ionisation
FID :	Flame Ionization Detector
EXAFS :	Extended X-ray Absorption Fine Structure
SAXS :	Small Angle X-ray Scaterring
DRX :	X-Ray diffraction
NMR :	Nuclear Magnetic Resonance

δ :	chemical shift			
J :	coupling constant			
s :	singulet	d:	doublet	t: triplet
q :	quadruplet	quint:	quintuplet	sext: sextuplet
m :	multiplet			

ROESY :	Rotational Overhauser Effect SpectroscopY
DOSY :	Diffusion Order SpectroscopY

Chemicals

IL :	Ionic Liquid
BMIM :	1-butyl-3-methylimidazolium
BBIM :	1,3-dibutylimidazolium
BMMIM :	1-butyl-2,3-dimethylimidazolium
EMIM :	1-ethyl-3-methylimidazolium
HMIM :	1-hexyl-3-methylimidazolium
OMIM :	1-octyl-3-methylimidazolium
COD :	1,5-cyclooctadiene
COA :	Cyclooctane
To :	Toluene
Bz	Benzene
CYD :	1,3-cyclohexadiene
CYE	Cyclohexene
CYA	Cyclohexane
Me :	Methyle
Ph :	Phenyle
OTf :	Trifluoromethylsulfonate
NTf_2 :	Bis-(trifluoromethylsulfonyl)imide
TPPMSNa :	Sodium (*m*-sulfophenyl)-diphenylphosphine
TPPMSBMMIM :	1-butyl-2,3-dimethylimidazolium (*m*-sulfophenyl)-diphenylphosphine
Ru(COD)(COT) :	(1,5-cycooctadiene)(1,3,5-cyclooctatriene)ruthenium
MNP	Metal Nanoparticles

SOMMAIRE

Introduction générale

Depuis deux décennies, les liquides ioniques (LI) sont devenus des solvants incontournables dans des domaines variés tels que :

- l'électrochimie notamment pour le dépôt électrolytique de métaux et les électrolytes de batteries
- le génie des procédés avec des utilisations en tant que thermofluides ou comme solvants de séparation ou d'extraction
- en synthèse et catalyse en tant que solvants de réactions organiques, catalytiques ou biochimiques

Initialement développés pour leurs propriétés électrochimiques, ces milieux ont été utilisés comme solvants de réaction à partir des années 80 et depuis, l'intérêt pour ce type de composés ne cesse de croître. Cet essor s'explique notamment par la nécessité de mettre au point des procédés plus respectueux de l'environnement.

Cependant, beaucoup de chimistes ont considéré les LI comme une gamme de solvants supplémentaire mise à leur disposition alors que ces composés présentent des propriétés spécifiques du fait de leur composition. En effet, les LI sont des associations de cations et d'anions et sont rapidement apparus comme des solvants non-inertes vis-à vis des réactifs mis en jeu dans les réactions chimiques. De nombreux résultats catalytiques n'ont pas pris en compte les phénomènes particuliers pouvant avoir lieu dans ces milieux.

Récemment, certains spécialistes tels que le Dr Welton, ont évoqué les problèmes de solvatation pouvant intervenir dans les LI et de nombreuses études physico-chimiques ont permis de mieux appréhender les propriétés spécifiques de ces solvants.

Les LI ont dans un premier temps été définis par les paramètres de classification classiques des solvants organiques (propriétés acido-basiques, pouvoir coordonnant, polarité). Puis l'étude de leur structure à l'état solide et liquide par diffusion de neutrons, diffraction des rayons X, résonance magnétique nucléaire, … ainsi que leur modélisation théorique ont démontré que ces milieux présentent une très grande organisation en réseaux 3D et sont constitués de microdomaines polaires et apolaires. Ces résultats récents ont mis en évidence la nécessité d'étudier de façon approfondie les phénomènes de solvation mis en jeu dans les LI.

L'objectif de ce travail est d'étudier le rôle spécifique des LI dans les réactions catalytiques en particulier l'influence de trois facteurs :

1. l'association anions/cations
2. l'auto-organisation des LI
3. la présence de microdomaines polaires et apolaires

En effet, de par leur nature, les LI peuvent donner lieu à :

- la spéciation de systèmes catalytiques ioniques. Ce phénomène a déjà été évoqué pour interpréter les résultats obtenus en isomérisation catalytique au laboratoire.
- des interactions entre ions et réactifs, en particulier la possibilité de former des interactions π-cation avec les substrats insaturés.
- une auto-organisation et une structuration en microdomaines pouvant générer des « nanoréacteurs » dont les propriétés seraient ajustables par variation de la nature du LI. Les LI pourraient alors jouer le rôle de moule supramoléculaire lors de la synthèse de catalyseur.

Pour conclure, la compréhension des phénomènes particuliers entre les LI, le substrat et le catalyseur lorsque les LI sont utilisés comme solvants de réaction catalytique est indispensable pour optimiser les résultats catalytiques.

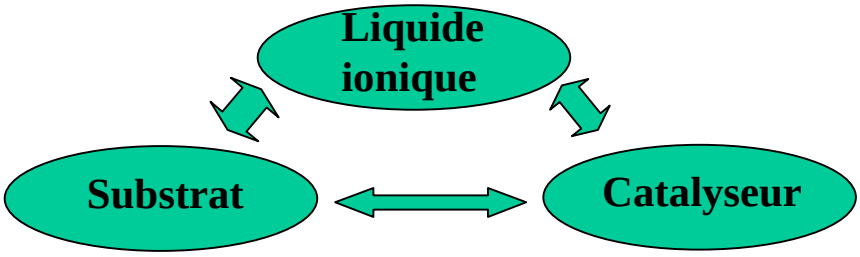

Schéma. *Relation entre les partenaires du système liquide ionique/substrat/catalyseur*

Chapitre I : Etude bibliographique : Les liquides ioniques, solvants de réaction catalytique

Introduction

Les solvants peuvent être classés en fonction du type de liaisons chimiques qu'ils mettent en jeu (Figure 1):

- les liquides moléculaires dans lesquels interviennent seulement des liaisons covalentes.
- les liquides ioniques où prédominent les interactions ioniques.
- les liquides atomiques tels que le mercure ou les alliages d'alcalins liquides, siège de liaisons métalliques.(amalgame Na-K liquide à température ambiante)

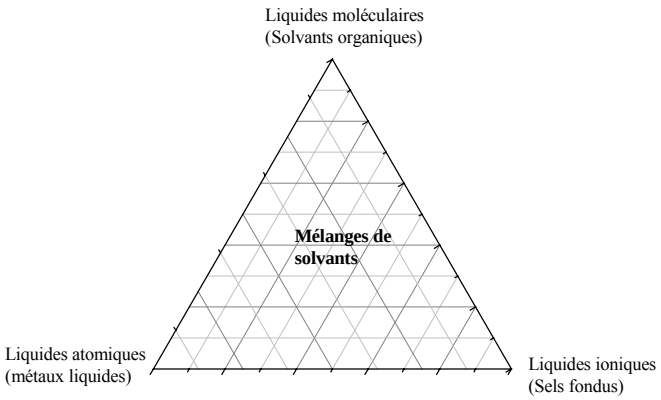

Figure 1. *Classification des solvants selon le type de liaisons chimiques mis en jeu*

Les liquides ioniques (LI) sont capables de dissoudre un grand nombre de composés organiques ou inorganiques mais présentent des effets de solvants particuliers par rapport aux solvants organiques classiques et sont par conséquent considérés comme des solvants néotériques. Les propriétés physico-chimiques des LI telles que leur grande stabilité thermique, leur bonne conductivité électrique, leur viscosité raisonnable, leur large domaine liquide, leur faible tension de vapeur, leur haute conductivité thermique, en font un milieu réactionnel très intéressant pour la chimie verte permettant notamment de travailler à haute température avec de bonne dispersion de la chaleur.[1]

De plus, les propriétés physiques et chimiques des LI sont modifiables par variation des combinaisons anion/cation et les LI sont souvent considérés comme des solvants modifiables.[2,3] Cela a permis de concevoir des systèmes adaptés à des applications variées (batteries thermiques, électrochimie, synthèse organique, inorganique et enzymatique, catalyse...) mais également d'ajuster les propriétés physico-chimiques des LI en fonction des besoins.[4]

Après avoir présenté les LI, leurs caractéristiques générales et leurs propriétés de solvants, ce chapitre bibliographique traitera de la problématique de l'utilisation des LI en tant que solvants de réaction catalytique.

La stratégie et la méthodologie des travaux entrepris pour étudier ces systèmes seront également exposées.

1 Généralités sur liquides ioniques

1.1 Définition

Les liquides ioniques (LI) sont des sels liquides se différenciant de l'ensemble des sels fondus par une température de fusion inférieure à 100°C (arbitrairement fixée en référence à la température d'ébullition de l'eau) mais un grand nombre d'entre eux sont liquides à température ambiante (Figure 2). Les LI sont constitués d'un cation le plus souvent organique, associé à un anion organique ou inorganique et les combinaisons cations/anions possibles sont très nombreuses (>10^6) et en constante évolution.[3]

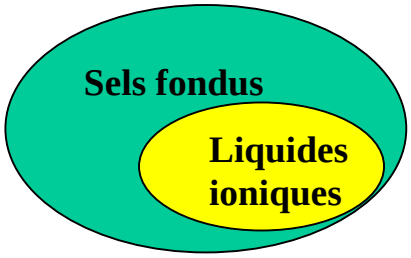

Figure 2. *Les LI, un sous-ensemble des sels fondus*

Les cations rencontrés sont généralement volumineux et dissymétriques. Les plus classiques sont des ammoniums ou phosphoniums quaternaires, tels que les tétraalkylammoniums ou tétraalkylphosphoniums mais de nombreux LI sont à base de systèmes hétéroaromatiques comme les alkylpyridiniums, les triazoliums ou encore des alkylpyrrolidiniums. Les plus étudiés sont les sels d'imidazoliums diversement substitués sur les atomes d'azote et de carbone.(Figure 3)

De plus, toute une série de cations fonctionnalisés a été récemment développée notamment des cations portant des groupements amines[5], alcools ou éthers,[6,7] acides carboxyliques ou esters,[8] thiols,[9] vinyl et allyl,[10-13] alcynes[14,15] ou encore nitriles[16,17]. Des cations chiraux ont également été synthétisés.[18-20]

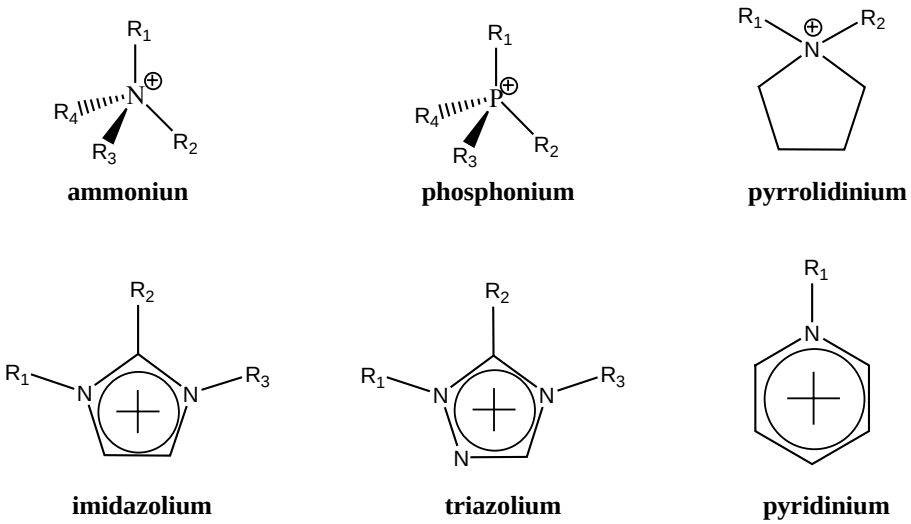

Figure 3. *Cations des LI*

Les anions mis en œuvre sont des anions inorganiques ou organiques (tableau 1). Les anions tétrafluoroborate (BF_4^-) et hexafluorophosphate (PF_6^-) très utilisés en chimie organique ou organométallique pour conférer une solubilité recherchée aux espèces ioniques sont à la base de très nombreux sels liquides. Pour ce qui est des anions organiques, les anions fluorés ($CF_3CO_2^-$) sont très intéressants notamment en catalyse organométallique. Les dérivés sulfoniques : $CF_3SO_3^-$, $C_4F_9SO_3^-$, $(CF_3SO_2)_2N^-$ et $(CF_3SO_2)_3C^-$ sont également très étudiés pour leur stabilité thermique et leur pouvoir faiblement coordonnant. Récemment d'autres anions à propriétés spécifiques ont été développés tels que des anions chiraux[21,22] ou des anions fonctionnalisés par des nitriles,[23] des hydroxyborates[24] ou des bases de Lewis.[25] Des systèmes anioniques à base d'hétéropolyanions ou de sels métalliques sont également étudiés.[4,26-28]

Anions inorganiques	Anions organiques
F^-, Cl^-, Br^-, I^-	$CH_3CO_2^-$, $CH_3SO_4^-$, $C_6H_5SO_3^-$ (=OTs)
BF_4^-, PF_6^-, SbF_6^-, AsF_6^-	$CF_3CO_2^-$, $C(CF_3SO_2)_3^-$
NO_3^-, ClO_4^-	$CF_3SO_3^-$ (=OTf)
$Al_xCl_{(3x+1)}^-$, $Al_xEt_xCl_{(2x+1)}^-$	$N(SO_2CF_3)_2^-$ (=NTf_2)
$CuCl_2^-$, $AuCl_4^-$, $ZnCl_3^-$, $SnCl_3^-$	BR_4^-, R_3BOH^-

Tableau 1 . *Exemple d'anions de LI*

1.2 Historique

La description du premier LI datent du milieu du 19ème siècle. Lors de la réaction de Friedel et Craft entre le benzène et le chlorométhane catalysée par un acide de Lewis, $AlCl_3$, une seconde phase apparaît sous la forme d'une « huile rouge ». La structure de ce composé sera identifiée plus tard par le Pr. Jerry Atwood à l'université du Missouri grâce à l'apparition de la RMN et correspond au complexe intermédiaire, jusqu'alors présupposé, de la réaction de Friedel et Craft : le sel d'heptadichloroaluminate **1**.

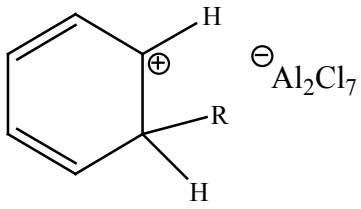

1

Des sels liquides de nitrate d'alkylammoniums furent ensuite découverts au début du 20ème siècle en particulier le nitrate d'éthylammonium (Walden, 1914) dont le point de fusion est de 12°C. Ces découvertes furent le début de l'ère des LI tels qu'ils sont connus à ce jour. Un programme sera lancé pour développer ce type de composés dans des applications comme les liquides de propulsion des fusils marins et de l'artillerie navale et débouchera sur la découverte de nitrates plus complexes et la prise de nombreux brevets.[29]

Dans les années soixante, le développement des LI sera relancé par la mise en évidence par le Pr. John Yoke à l'université d'état de l'Oregon de la formation d'un liquide résultant du mélange de deux solides, le chlorure de cuivre et le chlorure d'alkylammonium selon l'équation : $CuCl(s) + Et_3NHCl(s) \rightarrow Et_3NHCuCl_2(l)$

De nombreux LI de cette forme seront alors développés mais aucun n'aboutira à d'applications particulières excepté en spectroscopie. Par la suite, de nouveaux composés, appelés « clathrates liquides », seront mis au point par le Pr. Jerry Atwood et son groupe à l'université d'Alabama dans les années 70 par association de différents sels avec un alkyl aluminium conduisant à la formation à haute température de composés d'inclusion avec une ou plusieurs molécules aromatiques :

$$M[Al_2(CH_3)_6X] + n\ \text{Aromatiques} \leftrightarrows M[Al_2(CH_3)_6X].n\text{Aromatiques}$$

Ces clathrates liquides furent brevetées pour la liquéfaction du charbon et l'extraction du pétrole des schistes bitumineux. Mais dès le début des années 60, l'US Air Force Academy en collaboration avec la National Science Foundation lance un vaste projet de recherche initié par le Dr Lowell King puis repris par les Dr John Wilkes et Dr Richard Carlin visant à améliorer les caractéristiques des électrolytes de batteries thermiques constitués de sels de

chlorures fondus, généralement le mélange eutectique LiCl-KCl (température de fusion de 355°C), afin d'en abaisser le point de fusion. La recherche se concentre tout d'abord sur le développement de systèmes à base de chlorures alcalins et de chlorure d'aluminium. Les premiers travaux s'attachent à la caractérisation physico-chimiques de tels mélanges, en particulier $NaCl/AlCl_3$, qui se révèlent être des systèmes relativement complexes et qui seront utilisés en tant qu'électrolytes de batteries thermiques. Les travaux sur le dépôt électrolytique d'aluminium à partir d'électrolytes constitués de mélanges d'halogénures d'1-éthylpyridinium avec $AlCl_3$ inspireront les équipes de l'US Air Force menées par le Dr Charles Hussey qui développeront ce type de mélanges mais aucune application n'aboutira en raison d'une fenêtre électrochimique trop étroite. Puis de nouveaux cations organiques moins sensibles à la réduction électrochimique, en particulier le mélange de chlorure d'aluminium et d'un halogénure de 1-éthyl-3-méthylimidazolium seront mis au point. Ces LI à base de chloroaluminates sont hydrolysables et conduisent à la formation de gaz corrosif (HCl) d'où la recherche de nouveaux anions qui aboutira dans les années 1990 à l'élaboration des sels de dialkylimidazolium associés aux anions tétrafluoroborates, hexafluorophosphates, nitrates, sulfates et acétates par métathèse d'anions avec les sels d'argent correspondants.[30] Une très grande gamme de LI de ce type fut alors développée à l'US Air Force par le Pr Mike Zaworotko et le Dr Joan Fuller.[29]

Ce n'est qu'au début des années 1990 que les LI furent utilisés comme solvants. [31,32] Depuis ils sont utilisés dans de nombreux domaines tels que la synthèse organique, la catalyse, la spectroscopie, l'électrochimie, l'extraction, la séparation ou encore la préparation de nanomatériaux.

Dans la dernière décennie, les nombreuses applications des LI ont été motivées par le besoin de solvants compatibles avec l'environnement et signalons que de nombreux industriels : BASF (Allemagne), GlaxoSmithKline (RU), Merck (Allemagne), SASOL (Afrique du Sud), Novartis (Allemagne), Strata Technology Ltd (RU), Arkema et l'IFP (France) développent actuellement des procédés exploitant cette technologie nouvelle. Actuellement seulement 3 procédés basés sur les LI sont exploités à notre connaissance.

* Le procédé Difasol^{TM} (1995, IFP-Axens) : La dimérisation des butènes dans les LI à base de chloroaluminates est réalisée avec de bonnes conversions (70% de conversions du butène) et des sélectivités (95% de sélectivité en octène) 5 fois supérieures au procédé existant. La transposition de cette réaction dans les LI permet le recyclage du catalyseur à

base de nickel immobilisé dans la phase LI, la récupération aisée des produits en fin de réaction et la diminution des volumes réactionnels.[33]

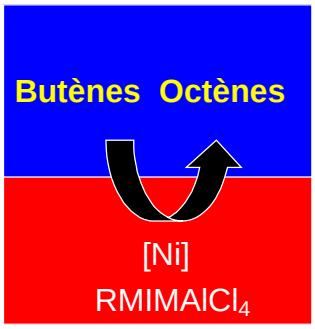

* La synthèse du 2,5-dihydrofurane est conduite dans un iodure de phosphonium.(1995, Eastman Chem Co)[34] Ce LI apolaire ainsi que l'acide de Lewis ont, dans ce cas, été choisis du fait de leur grande solubilité dans l'heptane permettant leur séparation en fin de réaction.[35]

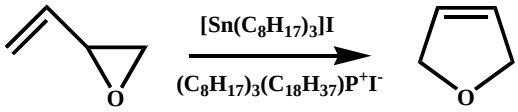

* Le procédé **BASIL**^{TM} (2003, BASF) : Le remplacement de la triéthylamine par l'imidazole comme base dans la synthèse de phosphites a considérablement simplifié le procédé existant. En effet, le cation imidazolium ainsi formé pendant la réaction décante spontanément et permet un récupération plus aisée des produits de réaction.[36]

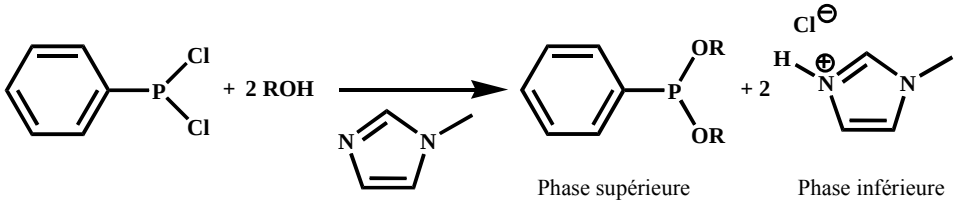

Le développement de ces procédés a considérablement encouragé l'utilisation des LI en démontrant leur intérêt comme solvants dans l'industrie et de nombreux LI sont actuellement commerciaux.[37]

1.3 Synthèses

Comme de nombreuses associations de cations et d'anions sont possibles, nous avons restreint cette partie bibliographique à la préparation de LI dérivés d'imidazoliums.

La synthèse de ces LI s'effectue en deux étapes :

- la quaternisation du noyau imidazole
- l'échange d'anion

1.3.1 Réaction de quaternisation du noyau imidazole

La préparation du cation peut être effectuée soit par protonation en milieu acide soit par quaternisation d'une amine par un halogénure d'alcane.

* La protonation des imidazoles par un acide conduit directement aux sels d'imidazoliums désirés. Cette technique ne permet pas la préparation de sels d'imidazoliums alkylés en position 3.[3,38]

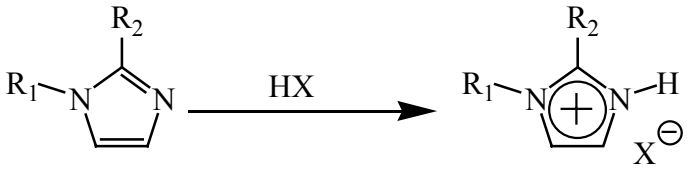

R_1 et R_2 = alkyl, H

X = Cl, NO_3, BF_4, PF_6

* La substitution nucléophile d'halogénures d'alcanes par les imidazoles conduit avec de bons rendements aux halogénures d'imidazoliums correspondants.[3,38] Cette méthode a l'avantage d'utiliser des réactifs commerciaux et bon marché mais nécessite souvent la distillation des réactifs et des temps de réaction importants (plusieurs jours avec les chloroalcanes) même s'ils peuvent être réduits par utilisation des micro-ondes,[39,40] des ultrasons[41] ou en opérant sous pression.

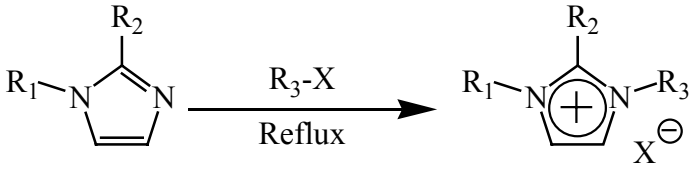

R_1, R_2 et R_3 = alkyl

X= Cl, Br, I, OTf ou OTs

La réactivité des halogénures d'alcanes croit dans l'ordre : Cl >Br >I, les fluorures ne pouvant être préparés de cette manière. La réaction de quaternisation d'amine par des triflates ou des tosylates est également possible du fait de la présence d'un très bon groupe partant et peut être réalisée à température ambiante. Ces réactions peuvent être effectuées sans solvant mais dans tous les cas, cette étape est réalisée sous atmosphère inerte du fait du caractère extrêmement hygroscopique voire hydrolysable des réactifs et des produits.

La décantation en fin de réaction permet d'éliminer l'excès de solvant et de réactifs, les sels d'imidazolium étant généralement plus denses que les solvants organiques mais par précaution, le produit est généralement traité sous vide avant usage pour éviter toutes traces d'eau ou de produits volatils. Le cation, une fois préparé, peut être également purifié par recristallisation ou lavé avec un solvant non-miscible.[3,38]

1.3.2 Réaction d'échange de l'anion

La réaction d'échange de l'anion peut se diviser en deux catégories : traitement direct du sel d'imidazolium par un acide de Lewis ou réaction d'échange par métathèse d'anions.

* Le traitement d'un halogénure d'imidazolium avec un acide de Lewis MX_n conduit à la formation d'un contre-ion métallique.[3,28,38,42]

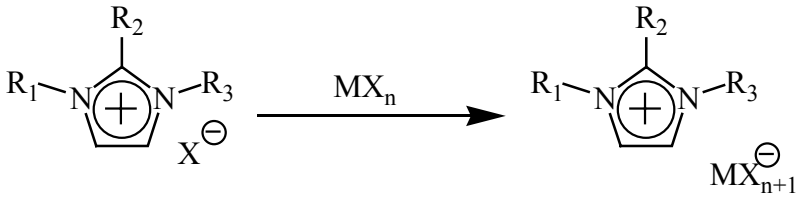

R_1, R_2 et R_3 = alkyl

X= Cl, Br, I

M = Al, Cu, Sn, Fe, Zn

Cette réaction est relativement exothermique et doit être réalisée en conditions anhydres.

* Il est possible de réaliser l'échange de l'anion des sels d'imidazoliums avec un autre sels inorganiques :[3,38]

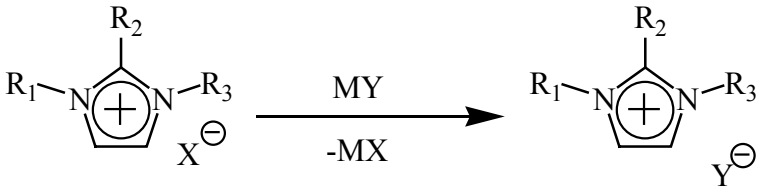

R_1, R_2 et R_3 = alkyl

X= Cl, Br, I

MY=$LiNTf_2$, NaOTf, $NaPF_6$, $NaBF_4$

Cette réaction conduit aux LI avec de hauts rendements et une très bonne pureté. L'inconvénient de cette technique est lié à l'échange incomplet des halogénures qui peut conduire à la contamination du LI. Par conséquent, un grand soin doit être apporté lors de la phase de lavage du LI.

Les LI obtenus par ces voies de synthèse sont généralement des liquides incolores bien que les sels d'imidazoliums à base de PF_6 ou BF_4 puissent présenter une légère coloration jaune. Il est indispensable de caractériser la pureté de ces composés et il est parfois nécessaire de les purifier avant usage.

1.3.3 Purification et pureté des LI

La pureté des LI est un paramètre important pour la plupart des applications car la présence d'impuretés peut gravement affecter les propriétés physico-chimiques des LI[43,44] et la réactivité des systèmes catalytiques.[45,46]

Comme les LI sont très peu volatils, la purification par distillation n'est pas envisageable excepté dans des conditions sévères.[47] La purification par chromatographie est également délicate dans la mesure où les LI ont tendance à s'absorber sur les phases stationnaires.[48] Par conséquent, un grand soin doit être apporté lors de la synthèse des LI afin de limiter tant que possible les impuretés présentes dans le produit final notamment les traces d'eau, d'halogénures et d'imidazole de départ.[27]

Il est possible de mesurer la quantité d'eau présente dans les LI par dosage Karl-Fischer,[44] par spectroscopie infra-rouge,[49] par spectroscopie UV ou par spectrométrie de masse.[50] La détection de traces d'halogénures est généralement réalisée par un test au nitrate d'argent mais ces impuretés peuvent être quantifiées par analyse élémentaire, par chromatographie ionique,[51] ou par électrophorèse capillaire.[52] La présence d'imidazole de départ peut être détectée par un test colorimétrique au chlorure de cuivre(II).[53]

1.3.4 Nomenclature et acronymes des LI

La dénomination des cations imidazolium ($R_1R_2R_3IM$) utilisés par la suite est présentée dans le tableau suivant :

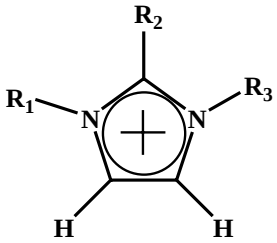

Nom du cation	acronyme	R_1	R_2	R_3
1-éthyl-3-méthylimidazolium	EMIM	CH_3	H	C_2H_5
1-butyl-3-méthylimidazolium	BMIM	CH_3	H	C_4H_9
1-hexyl-3-méthylimidazolium	HMIM	CH_3	H	C_6H_{13}
1-octyl-3-méthylimidazolium	OMIM	CH_3	H	C_8H_{17}
1-décyl-3-méthylimidazolium	DMIM	CH_3	H	$C_{10}H_{21}$
1,3-dibutylimidazolium	BBIM	C_4H_9	H	C_4H_9
1-butyl-2,3-diméthylimidazolium	BMMIM	CH_3	CH_3	C_4H_9

Tableau 2. Nomenclature utilisée pour la dénomination des cations imidazoliums

Les anions (X) bis(trifluorométhanesulfonyl)imides et trifluoromethylsulfonate seront désignés par NTf_2 et OTf respectivement.

1.4 Propriétés physico-chimiques et paramètres de solvant des LI

Les LI se sont récemment ajoutés à la gamme des composés potentiellement utilisables en tant que solvants de réaction et présentent un grand intérêt du fait de leur propriétés physico-chimiques particulières. En effet, les LI présentent des avantages évidents d'un point de vue d'ingénierie de procédés, en raison d'une grande plage de stabilité thermique et chimique, d'une conductivité élevée de la chaleur et d'une faible tension de vapeur. Certains LI sont complètement non-volatils jusqu'à leurs températures de décomposition (typiquement au-dessus de 300°C).[47] Ils présentent ainsi un risque considérablement réduit de décharge accidentelle de vapeurs dans l'atmosphère. De plus, la possibilité d'ajuster leurs caractéristiques physico-chimiques par variation de la nature de l'anion ou du cation ou en modifiant les substituants portés par le cation du LI est un atout majeur. Il faut aussi mentionner que les LI sont capables de dissoudre un grand nombre de composés organiques ou inorganiques.

1.4.1 Point de fusion, transition vitreuse, domaine liquide et surfusion

Les LI, caractérisés par des températures de fusion relativement basses et des températures de décomposition élevées (350-400°C), possèdent un très large domaine de température dans lequel ils sont à l'état liquide (de l'ordre de 200-300°C) et un domaine de stabilité thermique très grand.[54] La température de fusion des LI dépend de la nature du cation mais surtout de celle de l'anion.[55] Plus l'anion est volumineux, plus le point de fusion du LI est bas. De même, les cations encombrés et portant des substituants dissymétriques conduisent à des LI à plus bas point de fusion.[56]

L'analyse par calorimétrie différentielle (DSC) montre que les LI peuvent rester à l'état de surfusion, adopter des phases quasi-amorphes voire s'assembler sous forme de cristaux liquides et ainsi présenter un point de fusion (T_{fus}) et/ou une transition vitreuse (T_g).[57] Généralement les LI constitués de cations à courte chaîne alkyle sont des solides cristallins dans lesquels les interactions sont fortes à l'état solide. Ceux qui porte des chaînes alkyles de longueurs modérées possèdent de grands domaines liquides et ont tendance à se solidifier à l'état vitreux. Enfin les LI ayant de longues chaînes alkyles se comporte comme des composés amphiphiles et conduisent à la formation de mésophases et la cristallisation en feuillets.[58]

1.4.2 Viscosité et densité

Les LI présentent généralement des viscosités importantes, une à dix fois supérieures aux solvants organiques usuels, qui diminuent avec la température. Les LI comportant l'anion NTf_2 sont moins visqueux que ceux avec PF_6 et la viscosité de $RMIMNTf_2$ ($R=C_nH_{2n+1}$) augmente linéairement avec la longueur de la chaîne alkyle R (quand n augmente).(Figure 4)

Figure 4. *Evolution de la viscosité de $RMIMNTf_2$ avec la longueur de R : C_nH_{2n+1} avec $n=2\rightarrow10$*

A l'exception des tétraalkylborates, les LI sont généralement plus denses que l'eau avec des densités comprises entre 1 et 1.6 $g.cm^{-3}$. La densité des LI diminue lorsque la longueur de la chaîne alkyle portée par le cation imidazolium augmente.[56] En général, elle est contrôlée par la nature de l'anion et augmente linéairement lorsque la température diminue.[57]

L'alkylation du cation imidazolium en position 2 supprime la liaison hydrogène forte et devrait provoquer une diminution du point de fusion et de la viscosité mais la comparaison de $BMIMNTf_2$ et $BMMIMNTf_2$ indique le contraire. Cela s'explique par une perte d'entropie dans le système trialkylé.[55]

Les propriétés physico-chimiques des LI utilisés sont résumées dans le tableau suivant : [56,57,59-62]

	M ($g.mol^{-1}$)	Densité ($g.cm^{-3}$)	T_{fus} (°C)	T_g (°C)	T_{dec} (°C)	Viscosité (cP)
$BMIMPF_6$	284	1.368	-8	-77	349	257
$BMMIMPF_6$	298	1.363	35	X	X	x
$BMIMBF_4$	226	1.12	-80	-97 à -71	361-435	92-233
$BMMIMBF_4$	240	X	37-40	-68	347-389	243
$EMIMNTf_2$	391	1.519	-21	-87 à -78	480	34
$BMIMNTf_2$	419	1.436	-6 à -2	-104 à -86	423-439	44-69
$HMIMNTf_2$	447	1.372	-6	-84 à -81	X	60
$OMIMNTf_2$	475	1.320	X	-84 à -80	X	93
$DMIMNTf_2$	453	1.271	-29 à -2	-83	X	95
$BBIMNTf_2$	461	X	X	X	X	X
$BMMIMNTf_2$	433	1.421	15-20	-82	462	88-97

Tableau 3. *Principales données physico-chimiques des LI à 25°C*

Les différences importantes qui apparaissent entre certaines données de la littérature mettent de nouveau en exergue les problèmes liés à la préparation et à la pureté du LI et mettent en évidence la difficulté de comparer les résultats publiés par différents auteurs.

1.4.3 Toxicité et dangerosité

La toxicité des LI est pour l'instant mal connue bien que certaines études aient entreprises d'en évaluer les propriétés toxicologiques.[63-67] Il apparaît notamment que les sels d'imidazolium sont d'autant plus (éco-)toxique que la chaîne alkyle est longue.[66] Ainsi les LI à base de l'anion PF_6 n'ont pu être utilisés dans les batteries d'ordinateurs portables.

Il a par contre été montré que les LI étaient ininflammables.[68]

1.4.4 Propriétés électrochimiques et dépôt électrolytique

Les LI, composés uniquement d'ions, présentent des conductivités fortes (~10 mS/cm) et possèdent un domaine de stabilité électrochimique important avec des fenêtres électrochimiques pouvant aller jusqu'à 5-6 V.[69]

Ces propriétés ont été exploitées dans le domaine des piles à combustibles[70,71] mais aussi en tant que milieux pour le dépôt électrolytique de métaux. Par exemple, le dépôt électrolytique de l'aluminium est réalisable dans les LI.[72]

1.4.5 Stabilité chimique et acidité

Les sels d'imidazoliums généralement inertes peuvent dans certaines conditions engendrer des réactions parasites. Par exemple, les anions $AlCl_4$ sensibles à l'hydrolyse,

génèrent du HCl. Dans le cas du PF_6, l'hydrolyse conduit à la formation de l'oxyde $O_2PF_2^-$ et d'acide fluorhydrique dans le milieu.[73,74]

La réactivité du cation imidazolium est surtout liée à la forte acidité du proton en position 2 (pKa=21-24)[75,76] qui est connu pour se déprotoner en conditions basiques ou en présence de métaux de transition riche en électrons et générer des carbènes.[77] Certains LI peuvent même se comporter comme des superacides.[78,79] Mais la déalkylation du cation par élimination d'Hoffman est également envisageable en présence d'eau et de palladium,[80], en sonochimie[81] ou à hautes températures.[82] Le cation imidazolium est chimiquement plus stable lorsqu'il est substitué en position 2.[55]

1.4.6 Echelle de polarité et paramètres de Kamlet-Taft

Les échelles de polarité et autres paramètres de classification classiquement utilisés pour les solvants organiques se sont montrés inapplicables aux LI du fait des nombreux phénomènes pouvant intervenir dans ces systèmes : interactions ion-ion, dipôle-ion, dipôle-dipôle et dipôle induit-dipôle mais aussi interactions de type π et liaisons hydrogène.

Par conséquent, la détermination de ces paramètres a été réalisée aux travers de mesures indirectes et par combinaison de plusieurs techniques.

Les LI sont considérés comme polaires mais peu coordonnants. Il ressort que la polarité des LI (représentée par les valeurs E_T^N) est comparable au DMF ou à l'acétonitrile et proche des alcools à courte chaîne.[83] Leur pouvoir coordonnant est similaire au dichlorométhane.[84] Les effets dipolaires et de polarisabilité représentés par le paramètre π^* y sont importants par rapport aux solvants moléculaires notamment du fait d'interactions coulombiennes entre les ions du LI. Le caractère donneur de liaison H (acide) représenté par le paramètre α est relativement important et largement dominé par la nature du cation. Par contre, le facteur β lié au caractère accepteur de liaison H (basique) est fonction de l'anion et montre que les LI se comportent comme l'acétonitrile, considéré comme un solvant donneur.[4,38,85,86]

	E_T^N	α	β	π*
$BMIMBF_4$	0.673	0.627	0.376	1.047
$BMMIMBF_4$	0.576	0.402	0.363	1.083
$BMIMPF_6$	0.675	0.654	0.246	1.015
$BMMIMPF_6$	X	X	X	X
$EMIMNTf_2$	0.685	0.705	0.233	0.980
$BMIMNTf_2$	0.645	0.635	0.243	0.971
$HMIMNTf_2$	0.653	0.650	0.259	0.971
$OMIMNTf_2$	0.630	X	X	X
$DMIMNTf_2$	0.63	X	X	X
$BMMIMNTf_2$	0.541	0.381	0.239	1.010

Tableau 4. Paramètres de solvant des LI

1.5 Comportement vis-à vis des gaz, de l'eau et des solvants organiques

La solubilité des gaz, de l'eau et des solvants organiques dans les LI mais également la solubilité des LI dans ces produits sont des paramètres essentiels pour le développement de ces milieux en tant que solvants de réaction d'autant plus que la miscibilité des systèmes substrats/LI est fortement dépendante de la nature du cation et de l'anion. De plus, elle est ajustable par variation des substituants du cation du LI en particulier en fonction de la longueur de la chaîne alkyle R.

1.5.1 Solubilité des gaz dans les LI

La solubilité des gaz dans la plupart des LI est généralement très faible. Elle diminue quand la température augmente et elle augmente avec la pression. La loi de Henry est applicable pour tous les gaz excepté le dioxyde de carbone (CO_2).[87]

Le CO_2 et le protoxyde d'azote sont les gaz les plus solubles dans les LI suivi de l'éthylène et de l'éthane. L'argon, l'oxygène et le méthane ont une solubilité très faible comparativement aux solvants organiques usuels. Les concentrations en hydrogène, azote ou monoxyde de carbone dans les LI sont inférieures aux limites de détection des techniques gravimétriques.[88]

	ΔH (kJ/mol)				ΔS (J/mol.K)			
	$BMIMPF_6$	**$BMIMNTf_2$**	**Cyclohexane**	**Benzene**	**$BMIMPF_6$**	**$BMIMNTf_2$**	**Cyclohexane**	**Benzene**
CO_2	**-14.3 ± 0.2**	**-12.5 ± 0.4**	**-5.556**	**-9.337**	**-47.6 ± 0.7**	**-41.3 ± 1.4**	**-18.5**	**-31.4**
C_2H_4	**-8.2 ± 0.9**	**-9.0 ± 2.1**		**-9.006**	**-27.2 ± 2.9**	**-29.9 ± 6.9**		**-30.2**
C_2H_6	**-5.9 ± 2.9**	**-9.8 ± 2.9**	**-10.974**	**-9.211**	**-19.0 ± 9.4**	**-32.5 ± 9.6**	**-36.8**	**-30.9**
CH_4	**2.1 ± 5.6**		**-2.462**	**-1.277**	**0.7 ± 18**		**-8.3**	**-4.3**
O_2	**51.1 ± 12.2**	**20.6 ± 8.2**	**0.243**	**1.712**	**169 ± 40**	**67.4 ± 26.9**	**0.7**	**5.7**
Ar	**52.9 ± 11.1**		**-0.913**	**1.243**	**175 ± 37**		**-3.1**	**4.1**
CO	**nondetect**		**5.192**	**6.360**	**nondetect**		**17.4**	**21.3**
N_2	**nondetect**		**2.139**	**4.254**	**nondetect**		**7.0**	**14.2**
H_2	**nondetect**		**0.846**	**2.659**	**nondetect**		**2.7**	**8.9**

Tableau 5. *Enthalpies et entropies d'absorption des gaz dans $BMIMPF_6$ et d'autres solvants organiques*[89]

Bien que les LI forment des systèmes biphasiques avec le $scCO_2$, la solubilité du dioxyde de carbone dans les LI est relativement importante du fait de son haut moment quadripolaire et de la probable interaction acide/base de Lewis avec l'anion du LI. La solubilité du CO_2 est contrôlée par la nature de l'anion et ne varie pas linéairement avec la pression. L'utilisation de ce gaz à l'état supercritique est par conséquent envisageable et permet de i) diminuer la viscosité du système et ii) augmenter la solubilité des réactifs.[74] D'autre part, il apparaît que la solubilité des gaz nécessaire pour les réactions d'hydrogénation (H_2), d'oxydation (O_2) et d'hydroformylation (CO et H_2) est très faibles ce qui implique l'utilisation de systèmes à hautes pressions et des problèmes liés au transfert de masse aux interfaces.[37]

Figure 5. *Solubilité de CO_2 (●), N_2O (□), C_2H_4 (▲), C_2H_6(■)et O_2 (♦)dans $BMIMNTf_2$ à 25°C*

Figure 6. *Solubilité du CO_2 dans $BMIMNTf_2$ (Δ), $BMIMPF_6$ (●) et $BMIMBF_4$ (■) à 25 °C.*

La solubilité de différents gaz dans les LI décrit dans le tableau 6, a été estimée par mesure d'absorption.[88]

Constante de Henry (Bar)	**Ar**	**CO**	**CO_2**	**H_2**	**O_2**	**C_2H_4**
$BMIMPF_6$	7310+/-3690	nondetect	53.4+/-0.3	nondetect	7190+/-4190	144+/-2
$BMIMBF_4$		nondetect	59.0+/-2.6			
$BMIMNTf_2$			33.0+/-0.3		1730+/-560	70+/-4

Tableau 6. *Solubilité des gaz dans les LI*

Bien que l'étude rapporte une solubilité de l'hydrogène en-dessous du seuil de détection à pression atmosphérique, elle a pu être déterminé par RMN ^1H à partir d'une extrapolation de

la solubilité de l'hydrogène dans les LI à 100atm en supposant qu'elle changeait linéairement avec la pression partielle.[59]

	$[H_2]$ (mM)	Constante de Henry k_H(MPa)
$BMIMPF_6$	0.73	$6.6x10^2$
$BMIMBF_4$	0.86	$5.8x10^2$
$BMIMNTf_2$	0.77	$4.5x10^2$
$BMMIMNTf_2$	0.86	$3.8x10^2$
Toluene	3.50	$2.69x10^2$
Benzene	2.54	$4.47x10^2$
Cyclohexane	3.63	$2.57x10^2$

Tableau 7. *Solubilité de l'hydrogène dans les LI à 0,101MPa ($k_H=P(H_2)/X(H_2)$, avec la pression partielle en hydrogène exprimé en MPa)*

Il faut par ailleurs noté que la solubilité de l'hydrogène peut être augmenté en présence de $scCO_2$.[90]

L'utilisation des LI comme milieux pour la séparation des gaz [91-95]et leur stockage [93] commence à se développer.

1.5.2 Solubilité de l'eau dans les LI et des LI dans l'eau

Les LI dérivés d'imidazolium sont généralement hygroscopiques mais ils peuvent être soit totalement miscibles avec l'eau (LI hydrophile) soit partiellement (LI hydrophobe). Ce comportement est principalement gouverné par la nature de l'anion qui forme des liaisons hydrogène avec l'eau de force croissante dans la série : $PF_6 < BF_4 < NTf_2 <$ OTf.(Tableau 8) Les LI comportant l'anion OTf sont hydrophiles alors qu'avec l'anion NTf_2, ils sont hydrophobes.[49]

	$BMIMPF_6$	**$BMIMBF_4$**	**$BMIMNTf_2$**	**BMIMOTf**
ΔH (kJ.mol-1)	-7.5	-9.6	-10.5	-15.9

Tableau 8. *Enthalpies des liaisons H des systèmes eau/LI*

Pour un anion donné, la solubilité de l'eau diminue avec la longueur de la chaîne alkyle portée par l'azote en position 3 de l'imidazolium et avec le degré de substitution du cation di- ou trisubstitués du LI. Ainsi, $EMIMBF_4$ est totalement miscible avec l'eau tandis que $BMIMBF_4$ démixe dès –4°C et que $OMIMBF_4$/eau est un système biphasique à température ambiante.

	Teneur maximale en eau (ppm)
$BMIMPF_6$	2640
$BMMIMPF_6$	2540
$BMIMBF_4$	19500
$BMMIMBF_4$	13720
$EMIMNTf_2$	14000
$BMIMNTf_2$	3300
$HMIMNTf_2$	10900
$OMIMNTf_2$	8150
$DMIMNTf_2$	1450
$BBIMNTf_2$	X
$BMMIMNTf_2$	6380

Tableau 9. *Teneur maximal des LI en eau à température ambiante*[49,57]

La solubilité des LI dans l'eau a été déterminée par spectrométrie de masse[50] et par potentiométrie (Tableau 10)[96] :

	Solublité dans l'eau (%poids)
$BMIMPF_6$	2.12±0.02
$BMMIMPF_6$	1.6±0.2
$BMIMNTf_2$	0.77±0.05
$BMMIMNTf_2$	0.61±0.03

Tableau 10. *Solubilité des LI dans l'eau*[96]

La présence simultanée de l'anion NTf_2 et de substituants encombrés sur le cation imidazolium conduit donc aux LI les plus hydrophobes et les moins hygroscopiques.

1.5.3 Miscibilité des LI avec les solvants organiques.

En règle générale, les solvants organiques sont d'autant plus miscibles avec les LI qu'ils sont polaires.[87] Les LI sont donc miscibles avec les alcools à courte chaînes et les cétones, le dichlorométhane, l'acétonitrile et le THF. Ces composés seront donc choisis comme solvants d'analyse pour homogénéiser le milieu réactionnel en fin de réaction catalytique. En revanche, par un choix judicieux de la nature du cation et/ou de l'anion, les LI peuvent être non-miscibles avec les alcanes, le dioxane, le toluène et l'éther qui seront utilisés pour favoriser les systèmes biphasiques en catalyse.[38,97]

Les hydrocarbures insaturés étant des substrats modèles de choix, de nombreuses études ont examiné leur comportement dans les LI. Ces études de solubilité ont montré que les composés aromatiques sont presque 10 fois plus solubles dans les LI que les alcanes. [98]

%wt	$BMIMBF_4$	$BMIMPF_6$	$EMIMNTf_2$	$BMIMNTf_2$
Benzene	**29,3**	**29-35,5**	**37,4**	**39,5**
Toluene	**7,5**	**18,5**	**28,6**	**33,6**
Cyclohexane	**X**	**1,7-5,6**	**X**	**X**
1-hexene	**0,9**	**1,6**	**X**	**3,9**
hexane	**X**	**1,8**	**X**	**X**

Tableau 11. *Solubilité des solvants organiques dans les LI*

La solubilité des solvants organiques est fortement dépendante de la nature du LI. Les alcanes et les alcènes sont d'autant plus soluble dans RMIMX (R= C_nH_{2n+1} et X=BF_4, PF_6 et NTf_2) que la chaîne alkyle R est longue (quand n augmente) et/ou que l'anion est volumineux (X : $BF_4 < PF_6 < NTf_2$).

Il faut également signaler que les études de mélanges ternaires montrent une forte chute de la solubilité des aromatiques en présence d'alcanes dans les LI.[99]

Notons les LI sont très peu solubles dans les alcanes mais présentent une certaine solubilité dans les solvants aromatiques. La solubilité des LI dans les solvants organiques est un facteur important à prendre en compte mais très peu de travaux ont évalué ce paramètre. Une étude par équilibre liquide-liquide a évalué la solubilité de $BMIMPF_6$ dans certains hydrocarbures.[100]

Fraction molaire	Benzene	Toluene	Cyclohexane
$BMIMPF_6$	0.66	0.44	0.06

Tableau 12. *Solubilité de $BMIMPF_6$ dans les hydrocarbures à 30°C*

Dans cette première partie, il a été montré que les LI sont des solvants denses, relativement visqueux et de bons conducteurs. Il ressort également de l'étude des propriétés physico-chimiques des LI que :

- la stabilité thermique et chimique des LI permet une grande souplesse dans le choix des conditions réactionnelles
- les LI sont des solvants polaires, leur pouvoir coordonnant est modulable et ils sont peu dissociant ce qui aura des conséquences importantes sur la solvatation et la stabilité des systèmes catalytiques dans les LI

- la solubilité des différents substrats peut certes être modulée mais elle est régie soit par les forces électrostatiques (CO_2) soit par la présence de liaisons hydrogène fortes (eau) ou de liaisons π-π ou n-π (substrats aromatiques).

La compréhension des phénomènes de solvatation dans les LI est donc complexe et nécessite de prendre en compte l'ensemble de ces facteurs.

2 L'utilisation des LI comme solvants de réaction catalytique

L'utilisation des LI comme solvants de réaction catalytique est en plein essor ces dernières décennies. L'intérêt pour ces nouveaux milieux s'explique par la nécessité de trouver des procédés plus respectueux de l'environnement, les LI étant non-inflammables et très peu volatils. Cependant les effets de solvatation particuliers des LI induisent des différences de réactivités et de sélectivités des systèmes catalytiques mais restent mal compris et peu pris en compte.

Chauvin a envisagé que le caractère non-coordonnant des LI entraînait la formation d'intermédiaire « nu » lors de la réaction d'hydrogénation par des catalyseurs à base de rhodium expliquant la plus grande activité du système catalytique dans les LI comparativement aux solvants organiques.[101,102]

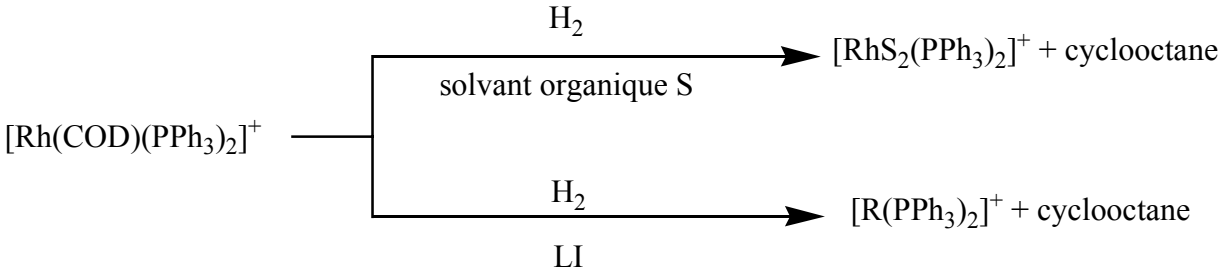

Par contre, le caractère non-dissociant des LI explique la chute de réactivité des catalyseurs à base de ruthénium **2**. En effet, l'absence de traces d'eau empêche la dissociation des ligands chlorure du catalyseur et inhibe la réaction.[45]

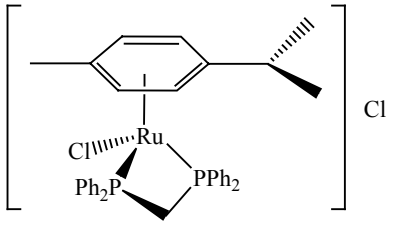

2

Les LI sont donc des milieux complexes dans lequel interviennent des interactions intra- et intermoléculaires mal identifiées.

Dans la partie suivante, les avantages et les limites de l'emploi des LI comme solvant sont exposés. Les problèmes et questions que soulèvent leur utilisation sont également abordés.

2.1 Leur intérêt en catalyse

Les LI offrent l'opportunité de :

- Travailler en phase liquide dans un large domaine de température
- Faciliter les échanges de chaleurs
- Utiliser des procédés électrochimiques
- Utiliser les micro-ondes pour accélérer les réactions[103]
- Travailler à pression réduite

De plus, la variation des anions et des cations du LI permettent d'ajuster les propriétés physico-chimiques du système selon les besoins en particulier modifier :

- la miscibilité relative des substrats/produits vis-à vis des LI
- la réactivité du LI vis-à vis du catalyseur
- le caractère acide et/ou protique des LI

Mais les principaux avantages de l'utilisation des LI en tant que solvants de réaction catalytique sont : la possibilité d'immobilisation du catalyseur dans la phase LI et une séparation aisée des produits de réaction du système catalytique.

2.1.1 Immobilisation du catalyseur dans les LI

L'immobilisation du catalyseur dans la phase LI, un des intérêts majeurs de leur utilisation, est réalisée selon quatre approches. :

1. utilisation du caractère ionique de certains catalyseurs en choisissant soit un précurseur ionique tels que $[Rh(COD)(PPh_3)_2]^+$ (COD=1,3-cyclooctadiène)[101] soit un ligand ionique comme $[Ni(TPPMSNa)_3]$ (TPPMS=triphénylphosphine monosuflonée).[104]

2. Greffage du catalyseur sur le cation[105] ou sur l'anion.[24]

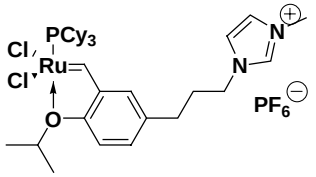

3. Greffer les LI sur un support solide inorganique par l'intermédiaire de l'anion (Voie A) ou du cation (Voie B) (Figure 7).[106]

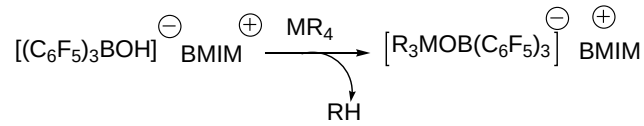

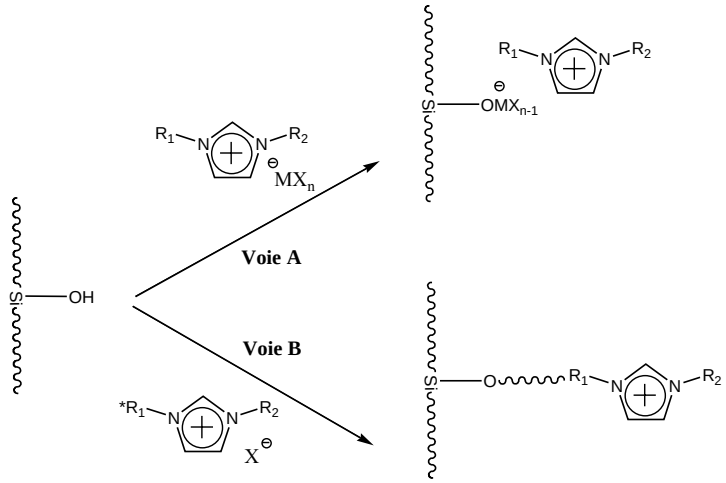

Figure 7. *Préparation de LI supportés sur silice*

4. Supporter le catalyseur dans une couche de LI déposée sur un support solide inorganique.[107-109]

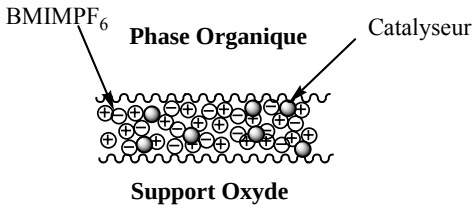

Figure 8. *Immobilisation de catalyseur dans une couche de LI.*

2.1.2 Séparation des produits en fin de réaction

L'utilisation des LI en tant que solvants de réaction catalytique permet également une récupération aisée des produits de réaction. En effet, les produits organiques présentent généralement des solubilités limitées dans les LI ce qui peut permettre une extraction efficace en fin de réaction. Deux cas sont envisageables :

* Si la solubilité du produit dans les LI est nulle ou faible, le produit sera séparé au cours de la réaction par formation d'un système biphasique. La décantation est alors une solution possible pour la récupération du ou des produits de réaction et le recyclage du système catalyseur/LI. Cette technique est particulièrement adaptée aux produits apolaires notamment les hydrocarbures. Il faut également souligner que les réactions secondaires sont limitées dans ce cas.

* Si le ou les produits de réaction présentent une miscibilité partielle ou totale avec les LI, la distillation, bien que coûteuse en énergie, est une méthode efficace de récupération des produits en fin de réaction. Malheureusement cette technique n'est adaptée qu'aux composés volatiles et implique la stabilité thermique du système catalytique. L'extraction par un solvant organique peu miscible avec les LI voire l'utilisation de systèmes triphasique LI/Eau/Solvant organique sont envisageables dans ce cas.

2.1.3 LI et $ScCO_2$

L'utilisation de systèmes multiphasiques donne généralement lieu à des problèmes de contamination des produits par le LI voire de perte du catalyseur du fait de la solubilisation partielle des LI dans la phase organique. L'utilisation du dioxyde de carbone à l'état supercritique permet d'éviter ces phénomènes même si elle implique l'utilisation de systèmes à hautes pressions. Il a effectivement été démontré que la combinaison des LI et du $scCO_2$ présentaient de nombreux avantages notamment du fait de la très grande solubilité du dioxyde de carbone dans les LI et de l'insolubilité des LI dans le $scCO_2$. De plus, ce type de système permet de diminuer considérablement la viscosité des LI et ainsi limiter les problèmes liés au transfert de masse.[90,110,111]

Pour conclure, l'utilisation de LI comme solvants de réaction catalytique présente de nombreux intérêts que ce soit pour le recyclage du catalyseur ou la séparation des produits de réaction. Cependant les LI ne peuvent pas toujours être considérés comme des solvants classiques et certains problèmes inhérents à leur nature chimique peuvent limiter leur utilisation dans les réactions industrielles.

2.2 Limitations de l'utilisation des LI en tant que solvants de réaction catalytique

Ces limites sont dues soit aux propriétés physico-chimiques des LI soit à « leur réactivité ».

2.2.1 Les contraintes dues aux propriétés physico-chimiques des LI

L'utilisation des LI en tant que solvants de réaction catalytique soulève certains problèmes. Tout d'abord, le manque de données toxicologiques les concernant mais aussi le

prix de revient élevé de ces produits sont des facteurs handicapants pour leur développement industriel. Mais, il apparaît également des limitations inhérentes à la nature du LI tels que :

- Une viscosité importante
- Une solubilité des gaz dans les LI très faible
- Une purification difficile

Ce dernier aspect est probablement un des principaux freins à l'utilisation des LI car les impuretés présentes sont généralement difficiles à éliminer[51] et peuvent fortement altérer les propriétés des ces milieux.[43,44,112] De plus, la présence d'impuretés, notamment des traces d'eau ou de chlorures peut avoir des conséquences néfastes (ou bénéfiques) sur l'activité catalytique.[45,46,113] Il a par exemple été montré que la réaction d'hydrogénation du styrène par un catalyseur à base de ruthénium n'avait pas lieu dans les LI totalement anhydre mais nécessitait la présence de traces d'eau.[45] Des précautions particulières doivent par conséquent être prises pour éviter la présence d'impuretés notamment le travail en atmosphère inerte et un grand soin lors de la synthèse des LI. Une caractérisation exhaustive de ces milieux est indispensable pour envisager l'ensemble des phénomènes pouvant avoir lieu dans les LI et ainsi obtenir des résultats reproductibles et comparables.

2.2.2 « Réactivité » inattendue

Mais les propriétés physico-chimiques ne peuvent pas totalement expliquer la réactivité des systèmes catalytiques dans les LI. En effet, bien que les LI soient généralement considérés comme des solvants inertes et relativement peu coordonnants, de nombreuses études rapportent des comportements non-conventionnels de certains systèmes à base de LI et des transformations indésirables.[114]

** LI, solvant inerte*

Le LI solubilise alors le ou les substrats et le système catalytique sans en modifier ni la nature ni la réactivité. Les LI ont été utilisés comme solvants pour de nombreuses réactions catalytiques telles que l'hydrogénation[115], l'hydroformylation[116] et les réactions d'oxydations.[117]

Des effets de solvant « classiques » peuvent alors être observés. Des effets d'interactions solvophobes ont été mis en évidence par Welton *et al* lors de la transposition de la réaction de Diels-Alder dans les LI. Ce phénomène, très étudié en phase aqueuse, génère une « pression

interne » localisée dans des cavités formées par le solvant qui d'une part favorise la mise en contact des réactifs et d'autre part oriente la stéréochimie vers le produit *endo*.[38]

** LI, ligand*

L'utilisation des LI comme solvants de réaction catalytique a montré que les constituants du LI pouvaient réagir avec le système catalytique et ainsi en modifier la nature.

- les réactions d'échange ioniques.

Il a été démontré que dans les réactions d'hydrogénation[118] ou d'hydroformylation,[119] les chlorostannates pouvaient réagir avec les catalyseurs à base de platine et générer un nouveau système catalytique : $[Pt(SnCl_3]_5]^{2-}$ et $[HPt(SnCl_3)_4]^-$. Plus généralement, l'utilisation de composés ioniques dans les LI peut donner lieu à des réactions d'échanges et conduire à la formation *in situ* de nouvelles paires d'ions :[120] 3 $BMIMBF_4$ + $K_3Co(CN)_5 \rightarrow$ $(BMIM)_3Co(CN)_5$ + 3 KBF_4

- la formation *in situ* de carbènes N-hétérocycliques (NHC).

Il est décrit que le cation imidazolium peut se coordonner au métal de transition par addition oxydante. Ces intermédiaires métalliques comportant des ligands imidazolidènes sont connus sous le nom de carbènes N-hétérocycliques (NHC) et ont été observés dans de nombreuses réactions catalytiques telles que la réaction de Heck ou les couplages de Suzuki.[121] L'étude de la réaction de télomérisation du 1,3-butadiène dans les LI réalisée au laboratoire par Magna *et al* en collaboration avec la société Celanese a montré que les sels de 1,3-dialkylimidazolium pouvaient réagir avec le système catalytique $Pd(OAc)_2/PPh_3$. Ceci conduit à la désactivation du catalyseur attribuée à la formation d'un carbène N-hétérocyclique :

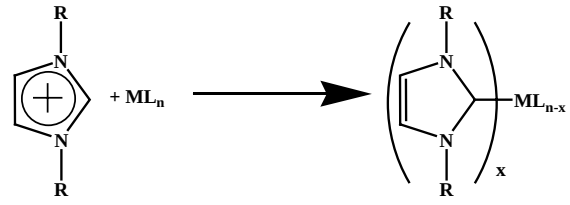

M=$Pd(OAc)_2$, $Ni(OAc)_2$

Le développement de nouveaux LI, notamment un sel de 1,2,3-trialkylimidazolium, a permis de palier ce problème.[46]

**LI, co-catalyseur*

Dans la réaction de dimérisation des oléfines par des catalyseurs à base de nickel, les anions chloroaluminates interviennent comme co-catalyseur et permettent d'éviter certaines réactions secondaires et d'immobiliser le catalyseur dans la phase LI.[31]

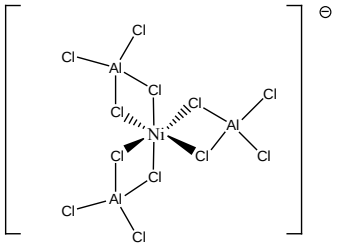

Figure 9. *Complexation du nickel dans les chloroaluminates.*[122]

** LI, catalyseur*

Dans certains cas, le LI peut générer le catalyseur de la réaction en particulier pour les substitutions électrophiles et les réactions de condensations mais également intervenir comme organocatalyseurs pour les réaction de Diels-Alder.

- Les substitutions électrophiles

Les chloroaluminates dont la fraction molaire en $AlCl_3$ est supérieure à 0,5 peuvent se comporter comme des catalyseurs acides. De nombreuses réactions de Friedel et Crafts sont réalisées dans ces milieux sans ajout de catalyseur.[123-125] L'acylation du benzène dans EMIMCl-$AlCl_3$ par le 1-chloropropane conduit aux produits de polyacylations par génération *in situ* de l'ion acylium lors de la réaction de l'ion $Al_2Cl_7^-$:[123]

$$CH_3COCl + Al_2Cl_7^- \rightarrow CH_3CO^+ + 2\ AlCl_4^-$$

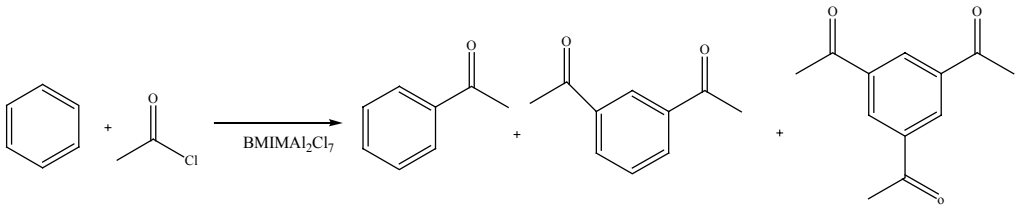

L'acidité de Lewis des chloroaluminates a été utilisée pour de nombreuses substitutions électrophiles des aromatiques telles la chloration,[126] la nitration[126] ou encore la suflonation.[127]

Les sels chlorozincates d'imidazoliums peuvent se dissocier de façon réversible par élévation de la température :[28]

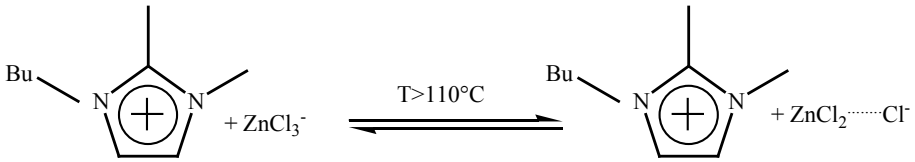

Des résultats préliminaires ont montré que le $ZnCl_2$ ainsi formé *in situ* permet de catalyser la réaction de Friedel et Crafts :

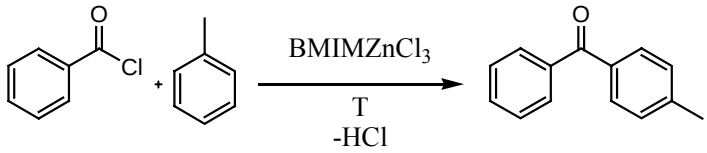

Cela conduit à la formation de la 4-méthylbenzophénone, au dégagement de HCl et à la production de BMIMCl qui constitue une nouvelle phase. Pour l'instant, il n'a pas été possible de recycler le LI de départ du fait du solubilisation du $ZnCl_2$ par la phase organique.[128]

- Les réactions de condensations

De nombreuses réactions ou condensations catalysées par les acides de Lewis ont été menées dans les chloroaluminates notamment la réaction de Pechmann,[129] de Knoevenagel,[130] la synthèse d'indole de Fischer[131] ou encore la condensation de Baeyer[132] mais la formation d'eau comme produit secondaire conduit à la destruction du LI par hydrolyse. On peut également citer la coupure d'éthers,[133] l'estérification[134] ou la réaction de Prins[135] malheureusement la formation de sous-produits ou le traitement du milieu réactionnel conduit généralement à la destruction du LI.

- LI, un organocatalyseur

Les cycloadditions de Diels-Alder ont été transposées dans les LI et il a été montré que le cation imidazolium jouait le rôle de donneur de liaison H et accélérait les réactions.

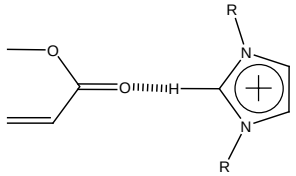

Cet aspect a également été utilisé par la suite pour les réactions d'additions de Michael[136] et autres additions conjuguées.[135,137]

Il a même été démontré que le cation imidazolium pouvaient générer par déprotonation un catalyseur nucléophile : l'imidazolidène, actif notamment en catalyseur de transésterification ou en polymérisation des lactones et lactides par ouverture de cycle.[138-140]

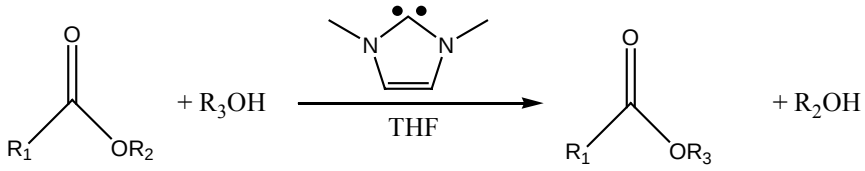

Mais aucun des exemples cités ci-dessus ne prend en compte le fait que les LI sont des associations de cations et d'anions qui peuvent donner lieu à des réactions d'échanges ioniques ou participer à des complexation du fait ses charges mais qui surtout induisent une structuration des LI qui peut influencer les réactions catalytiques.

3 Organisation du liquide ionique

Bien que de nombreux travaux aient étudiés la structure des LI à l'état solide, très peu d'études ont été menées sur leur organisation à l'état liquide. Cependant il est crucial de prendre en compte ces aspects structuraux pour comprendre le rôle des LI et la réactivité dans ces solvants.

La structure des LI est gouvernée par plusieurs paramètres : la taille des ions, la distribution de charge des ions, la présence de donneurs et/ou d'accepteur de liaison H ou encore les interactions π-π entre les cations imidazoliums. Mais la structure est en premier lieu dominée par les forces d'attractions coulombiennes entre ions de charges opposées. Pour les LI à bas point de fusion, la charge q est ± 1 et la distance interatomique r est grande.

Loi de Coulomb : $F = k\frac{q_1 q_2}{\varepsilon r^2}$ avec k : constante et ε : permittivité

Anion	Cl	PF_6	$AlCl_4$	NTf_2
R_{ion} (A)	1.7	2.4	2.8	
$R_{van\ der\ waals}$ (A)		2.54		3.26
Surface (A^2)	36	72	98	
Volume (A^3)	20	58	92	

Cation	EMIM	BMIM
R_{ion} (A)	2.7x2	
$R_{van\ der\ waals}$ (A)		3.3
Surface (A^2)	>80	
Volume ($A^{3)}$	>46	

Tableau 13. *Taille, surface et volume des constituants du LI*

L'organisation des LI est également due aux atomes accepteurs (facteur α) ou donneurs (facteur β) de liaisons hydrogène. Ces interactions dépendent de la nature du cation et de la délocalisation des charges de l'anion.[141]

Les interactions π-π entre les cations imidazoliums jouent aussi un rôle important dans l'organisation des LI et impliquent un arrangement dans lequel ces composés sont face à face. Par exemple, les structures par diffraction des rayons X (DRX) du cation 3-éthyl-1-méthylimidazolium ont montré que les cations étaient situés dans des plans parallèles séparés par des distances intermoléculaires de l'ordre de 4,5Å.[142] Ces résultats ont été confirmés par des études en diffusion des neutrons.[143] Il est évident que ces interactions seront dépendantes de la nature du cation (présence d'un système π planaire ou non) et de l'anion suivant la répartition de sa densité électronique dans l'espace.[141]

3.1 Structure à l'état solide.

Les études DRX des sels de 1,3-dialkylimidazoliums ont montré que ces LI forment, à l'état solide, un réseau de cations et d'anions interconnectés par des liaisons hydrogène, chaque cation étant entouré de trois anions et réciproquement. Cet arrangement génère des canaux dans lesquels les anions s'organisent en chaîne.[114]

La structure du bis(trifluorométhanesulfonyl)imide 1,3-diméthylimidazolium ($MMIMNTf_2$) déterminée par DRX (figure 10) montre que l'anion NTf_2 adopte une géométrie *cis* du fait des liaisons hydrogène C-H···O entre le cation et l'anion du LI provoquant l'apparition de couches fluorées.[144]

Figure 10. *Structure cristallographique de $MMIMNTf_2$ (type A)*

Par contre, les ions dans le bis(trifluorométhanesulfonyl)imide 1,2,3-triéthylimidazolium ($EEEIMNTf_2$) sont interconnectés par des liaisons C-H···O faibles à des distances proches de celle de la séparation de Van Der Waals et l'anion NTf_2 adopte une conformation intermédiaire entre la configuration *cis* et *trans*.[144]

Figure 11. *Structure cristallographique de $EEEIMNTf_2$ (Type B)*

En conclusion, cette étude structurale à l'état solide montre que l'arrangement local autour de l'anion est gouverné par la présence ou non d'un atome d'hydrogène en position C_2 qui conduit soit à des structures de type A (Figure 10) lorsque la liaison hydrogène est possible soit à des arrangements de type B (Figure 11) si le carbone en position 2 est alkylée.

3.2 Structure à l'état liquide

Les LI présentent une structure à l'état liquide semblable à celle observée dans la phase cristalline donc très bien organisée ce qui en fait des fluides supramoléculaires. Cette auto-organisation à l'état liquide est assurée par diverses interactions comme des liaisons hydrogène, des atomes dit pontants (atome oxygène, azote, chlore, fluor)[145] et par des interactions électrostatiques entre les charges qui s'accumulent en certaines régions des molécules. Plusieurs études ont montré que cette organisation était maintenue à l'échelle macroscopique.

Tout d'abord, les études de diffusion des rayons X aux petits angles (SAXS) ont montré qu'à l'état liquide, $BMIMPF_6$ présentait une organisation locale constituée de motifs de 4,4 et 6,3Å répétés sur des distances de 15Å mais qu'il n'était pas un cristal liquide du fait de l'absence de bande de réfraction de la lumière polarisante. Ce phénomène a été expliqué par la répétition de 3 couches successives de cations imidazoliums séparées de 4,4Å, la distance entre deux cations imidazoliums étant de 6,3 Å.[51] Ces résultats ont été validés par l'analyse DRX d'échantillons de LI initialement surfondus dont la cristallisation a été induite par un choc. Cette étude confirme une distance entre les cycles imidazoliums de 6,113Å mais distingue deux distances interplanaires de 4,3378 et 3,4618Å, deux de ces motifs se répétant sur une échelle de 15,6Å (Figure 12).[146]

Figure 12. *Les deux types d'arrangements interplanaires des cations imidazoliums dans les LI.(H omis)*

Les distances inter- et intramoléculaires de BMIMX et BMMIMX (X= Cl, Br,, BF_4 et NTf_2) ont été estimées par RMN NOE. L'absence d'interaction intermoléculaire dans le cas de $BMIMNTf_2$ et $BMMIMNTf_2$ est expliquée par la taille et le pouvoir peu coordonnant de l'anion NTf_2. Cette étude met en évidence la présence d'une organisation locale des cations imidazoliums qui forme un domaine polaire mais aucune association des chaînes alkyles n'est détectée. De plus, ces données ne permettent pas de conclure quant au parallélisme des cycles imidazoliums ou à la présence d'interactions π-π.[147]

Figure 13. *Différents arrangements des cations imidazoliums proposés par Mele et al.*

Les LI présentent un ordre analogue à celui existant à l'état solide conférant une structure « hétérogène » à ce milieu. Ceci conduit à se poser des questions sur :

1) la solvatation des réactifs dans les LI

2) le domaine dans lequel a lieu la réaction
3) les interactions des cations métalliques dans ce milieu ionique

Conclusion

Cette étude bibliographique a souligné les avantages et les limites des LI utilisés comme solvants de réaction catalytique. Les propriétés physico-chimiques, la stabilité thermique, le vaste domaine liquide, l'ininflammabilité et la très faible tension de vapeur en font des milieux propices pour leur utilisation dans les procédés industriels. Mais les réactions catalytiques étudiées dans les LI au laboratoire LCOMS : la télomérisation du butadiène (Celanese),[46] l'isomérisation du 2-méthyl-3-butènenitrile en 3-pentènenitrile[148] et l'hydrocyanation du 3-pentènenitrile en adiponitrile (Rhodia)[104] démontrent à l'évidence que lorsqu'ils sont utilisés comme milieux réactionnels, les LI peuvent intervenir en tant que solvants et donner lieu à des phénomènes de solvatation « classiques » mais qu'il est également envisageable qu'ils jouent le rôle de ligand, de co-catalyseur voire même de catalyseur et ainsi modifie la réactivité des systèmes lors de la réaction catalytique.

Une meilleure compréhension de ces milieux a permis de résoudre certains problèmes liés à l'utilisation des LI comme solvants tels que le remplacement de BMIM par BMMIM pour éviter la formation de NHC ou un meilleur contrôle des impuretés présentes afin de limiter les effets négatifs de traces de chlorures ou d'eau.

Cependant un certain nombre de questions subsiste quant à la solubilisation/solvatation des espèces organiques et organométalliques dans les LI notamment :

- Le type d'interaction responsable de la mise en solution et de la solvatation du substrat et des précurseurs du catalyseur
- L'élément le plus perturbé par ces interactions
- La réactivité relative du substrat libre ou « complexé »
- La localisation du milieu réactionnel (espace confinés, clathrates, domaines apolaires, milieux ioniques)

Par conséquent et dans l'état de connaissance actuel des milieux LI, notre stratégie est de tenter d'établir une relation « structure – activité » pour certains LI et leur comportement comme solvants dans certains types de catalyse.

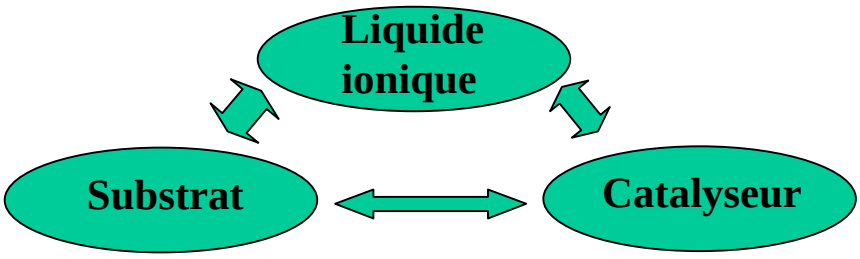

Figure 14. *Relation entre les partenaires du système liquide ionique/substrat/catalyseur*

Bibliographie

(1) Reichardt, C. *Solvents and Solvent Effects in Organic Chemistry. 3rd Ed*; Wiley-VCH: Weinheim, 2003.
(2) Wilkes, J. S. *J. Mol. Catal. A* **2004**, *214*, 11-17.
(3) Wasserscheid, P.; Welton, T. *Ionic Liquids in Synthesis*; Wiley-VCH: Weinheim, 2003.
(4) Welton, T. *Coord. Chem. Rev.* **2004**, *248*, 2459-2477.
(5) Herrmann, W. A.; Koecher, C.; Goossen, L. J.; Artus, G. R. J. *Chem. Eur. J.* **1996**, *2*, 1627-1636.
(6) Branco, L. C.; Rosa, J. N.; Ramos, J. J. M.; Afonso, C. A. M. *Chem. Eur. J.* **2002**, *8*, 3671-3677.
(7) Abbott, A. P.; Capper, G.; Davies, D. L.; Rasheed, R. *Inorg. Chem.* **2004**, *43*, 3447-3452.
(8) Fei, Z.; Ang, W. H.; Geldbach, T. J.; Scopelliti, R.; Dyson, P. J. *Chem. Eur. J.* **2006**, *12*, 4014-4020.
(9) Itoh, H.; Naka, K.; Chujo, Y. *J. Am. Chem. Soc.* **2004**, *126*, 3026-3027.
(10) Fei, Z.; Kuang, D.; Zhao, D.; Klein, C.; Ang, W. H.; Zakeeruddin, S. M.; Graetzel, M.; Dyson, P. J. *Inorg. Chem.* **2006**, *45*, 10407-10409.
(11) Chen, W.; Liu, F. *J. Organomet. Chem.* **2003**, *673*, 5-12.
(12) Zhao, D.; Fei, Z.; Geldbach, T. J.; Scopelliti, R.; Laurenczy, G.; Dyson, P. J. *Helv. Chim. Acta* **2005**, *88*, 665-675.
(13) Mazille, F.; Fei, Z.; Kuang, D.; Zhao, D.; Zakeeruddin, S. M.; Graetzel, M.; Dyson, P. J. *Inorg. Chem.* **2006**, *45*, 1585-1590.
(14) Schottenberger, H.; Wurst, K.; Horvath, U. E. I.; Cronje, S.; Lukasser, J.; Polin, J.; McKenzie, J. M.; Raubenheimer, H. G. *Dalton Trans.* **2003**, 4275-4281.
(15) Fei, Z.; Zhao, D.; Scopelliti, R.; Dyson, P. J. *Organometallics* **2004**, *23*, 1622-1628.
(16) Zhao, D.; Fei, Z.; Scopelliti, R.; Dyson, P. J. *Inorg. Chem.* **2004**, *43*, 2197-2205.
(17) Zhao, D.; Fei, Z.; Geldbach, T. J.; Scopelliti, R.; Dyson, P. J. *J. Am. Chem. Soc.* **2004**, *126*, 15876-15882.
(18) Bao, W.; Wang, Z.; Li, Y. *J. Org. Chem.* **2003**, *68*, 591-593.
(19) Baudequin, C.; Baudoux, J.; Levillain, J.; Cahard, D.; Gaumont, A.-C.; Plaquevent, J.-C. *Tetrahedron Asym* **2003**, *14*, 3081-3093.
(20) Baudequin, C.; Bregeon, D.; Levillain, J.; Guillen, F.; Plaquevent, J.-C.; Gaumont, A.-C. *Tetrahedron Asym* **2005**, *16*, 3921-3945.
(21) Fukumoto, K.; Ohno, H. *Chem. Comm.* **2006**, 3081-3083.
(22) Fukumoto, K.; Yoshizawa, M.; Ohno, H. *J. Am. Chem. Soc.* **2005**, *127*, 2398-2399.

(23) Yoshida, Y.; Baba, O.; Saito, G. *J. Phys. Chem. B* **2007**, *111*, 4742-4749.
(24) Bibal, C.; Santini, C. C.; Chauvin, Y.; Olivier-Bourbigou, H.; Vallée, C. In *PCT Int. Appl.*; IFP: France, 2007; Vol. 04 935, p 20p.
(25) MacFarlane, D. R.; Pringle, J. M.; Johansson, K. M.; Forsyth, S. A.; Forsyth, M. *Chem. Comm.* **2006**, 1905-1917.
(26) Olivier-Bourbigou, H.; Magna, L. *J. Mol. Catal. A* **2002**, *182-183*, 419-437.
(27) Olivier-Bourbigou, H.; Vallee, C. In *Multiphase Homogeneous Catalysis*; Wiley-VCH: Weinheim, 2005; Vol. 2, pp 413-431.
(28) Lecocq, V.; Graille, A.; Santini, C. C.; Baudouin, A.; Chauvin Y.; Basset, J.-M.; Bouchu, D.; Fenet, B. *New J. Chem.* **2005**, *2 9*, 700–706.
(29) Wilkes, J. S. *Green Chem.* **2002**, *4*, 73-80.
(30) Wilkes, J. S.; Zaworotko, M. J. *Chem. Comm.* **1992**, 965-967.
(31) Chauvin, Y.; Gilbert, B.; Guibard, I. *Chem. Comm.* **1990**, 1715-1716.
(32) Jaeger, D. A.; Tucker, C. E. *Tetrahedron Lett.* **1989**, *30*, 1785-1788.
(33) Favre, F.; Forestiere, A.; Hugues, F.; Olivier-Bourbigou, H.; Chodorge, J. A. *Petrol. Tech.* **2002**, *441*, 104-109.
(34) Falling, S. N.; Godleski, S. A.; McGarry, L. W. In *U.S. Pat.*; (Eastman Kodak Co., USA).: US, 1993; p 8 pp.
(35) Cole-Hamilton, D. J.; Tooze, R. P. *Catalyst separation, recovery and recycling: Chemistry and Process Design*; Springer: Dordrecht, 2006.
(36) Maase, M.; Massonne, K.; Halbritter, K.; Noe, R.; Bartsch, M.; Siegel, W.; Stegmann, V.; Flores, M.; Huttenloch, O.; Becker, M. In *PCT Int. Appl.*; Basf: Germany, 2003; Vol. 2003062171, p 60 pp.
(37) Cornils, B.; Herrmann, W. A.; Horvath, I. T.; Leitner, W.; Mecking, S.; Olivier-Bourbigou, H.; Vogt, D. *Multiphase Homogeneous Catalysis, Volume 2*; Wiley-VCH: Weinheim, 2005.
(38) Welton, T. *Chem. Rev.* **1999**, *99*, 2071-2083.
(39) Deetlefs, M.; Seddon, K. R. *Green Chem.* **2003**, *5*, 181-186.
(40) Namboodiri, V. V.; Varma, R. S. *Tetrahedron Lett.* **2002**, *43*, 5381-5383.
(41) Leveque, J.-M.; Luche, J.-L.; Petrier, C.; Roux, R.; Bonrath, W. *Green Chem.* **2002**, *4*, 357-360.
(42) Abbott, A. *Chem. Soc. Rev.* **1993**, *22*, 435-440.
(43) Noda, A.; Hayamizu, K.; Watanabe, M. *J. Phys. Chem. B* **2001**, *105*, 4603-4610.
(44) Seddon, K. R.; Stark, A.; Torres, M.-J. *Pure Appl. Chem.* **2000**, *72*, 2275-2287.
(45) Daguenet, C.; Dyson, P. J. *Organometallics* **2004**, *23*, 6080-6083.
(46) Magna, L.; Chauvin, Y.; Niccolai, G. P.; Basset, J.-M. *Organometallics* **2003**, *22*, 4418-4425.
(47) Earle, M. J.; Esperanca, J. M. S. S.; Gilea, M. A.; Canongia Lopes, J. N.; Rebelo, L. P. N.; Magee, J. W.; Seddon, K. R.; Widegren, J. A. *Nature* **2006**, *439*, 831-834.
(48) Stepnowski, P.; Nichthauser, J.; Mrozik, W.; Buszewski, B. *Anal. Bioanal. Chem.* **2006**, *385*, 1483-1491.
(49) Cammarata, L.; Kazarian, S. G.; Salter, P. A.; Welton, T. *Phys. Chem. Chem. Phys.* **2001**, *3*, 5192-5200.
(50) Alfassi, Z. B.; Huie, R. E.; Milman, B. L.; Neta, P. In *Anal. Bioanal. Chem.*, 2003; Vol. 377, pp 159-164.
(51) Billard, I.; Moutiers, G.; Labet, A.; El Azzi, A.; Gaillard, C.; Mariet, C.; Luetzenkirchen, K. *Inorg. Chem.* **2003**, *42*, 1726-1733.
(52) Berthier, D.; Varenne, A.; Gareil, P.; Digne, M.; Lienemann, C.-P.; Magna, L.; Olivier-Bourbigou, H. *Analyst* **2004**, *129*, 1257-1261.
(53) Holbrey, J. D.; Seddon, K. R.; Wareing, R. *Green Chem.* **2001**, *3*, 33-36.

(54) Anthony, J. L.; Brennecke, J. F.; Holbrey, J. D.; Maginn, E. J.; Mantz, R. A.; Rogers, R. D.; Trulove, P. C.; Visser, A. E.; Welton, T. In *Ionic Liquids in Synthesis*; Wasserscheid, P., Welton, T.,, Ed.; Wiley-VCH: Weinheim, 2003; pp 41-55.
(55) Hunt, P. A. *J. Phys. Chem. B* **2007**, *111*, 4844-4853.
(56) Endres, F.; Zein El Abedin, S. *Phys. Chem. Chem. phys.* **2006**, *8*, 2101-2116.
(57) Dzyuba, S. V.; Bartsch Richard, A. *Chem. Phys. Phys. Chem* **2002**, *3*, 161-166.
(58) Holbrey, J. D.; Seddon, K. R. *Dalton Trans.* **1999**, 2133-2139.
(59) Dyson, P. J.; Laurenczy, G.; Ohlin, C. A.; Vallance, J.; Welton, T. *Chem. Comm.* **2003**, 2418-2419.
(60) Dzyuba, S. V.; Bartsch, R. A. *Tetrahedron Lett.* **2002**, *43*, 4657-4659.
(61) McLean, A. J.; Muldoon, M. J.; Gordon, C. M.; Dunkin, I. R. *Chem. Comm.* **2002**, 1880-1881.
(62) Huddleston, J. G.; Visser, A. E.; Reichert, W. M.; Willauer, H. D.; Broker, G. A.; Rogers, R. D. *Green Chem.* **2001**, *3*, 156-164.
(63) Ranke, J.; Stolte, S.; Stoermann, R.; Arning, J.; Jastorff, B. *Chem. Rev.* **2007**, *107*, 2183-2206.
(64) Ranke, J.; Mueller, A.; Bottin-Weber, U.; Stock, F.; Stolte, S.; Arning, J.; Stoermann, R.; Jastorff, B. *Ecotox. Environ. Safe.* **2007**, *67*, 430-438.
(65) Stolte, S.; Arning, J.; Bottin-Weber, U.; Matzke, M.; Stock, F.; Thiele, K.; Uerdingen, M.; Welz-Biermann, U.; Jastorff, B.; Ranke, J. *Green Chem.* **2006**, *8*, 621-629.
(66) Jastorff, B.; Moelter, K.; Behrend, P.; Bottin-Weber, U.; Filser, J.; Heimers, A.; Ondruschka, B.; Ranke, J.; Schaefer, M.; Schroeder, H.; Stark, A.; Stepnowski, P.; Stock, F.; Stoermann, R.; Stolte, S.; Welz-Biermann, U.; Ziegert, S.; Thoeming, J. *Green Chem.* **2005**, *7*, 362-372.
(67) Ranke, J.; Moelter, K.; Stock, F.; Bottin-Weber, U.; Poczobutt, J.; Hoffmann, J.; Ondruschka, B.; Filser, J.; Jastorff, B. *Ecotox. Environ. Safe.* **2005**, *60*, 350.
(68) Smiglak, M.; Reichert, W. M.; Holbrey, J. D.; Wilkes, J. S.; Sun, L.; Thrasher, J. S.; Kirichenko, K.; Singh, S.; Katritzky, A. R.; Rogers, R. D. *Chem. Comm.* **2006**, 2554-2556.
(69) Endres, F.; Bukowski, M.; Hempelmann, R.; Natter, H. *Angew. Chem. Int. Ed.* **2003**, *42*, 3428-3430.
(70) Ohno, K. *Electrochemical Aspects of Ionic Liquids*; John Wiley & Sons: Chichester, 2004.
(71) Ohno, H.; Yoshizawa, M. *Electrochemistry* **2002**, *70*, 136-140.
(72) Moustafa, E. M.; Zein El Abedin, S.; Shkurankov, A.; Zschippang, E.; Saad, A. Y.; Bund, A.; Endres, F. *J. Phys. Chem. B* **2007**, *111*, 4693-4704.
(73) Smith, G.; Cole-Hamilton, D. J.; Gregory, A. C.; Gooden, N. G. *Polyhedron* **1982**, *1*, 97-103.
(74) Webb, P. B.; Sellin, M. F.; Kunene, T. E.; Williamson, S.; Slawin, A. M. Z.; Cole-Hamilton, D. J. *J. Am. Chem. Soc.* **2003**, *125*, 15577-15588.
(75) Thomazeau, C.; Olivier-Bourbigou, H.; Magna, L.; Luts, S.; Gilbert, B. *J. Am. Chem. Soc.* **2003**, *125*, 5264-5265.
(76) Amyes, T. L.; Diver, S. T.; Richard, J. P.; Rivas, F. M.; Toth, K. *J. Am. Chem. Soc.* **2004**, *126*, 4366-4374.
(77) Arduengo, A. J. *Acc. Chem. Res.* **1999**, *32*, 913-921.
(78) Smith, G. P.; Dworkin, A. S.; Pagni, R. M.; Zingg, S. P. *J. Am. Chem. Soc.* **1989**, *111*, 5075-5077.
(79) Smith, G. P.; Dworkin, A. S.; Pagni, R. M.; Zingg, S. P. *J. Am. Chem. Soc.* **1989**, *111*, 525-530.
(80) Dullius, J. E. L.; Suarez, P. A. Z.; Einloft, S.; de Souza, R. F.; Dupont, J.; Fischer, J.; De Cian, A. *Organometallics* **1998**, *17*, 815-819.

(81) Oxley, J. D.; Prozorov, T.; Suslick, K. S. *J. Am. Chem. Soc.* **2003**, *125*, 11138-11139.
(82) Campbell, P.; Santini, C. C. In;; CNRS-CPE Lyon: Lyon, 2007; p 60.
(83) Baker, S. N.; Baker, G. A.; Bright, F. V. *Green Chem.* **2002**, *4*, 165-169.
(84) Poole, C. F. *J. Chromatography* **2004**, *1037*, 49-82.
(85) Chiappe, C.; Pieraccini, D. *J. Phys. Chem. B* **2006**, *110*, 4937-4941.
(86) Muldoon, M. J.; Gordon, C. M.; Dunkin, I. R. *Perkin Trans.* **2001**, 433-435.
(87) Moutiers, G. B., I. *Techniques de l'ingénieur* **2005**.
(88) Anthony, J. L.; Anderson, J. L.; Maginn, E. J.; Brennecke, J. F. *J. Phys. Chem. B* **2005**, *109*, 6366-6374.
(89) Anthony, J. L.; Maginn, E. J.; Brennecke, J. F. *J. Phys. Chem. B* **2002**, *106*, 7315-7320.
(90) Solinas, M.; Pfaltz, A.; Cozzi Pier, G.; Leitner, W. *J. Am. Chem. Soc.* **2004**, *126*, 16142-16147.
(91) Jiang, Y.-Y.; Zhou, Z.; Jiao, Z.; Li, L.; Wu, Y.-T.; Zhang, Z.-B. *J. Phys. Chem. B* **2007**, *111*, 5058-5061.
(92) Gan, Q.; Rooney, D.; Zou, Y. *Desalination* **2006**, *199*, 535-537.
(93) Tempel, D. J.; Henderson, P. B.; Brzozowski, J. R.; Pearlstein, R. M.; Garg, D. In *U.S. Pat. Appl. Publ. N°2006060818*: USA, 2006; Vol. 948, p 15 pp.
(94) Chinn, D.; Vu, D.; Driver, M. S.; Boudreau, L. C. In *U.S. Pat. Appl. Publ. N°2005129598*; (Chevron U.S.A. Inc., USA).: USA, 2005; p 17 pp.
(95) Baltus, R. E.; Counce, R. M.; Culbertson, B. H.; Luo, H.; DePaoli, D. W.; Dai, S.; Duckworth, D. C. *Separation Science and Technology* **2005**, *40*, 525-541.
(96) Shvedene, N. V.; Borovskaya, S. V.; Sviridov, V. V.; Ismailova, E. R.; Pletnev, I. V. *Anal. Bioanal. Chem.* **2005**, *381*, 427-430.
(97) Bonhote, P.; Dias, A.-P.; Papageorgiou, N.; Kalyanasundaram, K.; Graetzel, M. *Inorg. Chem.* **1996**, *35*, 1168-1178.
(98) Holbrey, J. D.; Reichert, W. M.; Nieuwenhuyzen, M.; Sheppard, O.; Hardacre, C.; Rogers, R. D. *Chem. Comm.* **2003**, 476-477.
(99) Selvan, M. S.; McKinley, M. D.; Dubois, R. H.; Atwood, J. L. *J. Chem. Eng. Data* **2000**, *45*, 841-845.
(100) Domanska, U.; Marciniak, A. *J. Chem. Eng. Data* **2003**, *48*, 451-456.
(101) Chauvin, Y.; Mussmann, L.; Olivier, H. *Angew. Chem. Int. Ed.* **1996**, *34*, 2698-2700.
(102) Schrock, R. R.; Osborn, J. A. *J. Am. Chem. Soc.* **1976**, *98*, 4450-4455.
(103) Ley, S. V.; Leach, A. G.; Storer, R. I. *Perkin Trans.* **2001**, 358-361.
(104) Vallee, C.; Chauvin, Y.; Basset, J.-M.; Santini, C. C.; Galland, J.-C. *Adv. Synth. Catal.* **2005**, *347*, 1835-1847.
(105) Audic, N.; Clavier, H.; Mauduit, M.; Guillemin, J.-C. *J. Am. Chem. Soc.* **2003**, *125*, 9248-9249.
(106) Valkenberg, M. H.; de Castro, C.; Hoelderich, W. F. *Green Chem.* **2002**, *4*, 88-93.
(107) Virtanen, P.; Karhu, H.; Kordas, K.; Mikkola, J.-P. *Chem. Eng. Sc.* **2007**, *62*, 3660-3671.
(108) Haumann, M.; Dentler, K.; Joni, J.; Riisager, A.; Wasserscheid, P. *Adv. Synth. Catal.* **2007**, *349*, 425-431.
(109) Mehnert, C. P.; Mozeleski, E. J.; Cook, R. A. *Chem. Comm.* **2002**, 3010-3011.
(110) Ballivet-Tkatchenko, D.; Picquet, M.; Solinas, M.; Francio, G.; Wasserscheid, P.; Leitner, W. *Green Chem.* **2003**, *5*, 232-235.
(111) Hintermair, U.; Zhao, G.; Santini, C. C.; Muldoon, M. J.; Cole-Hamilton, D. J. *Chem. Comm.* **2007**, 1462-1464.
(112) Mele, A.; Tran, C. D.; De Paoli Lacerda, S. H. *Angew. Chem. Int. Ed.* **2003**, *42*, 4364-4366.

(113) Zhao, Y.-B.; Yan, Z.-Y.; Liang, Y.-M. *Tetrahedron Lett.* **2006**, *47*, 1545-1549.
(114) Dupont, J. *J. Braz. Chem. Soc.* **2004**, *15*, 341-350.
(115) Dyson, P. J.; Zhao, D. In *Multiphase Homogeneous Catalysis*; Wiley-VCH: Weinheim, 2005; Vol. 2, pp 494-511.
(116) Cole-Hamilton, D. J. *Science* **2003**, *299*, 1702-1706.
(117) Howarth, J. *Tetrahedron Lett.* **2000**, *41*, 6627-6629.
(118) Parshall, G. W. *J. Am. Chem. Soc.* **1972**, *94*, 8716-8719.
(119) Wasserscheid, P.; Eichmann, M. *Catal. Today* **2001**, *66*, 309-316.
(120) Suarez, P. A. Z.; Dullius, J. E. L.; Einloft, S.; de Souza, R. F.; Dupont, J. *Inorg. Chim. Acta* **1997**, *255*, 207-209.
(121) Xu, L.; Chen, W.; Xiao, J. *Organometallics* **2000**, *19*, 1123-1127.
(122) Dent, A. J.; Seddon, K. R.; Welton, T. *Chem. Comm.* **1990**, 315-316.
(123) Boon, J. A.; Levisky, J. A.; Pflug, J. L.; Wilkes, J. S. *J. Org. Chem.* **1986**, *51*, 480-483.
(124) Earle, M. J.; Hakala, U.; Hardacre, C.; Karkkainen, J.; McAuley, B. J.; Rooney, D. W.; Seddon, K. R.; Thompson, J. M.; Waehaelae, K. *Chem. Comm.* **2005**, 903-905.
(125) Stark, A.; MacLean, B. L.; Singer, R. D. *Dalton Trans.* **1999**, 63-66.
(126) Boon, J. A.; Lander, S. W., Jr.; Levisky, J. A.; Pflug, J. L.; Skrazynecki-Cooke, L. M.; Wilkes, J. S. *Proc- Electrochem.Soc.* **1987**, *87-7*, 979-990.
(127) Nara, S. J.; Harjani, J. R.; Salunkhe, M. M. *J. Org. Chem.* **2001**, *66*, 8616-8620.
(128) Santini, C. C. "Chlorozincates ionic liquid as solvent for Friedel-Crafts acylation reaction,", 2007.
(129) Potdar, M. K.; Mohile, S. S.; Salunkhe, M. M. *Tetrahedron Lett.* **2001**, *42*, 9285-9287.
(130) Harjani, J. R.; Nara, S. J.; Salunkhe, M. M. *Tetrahedron Lett.* **2002**, *43*, 1127-1130.
(131) Rebeiro, G. L.; Khadilkar, B. M. *Synthesis* **2001**, 370-372.
(132) Paul, A. M.; Khandekar, A. C.; Khadilkar, B. M. *J. Chem. Res.* **2003**, 168-169.
(133) Green, L.; Hemeon, I.; Singer, R. D. *Tetrahedron Lett.* **2000**, *41*, 1343-1346.
(134) Gu, Y.; Shi, F.; Deng, Y. *J. Mol. Catal. A* **2004**, *212*, 71-75.
(135) Yadav, J. S.; Reddy, B. V. S.; Reddy, M. S.; Niranjan, N.; Prasad, A. R. *Eur. J. Org. Chem.* **2003**, 1779-1783.
(136) Dere, R. T.; Pal, R. R.; Patil, P. S.; Salunkhe, M. M. *Tetrahedron Lett.* **2003**, *44*, 5351-5353.
(137) Ranu, B. C.; Dey, S. S.; Hajra, A. *Tetrahedron* **2003**, *59*, 2417-2421.
(138) Grasa, G. A.; Gueveli, T.; Singh, R.; Nolan, S. P. *J. Org. Chem.* **2003**, *68*, 2812-2819.
(139) Grasa, G. A.; Kissling, R. M.; Nolan, S. P. *Organic Lett.* **2002**, *4*, 3583-3586.
(140) Nyce, G. W.; Lamboy, J. A.; Connor, E. F.; Waymouth, R. M.; Hedrick, J. L. *Organic Lett.* **2002**, *4*, 3587-3590.
(141) Bradley, A. E.; Hardacre, C.; Holbrey, J. D.; Johnston, S.; McMath, S. E. J.; Nieuwenhuyzen, M. *Chem. Mat.* **2002**, *14*, 629-635.
(142) Wilkes, J. S.; Zaworotko, M. J. *Supramol. Chem.* **1993**, *1*, 191-193.
(143) Hardacre, C.; Holbrey, J. D.; McMath, S. E. J.; Bowron, D. T.; Soper, A. K. *J. Chem. Phys.* **2003**, *118*, 273-278.
(144) Holbrey, J. D.; Reichert, W. M.; Rogers, R. D. *Dalton Trans.* **2004**, 2267-2271.
(145) Loc Nguyen, H.; Horton, P. N.; Hursthouse, M. B.; Legon, A. C.; Bruce, D. W. *J. Am. Chem. Soc.* **2004**, *126*, 16-17.
(146) Dibrov, S. M.; Kochi, J. K. *Acta Cryst. C* **2006**, *62*, 19-21.
(147) Mele, A.; Romano, G.; Giannone, M.; Ragg, E.; Fronza, G.; Raos, G.; Marcon, V. *Angew. Chem. Int. Ed.* **2006**, *45*, 1123-1126.
(148) Vallee, C.; Valerio, C.; Chauvin, Y.; Niccolai, G. P.; Basset, J.-M.; Santini, C. C.; Galland, J.-C.; Didillon, B. *J. Mol. Catal. A* **2004**, *214*, 71-81.

Chapter II : Ionic solute speciation in ionic liquids

Introduction

Industrial objectives in the field of catalytic reaction deal with enhancing selectivity by the development of new ligand structures and recycling the catalysts using heterogeneous catalysts and potentially biphasic systems.[1,2] With a strong drive for environmentally friendly solvents, the applications of ionic liquid (IL) solvents in biphasic catalysis have been studied in detail.[3,4] Although many organic, inorganic and organometallic compounds are easily dissolved in IL, there are some organic solvents, particularly alkanes remain immiscible even at high temperatures. Moreover it is also possible to change the chemical and physical properties of IL by simply varying the nature of the cations and/or anions.[1,2]

The development of IL in biphasic catalysis has clearly demonstrated that catalytic systems have to be ionic in order to avoid catalyst leaching from IL phase.[5,6] Two strategies can be used to synthesize an ionic catalyst : either the catalyst is charged itself such $K_3Co(CN)_5$,[7] $Ni(CH_3CN)_6BF_4$,[8] or $Rh(COD)(PPh_3)_2BF_4$ (COD=1,5-cyclooctadiene)[9] or it possesses ionic ligands. Several ionic ligands have been tested but the most versatile is the (m-sulfophenyl)diphenylphosphine sodium salt : $TPPMS^-Na^+$ [10] which has been extensively used in a biphasic aqueous/organic systems[11,12] and in IL.[3,5,13]

EXAFS studies showed the non-innocent nature of IL on dissolved species. The coordination of cobalt in $K_3Co(CN)_5$ and of nickel in $Ni(CH_3CN)_6BF_4$ in presence of $(EMIM)MCl_4$ (M=Mn, Co, Ni) was found to change during the catalysis. For instance, $K_3Co(CN)_5$ is totally converted in $(BMIM)_3Co(CN)_5$ and $Ni(CH_3CN)_6BF_4$ into $Ni(AlCl_4)_3^-$.[8] At the opposite, to our knowledge, there are no study reports the speciation of ionic ligand during the catalysis. However it has also been described that sodium cation could be exchange for the cation of IL by dissolving cationic nanoclays in IL.[14]

Recent work carried out in our laboratory proved that the synthesis of adiponitrile in a biphasic system IL/organic solvent is possible.[5,6,15,16] Adiponitrile is a nylon-6,6 intermediate that is industrially prepared by hydrocyanation of butadiene. The process is usually catalyzed by homogeneous Ni(0)-phosphite catalysts and in a 3-step process. First of all, addition of HCN to butadiene results in a mixture of branched and linear pentenenitriles. Secondly, the branched molecules are isomerized into the linear analogues, and finally, a second hydrocyanation results in the desired product.[5]

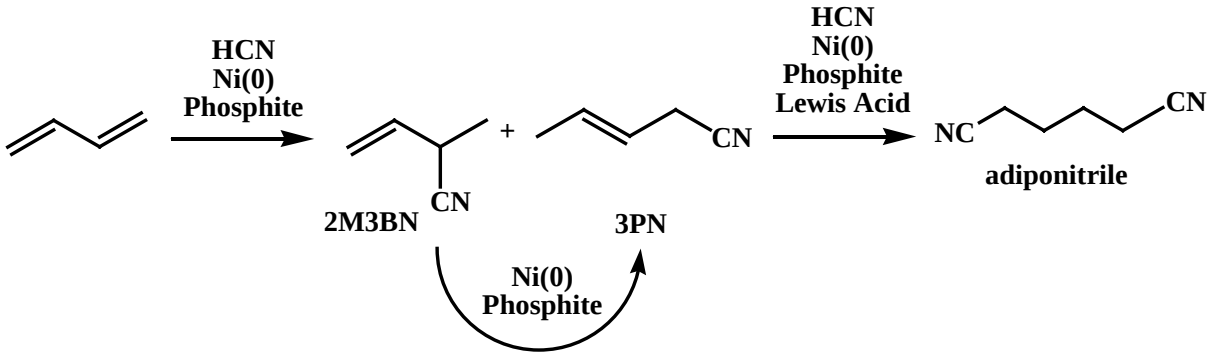

In particular, the catalytic isomerization of 2-methyl-3-butenenitrile (2M3BN) into 3-pentenenitrile (3PN), step 2 of the adiponitrile synthesis, has been more carefully studied under biphasic conditions in an IL/organic solvent system using bis(1,5-cyclooctadiene)nickel(0) ($Ni(COD)_2$). IL based on 1-butyl-2,3-dimethylimidazolium cation ($BMMIM^+A^-$ with A^- equal to Cl^-, $SnCl_3^-$, $ZnCl_3^-$, $Zn_3Cl_7^-$, $AlCl_4^-$, BF_4^-, PF_6^-, OTf^-, NTf_2^-) and the phosphine ligands : triphenylphosphine (TPP), and (*m*- sulfophenyl)-diphenyl-phosphine sodium salt ($TPPMS^-Na^+$) have been used.[5]

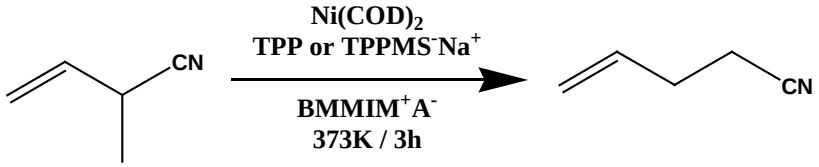

(1)

In contrast to the results obtained with TPP, the observed conversion with $TPPMS^-Na^+$ was strongly dependent on the nature of the anion A^- of the IL.[5] Using 1-butyl-2,3-dimethylimidazolium bis(trifluoromethanesulfonyl)imide ($BMMIM^+NTf_2^-$) as IL in the presence of $Ni(COD)_2$ and $TPPMS^-Na^+$, 96% conversion of 2M3BN and 93% selectivity to 3PN are obtained for reaction (1). Partition experiments proved that the catalyst was immobilized in the ionic phase. Turnover number (TON) (1020) and turnover frequency (TOF) ($103h^{-1}$) of the catalyst were measured. However, the other anion based IL afford poor conversion and selectivity into 3PN. While for the IL based on PF_6^- anion higher conversion (>90%) and selectivity (>90%) are observed.[5] Moreover, during the recycling of the catalyst, the deactivation of catalyst is higher for the IL based on PF_6^- (conversion ≅ 10% after two recycling of catalytic system) than for the IL based on NTf_2^- anion (conversion ≅ 50% after two recycling of catalytic system). Furthermore during subsequent experiments using $TPPMS^-BMMIM^+$ as ligand, the selectivity to 3PN was lower than 20%.

The question arises then of the possibility of an exchange between the sodium cation Na^+ of $TPPMS^-Na^+$ and the imidazolium ones $BMMIM^+$ of the IL, reaction (2). This exchange

would induce a change of the nature of the ligand $TPPMS^-Na^+$ into $TPPMS^-BMMIM^+$ thereby altering the nature of the catalyst and the catalytic activity :

$$TPPMS^-Na^+ + BMMIM^+A^- \rightarrow TPPMS^-BMMIM^+ + Na^+A^- \quad (2)$$

The main question then is the parameter which governs this cation exchange : Is-it due to the fact that sodium cations in IL are present under the form of ion pair or dissociated pairs or is-it another factor? Is-it due to specific interaction with IL derivatives ?

In order to solve this problem and understand which factors are involved in the difference of activity between $TPPMS^-Na^+$ and $TPPMS^-BMMIM^+$ catalytic based system, several NMR experiments have been performed.

Eventually to validate our hypothesis, we have studied the consequences of this exchange reaction (2) in the catalytic hydrogenation of 1,3-cyclohexadiene in the presence of $[Rh(COD)L_2]^+NTf_2^-$ (L = TPP, $TPPMS^-Na^+$ or $TPPMS^-BMMIM^+$).

RESULTS

1 Behavior of sodium salt in IL

In order to prove that the reaction (2) occurs, (*m*- sulfophenyl)-diphenyl-phosphine sodium salt ($TPPMS^-Na^+$) dissolved at 298K and 373K in a range of IL (C^+A^- with $A^- = Cl^-$, Br^-, $ZnCl_3^-$, $Zn_3Cl_7^-$, BF_4^-, PF_6^-, OTf^-, NTf_2^-) have been studied by solid state ^{23}Na NMR.

The ^{23}Na chemical shifts of $TPPMS^-Na^+$ but also of potentially formed sodium salt are reported in table 1.

N°	neat sodium salt	δ^{23}_{Na} ±2 ppm
1	anhydrous $TPPMS^-Na^+$	-17
2	hydrated $TPPMS^-Na^+$	-20
3	Na^+Cl^-	0
4	Na^+Br^-	-2
5	$Na^+PF_6^-$	-27
6	$Na^+BF_4^-$	-27
7	Na^+OTf^-	-13
8	$Na^+NTf_2^-$	-21

Table 1. ^{23}Na chemical shifts of reference sodium. Note that $Na^+NTf_2^-$ has been prepared by reaction of sodium hydroxide with bis(trifluoromethanesulfonyl)imide acid : $Na^+OH^- + HNTf_2 \rightarrow Na^+NTf_2^- + H_2O$

Neat anhydrous $TPPMS^-Na^+$ exhibits a chemical shift $\delta_{Na} = -17 \pm 2$ppm and the hydrated form δ_{Na} = -20± 2ppm. Note that even if the ^{23}Na line widths are relatively large due to the quadruple interaction, however each signals can be distinguished easily from one another due to their great different chemical shifts.[17]

1.1 Reaction of $TPPMS^-Na^+$ with various IL

Reaction in anhydrous conditions at 298K

The $TPPMS^-Na^+$ was mixed in various IL and the ^{23}Na chemical shifts of the resulting mixture (liquid solution, suspension or solid) obtained after reaction of $TPPMS^-Na^+$ with IL at 298K for 3h are gathered in table 2.

N°	nature of IL added to TPPMSNa	resulting δ^{23}Na ±2 ppm	Exch. %
9	$EMIM^+OTf^-$	-14	partial
		-10	
10	$EMIM^+BF_4^-$	-14	0
11	$EMIM^+NTf_2^-$	-16	0
12	$BMIM^+OTf^-$	-13	100
13	$BMIM^+BF_4^-$	-26	partial
		-17	
14	$BMIM^+NTf_2^-$	-14	0

Table 2. ^{23}Na chemical shift of $TPPMS^-Na^+$ in different IL in a molar ratio 1 : 1 for 3 h.at 298K

Whatever cation of IL is, the only observed sodium resonance in case of NTf_2^- anion corresponds to $TPPMS^-Na^+$ which indicates that no exchange occurs in these type of IL. As the chemical shift of Na^+OTf^- appeared in OTf^- based IL mixtures, there is total exchange in the case of $BMIM^+OTf^-$ but partial for $EMIM^+OTf^-$. In the case of BF_4^-, this exchange is

partial with $BMMIM^+$ (resonance of $Na^+BF_4^-$ and $TPPMS^-Na^+$ observed simultaneously) and do not occur in the case of $EMIM^+$ cation (only the resonance corresponding to $TPPMS^-Na^+$). These differences of reactivity in both latter case could be explained to a stronger cation-anion hydrogen bond between $EMIM^+$ and A^-. Indeed IR and Raman spectroscopies have been shown that the ion pair $EMIM^+BF_4^-$ is strong and can not be cleaved by adding CH_2Cl_2.[18]

Reaction in anhydrous conditions at 373 K

The reaction of $TPPMS^-Na^+$ with IL were performed in the experimental conditions of the catalytic reaction of isomerization (3h, 373 K). In table 3 are given the ^{23}Na chemical shifts of the residual solid at room temperature obtained after reaction of $TPPMS^-Na^+$ with IL, at 373 K for 3h and the amount of 2M3BN converted into 3PN from previous catalytic results of reaction (1) in identical systems.

N°	nature of IL added to TPPMSNa	resulitng $\delta^{23}Na$ ±2 ppm	Exch. %	Conversion in 3PN (%) [a]
15	$BMMIM^+Cl^-$	0	100	0
16	$BMMIM^+ZnCl_3^-$	0	100	17 [b]
17	$BMMIM^+Zn_3Cl_7^-$	-13	0	47
18	$BMIM^+OTf^-$	-13	100	27
19	$BMMIM^+BF_4^-$	-17	0	27
20	$BMIM^+BF_4^-$	-17	0	22
21	$BMMIM^+PF_6^-$	-15 -24	37	93
22	$BMMIM^+NTf_2^-$	-17	0	96
23	$BMIM^+NTf_2^-$	-16	0	88

Table 3. ^{23}Na chemical shifts of residual solid after reaction of $TPPMS^-Na^+$ in IL, in a molar ratio 1 : 1, at 373 K for 3 h.
a Conditions: $Ni(COD)_2$ (0.036 mmol) + $TPPMS^-Na^+$ (0.18 mmol) + 2M3BN (4.94 mmol) + IL (2.0 g) + heptane (1.2 ml) were stirred for 3 h at 373 K
b Conditions: $Ni(COD)_2$ (0.036 mmol) + $TPPMS^-Na^+$ (0.18 mmol) + 2M3BN (4.94 mmol) + IL (2.0 g) were stirred for 3 h at at 373 K

After reaction with $BMMIM^+Cl^-$, N° 15, and $BMMIM^+ZnCl_3^-$, N° 16, the spectra show only one resonance at $\delta^{23}Na = 0 \pm 2$ ppm, corresponding to the resonance of Na^+Cl^- indicating that $TPPMS^-Na^+$ has been totally converted into $TPPMS^-BMMIM^+$ in these IL. At the opposite, in the case of $BMMIM^+NTf_2^-$, N° 22, as with $BMMIM^+Zn_3Cl_7^-$, N° 17, the resonance of $TPPMS^-Na^+$ is the only one which is observed after 3h, consequently no exchange occurs with these two IL.

With $BMMIM^+PF_6^-$, N° 21, the spectrum shows two peaks at $\delta^{23}Na$ = -15 ± 2 and -24 ± 2 ppm in a 62 : 37 ratio (determined by deconvolution of the spectra, figure 2). The former is due to the resonance of sodium in $TPPMS^-Na^+$ (figure 1c) and the latter to that of the Na atom in $Na^+PF_6^-$. With $BMMIM^+PF_6^-$, the exchange reaction (2) is partial (37 % at 373 K) and temperature dependent (58 % at 393 K), (figure 1b).

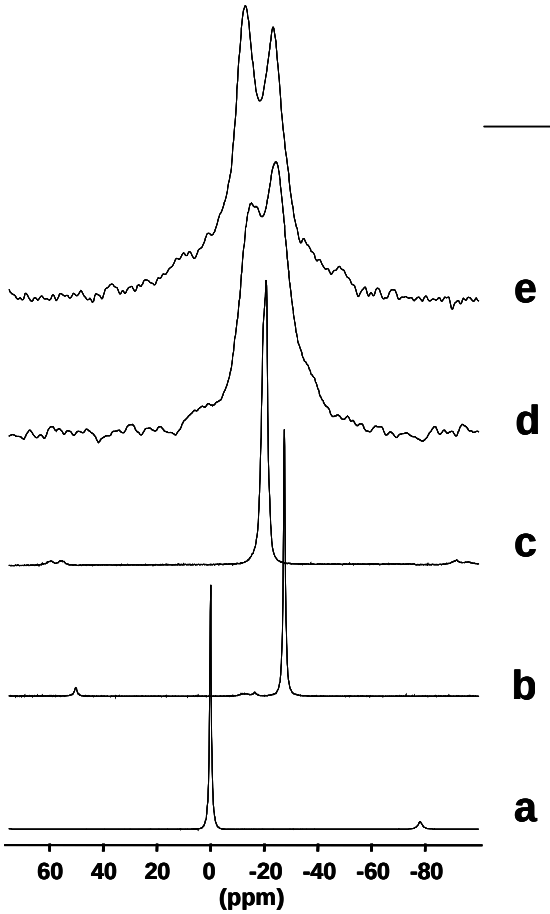

Figure 1. MAS ^{23}Na CP NMR spectra of (a) Na^+Cl^-; (b) $Na^+PF_6^-$; (c) $TPPMS^-Na^+$; (d) $BMMIM^+PF_6^-$ + $TPPMS^-Na^+$ at 393°K ; (e) $BMMIM^+PF_6^-$ + $TPPMS^-Na^+$ at 373°K

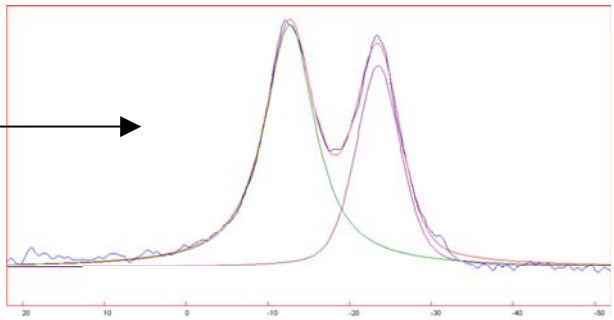

Figure 2. Deconvolution of spectrum (e) $BMMIM^+PF_6^-$ + $TPPMS^-Na^+$, 3h at 373°K

Influence of the temperature

In order to study the role of the temperature, the exchange reaction between $BMMIM^+PF_6^-$ and $TPPMS^-Na^+$ has been carried out at 393°K. It appears that the exchange is partial (58%) but superior to that at 373°K. Consequently, this phenomena is temperature dependent : the higher temperature is, the more important is the exchange.

Reaction in presence of water

Exchange reactions between the Na^+ cation of $TPPMS^-Na^+$ and either 1-propyl-3-methylimidaziolium chloride ($PMIM^+Cl^-$) or ammonium and alkaline cation has largely been reported especially in water or protic solvent.[13,19,20] Even if the structure of $TPPMS^-Na^+$ has not been reported to our knowledge, in the case of (m-sulfophenyl)-diphenylphosphine benzyltriethyl ammonium salt, X-ray structure has evidenced hydrogen bond between $TPPMS^-$ anion and H_2O molecules.[20] Consequently the ions are dissociated in this media $\{[TPPMS^-]_{H2O}$ // $[NEt_3CH_2Ph]^+\}_{H2O}$. As the synthesis and purification procedure of $TPPMS^-Na^+$ imply several treatments in water, the presence of coordinated water can not be excluded even after drying treatment (17 h at 45°C, 10^{-6} mm Hg).[10,12] Due to the high relative permittivity of water (ε_T = 78.4) in $TPPMS^-Na^+$, the ions could be supposed to be dissociated $(TPPMS^-$ // $Na^+)_{H2O}$.[21] Moreover, the presence of water is known to have strong influence in IL on the dissociation as well as on sodium salt[22] that chloride transition-metal bond.[23]

To demonstrate that the exchange reaction (2) is or not related to the presence of the residual water molecules, two series of experiments have been performed (table 4).

N°	Exp.	δ^{23}_{Na} ±2 ppm	Exch. %
24	$BMMIM^+PF_6^-$ + $TPPMS^-Na^+$ +H_2O	0	0
		-17	
25	$BMMIM^+NTf_2^-$ + $TPPMS^-Na^+$ + H_2O	-14	0

Table 4. ^{23}Na NMR chemical shifts of residual solid after reaction of $TPPMS^-Na^+$ in IL, in a molar ratio 1:1, at 373 K for 3h in presence of traces of water.

Firstly, the reaction (2) was performed in presence of water, with $BMMIM^+PF_6^-$ and $BMMIM^+NTf_2^-$. With $BMMIM^+PF_6^-$ instead of observing in the ^{23}Na spectrum, two peaks at –15 ± 2 and –24 ± 2 ppm in a 62:37 ratio as in experiment N° 21, the spectrum exhibits besides the resonance of $TPPMS^-Na^+$, a resonance at 0 ± 2 ppm which is attributed to Na^+F^-. Indeed, $BMMIM^+PF_6^-$ is easily hydrolyzed with concomitant formation of HF, this latter can react with $TPPMS^-Na^+$ and by substitution of Na^+ by H^+ leads to Na^+F^-.[3,24] At the opposite, with $BMMIM^+NTf_2^-$, even in the presence of water (up to 10% in weight), no exchange is observed, as in absence of water. These two series of experiments evidently prove that the water has no effect on the exchange reaction (2).

To confirm these results, the reactivity of anhydrous sodium acetate (AcO^-Na^+) with IL has been studied. In table 5 are given the ^{23}Na chemical shifts for neat sodium acetate and for the sodium salts after heating at 373 K for 3h in IL.

N°	Exp.	δ^{23}_{Na} ±2 ppm	Exch. %
26	AcO^-Na^+	-11	X
27	$BMMIM^+Cl^- + AcO^-Na^+$	0	≈ 30
		-11	
28	$BMMIM^+PF_6^- + AcO^-Na^+$	-11	0
29	$BMMIM^+NTf_2^- + AcO^-Na^+$	-11	0

Table 5. ^{23}Na NMR chemical shifts in solid-state AcO^-Na^+ after heating at 373 K for 3h, in IL

The chemical shift of anhydrous AcO^-Na^+ is $\delta^{23}Na$ = -11± 2 ppm. After the reaction with $BMMIM^+PF_6^-$ and $BMMIM^+NTf_2^-$, this resonance is the only one observed in the solid state ^{23}Na NMR spectrum. No resonance at $\delta^{23}Na$= -27± 2 and –21± 2ppm corresponding to $Na^+PF_6^-$ and $Na^+NTf_2^-$ respectively are observed. At the opposite in $BMMIM^+Cl^-$, the ^{23}Na NMR spectrum exhibits besides the peak of anhydrous AcO^-Na^+ at -11± 2 ppm, another resonance at 0 ± 2 ppm, corresponding to the resonance of Na^+Cl^-. These results prove that in the case of anhydrous AcO^-Na^+, there is a cation exchange reaction with $BMMIM^+Cl^-$.

$$BMMIM^+Cl^- + AcO^-Na^+ \rightarrow BMMIM^+AcO^- + Na^+Cl^- \qquad (3)$$

Consequently, the ionic exchange between IL and sodium acetate could also occur in IL.

These two series of experiments proved that water has no effect on the reactions (2) and (3) but that the exchange reaction is strongly dependent on the nature of the anion of IL.

The solvation of Na^+ by hard anions, such as Cl^-, leads to the dissociation of the ion pair. Reaction (2) and (3) can be simply predicted by the Pearson's principle of hard and soft acids and bases (HSAB Theory).

But is it also dependent on the nature of the cations ?

1.2 influence of the nature of the cation on exchange reaction

Several kinds of cations (C^+) such imidazolium ones with 1-ethyl-3-methylimidazolium ($EMIM^+$), 1-butyl-3-methylimidazolium ($BMIM^+$) or 1-butyl-2,3-dimethylimidazolium ($BMMIM^+$) but also quaternary ammonium salt like tetrabutylammonium (Bu_4N^+) or N-butyl-

N-methylpyrrolidinium ($bmpy^+$) and phosphoniums based IL such as tetrabutylphosphoniums (Bu_4P^+) have been studied.

The reaction of $TPPMS^-Na^+$ with those IL have been performed at 373K during 3h. The resulting ^{23}Na chemical shifts have been reported in table 6.

N°	nature of IL added to $TPPMS^-Na^+$	resulitng $\delta^{23}Na$ ±2 ppm	Exch. %
30	$bmpy^+Cl^-$	0	100
31	$Bu_4N^+Cl^-$	0	100
32	$Bu_4P^+Cl^-$	0	100
33	$BMMIM^+Br^-$	-1	100
34	$Bu_4N^+Br^-$	-2	100
35	$Bu_4P^+Br^-$	-2 -13	partial
36	$Bu_4N^+OTf^-$	-13	100
37	$EMIM^+BF_4^-$	-15	0
38	$Bu_4P^+BF_4^-$	-13 -28	partial
39	$EMIM^+PF_6^-$	-13	0
40	$Bu_4N^+NTf_2^-$	-15,8	0

Table 6. ^{23}Na NMR chemical shifts in solid-state $TPPMS^-Na^+$ after heating at 373 K for 3h in IL

After the reaction of $TPPMS^-Na^+$ with $bmpy^+Cl^-$, $Bu_4N^+Cl^-$ and $Bu_4P^+Cl^-$, the ^{23}Na NMR spectra show only one resonance at 0 ± 2 ppm, corresponding to the resonance of Na^+Cl^-.

In case of $BMMIM^+Br^-$ and $Bu_4N^+Br^-$, the ^{23}Na chemical shift is analogous to one of Na^+Br^-. In the case of $Bu_4P^+Br^-$, the exchange is partial.

These observations can only be explain by **ionic exchange** between sodium salts and IL (C^+A^-) and indicate that $TPPMS^-Na^+$ has been totally converted into $TPPMS^-C^+$ in these two IL according to reaction 2 :

$$TPPMS^-Na^+ + C^+A^- \rightarrow TPPMS^-C^+ + Na^+A^- \text{ with } A^- = Cl^- \text{ or } Br^- \qquad (4)$$

$TPPMS^-Na^+$ dissolved in $Bu_4N^+OTf^-$ also leads to complete exchange reaction.

After the reaction of $TPPMS^-Na^+$ with $EMIM^+BF_4^-$, no exchange reaction is detected but it was partial in $Bu_4P^+BF_4^-$.

The exchange is total between $TPPMS^-Na^+$ with $EMIM^+PF_6^-$. No exchange happens in $Bu_4N^+NTf_2^-$.

Consequently it appears that the nature of the cation affected the importance of the exchange but it is the nature of the anion which determines if this reaction occurs or not.

1.3 Conclusion on ionic exchange in LI

It clearly appears that there is an ionic exchange at 373K between both studied sodium salt : $TPPMS^-Na^+$ and AcO^-Na^+ with several IL :

- **total exchange** with IL when A^- = Cl^-, Br^-, $ZnCl_3^-$ and OTf^- whatever cation C^+ is
- **no exchange** with IL when $A^- = NTf_2^-$ and $Zn_3Cl_7^-$ whatever cation C^+ is
- **partial to total exchange** with IL when A^- = PF_6^- and BF_4^- whatever cation C^+ is

These exchange reactions (2) or (3) can obviously be predicted by the Pearson's principle (Hard and Soft Acid Base theory) but even if this exchange is largely governed by the nature of the anion, it appears that the strength of hydrogen bond between cation and anion of IL and of the ionic pair also intervene in the exchange reaction : the stronger the ion pair C+A- is, the less important the exchange reaction is.

$$Bu_4P^+A^- > EMIM^+A^- > Bu_4N^+A^- \approx BMMIM^+A^-$$

This exchange would induce a change of the nature of the ligand $TPPMS^-Na^+$ into $TPPMS^-C^+$, thereby altering the nature of the catalyst and the catalytic activity : the conversion decreases when $TPPMS^-Na^+$ is transformed into $TPPMS^-BMMIM^+$.

1.4 Is there a relationship between the results of exchange reaction(2) and reaction (1)?

The data of the above experiments have been compared to previous catalytic results of reaction (1) in identical systems i.e. to the conversion into 3PN and recycling experiments, Table 7.[5]

N°	nature of IL	HSAB prediction of exchange	Conversion in 3PN (%) [a]
15	$BMMIM^+Cl^-$	Y	0
41	$BMMIM^+AlCl_4^-$	Y	2 [b]
42	$BMIM^+AlCl_4^-$	Y	17 [b]
43	$BMMIM^+SnCl_3^-$	Y	15 [b]
44	$BMMIM^+Cl^- / SnCl_2$ 1/2	Y	17 [b]
16	$BMMIM^+ZnCl_3^-$	Y	17 [b]
21	$BMMIM^+Cl^- /ZnCl_2$ 1/2	partial	34 [b]
17	$BMMIM^+Zn_3Cl_7^-$	N	47
45	$BMMIM^+OTf^-$	Y	25
18	$BMIM^+OTf^-$	Y	27
19	$BMMIM^+BF_4^-$	N	27
20	$BMIM^+BF_4^-$	N	22
21	$BMMIM^+PF_6^-$	partial	93 (72, 13)
28	$BMIM^+PF_6^-$	partial	42
22	$BMMIM^+NTf_2^-$	N	96 (79, 35)
23	$BMIM^+NTf_2^-$	N	88

Table 7. Conversion of 2M3BN into 3PN in various IL (conversion during the 2nd and 3rd runs)
Conditions: **a** $Ni(COD)_2$ (0.036 mmol) + TPPMSNa (0.18 mmol) + 2M3BN (4.94 mmol) + IL (2.0 g) + heptane (1.2 ml) were stirred for 3 h at 373K. **b** $Ni(COD)_2$ (0.036 mmol) + TPPMSNa (0.18 mmol) + 2M3BN (4.94 mmol) + IL (2.0 g) were stirred for 3 h at 373K

When a total or partial exchange reaction is observed, no or very low conversion is observed.

In $BMMIM^+Cl^-$, $TPPMS^-Na^+$ is converted into $TPPMS^-BMMIM^+$ and there is no conversion of 2M3BN into 3PN.

With $BMMIM^+ZnCl_3^-$, ^{35}Cl NMR spectra, at 337-383 K, prove that there is dissociation of $ZnCl_3^-$ anion into $BMMIM^{\cdots}Cl^{\cdots}ZnCl_2$ generating Cl^- anions in the media.[25] Concomitantly, $TPPMS^-Na^+$ is converted into $TPPMS^-BMMIM^+$ and there is a very low conversion into 3PN (17 %). While in the case of the polynuclear anion $Zn_3Cl_7^-$ containing excess of $ZnCl_2$, the generated Cl^- anions are neutralized avoiding the exchange reaction (2), then the conversion into 3PN is up to 45% in $BMMIM^+Zn_3Cl_7^-$.

The best results in conversion of 2M3BN (≅90%) are obtained in $BMMIM^+PF_6^-$ and in $BMMIM^+NTf_2^-$. In the former, a partial exchange reaction is evidenced that affords a rapide deactivation of catalyst : after three recycling, the conversion is lower than 15%. In the IL

based on NTf_2^- anion, in which no exchange (2) is observed the catalyst is still active after the 3^d run (conversion > 30%).

Therefore it might seems that there is a relationship between the catalytic activity in the rearrangement reaction of 2M3BN into 3PN.

To conclude, we have provided that when sodium salts are dissolved in IL, ionic exchange reaction is possible and is mainly governed by the HSAB theory. When this exchange occur, the nature of the catalytic system is altered and in case of $TPPMS^-Na^+$, it inhibits catalytic isomerization of 2M3BN into 3PN. Even if the parameters which governs this exchange has been fully understand, to our knowledge, the explanation of this decrease of activity is still unknown and needs further investigation.

2 How explain the difference of activity ?

In order to attempt to answer to this question, the synthesis and characterization of Ni and Rh complexes have been realized. These experiments enable the preparation the NiL_4 (L= phosphine ligand) catalysts involved in isomerization reaction and investigates their behaviour in organic and IL media using NMR techniques.

Firstly, the reaction of ligands : L = TPP, $TPPMS^-Na^+$ and $TPPMS^-BMMIM^+$ with $Ni(COD)_2$ (L / Ni = 5) in THF-d_8 / $BMMIM^+NTf_2^-$ mixture (0.5:1) in the presence of 2M3BN (2M3BN / Ni = 12) was monitored by ^{31}P NMR spectroscopy.

$$Ni\ (COD)_2 + 4L \rightarrow NiL_4 + 2COD \quad (5)$$

In $Ni(COD)_2$ / TPP, the ^{31}P NMR spectrum at 295°K exhibits a large peak at δ = 23.1 and –6.0 ppm, which splits at 258°K into several peaks around 25 ppm attributed to $Ni(TPP)_3$ and $Ni(TPP)_4$. These complexes are respectively associated to peaks at δ 26.33 and 28.60 ppm at –183°K in toluene,[26] and a peak at -5.6 ppm for free TPP. Thus, there is a fast exchange between TPP and the nickel complexes.

The same behaviour is observed with $Ni(COD)_2$ / $TPPMS^-Na^+$, the ^{31}P NMR spectrum at 295°K exhibits broad peaks at δ -4.0, 23.8 and 26.5 ppm attributed to free ligand $TPPMS^-Na^+$, NiL_3 and NiL_4 complex. Fast exchange (6) also occurred in the case of $TPPMS^-Na^+$.

$$Ni(TPPMS^-Na^+)_4 \rightleftharpoons Ni(TPPMS^-Na^+)_3 + TPPMS^-Na^+ \quad (6)$$

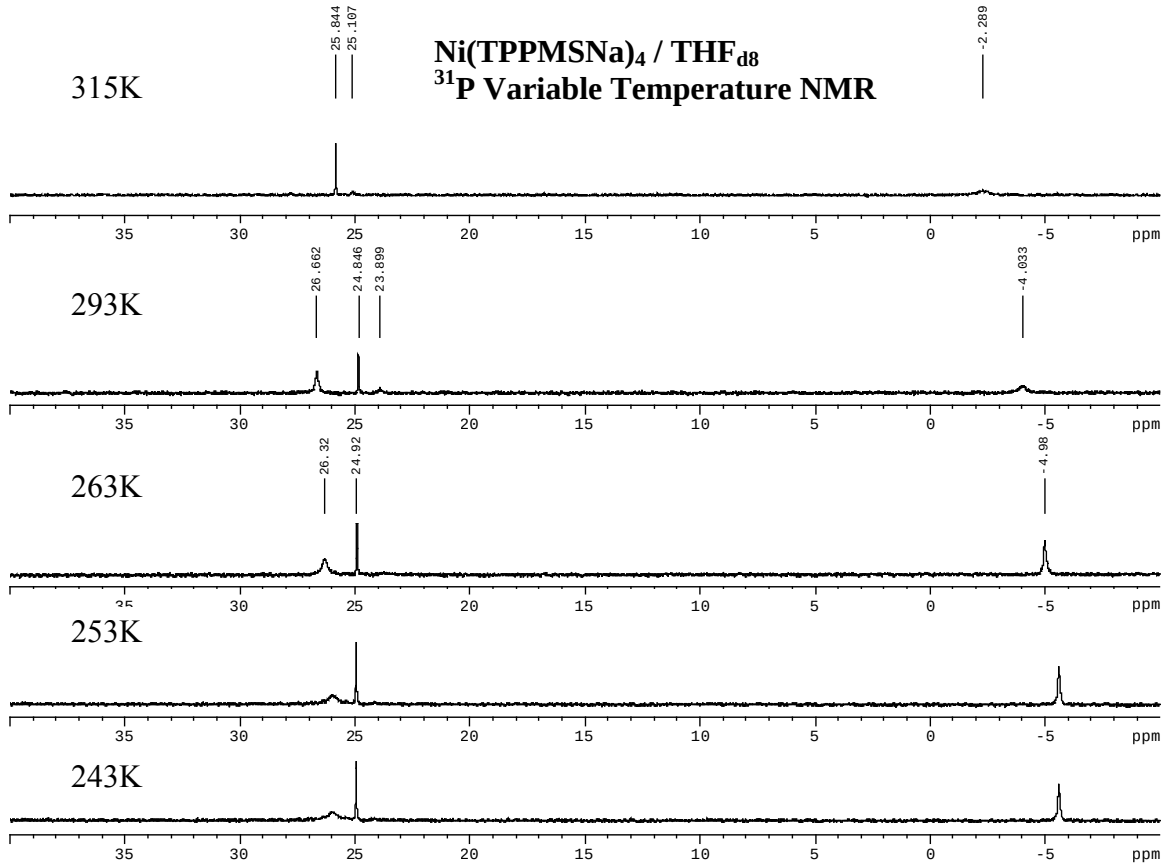

Figure 3. Variable Temperature ^{31}P NMR for Ni $(TPPMSNa)_4$

With $TPPMS^-BMMIM^+$, the ^{31}P NMR spectrum at 295°K exhibits two thin peaks at δ -4.1 and 25.0 ppm attributed to free ligand $TPPMS^-BMMIM^+$ and to NiL_3 or NiL_4 complex. No exchange occurred in the case of $TPPMS^-BMMIM^+$.

In order to investigate the difference between $TPPMS^-Na^+$ and $TPPMS^-BMMIM^+$ phosphine, both ligands dissolved in $BMIM^+NTf_2^-$ have been studied in DOSY NMR (Diffusion Order Spectroscopy). It appears that the mobility of $TPPMS^-BMMIM^+$ (diffusion coefficient : $D=6.91x10^{-12}m^2.s^{-1}$) is very low compared to that of $TPPMS^-Na^+$ ($D=10x10^{-12}m^2.s^{-1}$).

To conclude $TPPMS^-BMMIM^+$ due to its lower mobility is statistically more present in Ni coordination sphere. ^{31}P NMR study shows that the exchange reaction (6), first step of isomerization reaction, is slower and consequently the conversion of 2M3BN is slower.[27] This

could explain the lower activity of the catalyst $Ni(COD)_2$ / $TPPMS^-BMMIM^+$ compare to the catalyst $Ni(COD)_2$ / $TPPMS^-Na^+$.

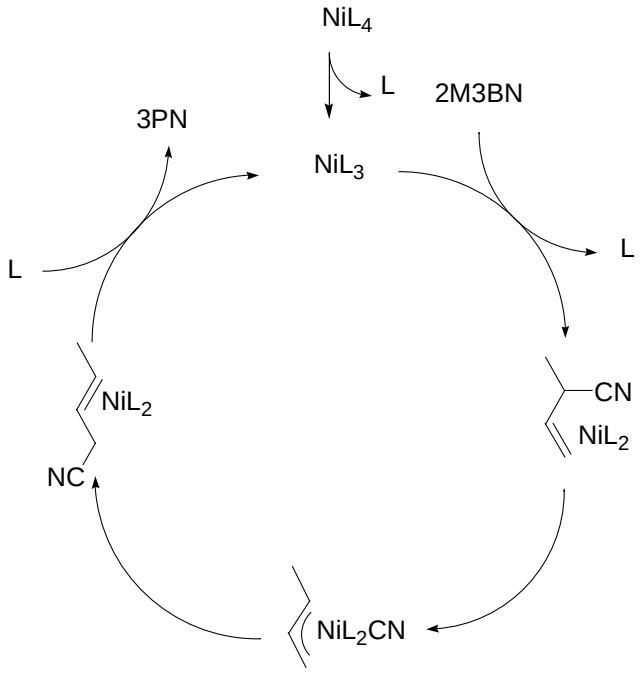

3 Influence of the nature of the IL on catalytic hydrogenations

We have provided that there is an exchange reaction between ionic ligand and IL in some cases and that it perturbed considerably the reactivity of isomerization catalyst system. But if the exchange reaction seems to take place when ionic species are used, we wondered if this exchange is always unfavorable for catalytic activity.

It is possible to hydrogenate selectively 1,3-cyclohexadiene into cyclohexene with good conversion and selectivity using Osborn's type complex : $[Rh(NBD)(PPh_3)_2]^+PF_6^-$ (NBD=norbornadiene) in IL media such $BMIMSbF_6$ or $BMIMPF_6$.[9]

The hydrogenation of 1,3-cyclohexadiene has been performed using three different phosphine ligand (L=TPP, $TPPMS^-Na^+$ and $TPPMS^-BMMIM^+$) based catalytic system but to avoid any anion exchange between IL and the catalyst, NTf_2 based catalyst has been developed : $[Rh(COD)L_2]^+NTf_2^-$.

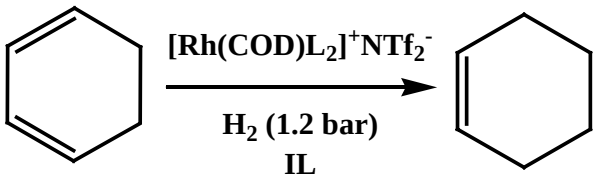

L = TPP, $TPPMS^-Na^+$, $TPPMS^-BMMIM^+$

The reactions have been performed in two different IL : 1-butyl-3-methylimidazolium bis(trifluoromethanesulfonyl)imide $BMIM^+NTf_2^-$ and 1-butyl-2,3-dimethylimidazolium bis(trifluoromethanesulfonyl)imide $BMMIM^+NTf_2^-$.

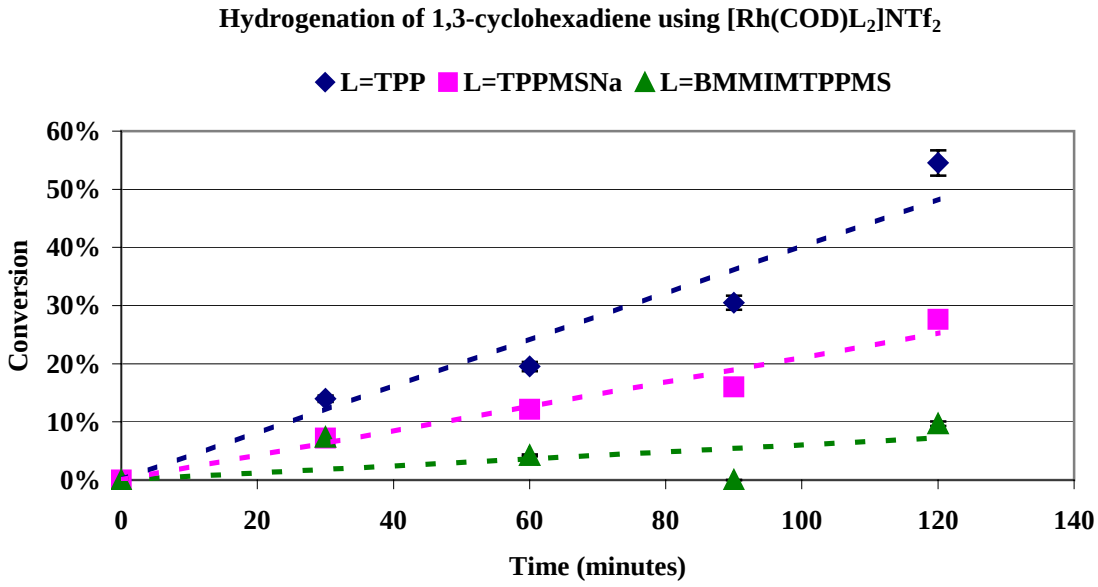

Figure 4. Conversion curves for the 3 different catalysts in $BMIM^+NTf_2^-$ with R=moles of 1,3-cyclohexadiene for one mole of IL=0.5 and r = n($[Rh(COD)L_2]^+NTf_2^-$)/n(1,3-cyclohexadiene)=1000

As it observed in the case of isomerization reaction, it appears that $TPPMS^-BMMIM^+$ based catalytic system is less active than with $TPPMS^-Na^+$ while $[Rh(COD)(TPP)_2]^+NTf_2^-$) is more active.

The order of reactivity of the ligands can be expressed as below:

$$TPP >> TPPMS^-Na^+ > TPPMS^-BMMIM^+$$

In this case, the dissociation of ligand is not implied. The ROESY experiment on $TPPMS^-Na^+$ and $TPPMS^-BMMIM^+$ in $BMIMNTf_2$ do not support stronger interaction between phenyl group of phosphine and imidazolium rings. To explain this difference, we proposed that the accessibility of the catalyst is reduced probably due to the intermolecular imidazolium interactions which creates around the catalyst a second shell of solvation in the case of $TPPMS^-BMMIM^+$.[28,29]

Conclusion

The goal of this chapter was to understand the interactions between ionic ligand and IL. It has been demonstrated that IL is not innocent and the speciation of ligand depends on the nature of IL.

In the catalytic isomerization of 2M3BN into 3PN, the influence of the nature of IL on the catalytic activity has been shown.

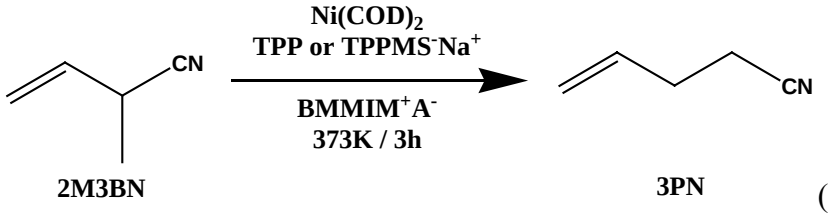

(1)

The result has been explained by the presence or not of an exchange reaction (2). In the case of $TPPMS^-Na^+$ ligand and several other inorganic salts (C^+A^-), the exchange reaction was governed by HSAB theory and has been demonstrated by ^{23}Na NMR.

$$TPPMS^-Na^+ + BMMIM^+A^- \rightarrow TPPMS^-BMMIM^+ + Na^+A^- \quad (2)$$

NMR DOSY experiments explain that the reactivity in (1) decreases in presence of $TPPMS^-BMMIM^+$ due to a slower diffusion in IL which reduces the dissociation of the catalyst : $NiL_4 \leftrightarrow NiL_3 + L$ compared to $TPPMS^-Na^+$ and TPP.

Consequently the activity in isomerization decreases in the range :

$$TPP > TPPMS^-Na^+ > TPPMS^-BMMIM^+$$

Moreover, the same tendency is observed in catalytic hydrogenation of 1,3-cyclohexadiene with $[Rh(COD)L_2]^+NTf_2^-$ (L=phosphine ligand). It could be related to a reduce accessibility of catalyst due to interaction between imidazolium ligand and imidazolium ring of IL.

Experimental part

1-methylimidazole (>99%), 1,2-dimethylimidazole (>98%) (Aldrich) were distilled prior to use. Triphenylphoshpine (Aldrich), (m-sulfophenyl)diphenylphosphine sodium salt (Strem), sodium acetate (Aldrich), $Ni(COD)_2$ (Strem) and $[Rh(COD)Cl]_2$ (>99%, Strem) were used as received. Bis(trifluoromethanesuflonyl)imide lithium salt and IL : BMIMOTf, $EMIMNTf_2$, $EMIMBF_4$ and $EMIMPF_6$ but also Bu_4NCl, Bu_4NBr, Bu_4NOTf, Bu_4NNTf_2, Bu_4PCl, Bu_4PBr and Bu_4PBF_4 (Solvionic company) were used as received.

Liquid state NMR

^{1}H, ^{13}C and ^{31}P NMR at liquid state data were collected at room temperature on a Bruker AC 300 MHz spectrometer with the resonance frequency at 300,130 MHz.

The solvents used (CD_2Cl_2, $CDCl_3$, C_6D_6, THF d_8) were purchased from SDS and used as received. Chemicals shifts are expressed in ppm (singlet = s, doublet = d, doublet of doublet = dd, and multiplet = m) and were measured relative to residual proton of the solvent to $CHDCl_2$ for ^{1}H, to CD_2Cl_2 for ^{13}C and to H_3PO_4 for ^{31}P.

Solid state ^{23}Na NMR

Solid state NMR spectra were recorded on a Bruker DSX-500 spectrometer equipped with a standard 4 mm double-bearing probe head and operating at 132.5 MHz for ^{23}Na. The spinning rate was typically 10 kHz and the delay between successive scans was sufficiently high to allow a complete relaxation of the sodium nuclei as shown by recording different spectra. The chemical shifts were given with respect to external references (NaCl at 0 ppm)

As ^{23}Na is a quadrupolar nuclei and as quantitative information were expected, we used a simple sequence for the acquisition of the spectra: the FID was acquired after a very short pulse (less than $\pi/10$) and a sufficient delay between successive scans was used. The determination of this delay, varying from one sample to another but always between 1 and 30 s was determined by recording the spectra with variable delays. When the spectrum remained unchanged, a sufficient delay was used.

Ionic liquids and $TPPMS^{-}BMMIM^{+}$ are synthesized as previously reported.[5,13,25]

1-butyl-3-methylimidazolium chloride [BMIMCl]

1-chlorobutane (106mL, 1.01mol) was added to 1-methylimidazole (50mL, 0.63mol) freshly distilled. The mixture was stirred for 48h at 65°C. The hot solution was then transferred to a dropping funnel and the lower phase was added dropwise under vigorous stirring to toluene (200mL). The white precipitate formed was filtered and then washed repeatedly with toluene (3*200mL) and dried overnight under vacuum, giving white powder (83.6g, 76%). ^{1}H-NMR (CD_2Cl_2) : δ (ppm) : 11.03 (s, 1H) ; 7.33 (d, 2H) ; 7.28 (d, 2H) ; 4.29 (t, 2H) ; 4.06 (s, 3H) ; 1.88 (qt, 2H) ; 1.38 (st, 2H) ; 0.97 (t, 3H) ; ^{13}C{^{1}H}-NMR (CD_2Cl_2) : δ (ppm) : 139.2 (CH) ; 123.5 (CH) ;122.0 (CH) ; 50.1 (NCH_2) ; 36.8 (NCH_3) ; 32.5 (CH_2) ; 19.8 (CH_2) ; 13.6 (CH_3)

1-butyl-2,3-dimethylimidazolium chloride [BMMIMCl]

The procedure previously described for BMIMCl was used. From 36g (0.37mol) of 1,2-dimethylimidazole and 63mL (0.60mol) of 1-chlorooctane, there were obtained 54.9g (78%) of BMMIMCl as an hygroscopic white solid. ^{1}H-NMR (CD_2Cl_2) : δ (ppm) : 7.80 (s, 1H) ; 7.49 (s, 1H) ; 4.17 (t, 2H) ; 3.98 (s, 3H) ; 2.73 (s, 3H) ; 1.79 (qt, 2H), 1.38 (st, 2H), 0.96 (t, 3H) ; ^{13}C{^{1}H}-NMR (CD_2Cl_2) : 144.0 (C) ; 123.6 (CH) ; 121.7 (CH) ; 48.9 (NCH_2) ; 36.1 (NCH_3) ; 32.3 (CH_2) ; 20.0 (CH_2) ; 13.7 (CH_3) ; 10.7 (CH_3)

1-butyl-1-methylpyrrolidinium chloride [bmpyCl]

1-chlorobutane (65mL, 0.62mol) was added to N-methylpyrrolidine (50mL, 0.48mol) freshly distilled in acetonitrile (60mL). The mixture was then stirred for 48h at 80°C. After cooling, the solvent was removed under vacuum. The solid formed was re-crystallized with a mixture acetonitrile/ethyl acetate, giving white crystals. (47.5g, 56%)

^{1}H-NMR (CD_2Cl_2) : δ (ppm) : 3.75 (m, 2H) ; 3.57 (m, 2H) ; 3.21 (s, 3H) ; 2.20 (s, 2H) ; 1.70 (qt, 2H) ; 1.37 (st, 2H) ; 0.94 (t, 3H) ; ^{13}C{^{1}H}-NMR (CD_2Cl_2) : δ (ppm) : 64.2 (CH_2) ; 63.8 (CH_2) ; 48.3 (CH_3) ; 25.9 (CH_2) ; 21.6 (CH_2) ; 19.8 (CH_2) ; 13.6 (CH_3)

1-butyl-3-methylimidazolium bis(trifluoromethylsulfonyl)imide [BMIMNTf$_2$]

A solution of lithium bis(trifluoromethylsuflonyl)imide [$LiNTf_2$] (50g, 0.17mol) in water (50mL) was added to a solution of BMIMCl (30.4g, 0,17mol) in water (100mL). The solution was stirred 2h at room temperature, dichloromethane (50mL) was added and the mixture transferred in a separating funnel. The lower phase was collected and washed repeatedly with water (8x100mL) until no traces of chloride salt was detected in the washing

water (test with sliver nitrate). The ionic liquid in dichloromethane was purified through a short alumina column and the solvent was removed under vacuum, giving colourless viscous liquid. ^{1}H-NMR (CD_2Cl_2) : δ (ppm) : 8.53 (s, 1H) ; 7.44 (s,1H) ; 7.36 (s, 1H) ; 4.13 (t, 2H) ; 3.86 (s, 3H) ; 1.81 (qt, 2H) ; 1.29 (st, 2H) ; 0.86 (t, 3H) ; ^{13}C{^{1}H}-NMR (CD_2Cl_2) : δ (ppm) : 136.2 (CH) ; 124.1 (CH) ; 122.4 (CH) ; 120.3 (CF_3) ; 50.4 (NCH_2) ; 36.7 (NCH_3) ; 32.3 (CH_2) ; 19.7 (CH_2) ; 13.4 (CH_3)

1-butyl-2,3-dimethylimidazolium bis(trifluoromethylsulfonyl)imide [BMMIMNTf$_2$]

The procedure previously described for BMIMNTf$_2$ was used. From 33g (0.17mol) of BMMIMCl and 50g (0.17mol) of LiNTf$_2$, there were obtained 66.7g (88 %) of BMMIMNTf$_2$ as a colourless viscous liquid. ^{1}H-NMR (CD_2Cl_2) : δ (ppm) : 7,30 (s, 1H) ; 7,23 (s, 1H) ; 4,03 (t, 2H) ; 3,72 (s, 3H) ; 2,53 (s, 3H) ; 1,73 (qt, 2H) ; 1,30 (st, 2H) ; 0,87 (t, 3H) ; ^{13}C{^{1}H}-NMR (CD_2Cl_2) : δ (ppm) : 144.2 (CCH_3) ; 122.9 (CH) ; 121.4 (CH) ; 120.5 (CF_3) ; 49.0 (NCH_2) ; 35.6 (NCH_3) ; 31.9 (CH_2) ; 19.9 (CH_2) ; 13.5 (CH_3) ; 9.8 (CH_3) Anal. Calcd for $C_{11}H_{17}F_6N_3O_4S_2$: C, 30,48 ; H, 3.95 ; N, 9,70 ; Cl, 0.00. Found : C, 30.60 ; H, 4,19 ; N, 9,83 ; Cl, 56ppm.

1-butyl-3-methylimidazolium hexafluorophosphate [BMIMPF$_6$]

A solution of sodium hexafluorophosphate (31.4g, 0,18mol) in acetone (75mL) was added to a solution of [BMIMCl] (32.6g, 0,18mol) in acetone (150mL). The solution was vigorously stirred during 72h at room temperature then filtered through celite. The filtrate was purified through little column of neutral alumina and the solvent removed under vacuum. The product was then washed 5 times with 75mL of water and dried 3h under vacuum at 50°C, giving a pale yellow liquid. (43,5g, 82%) ^{1}H-NMR (CD_2Cl_2) : δ (ppm) : 8.28 (s, 1H) ; 7.26 (d, 2H) ; 7.23 (d, 2H); 3.99 (t, 2H) ; 3.73 (s, 3H) ; 1.60 (qt, 2H) ; 1.13 (st, 2H) ; 0.68 (t, 3H) ; ^{13}C{^{1}H}-NMR (CD_2Cl_2) : δ (ppm) : 136.0 (C) ; 124.1 (CH) ; 122.7 (CH) ; 50.3 (NCH_2) ; 36.6 (NCH_3) ; 32.2 (NCH_2) ; 19.7 (CH_2) ; 13.5 (CH_2)

1-butyl-2,3-dimethylimidazolium hexafluorophosphate [BMMIMPF$_6$]

A solution of sodium hexafluorophosphate (31,4g, 0,18mol) in acetone (75mL) was added to a solution of [BMMIMCl] (32,6g, 0,18mol) in acetone (150mL). The solution was vigorously stirred during 72h at room temperature then filtered through celite. The filtrate was purified through little column of neutral alumina and the solvent removed under vacuum. The

product was then washed 5 times with 75mL of water and dried 3h under vacuum at 50°C, giving a pale yellow liquid. (43,5g, 82%) ^{1}H-NMR (CD_2Cl_2) : δ (ppm) : 7.21 (s, 1H) ; 7.18 (s, 1H) ; 4.06 (t, 2H) ; 3.79 (s, 3H) ; 2.59 (s, 3H) ; 1.74 (qt, 2H) ; 1.42 (st, 2H) ; 0.97 (t, 3H) ; ^{13}C{^{1}H}-NMR (CD_2Cl_2) : δ (ppm) : 144.1 (C) ; 122.8 (CH) ; 121.2 (CH) ; 48.9 (NCH_2); 35.5 (NCH_3) ; 31.8 (NCH_2) ; 19.8 (CH_2) ; 13.5 (CH_2) ; 9.6 (CH_3)

1-butyl-3-methylimidazolium tetrafluoroborate [BMIMBF$_4$]

A solution of sodium tetrafluoroborate (31,5g, 0.28mol) in acetone (100mL) was added to a solution of [BMIMCl] (50g, 0.28mol) in acetone (200mL). The solution was vigorously stirred during 72h at room temperature then filtered through celite. The filtrate was dissolved in water (100mL) and extract from the aqueous solution with dichloromethane 5x100mL. The product was purified through little column of neutral alumina and the solvent removed under vacuum giving a pale yellow liquid. (44.1g, 70%) ^{1}H-NMR (CD_2Cl_2) : δ (ppm) : 8.69 (s, 1H) ; 7.36 (d, 2H) ; 7.34 (d, 2H); 4.15 (t, 2H) ; 3.91 (s, 3H) ; 1.83 (qt, 2H) ; 1.32 (st, 2H) ; 0.93 (t, 3H) ; ^{13}C{^{1}H}-NMR (CD_2Cl_2) : δ (ppm) : 136.5 (C) ; 124.1 (CH) ; 122.7 (CH) ; 50.1 (NCH_2) ; 36.5 (NCH_3) ; 32.3 (NCH_2) ; 19.7 (CH_2) ; 13.5 (CH_2)

1-butyl-2,3-dimethylimidazolium tetrafluoroborate [BMMIMBF$_4$]

A solution of sodium tetrafluoroborate (31,4g, 0.26mol) in water (125mL) was added to a solution of [BMMIMCl] (32,6g, 0.26mol) in water (250mL). The solution was vigorously stirred during 48h at room temperature, dichloromethane (500mL) was added and the lower phase was collected. The ionic liquid was purified through a short alumina column and the solvent removed under vacuum. giving a pale yellow liquid. (49.7g, 80%) ; ^{1}H-NMR (CD_2Cl_2) : δ (ppm) : 7.24 (s, 1H) ; 7.21 (s, 1H) ; 3.93 (t, 2H) ; 3.60 (s, 3H) ; 2.42 (s, 3H) ; 1.54 (qt, 2H) ; 1.11 (st, 2H) ; 0.66 (t, 3H) ; ^{13}C{^{1}H}-NMR (CD_2Cl_2) : δ (ppm) : 144.2 (C) ; 122.8 (CH) ; 121.2 (CH) ; 48.6 (NCH_2); 35.3 (NCH_3) ; 31.9 (NCH_2) ; 19.7 (CH_2) ; 13.5 (CH_2) ; 9.5 (CH_3)

^{23}Na NMR samples

In a glovebox, sodium salt (0.14mmol) was mixed with IL (0.14mmol) and stirred overnight at 373 K (or 393 K). The obtained mixture is a liquid solution, a suspension or a solid. Then the samples were introduced in the zirconia rotor in a glovebox and tightly closed.

The samples heated at 373 K (or 393 K) have a higher line width than pure compounds. The line width, in these compounds (where the asymmetry around sodium is low and has no influence on the line shape), is mainly due to a distribution of chemical shifts arising from the fact that in the solid the neighbors are not always the same. Such a broadening can for example be observed for amorphous compounds compared to the same products in a crystalline form. The deconvolution of spectra was made by using the lowest number of peaks. A good fit was obtained with two peaks, the discrepancies between experimental and calculated spectra being of the same order of magnitude as the noise.

^{31}P NMR samples

In glovebox, in a Schlenk tube, a mixture of TPP [41.3 mg (0.113 mmol) and 22.95 mg of BMMIMCl (0.122 mmol- 1.1 equiv.) was prepared then the solid were stirred at 110 °C. Then the samples were introduced in the zirconia rotor in a glovebox and tightly closed

TPPMSBMMIM

BMMIMCl (1.14g, 6.04×10^{-3}mol) and TPPMSNa.$2H_2O$ (2.20g, 6.04×10^{-3}mol) in water (17ml) were stirred for 18 hours at room temperature. The product was extracted with dichloromethane (5×20ml) and the solvent removed *in vacuo*. The residue was washed with distilled pentane (30ml) and dried *in vacuo* for 48 hours. This gave TPPMSBMMIM (2.10g, 71%) as a white powder. ^{1}H NMR (300 MHz, CD_2Cl_2): δ = 7.59 (d, 1 H), 7.47 (d, 1 H), 7.22(m, 14 H), 4.01 (t, 3J = 6 Hz, 2 H), 3.77 (s, 3 H), 2.57 (s, 3H), 1.73 (qn, 3J = 7.5 Hz, 2 H), 1.34 (qn, 3J = 7.8 Hz, 2 H), 0.92(t, 3 H), ^{31}P NMR (CD_2Cl_2): δ = -9.72 ppm.

Ni(TPP)$_4$

Triphenylphosphine (1.00g, 3.81 mmol) and Ni(COD)$_2$ (0.262g, 0.953 mmol) in distilled THF (10ml) was stirred for 1 hour at room temperature producing a red solution. The solvent was removed *in vacuo*. The residual solid washed with pentane (10ml) and dried *in vacuo*. ^{31}P NMR (THF_{d8}): δ = 23.13 (complexed TPP), -6.03 (remnant TPP) ppm.

Ni(TPPMSNa)$_4$

TPPMSNa (0.50g, 1.37 mmol) and Ni(cod)$_2$ (0.095g, 0.343mmol) in THF (10ml) was stirred for an hour at room temperature. The solvent was removed from the resulting red/brown solution *in vacuo*. The residual brown solid was washed with pentane (10ml) and

dried *in vacuo*. ^{31}P NMR (298K) (THF_{d8}): δ = 26.58, 24.72, 23.82 (complexed TPPMSNa), -4.03 (remnant TPPMSNa) ppm. VT ^{31}P NMR was then performed on this complex.

$Ni([TPPMS][BMMI])_4$

TPPMSBMMIM (0.40g, 0.812 mmol) and $Ni(COD)_2$ (0.056g, 0.203mmol) in THF (15ml) was stirred for an hour at room temperature. The solvent was removed from the resulting pale orange solution *in vacuo*. The residual orange solid was washed with pentane (10ml) and dried *in vacuo*. ^{31}P NMR (THF_{d8}): δ = 25.03 (complexed ligand), -4.16 (remnant free-ligand) ppm.

DOSY (Diffusion Order SpectroscopY)

Molecules in liquid or solution state move. This translational motion is, in contrast to rotational motion, known as Brownian molecular motion and is often simply called diffusion or self-diffusion. It depends on a lot of physical parameters like size and shape of the molecule, temperature, and viscosity. Assuming a spherical size of the molecule the diffusion coefficient ***D*** is described by the Stokes-Einstein equation:

$$D = \frac{kT}{6\pi\eta r_s}$$

k : Boltzman constant
T : temperature
η : viscosity of the liquid
r_s : (hydrodynamic) radius of the molecule.

Pulsed field gradient NMR spectroscopy can be used to measure translational diffusion of molecules and is sometimes referred to as q-space imaging. By use of a gradient, molecules can be spatially labelled, i.e. marked depending on their position in the sample tube. If they move after this encoding during the following diffusion time Δ, their new position can be decoded by a second gradient. The measured signal is the integral over the whole sample volume and the NMR signal intensity is attenuated depending on the diffusion time Δ and the gradient parameters ($\mathbf{g}$, δ). This intensity change is described by

$$I = I_0 \, e^{-D\gamma^2 g^2 \delta^2 (\Delta - \delta/3)}$$

I : the observed intensity

I_0 : reference intensity (unattenuated signal intensity)

D : diffusion coefficient

γ: the gyromagnetic ratio of the observed nucleus

g the gradient strength

δ the length of the gradient

Δ the diffusion time.

To simplify this equation some parameters are often combined to emphasize the exponential decay behaviour :

$$I = I_0 \, e^{-Dq^2(\Delta - \delta/3)} \quad \text{or} \quad I = I_0 \, e^{-DQ}$$

If bipolar gradients are used for dephasing and rephasing a correction for the time τ between those bipolar gradients has to be applied :

$$I = I_0 \, e^{-D\gamma^2 g^2 \delta^2 (\Delta - \delta/3 - \tau/2)}$$

2D DOSY experiments used a slightly modified Bruker experiment ledbpgp2s to improve lineshape and trapezoidal gradients where implemented for shorter pulses gradients. The diffusion evolution time was set to 100ms, the constant amplitude part of the gradient was set to 3ms, and the cosine raising and falling part of gradient where set to 150µs. The diffusion space where sampled by 32 linearly spaced gradients.

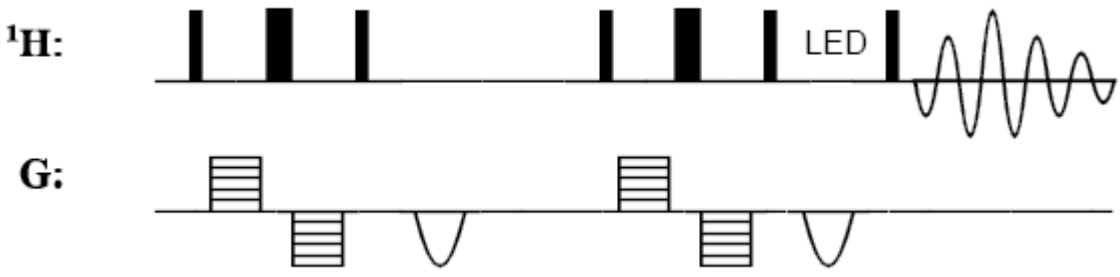

DOSY pulse sequences.

DOSY NMR

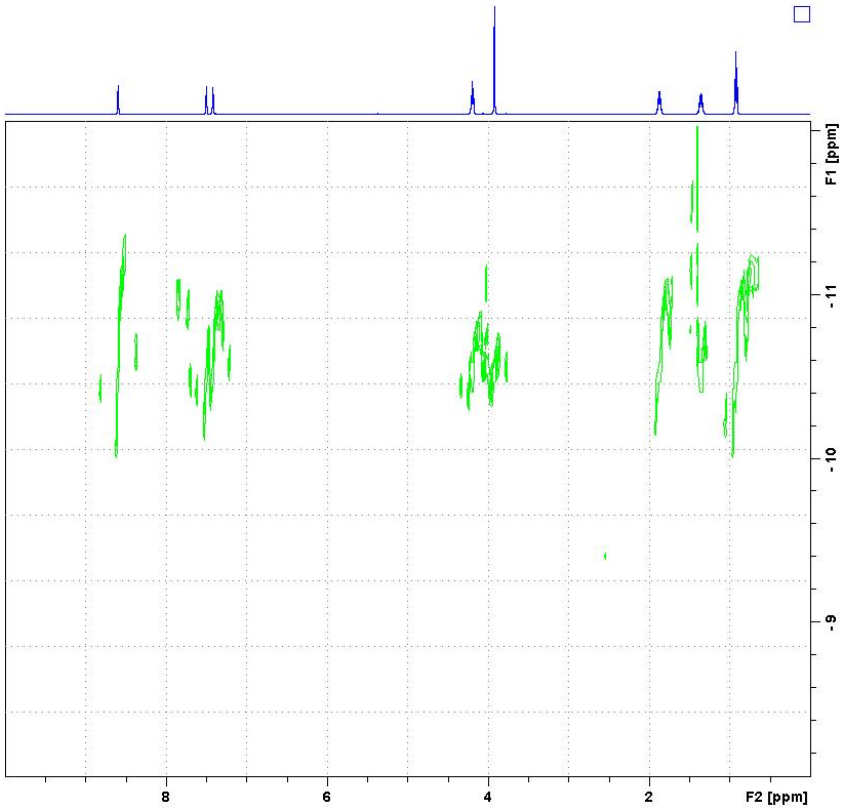

DOSY NMR of $TPPMS^{-}Na^{+}$ dissolved in $BMIM^{+}NTf_2^{-}$

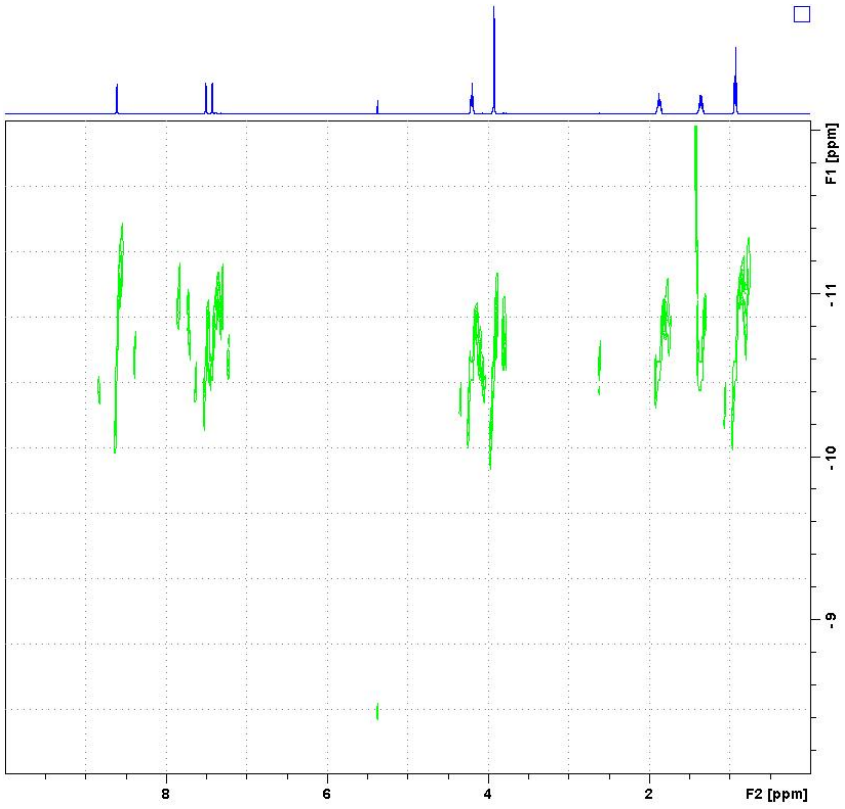

DOSY NMR of $TPPMS^{-}BMMIM^{+}$ dissolved in $BMIM^{+}NTf_2^{-}$

Hydrogenation of 1,3-cyclohexadiene

Four hydrogenations were started at the same time, using identical amounts of the same catalyst : $[Rh(COD)L_2]NTf_2$ with L=TPP, TPPMSNa and TPPMSBMMIM (1,6µmol), 1,3-cylohexadiene (0.12mL, 1.6mmol) with 1ml IL in each. After each desired time interval, one Schlenk was opened to air and dissolved with 4ml CH_3CN (1% toluene) and a 1ml sample taken for GC analysis.

Bibliography

(1) Cornils, B.; Herrmann, W. A.; Horvath, I. T.; Leitner, W.; Mecking, S.; Olivier-Bourbigou, H.; Vogt, D. *Multiphase Homogeneous Catalysis, Volume 2*; Wiley-VCH: Weinheim, 2005.
(2) Olivier-Bourbigou, H.; Vallee, C. In *Multiphase Homogeneous Catalysis*; Wiley-VCH: Weinheim, 2005; Vol. 2, pp 413-431.
(3) Wasserscheid, P.; Welton, T. *Ionic Liquids in Synthesis*; Wiley-VCH: Weinheim, 2003.
(4) Welton, T. *Coord. Chem. Rev.* **2004**, *248*, 2459-2477.
(5) Vallee, C.; Valerio, C.; Chauvin, Y.; Niccolai, G. P.; Basset, J.-M.; Santini, C. C.; Galland, J.-C.; Didillon, B. *J. Mol. Catal. A* **2004**, *214*, 71-81.
(6) Vallee, C.; Chauvin, Y.; Basset, J.-M.; Santini, C. C.; Galland, J.-C. *Adv. Synth. Catal.* **2005**, *347*, 1835-1847.
(7) Suarez, P. A. Z.; Dullius, J. E. L.; Einloft, S.; de Souza, R. F.; Dupont, J. *Inorg. Chim. Acta* **1997**, *255*, 207-209.
(8) Hardacre, C.; Holbrey, J. D.; Nieuwenhuyzen, M.; Youngs, T. G. A. *Acc. Chem. Res.*,, ACS ASAP.
(9) Chauvin, Y.; Mussmann, L.; Olivier, H. *Angew. Chem. Int. Ed.* **1996**, *34*, 2698-2700.
(10) Ahrland, S.; Chatt, J.; Davies, N. R.; Williams, A. A. *J. Chem. Soc.* **1958**, 1403-1405.
(11) Kuntz, E. G. *Chemtech* **1987**, *17*, 570-575.
(12) Joo, F. *Aqueous organometallic catalysis*; Kluwer Academic Publishers: Dordrecht, 2001; Vol. 23.
(13) Webb, P. B.; Sellin, M. F.; Kunene, T. E.; Williamson, S.; Slawin, A. M. Z.; Cole-Hamilton, D. J. *J. Am. Chem. Soc.* **2003**, *125*, 15577-15588.
(14) Kim, N. H.; Malhotra, S. V.; Xanthos, M. *Micro. Meso. Mat.* **2006**, *96*, 29-35.
(15) Galland, J. C.; Basset, J. M.; Vallee, C. In *Fr. Demande*; (Rhodia Chimie, Fr.).: Fr, 2006; p 46 pp.
(16) Basset, J. M.; Y., C.; Galland, J. C. In *2829763*; Rhodia Polyamide Intermediates, Fr: France, 2003.
(17) Amoureux, J. P.; Fernandez, C.; Lefebvre, F. *Magnetic Resonance in Chemistry* **1990**, *28*, 5-10.
(18) Katsyuba, S. A.; Dyson, P. J.; Vandyukova, E. E.; Chernova, A. V.; Vidis, A. *Helv. Chim. Acta* **2004**, *87*, 2556-2565.
(19) Burrows, A. D.; Harrington, R. W.; Mahon, M. F.; Teat, S. J. *Eur. J. Inorg. Chem.* **2003**, 1433-1439.
(20) Roman, J. P. J.; Paterniti, D. A.; See, R. F.; Churchill, M. R.; Atwood, J. D. *Organometallics* **1997**, 1484-1490.

(21) Reichardt, C. *Solvents and Solvent Effects in Organic Chemistry. 3rd Ed*; Wiley-VCH: Weinheim, 2003.
(22) Zhao, Y.-B.; Yan, Z.-Y.; Liang, Y.-M. *Tetrahedron Lett.* **2006**, *47*, 1545-1549.
(23) Daguenet, C.; Dyson, P. J. *Organometallics* **2004**, *23*, 6080-6083.
(24) Fonseca, G. S.; Umpierre, A. P.; Fichtner, P. F. P.; Teixeira, S. R.; Dupont, J. *Chem. Eur. J.* **2003**, *9*, 3263-3269.
(25) Lecocq, V.; Graille, A.; Santini, C. C.; Baudouin, A.; Chauvin Y.; Basset, J.-M.; Bouchu, D.; Fenet, B. *New J. Chem.* **2005**, *2 9*, 700–706.
(26) Chaumonnot, A.; Lamy, F.; Sabo-Etienne, S.; Donnadieu, B.; Chaudret, B.; Barthelat, J.-C.; Galland, J.-C. *Organometallics* **2004**, *23*, 3363-3365.
(27) Tolman, C. A.; McKinney, R. J.; Seidel, W. C.; Druliner, J. D.; Stevens, W. R. *Adv. Catal.,* **1985**, *33*, 1-46.
(28) Sieffert, N.; Wipff, G. *J. Phys. chem. B* **2007**, *111*, 7253-7266.
(29) Mele, A.; Romano, G.; Giannone, M.; Ragg, E.; Fronza, G.; Raos, G.; Marcon, V. *Angew. Chem. Int. Ed.* **2006**, *45*, 1123-1126.

Chapter III : Attempts to demonstrate an interaction between π-system of substrates and imidazolium ring of ionic liquid. Consequences on the catalytic activity

Introduction

Ionic liquids (IL), also known as room temperature molten salts, are rapidly emerged as a new class of solvents for a variety of catalytic reactions. In many reports, differences in the rates and selectivities of the processes in IL are observed when compared to the corresponding reactions in molecular solvents. However, very little has been reported detailing the origin of these changes. In some catalytic reactions, the difference could be related to the fact that IL are a source of new ligand for the catalytic metal centre, a catalyst activator or even a co-catalyst or a catalyst itself.[1,2]

Moreover, we have demonstrated in chapter II that other phenomena could be involved to explain these differences of reactivity, in particular the interaction between π-system of ligand and the cation of IL. Generally speaking, the interactions described in the literature concern either the π-stacking or H-bonding and take place between the components of IL (cation/anion, cation/cation or anion-anion).[3-5] Although H-bond interactions are often evocated to explain specific reactivity in IL, to our knowledge, no catalytic results have been related to the presence of π-interactions.

However, recent works explain the unusual high solubility of aromatic compounds in IL in comparison with aliphatic compounds by the electrostatic interactions between the cations and the π-system of the aromatic compounds.[6] This higher solubility is related to the formation of liquid clathrates.[7] The presence of the aromatic compounds alters the structure of IL in particular, in the cation-cation interactions/distances, but a strong ionic ordering is still observed.[6,8,9] But these works do not suggest any interaction between the π-system of the aromatic compound and the charged ions of IL.

Nevertheless, the significance and the importance of the interactions between aromatic rings and metallic ions (Li^+, Na^+, K^+,et Ag^+) or ammonium ions (NH_4^+, NMe_4^+) are widely recognized and studied in recent years.[10] This interaction, known as "π-cation interaction", are playing an important role in both chemical and biological recognition and the crucial role of such interactions was widely used in organometallic systems for a long time.[11] The interaction of a metal cation with π-system of aromatics residues is arguably

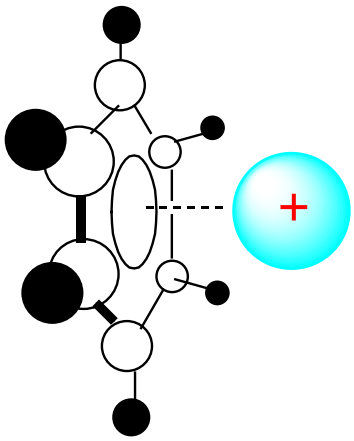

the strongest non-covalent force which can present a relatively high binding energy (from 10 to 30 kcal/mol). In Addition, the conformation-controlling ability has opened up new methods for stereoselective synthesis.[12]

Moreover, although most of the reported π-cation interactions are observed between a cationic moiety and aromatic π-component,[13] little is known about non aromatic π-systems except for the complexes of ethylene-ammonium cation[14,15] and acetylene-Ca^{+}[16]. Therefore, the disclosure of a new type of π-cation interaction would be of significant interest.

Except data provided by calculations, this π-cation interaction has been experimentally demonstrated by mass spectrometry. Positive secondary ion and positive electrospray ionisation have been used to reveal the presence of this interaction in cyclophane and calix[4]arene/metal ions systems.[17] But it is also possible to use NMR techniques. Indeed the study of evolution of NMR chemical shifts and/or NOE experiments also enable the detection of such interactions.[18,19]

Although the cations of IL and particularly imidazolium based IL present all criteria for the formation of π-cation interaction in presence of unsaturated compounds, no direct evidence of this phenomenon has been reported in the literature. However, this concept has already been proposed in chromatographic applications. A possible π···π interaction between alkylimidazolium or pyridinium cations and the aromatic π···π active moiety of the stationary phase could explain the selective separation by IL. Moreover, the fact that adding acetonitrile as a electron-rich modifier suppresses the separation is a consequence of the suppression of the π…π interaction. Unfortunately, this separation also used some hydrophobic interactions between alkyl chains of IL and stationary phase and some hydrogen bond formation between proton of imidazolium rings and ether-linked phenyl phase which improve the efficiency of the column.[20]

The aim of this work is to attempt to identify and to experimentally demonstrate the nature of potential interactions between **unsaturated substrate and IL** and to evaluate their consequences in catalytic reaction.

In order to favour the formation of π-cation interaction, imidazolium based IL have been studied because their aromatic character leads to planar molecules. In the case of imidazolium based IL, X-Ray spectroscopy demonstrates that the type of structure is almost only dependent on the nature of the cation while the anion determine the strength of hydrogen bond and the cation-cation and cation-anion distances.[21,22] Moreover it is clear that the presence or

not of hydrogen H(2) at the position C2 of imidazolium ring controls the 3D organization of IL due to strong hydrogen bonding with the anion and would determine the availability of imidazolium cation to interact with unsaturated substrates.[23,24] Indeed it has been shown that the cation-anion association energies are lower (<20kJ.mol^{-1}) for the ion pairs of 1-butyl-2,3-dimethylimidazolium chloride (BMMIMCl) compared to those of 1-butyl-3-methylimidazolium chloride (BMIMCl).[25] Consequently the imidazolium ring BMIM and BMMIM have been chosen.

Due to the relative weakness of π-cation interaction, it is necessary to study unsaturated compounds/IL systems at low temperature in order to maintain the local structure but also in the absence of water (or other impurities such chloride) in order to avoid competition with hydrogen-bonding. Consequently, tetrafluoroborate (BF_4), hexafluorophosphate (PF_6) and bis(trifluoromethylsulfonyl)imide (NTf_2) based IL could be used because the corresponding IL are hydrophobic and liquid at room temperature but also because their purification is well controlled.[26,27]

IL are excellent solvents for conducting hydrogenation reactions in homogeneous or heterogeneous catalysis and in mono- or biphasic conditions.[28] In particular, successful examples of hydrogenation reactions of benzene with ruthenium nanoparticles[29] and of 1,3-cyclohexadiene, cyclohexene with $[Rh(COD)(PPh_3)_2]^+A^-$(COD=1,5-cyclooctadiene ; $A^- = BF_4$ or PF_6)[30] in several IL have already been reported.

Consequently we have chosen these two catalytic hydrogenations as model reactions and benzene (Bz) and its hydrogenated products : 1,3-cyclohexadiene (CYD), cyclohexene (CYE) and cyclohexane (CYA) as model compounds of aromatic, diene, alkene and alkane systems. Toluene (To) has also been studied in NMR studies because the methyl group provide a supplementary probe.

To reach this goal, we have firstly determined the solubility of theses substrates in IL based on both cation 1-butyl-3-methylimidazolium (BMIM) and 1-butyl-2,3-dimethylimidazolium (BMMIM) associated to three different anions : BF_4, PF_6 and NTf_2 resulting in six IL : $BMIMBF_4$, $BMIMPF_6$, $BMIMNTf_2$, $BMMIMBF_4$, $BMMIMPF_6$ and $BMMIMNTf_2$. Then, NMR (1D and 2D NMR, Rotating-frame Overhauser Effect SpectroscopY **(**ROESY) and Diffusion Order SpectroscopY (DOSY)) experiments have been used to obtain information on solute-solvent interactions and about site-site distance. Eventually, the influence of this potential interaction on the evolution of the activity of the model heterogeneous and homogeneous catalytic reactions has been studied.

RESULTS

IL have been carefully synthesized using Schlenk techniques according to the procedure established in our laboratory (See details in chapter I and experimental section).[26]

1 Solubility of hydrocarbons in IL

1.1 Experimental determination of the solubilities of hydrocarbons in IL

All these experiments have been performed in a glove box in temperature controlled bath. All chosen substrates are only partially miscible with IL. Saturated solutions of hydrocarbons in IL have been prepared in closed containers by adding excess amount (until a second phase appears) of toluene, benzene, 1,3-cyclohexadiene, cyclohexene and cyclohexane to each IL.

After 24h of vigorously stirring at 30°C to ensure equilibrium, precise quantities of the lower phases (IL phase) were dissolved in acetonitrile and their compositions were evaluated by GC analyses (Figure 1) in presence of an internal standard (toluene or benzene). IL are totally soluble in acetonitrile which suppresses H-bond network and π-stacking, releasing in organic media hydrocarbons molecules trapped in IL. The experimental values, resulting from three measures in order to guarantee reproducible results (+/-2%wt), are presented in figure 1.

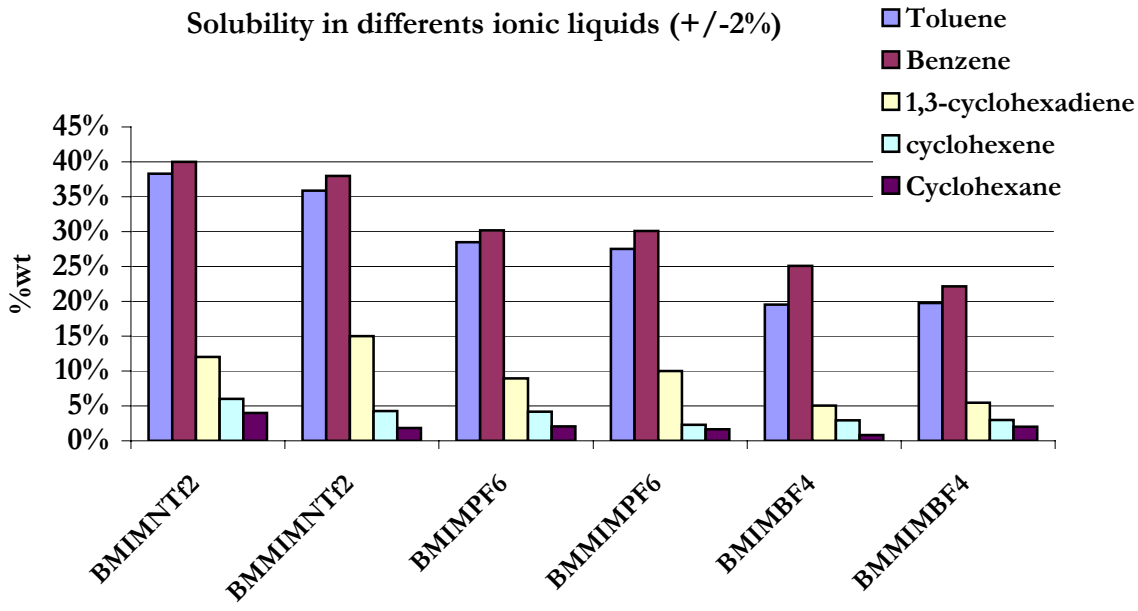

Figure 1. Solubility of various hydrocarbons in IL.

The solubility of benzene is about 40±2%wt in $BMIMNTf_2$ which correspond to 3 moles of aromatics for one mole of IL (molar ratio R=3) but only 30±2%wt with in $BMIMPF_6$ and 25±2%wt in $BMIMBF_4$. The same tendency is observed with 1,3-cyclohexadiene with a solubility of 12±2%wt in $BMIMNTf_2$, 9±2% in $BMIMPF_6$ and 5±2% in $BMIMBF_4$. For cyclohexene and cyclohexane, their solubilities are about 6 and 4%wt respectively in $BMIMNTf_2$, 4 and 3%wt in $BMIMPF_6$ and 2 and 1%wt in $BMIMBF_4$. Similar values were obtained in BMMIM based IL. For instance, the solubilities of toluene, benzene, 1,3-cyclohexadiene, cyclohexene and cyclohexane are 36, 38, 15, 4 and 2%wt respectively in $BMMIMNTf_2$.

The values of the solubility of aromatic in the same IL using ^{1}H NMR[7], gravimetric analysis or quantitative method based on UV-Visible spectroscopy[31] are very similar in the literature. For instance, the mass fractions of benzene and toluene in $BMIMNTf_2$ are about 39 and 34%wt respectively[7] while 38 and 40±2%wt have been found following our procedure. As reported, aromatics are really more soluble in IL than alkanes and even alkenes.

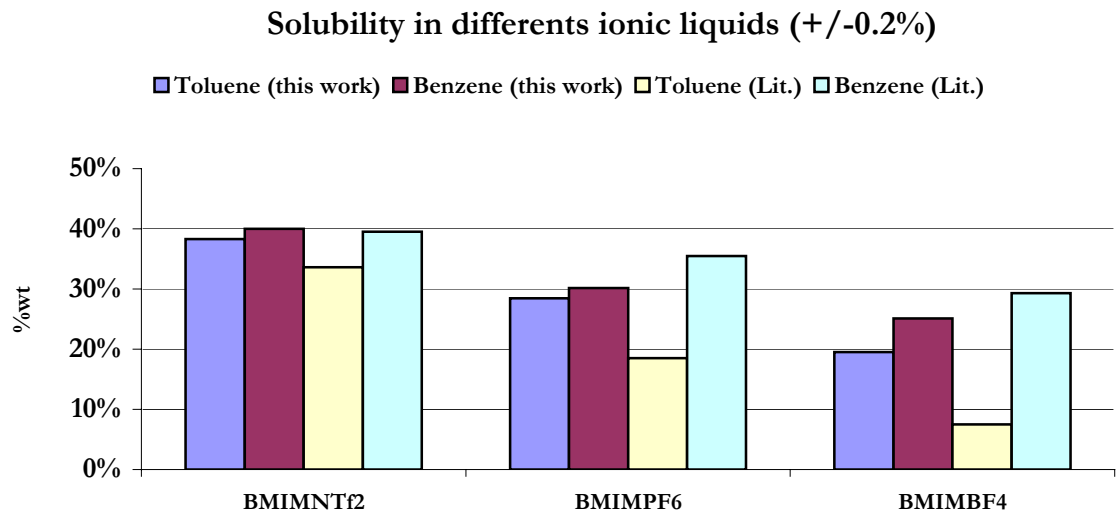

Figure 2. Comparison of our result with data providing by literature from ^{1}H NMR[7]

Important differences between solubilities of toluene given in literature and our result have been observed in $BMIMPF_6$ and $BMIMBF_4$. Obviously our method is not very precise due to a possible contamination of the sample by the upper phase (organic phase) during its preparation. But the very low solubilities of toluene compare with benzene reported by

Holbrey *et al* is surprising and probably due to a problem in toluene quantification or of homogenization of the mixture, especially if the sample is prepared in NMR tubes.

1.2 Effect of the nature of IL on the solubilities

For a given cation BMIM, the solubility of all hydrocarbons increases in the range :

$$BF_4 < PF_6 < NTf_2$$

As described in literature, the solubility is drastically dependent of the nature of the anion which indicates that more coordinating anion is, lower the solubility of hydrocarbons is. The strength of hydrogen bond between imidazolium ring and anion controls intermolecular distances in network of IL and seems to intervene strongly on the solubility of organic compounds.[32]

For the same anion, the methylation of C2 of imidazolium ring tends to slightly decrease the solubility of all hydrocarbons. For instance, the solubility of toluene is 38 and 36±2%wt in $BMIMNTf_2$ and $BMMIMNTf_2$ respectively.

1.3 Conclusion on the study of solubilities of hydrocarbons in IL

For all IL, the solubility of hydrocarbons increases when the number of double bonds increases :

benzene ≥ toluene > 1,3-cyclohexadiene > cyclohexene > cyclohexane

Although saturated hydrocarbons are poorly soluble in IL, they are not insoluble.

These results are consistent with those provided in the literature.[7] Some previous work based on calculations show that the difference in the average electrostatic fields is sufficient to explain the difference in solubility of aromatic and aliphatic compounds. On one hand, all these products are similar in size but present different electronic factors because the existence of π electrons in orbitals of aromatic ring results in a much stronger electrostatic field around an aromatic molecule compared to a saturated aliphatic molecule. In general, alkanes and alkyl side chains give very small electrostatic fields. On the other hand, benzene has a significant quadrupole moment of about an order of magnitude greater than that for cyclohexane and it is more polarisable than cyclohexane. Any effects of the fluctuations in the electronic structure of the aromatic system due to local fields will just exacerbate the difference.[6]

1.4 Solubility of IL in hydrocarbons

Few data are reported on the solubility of IL in hydrocarbons.[33] These solubilities have been determined in $BMIMNTf_2$ and $BMMIMNTf_2$ for toluene, benzene, cyclohexene and cyclohexane by analysing the upper phase (organic phase) of previous mixture following the same procedure.

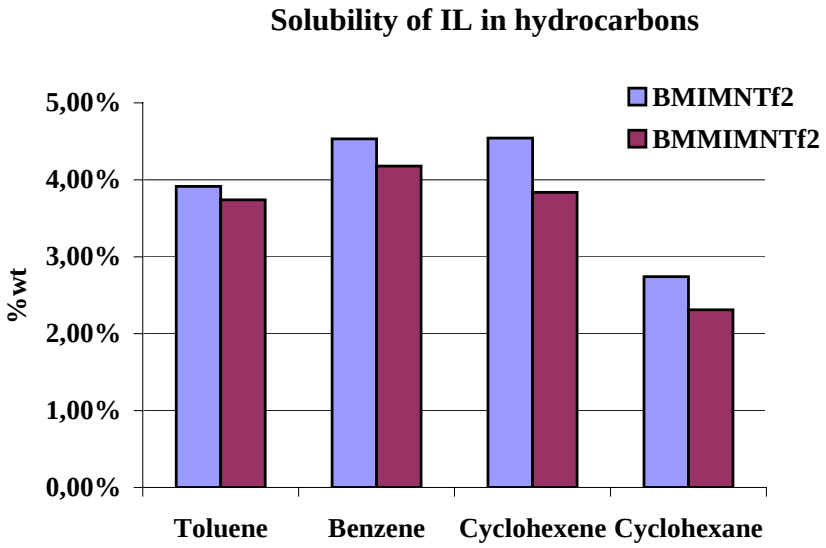

Figure 3. Solubility of IL in hydrocarbons at 30°C. (1mL of IL + 2-3mL of substrates)

The solubility of IL in hydrocarbons have been found relatively low but **not negligible**. The content of IL in aromatics is about 4-5%wt and decreases to 2%wt in cyclohexane. This factor is a major inconvenient for biphasic catalysis as IL phase can be extracted in organic phase and involves the use of distillation at the end of the reaction.

As the higher solubility for any hydrocarbons is obtained in NTf_2 based IL, these IL have been selected to perform all NMR experiments and catalytic reaction. Moreover these IL are known to be the more hydrophobic and less hygroscopic.[3]

2 NMR studies of hydrocarbons/IL systems.

To investigate the interaction and the specific local structure of the different hydrocarbons in IL, all systems have been studied by ^1H NMR, ROESY and DOSY experiments. The NMR study of aromatic/IL systems has been performed with toluene because the methyl proton is a supplementary probe in NMR.

2.1 General procedure for preparation of NMR Samples

Samples with various toluene, 1,3-cyclohexadiene and cyclohexene concentrations in IL were prepared by adding compound to reach specified molar ratios (R=number of moles of hydrocarbon in one mole of IL). Each saturated samples is prepared as described for solubility experiment. For toluene, R varies from 0.1 to 3, for 1,3-cyclohexadiene from 0.1 to 0.5 and 0.1 for cyclohexene. In all case, the mixture leads to an **homogeneous monophasic solution**. Approximately 0.3mL of a system was introduced into a 5 mm NMR tube. A stem coaxial capillary tube loaded with CD_2Cl_2 was inserted into the 5 mm NMR tube to avoid any contact between deuterated solvent and the analysed mixture. The deuterium in CD_2Cl_2 was used for the external lock of the NMR magnetic field and the residual $CHDCl_2$ in CD_2Cl_2 was used as the ^1H NMR external reference at 5.32ppm. When ^1H NMR data are obtained in this way, the reference signal of $CHDCl_2$ will remain as a constant and not be affected by change in sample concentration.

First, the evolution of the ^1H chemical shifts of each protons of toluene and imidazolium rings was followed in function of the molar ratio in order to identify potential specific structure of this system for a particular composition. This study could not be carried out on other hydrocarbons/IL systems due to too low solubilities resulting in insufficient numbers of experiments. Secondly, ROESY an DOSY experiments have been realized with toluene, 1,3-cyclohexadiene and cyclohexene.

Assignments of the ^1H NMR signals corresponding to the protons on hydrocarbons and to those on the imidazolium cation of IL for these systems are shown on Figure 4.

1-butyl-3-methylimidazolium (BMIM)

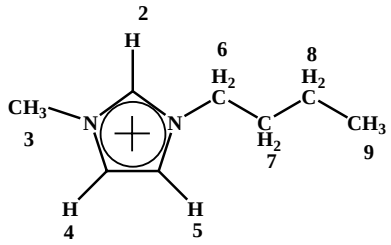

1-butyl-2,3-dimethylimidazolium (BMMIM)

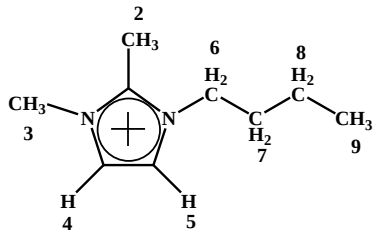

Toluene (To)

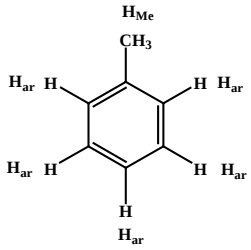

Benzene (Bz)

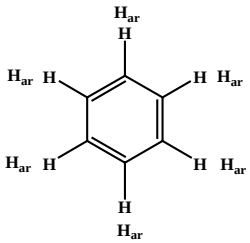

1,3-cyclohexadiene (CYD)

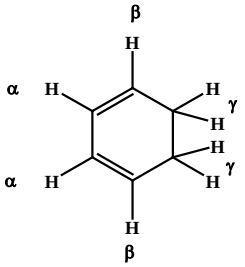

Cyclohexene (CYE)

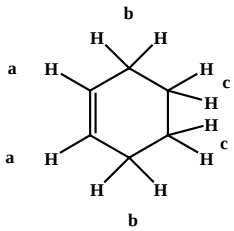

Figure 4. Proton NMR signals assignment of toluene, benzene, 1,3-cyclohexadiene, cyclohexene, 1-n-butyl-3-methylimidazolium and 1-n-butyl-2,3-dimethylimidazolium cations.

2.2 Study of the evolution of the ^{1}H NMR Spectra of a solution of toluene in IL as a function of the molar ratio R

The first study concerns the systems To/BMIMNTf$_2$ and To/BMMIMNTf$_2$. The ^{1}H NMR spectra (Figure 5), an array of representative expanded ^{1}H NMR spectra (Figure 6) and signal assignment for protons in aromatic rings of toluene and imidazolium cation are shown.

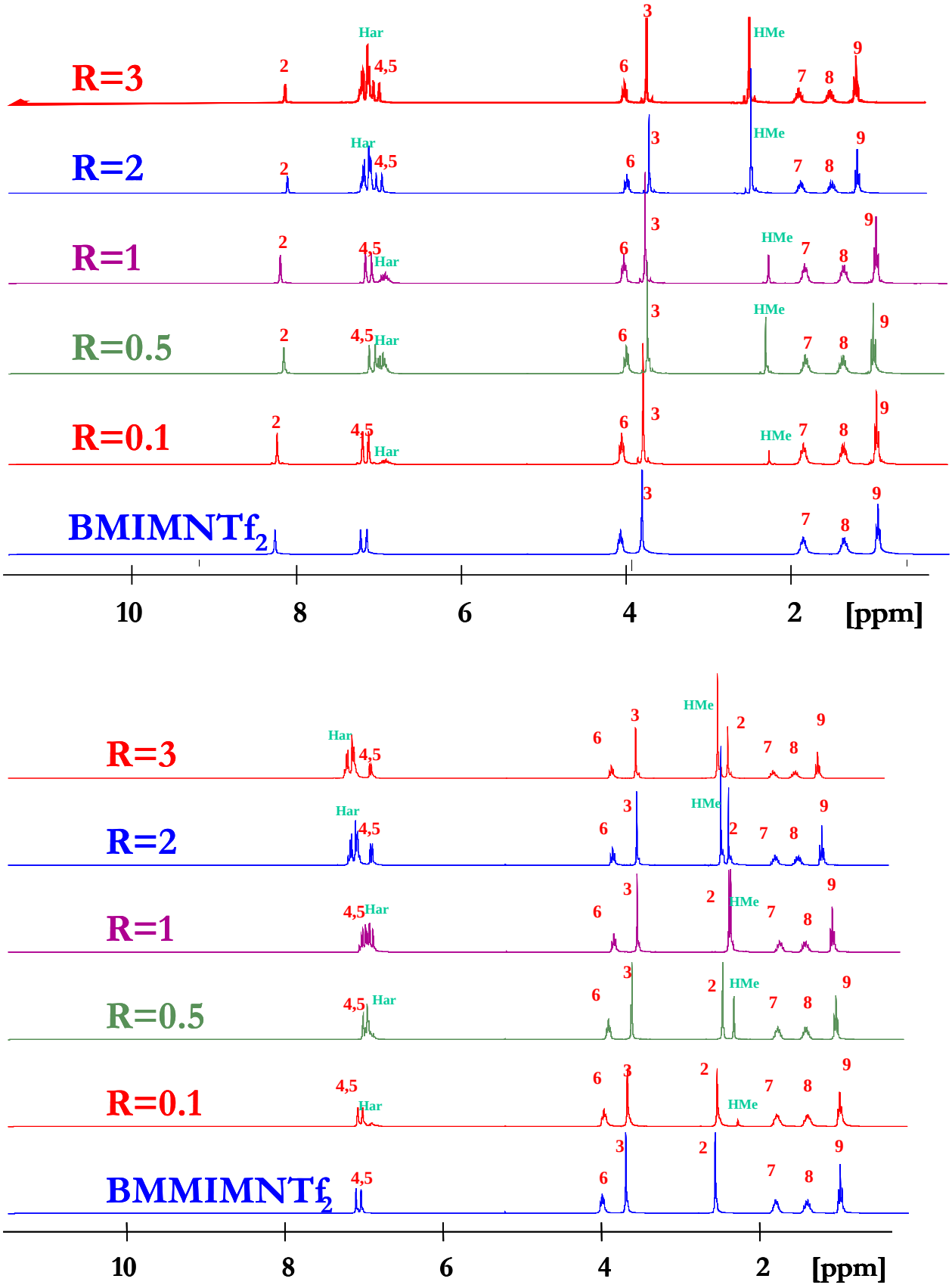

Figure 5. ^{1}H NMR signals assignment of the ring protons in To, $BMIMNTf_2$ and $BMMIMNTf_2$ at various mole ratios of To/IL. (The top spectrum is the saturated solution and the bottom spectrum is pure IL. The proton assignments to each signal is reported)

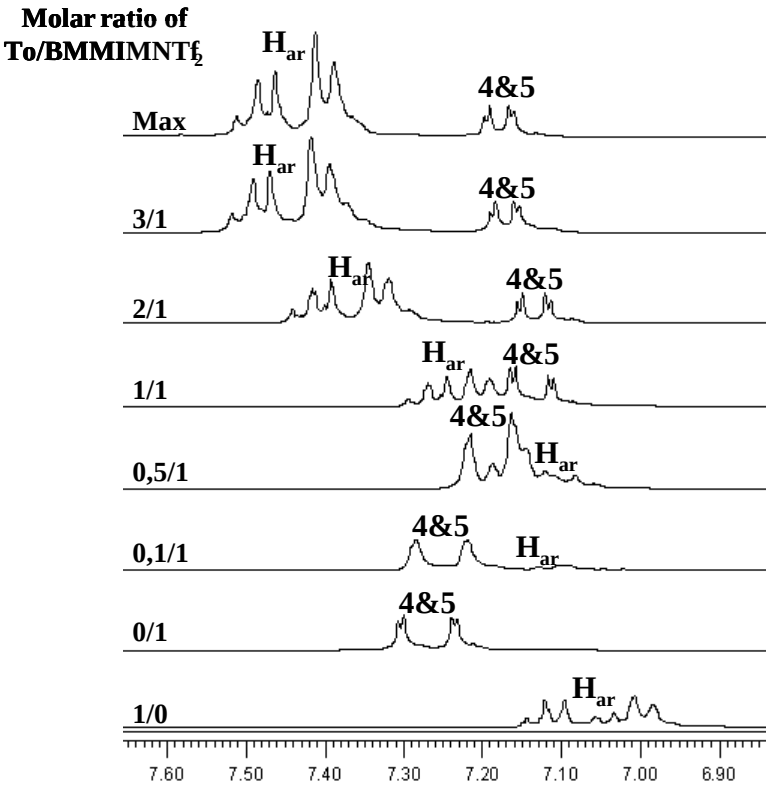

Figure 6. Expanded ^{1}H NMR spectra of To/BMMIMNTf$_2$

The ring protons H(4) and H(5) as all resonances of imidazolium cycle of BMMIM cation in BMMIMNTf$_2$ are gradually shifted upfield when the concentration of toluene increases (R = 0 to 3). Concomitantly all resonances of toluene are shifted downfield.

The variation of the proton chemical shift of toluene and BMMIM cation in the different systems could be due to several contributing factors, such as (a) aromatic ring current effect (i.e. π-π interaction), (b) C-H-π interaction between cation and toluene, (c) anion effect, (d) dilution effect, and (e) electrostatic field effect.[34]

a)*The aromatic ring current effects* in aromatic compounds have been well studied and documented.[35] It is known that NMR signals of a compound situated above or below the shielding cone of the aromatic ring will shift upfield (i.e. shielding effect), whereas those for a compound located outside the shielding cone will shift downfield. In this system, both toluene and BMMIM cation have an aromatic ring. The aromatic ring current effect in neat toluene is stronger than in a neat BMMIMNTf$_2$ because toluene molecules are tightly packed[9] whereas BMMIM cations are separated by NTf$_2$ anions. The bulky NTf$_2$ anions prevent BMMIM cations from coming too close and greatly reduce the aromatic current effect.[36] Therefore, the NMR chemical shift of a neat toluene is more upfield than a neat BMMIMNTf$_2$.[34] The trend

of chemical shift change observed in our spectra indicates that the BMMIM cation is located in the shielding cone of toluene ring current and the toluene is located near the deshielding zone of BMMIM ring current. This local structure arrangement caused NMR chemical shift of BMMIM to move upfield and the signal for toluene to move downfield.

b) *The C-H-π interaction* between the BMMIM cation and toluene aromatic ring could also induce an upfield chemical shift of BMMIM cation with different extent on each aromatic proton. Indeed H(4) and H(5) are known to form strong hydrogen bond but in this case, aromatics are in competition with anions of IL, which should be better hydrogen bond acceptor.[25]

c) *The NTf_2 anion* is a potential hydrogen acceptor, but it will introduce a downfield shift. It was known that NTf_2 anion is not such a good acceptor as Cl or $AlCl_4$. This effect is probably negligible.

d) *Effect of the dilution.* The NMR spectra that we have run at various molar ratio of toluene in pentane and 1,2-dimethylimidazole show no significant evolution of the chemical shifts, this effect is also probably negligible.

e) *The electrostatic field effect* is important when electrons surrounding the resonating nucleus were displaced by a chemically bonded polar atom such as fluorine. Studies of the electric field effect have been reported in several open chain and cyclic fluorine-substituted alkanes. The electric field effect arising from the physical interaction between fluoride anions and cations or toluene is not a dominant factor in determining the absorption capacity of toluene in these systems. Otherwise, a similar chemical shift effect on the imidazolium cation will be observed in the nonaromatic systems such as alkanes (pentane) or imidazole (1,2-dimethylimidazole) but in the experiments that we run, no chemical shift effect was observed.

With the consideration of all these possible factors and the observed NMR results, the **aromatic ring current effect seems the dominant factor** to influence the trend of chemical shift change of cation and toluene. Indeed the electronic density of π-system of toluene decreases due to interaction with electron-deficient π-system of positive charge imidazolium rings and inversely.

2.3 Comparison of the evolution of the ^{1}H NMR Spectra of a solution of toluene in $BMMIMNTf_2$ and $BMIMNTf_2$ as function of the molar ratio R

These experiments have been run with different systems To/IL. The figure 7 described the ^{1}H NMR chemical shifts of toluene in $BMMIMNTf_2$ and $BMIMNTf_2$ in function of the molar ratio R (R= 0 ; 0.1 ; 0.5 ; 1 ; 2 ; 3) and also for saturated solution and neat toluene.

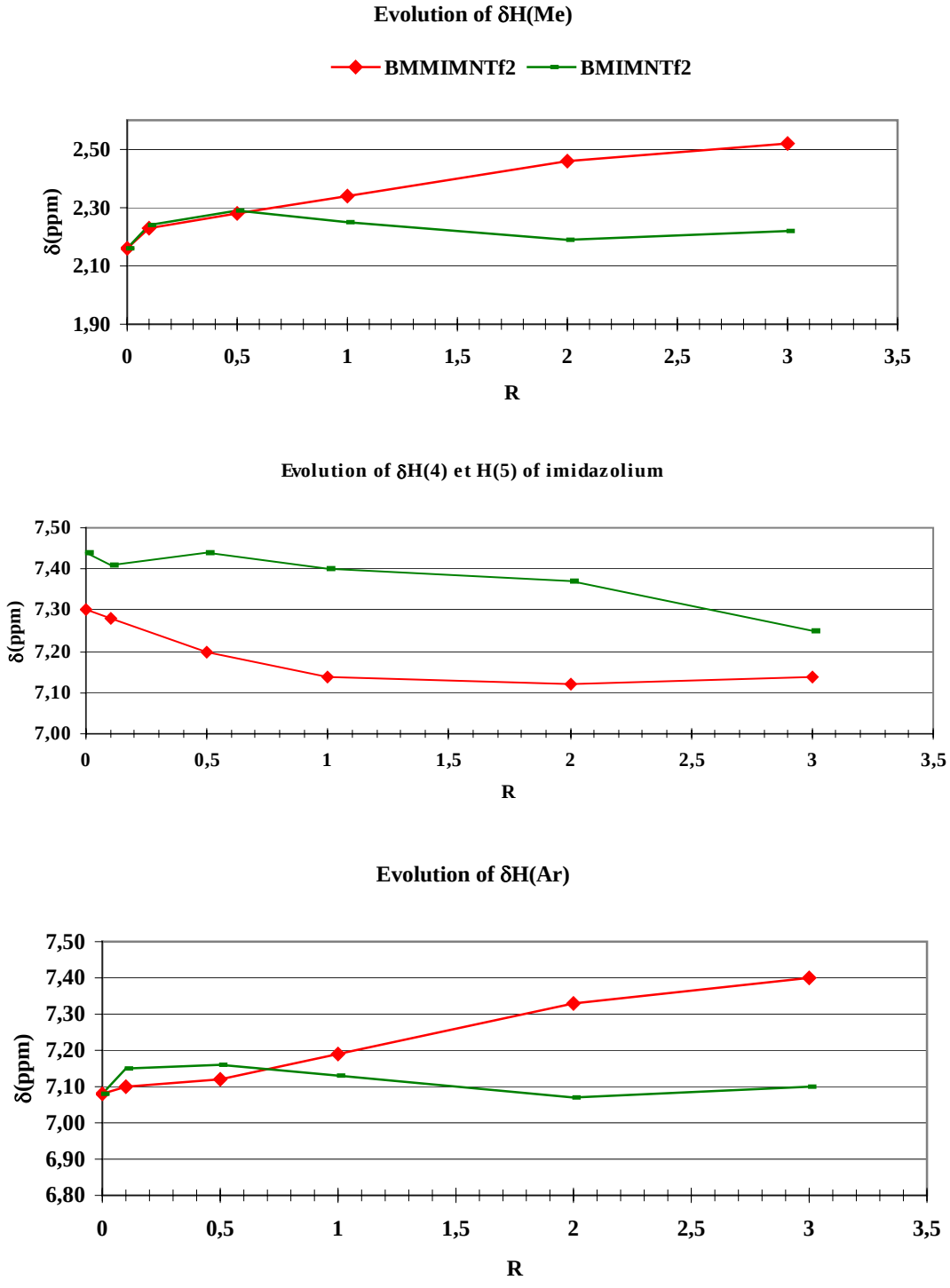

Figure 7. Evolution of the ^{1}H NMR spectra of a solution of toluene in $BMIMNTf_2$ and $BMMIMNTf_2$ in function of the molar ratio R (R= 0 ; 0.1 ; 0.5 ; 1 ; 2 ; 3)

The evolution of chemical shifts in function of molar ratio R is different. There is no significant variation of the chemical shift of the proton of the toluene in $BMIMNTf_2$ for molar ratio inferior to R=1. The variation H(2) chemical shift of BMIM is relatively small ($\Delta\delta$=0.1ppm) compare to that is observed in other organic solvent. For instance, the H(2) chemical shift shows a marked change to upfield when mole fraction of IL increases in acetone d_6. ($\Delta\delta$=0.4ppm when molar fraction of IL increase from 0,05 to 0,95).[37] For R≥1, a strong decrease is observed for hydrogen of imidazolium ring H(4) and H(5) of $BMIMNTf_2$ which could be explained by a partial dissolution of IL into toluene and the formation of an ionic solution.

It appears that a particular phenomenon which can mainly be attributed to aromatic ring current effect is detected in To/$BMMIMNTf_2$ system **but not** in To/$BMIMNTf_2$.

2.4 Study of the interaction between toluene and IL by ROESY experiments

^1H-^1H ROESY techniques is based on space correlations *via* the Rotational nuclear Overhauser Effect (ROE). A selective irradiation of one group of protons affects the intensities of integrals of group of protons which are spatially close but not necessary connected by chemical bonds. ROESY is especially useful for cases where NOESY (Nuclear Overhauser Effect SpectroscopY) signals are weak because they are near the transition between negative and positive while ROESY cross peaks are always negative.

NMR ROESY spectra of the previous systems of To/$BMIMNTf_2$ and To/$BMMIMNTf_2$ at various molar ratio have been recorded. The irradiation of protons of Me group of toluene involves a response of each imidazolium ring proton quantified by negative integrals which is proportional to the intensity of the intermolecular interactions. The variation of the intensities of integrals of methyl of toluene H(Me) and methyl groups H(3) and H(6) linked to nitrogen atom of imidazolium cations is represented in figure 8.

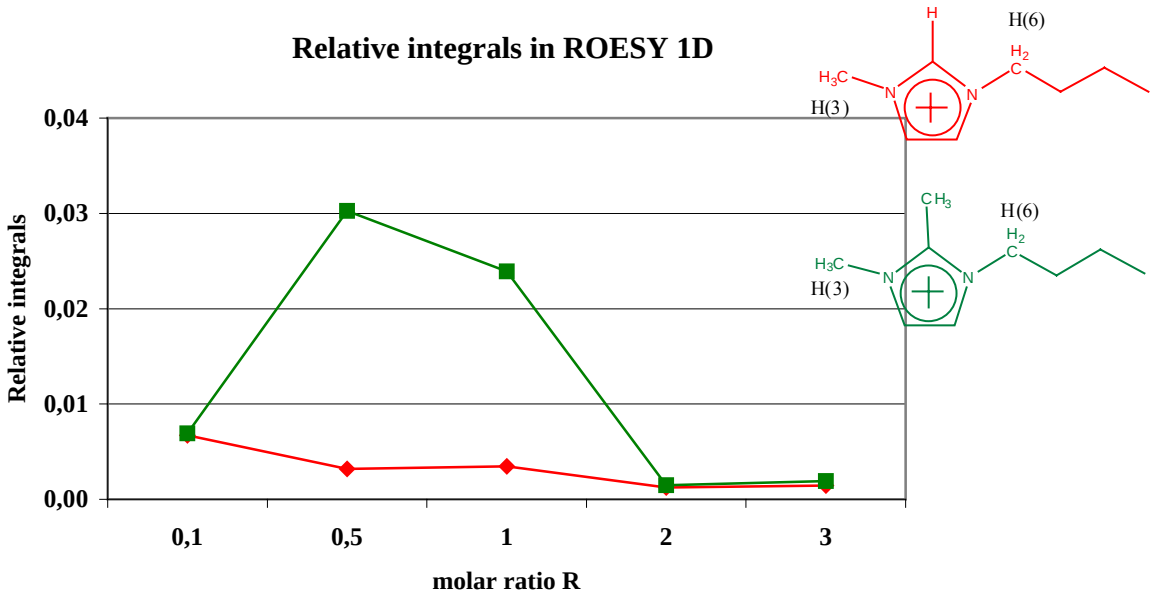

Figure 8. Normalized intensity of integrals of ROESY experiments at various molar ratio (R) for the systems : H(3) and H(6) in To/BMIMNTf$_2$ (red curve) and in To/BMMIMNTf$_2$ (green curve)

In the system To/BMMIMNTf$_2$, ROESY intensity increases when R varies from 0 to 0.5 then sharply decreases to zero when R varies from 1 to 2.

On the contrary, in the systems To/BMIMNTf$_2$, no particular interaction is evidenced. ROESY intensity is weak when R varies from 0 to 1 and decreases to zero for R equal to 2.

2.5 Estimation of intermolecular distances by extrapolation of ROESY experiments

The measures of ROESY intensities are related to the mean distances between toluene molecules and imidazolium rings and the treatment of data collected in a ROESY spectrum can be used to calculate the interproton-distances. Consequently it is possible to determine precisely the distance ($r_{To\text{-}IL}$) separating irradiated methyl group of toluene (H(Me)) and H(3) and H(6) of imidazolium rings because the intensity of the integrals ($I_{To\text{-}IL}$) is inversely proportional to intermolecular distances (figure 9).

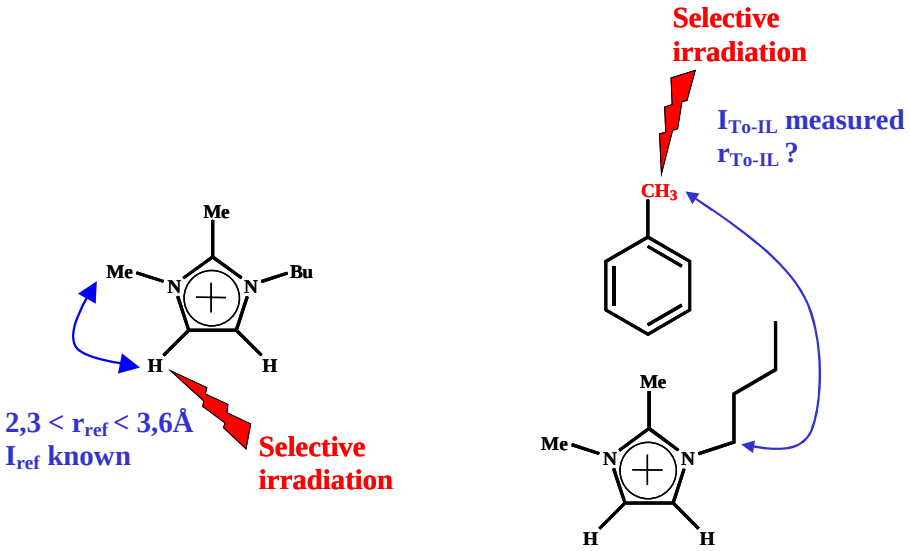

Figure 9. Representation of method to calculate intermolecular distances from ROESY experiments

Note that the intensity of reference integral (I_{ref}) has been measured in the same experimental conditions. The reference distance (r_{ref}) between H(4) and H(3) of imidazolium rings has been determined by modelling using crystallographic data.[21] As methyl protons group (H(3)) are very mobile, the minimal and the maximal distances in respect with H(4) have been considered and the exact value have been surrounded.

Using the ROESY integrals, one can directly use the following relation to calculate the distances r_{To-IL} from a known reference distance r_{ref}[38] :

$$r_{To-IL} = r_{ref} \left(\frac{I_{ref}}{I_{To-IL}}\right)^{\frac{1}{6}}$$

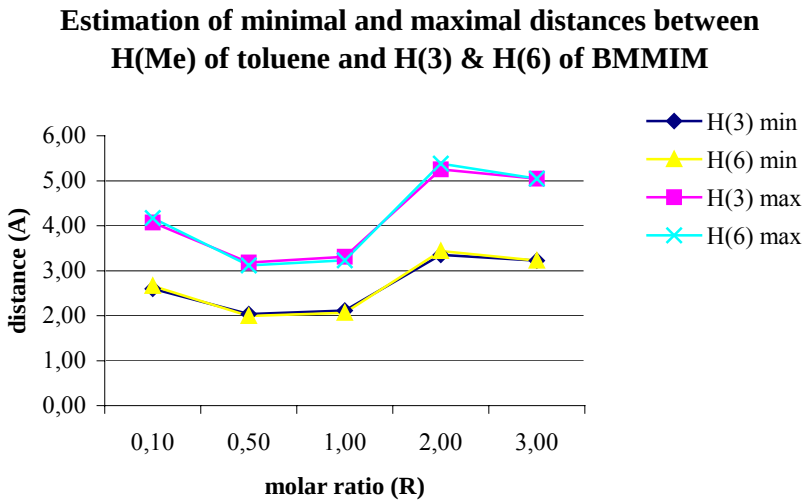

Figure 10. Evaluation of distances between methyl proton of toluene and BMMIM

As the maximal and minimal distances between H(Me) of toluene and both proton groups H(3) and H(6) of BMMIM are almost identical, the methyl group of toluene have to be in a parallel plan of imidazolium ring.

Moreover it indicates a strong interaction between toluene and BMMIM for molar ratio R=0.5 or R=1 and that toluene is the closest to cation BMMIM for molar ratio R=0.5 which corresponds to one molecule of toluene for two cations i.e. a "sandwich" structure. The extrapolation of ROESY integrals shows that toluene molecules are located at about 3Å from imidazolium rings which is consistent with data given in the literature. Indeed neutron diffraction study have evaluated that benzene-MMIMPF$_6$ distance is about 3.5Å.[8]

2.6 Study of the Interaction between toluene and IL by DOSY experiments

DOSY (Diffusion Order SpectroscopY) uses pulsed field gradient NMR spectroscopy to measure translational diffusion and enables the determination of diffusion coefficients of a molecule dissolved in a medium. Assuming a spherical size of the molecule, the diffusion coefficient D is described by the Stokes-Einstein equation:

$$D = \frac{kT}{6\pi\eta r_s}$$

k : Boltzman constant

T : temperature

η : viscosity of the liquid

r_s : (hydrodynamic) radius of the molecule.

Consequently, the diffusion coefficient D value of the same molecule in two different solvents is dependent on the viscosity value η of the solvent : $D_1 x \eta_1 = D_2 x \eta_2$.[39]

NMR DOSY spectra of the systems To/BMIMNTf$_2$ and To/BMMIMNTf$_2$ at molar ratio R=0.5 has been recorded. It has been determined that toluene diffuse in BMIMNTf$_2$ at D=220 μm^2/s but only at D=121μm^2/s in BMMIMNTf$_2$. The viscosity of IL dramatically decreases upon addition of molecular solvents. Surprisingly, for each IL, the viscosity variations according to the molar fraction of molecular solvent are practically independent of the solvent nature. In agreement with results previously reported, the experimental data obtained with different organic solvents can be fitted to a single exponential equation: $\eta = \eta_i e^{-x/a}$ where η and η_i are the viscosity of the mixture and of pure IL respectively, x the molar fraction of organic solvent and a is a constant depending on IL nature.[40] For BMIMNTf$_2$, the value of a is found equal at 0.351±0.012.[41] Consequently, for molar ratio of To/BMIMNTf$_2$ of 0.5 corresponding to molar fraction of 0.66, the viscosity of the medium is about 8cP versus

52cP in neat $BMIMNTf_2$. Unfortunately, *a* value for $BMMIMNTf_2$ is unknown. However as the *a* value is related to the strength of the interaction anion-cation, which is stronger in $BMIMNTf_2$ compare to $BMMIMNTf_2$ due to the presence of hydrogen bond with H(2) in the first one,[25] consequently the *a* value of $BMMIMNTf_2$ is expected to be lower than 0.351±0.012 and a sharp decrease of the viscosity in the system To/$BMMIMNTf_2$ is expected to about 16cP compared to 97cP in neat $BMMIMNTf_2$.[40-42] The experimental D value in To/$BMMIMNTf_2$ ($D_{exp.}$=121μm^2/s) is found slightly higher than the D value calculated from equation ($D_{cld.}$≈110μm^2/s). Consequently the difference of viscosity can not totally explain why the mobility of toluene is so much reduced in $BMMIMNTf_2$.

To conclude, the use of NMR techniques such as evolution of ^{1}H chemical shifts, ROESY and DOSY experiments enable the detection of intermolecular interactions between the π-system of toluene and imidazolium cation based IL.

^{1}H chemical shift changes at molar ratio inferior to R=1 in To/$BMMIMNTf_2$ have been attributed to the aromatic ring current effect. Indeed the interaction between two π-systems of aromatics and imidazolium rings leads to share electronic densities of both compounds. Toluene which is electron-rich increases the electronic density of electron-deficient imidazolium rings and *vice versa*. **ROESY experiments** confirm that BMMIM interacts strongly with toluene molecule and aromatic molecules are located very close to imidazolium ring compared with $BMIMNTf_2$. **DOSY studies** also demonstrated that the mobility of toluene in $BMMIMNTf_2$ is reduced due to this interaction.

These preliminary results of the representation of To/$BMIMNTf_2$ and To/$BMMIMNTf_2$ systems by explicit force fields[43,44] confirm that for molar ratio R=1, the H(Me) and H(Ar) of toluene is closer to H(9) of the butyl chain of $BMIMNTf_2$ but on the contrary, both methyl H(Me) and aryl group H(Ar) of toluene are significantly closer to carbon in position 2 of imidazolium ring (C-Me) in $BMMIMNTf_2$.[45]

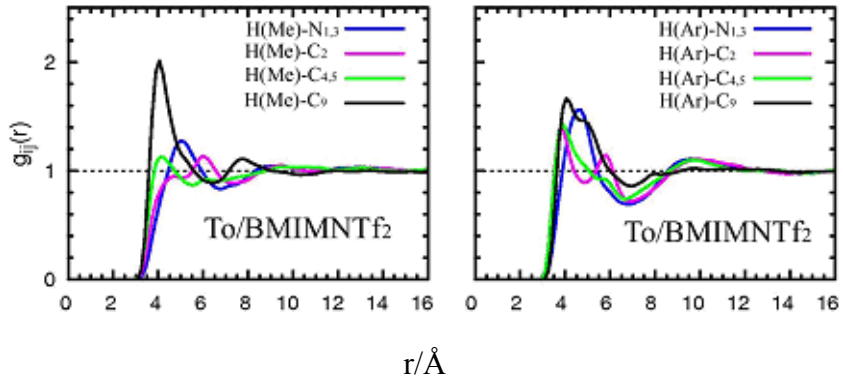

Figure 11. Radial distribution of To/BMIMNTf$_2$

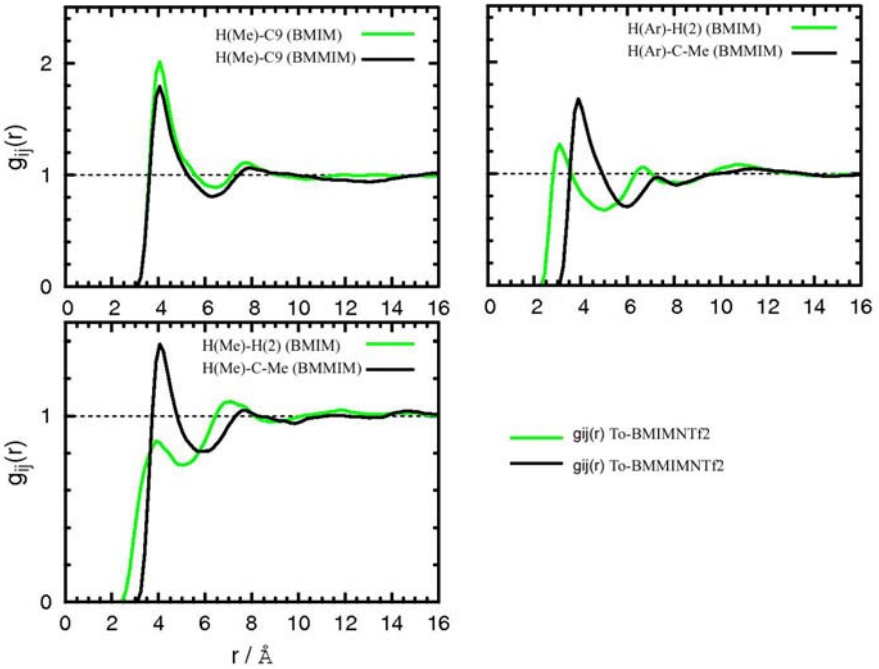

Figure 12. Comparison of radial distribution of To/BMIMNTf$_2$ and To/BMMIMNTf$_2$

Considering the mixture of To/IL at various molar ratio, important differences between both IL have been observed. Indeed it appears that in case of To/BMIMNTf$_2$, toluene molecules are very close ones from the others in molar ratio R=1 and R=3 and concomitantly imidazolium rings are probably efficiently packed. On the contrary, the distance between toluene and imidazolium ring in To/BMMIMNTf$_2$ system is probably less important.

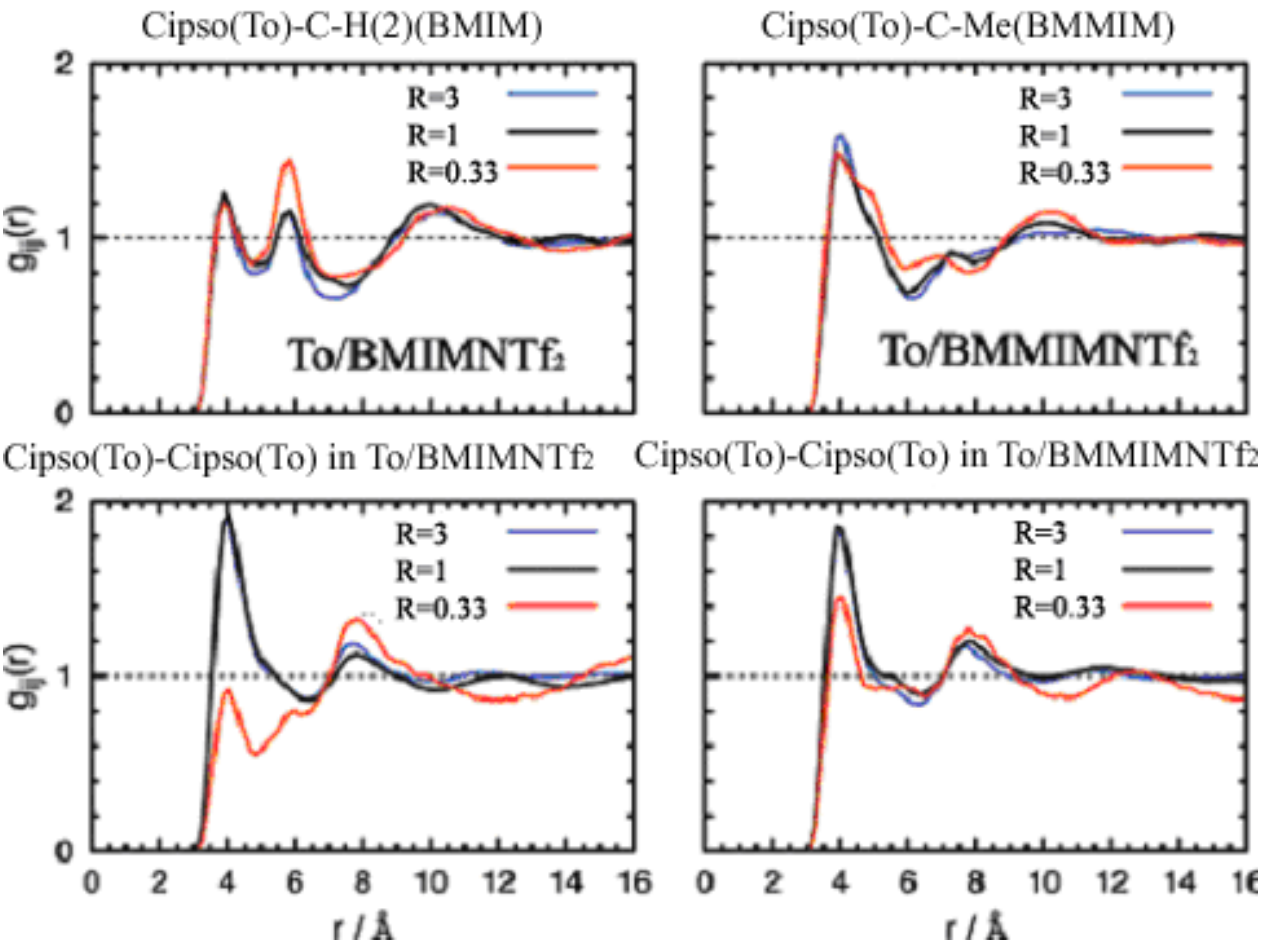

Figure 13. Radial distribution of To/BMIMNTf$_2$ and To/BMMIMNTf$_2$ at various molar ratio R

Since, all experimental factors are the same (concentration, temperature, identical conditions for NMR experiments), the difference in the observed phenomena result from the nature of IL. As the anion NTf_2 is the same, therefore the difference in these experiment are mainly due to the nature of cation. The alkylation at position C_2 of the imidazolium cation reduces the H-bond acidity of the cation (for instance, Kamlet-Taft α value of $EMIMBF_4$ and $EMMIMBF_4$ are 0.73 and 0.40 respectively) influencing drastically its 3D-organization and its ability to H-bond with the coexisting components. Indeed it has been shown that the cation-anion association energies are slightly lower (<20kJ.mol-1) for the ion pairs of BMMIMCl compared to those of BMIMCl. Moreover, the cations and anions of BMMIMCl are in general more ionic that those of BMIMCl and the positive charges in BMIMCl are localized on the peripheral H atoms and spread out over the C2-H moiety, while in BMMIMCl, the charge spread out over the C2-H moiety resides entirely on C2. Such localization of charge facilitates stronger Coulombic interactions.[25]

In molar ratio R inferior to 1, in 1,3-dialkylimidazolium cation (BMIM), the H(2) acidic proton are strongly linked to the anion by hydrogen-bond and consequently, BMIM cation can not interact with π-systems because aromatic molecules are not able to cleave hydrogen-bond. This assessment is supported by two recent results. On one hand, the IR and Raman spectra of the dilute solution of $EMIMBF_4$ in CH_2Cl_2 prove that ion pairing is not destroyed by the solvent.[46] On the other hand, solid-liquid phase diagram study and X-ray structure determination experimentally demonstrate that the aromatic plane of benzene and the EMIM cation are not stacked in piles of parallel arrangements, rather they exhibit two orientations quasi perpendicular to each other[47], contrary to Holbrey's clathrates in which MMIM cation occupies positions above and below the plan of the benzene aromatic ring.[7]

On the contrary, in case of $BMMIMNTf_2$, NMR studies and modelling results indicate that toluene is coplanar to the imidazolium ring plans and presents a very strong interaction for molar ratio R=0.5 or R=1. Consequently, toluene has probably penetrated the IL network and is located between two imidazolium ring plans with which it strongly interacts. (Figure 13)

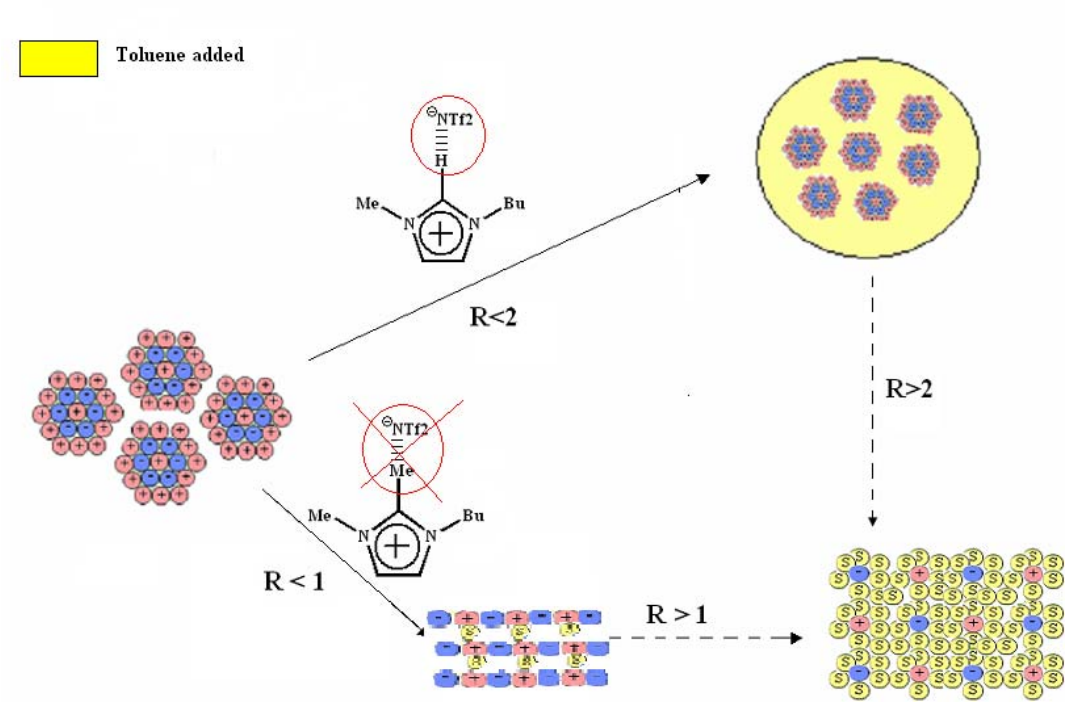

Figure 14. Attempts to represent IL structure in function molar ratio To/IL

2.7 Generalization : presence of interaction between 1,3-cyclohexadiene, cyclohexene and IL

Even if π-cation interaction are only reported between cations and aromatic compounds, we wondered if it can occur with dienes or monoenes.

Due to the low solubility of these two substrates, only ROESY and DOSY NMR experiments have been performed on systems CYD/IL (R=0.5) and CYE/IL (R=0.1) with IL : $BMIMNTf_2$ and $BMMIMNTf_2$.

- ROESY experiments

NMR ROESY performed on the system CYD/IL enables measurement of the intensity of the intermolecular interactions and the determination of mean distances between cation and CYD. Molecular dynamics have been performed using SYBYL software (version 7.0, Tripos Inc.1699 South Hanley Rd., St.Louis, Missouri, 63144, USA) according the TRIPOS force field developed by Clark *et al.*[48] Intermolecular distances have been fixed using results from NMR ROESY experiments and the energy of systems : CYD/BMIM and CYD/BMMIM have been minimized.

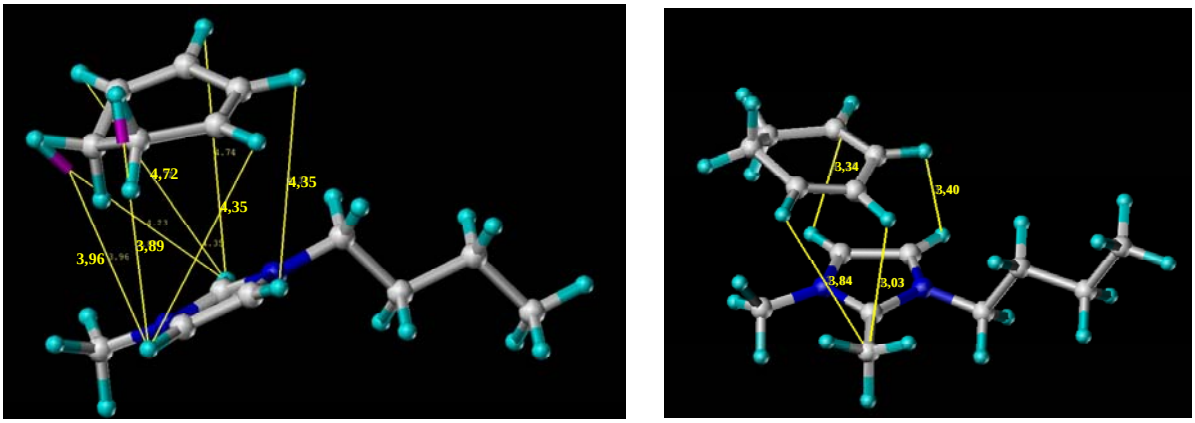

a **b**

Figure 15. SYBYL Representation of a) CYD/$BMIMNTf_2$ and b) CYD/$BMMIMNTf_2$ from ROESY NMR extrapolation

The CYD is found at 3-3,5Å from $BMMIMNTf_2$ and 4-4,5Å from $BMIMNTf_2$.

For CYE, the same experiments show that CYE is closer to BMMIM (3-4Å) than to BMIM (4-5Å).

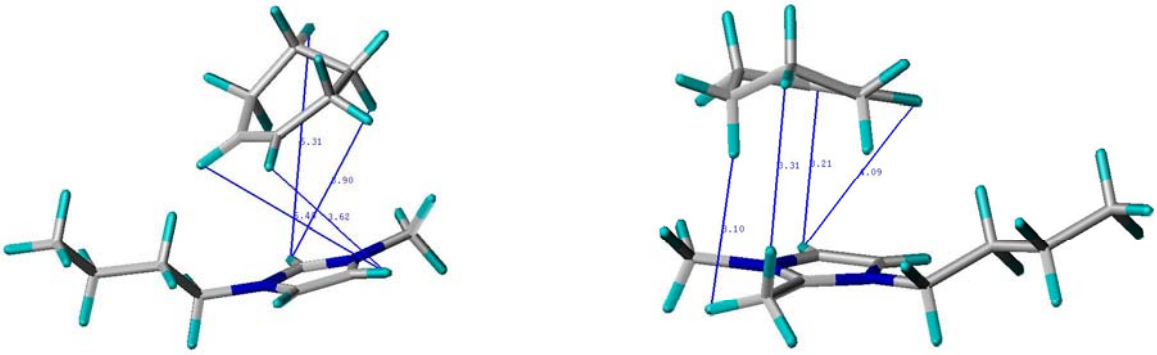

a **b**

Figure 16. SYBYL Representation of saturated solutions of a) CYE/BMIMNTf$_2$ and b) CYE/BMMIMNTf$_2$ from ROESY NMR extrapolation

Like To, ROESY experiments demonstrate that CYD and CYE are significantly closer to BMMIM cations.

- DOSY experiments.

Diffusion coefficients (D) of 1,3-cyclohexadiene in both IL determined from extrapolation of DOSY data are D=187,5 µm^2/s in BMIMNTf$_2$ while two different forms of CYD have been detected in BMMIMNTf$_2$ diffusing at D=78µm^2/s and D=97µm^2/s.

For the same reason as in To/BMMIMNTf$_2$, the strong interaction of 1,3-cyclohexadiene decreases its mobility in the media.

2.8 Conclusion of NMR studies

For toluene, 1,3-cyclohexadiene and cyclohexene, ^{1}H chemical shift studies or ROESY experiments demonstrated that interactions between all substrates are more important with BMMIMNTf$_2$ than with BMIMNTf$_2$. DOSY studies show that all substrates have a reduced mobility in BMMIMNTf$_2$.

3 Consequences on catalytic activity in hydrogenation

We have demonstrated that unsaturated hydrocarbons have a particular behaviour in BMMIMNTf$_2$ due to strong interactions between imidazolium rings and the π-system of cyclic hydrocarbons. What are the consequences of these interactions on catalytic hydrogenation ?

Two model reactions, one in heterogeneous and the other in homogeneous conditions, have been studied : hydrogenation of benzene using ruthenium nanoparticles (RuNP) and hydrogenation of 1,3-cyclohexadiene and cyclohexene by an ionic homogeneous rhodium catalytic system.

In order to compare specific solvation effects of both IL systems in hydrogenation reactions, all experimental conditions have to be identical. But some parameters are only governed by the nature of IL and could be different in respect with the medium. For instance, the solubility of reactants is dependent on the concentration of other organic substrates and products :

- At atmospheric pressure, the solubility of hydrogen in neat IL is $0.77x10^{-3}$ and $0.86x10^{-3}$ $mol.L^{-1}$ in $BMIMNTf_2$ and $BMMIMNTf_2$ respectively. But in presence of benzene (Bz/IL : 1:3 V:V i.e R≈1), the solubility increases to $1.4x10^{-3}$ and $1.5x10^{-3}$ $mol.L^{-1}$ in $BMIMNTf_2$ and $BMMIMNTf_2$ respectively.[49] As the solubility of H_2 in both LI is similar, the effect of this factor in the possible difference of activity could be considered as negligible.
- The solubility of benzene is 40 and 38%wt in $BMIMNTf_2$ and $BMMIMNTf_2$ respectively and the solubility of cyclohexane is 4 and 2%wt in $BMIMNTf_2$ and $BMMIMNTf_2$ respectively. Moreover, when a molar mixture of CYA/Bz (1/1) is dissolved in IL, in the identical experimental conditions, the solubility of benzene has been found at 12 % and 11 %wt in $BMIMNTf_2$ and $BMMIMNTf_2$ respectively. These results implies that during the catalytic reaction, when the benzene is converted into CYA (low soluble in IL) the aromatic, which is more soluble in CYA, is extracted from the IL phase and consequently no more in contact with the catalyst system. The initial monophasic system becomes biphasic.

Consequently only the data obtained at low concentration and low conversion could be compared. For this reason, all hydrogenations have been performed at 30°C (temperature controlled bath) and atmospheric hydrogen pressure (1.2atmH_2).

3.1 Hydrogenation of benzene in IL using ruthenium nanoparticles

Recent studies show that IL is a good media to generate metal nanoparticles and ruthenium nanoparticles (RuNP) are promising catalysts for hydrogenation of aromatic compound (for details see Chap IV).[50]

The synthesis of RuNP in imidazolium based IL have been performed in a stirred reactor by decomposition of (η^4-1,5-cyclooctadiene)(η^6-1,3,5-cyclooctatriene)ruthenium (0) complex (Ru(COD)(COT)) under 4 bar of hydrogen at 25°C for 18h. After a treatment under vacuum in order to remove formed cyclooctane (COA), it affords a stable colloidal suspension of RuNP dispersed in IL. Note that no precipitation have been detected for several months.

$$\mathbf{Ru(COD)(COT)} \xrightarrow[\mathbf{IL\ or\ solvent}]{\mathbf{H_2\ (4atm),\ 18h,\ 25°C}} \mathbf{RuNP} \quad + \quad \mathbf{2\ COA}$$

The size and size distribution of RuNP in IL were determined *in situ* by transmission electronic microscopy (TEM) depositing a droplet on holey carbon film supported by a copper grid (Figure 15).

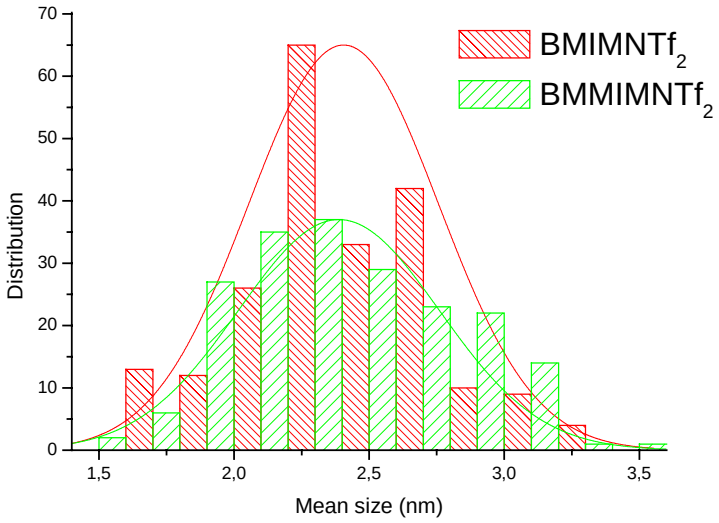

Figure 17. Size histograms of RuNP synthesized in $BMIMNTf_2$ and $BMMIMNTf_2$

The mean size of RuNP in $BMIMNTf_2$ and $BMMIMNTf_2$ are 2,4+/-0,3 and 2,4+/-0,4nm respectively and their distributions are homogeneous. Even if the distribution is narrower in the case of $BMIMNTf_2$, it has been assumed that RuNP catalysts are similar. Some

differences of catalyst surface ligand or stabilization could also be discerned (see details chapter IV), but the catalytic activity should be related to the available surface active sites determined by the size of RuNP.

These Ru catalysts prepared *in situ* have been used for the hydrogenation of benzene into cyclohexane. To a solution of RuNP nanoparticles, benzene was added to reach molar ratio of R=0.5 (one mole of benzene for 2 moles of IL) and the reactor was pressurized at 4 bar of dihydrogen for 4h at 30°C :

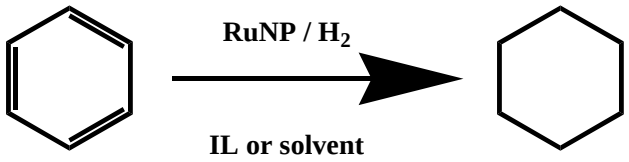

The resulting solutions have been dissolved in acetonitrile (known to prevent IL from organization) and their compositions were evaluated by GC analyses in presence of an internal standard (toluene).

The observed conversion of benzene into cyclohexane at 30°C under 4 bar of hydrogen after 4h in $BMIMNTf_2$ (37%) is higher than in $BMMIMNTf_2$ (20%). No significant formation of cyclohexene has been detected in these conditions.

The study of the conversion of benzene into cyclohexane as a function of time in both IL has been performed at room temperature under 1.2bar of H_2. To have a correct mass balance, the conversions have been determined by GC-analyses by dissolving the entire reaction system in acetonitrile in the presence of an internal standard. As a result, each point corresponds to one experiment.

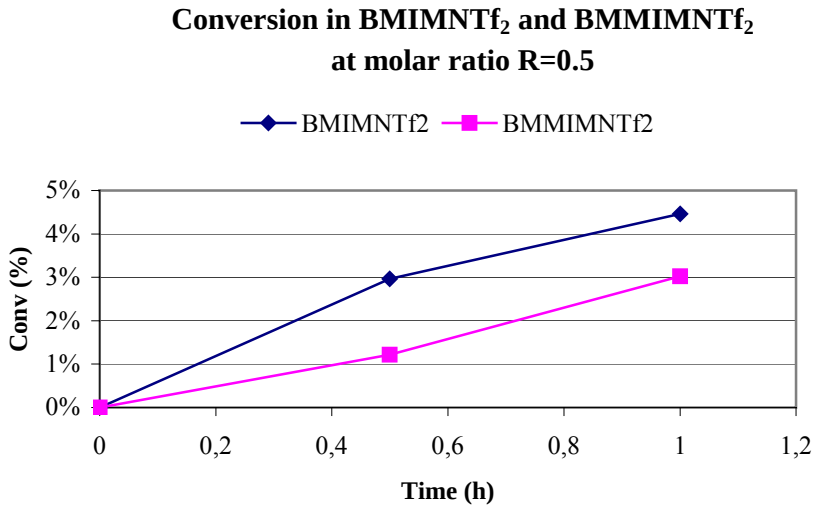

Figure 18. Conversion of benzene into cyclohexane in $BMIMNTf_2$ and $BMMIMNTf_2$ at molar ration R=0.5

The conversion which is almost twice as fast in $BMIMNTf_2$ than in $BMMIMNTf_2$ confirms that the hydrogenation of benzene is less efficient in $BMMIMNTf_2$.

These observations could be related to the presence of stronger interactions, detected in NMR, between BMMIM cations and aromatic π-system which reduce the mobility and the accessibility of benzene in this medium compared to $BMIMNTf_2$.

3.2 Hydrogenation of 1,3-cyclohexadiene using ionic rhodium based catalyst

It is possible to hydrogenate selectively 1,3-cyclohexadiene into cyclohexene with good conversion and selectivity using Osborn's type complex : $[Rh(NBD)(PPh_3)_2]PF_6$ (NBD=norbornadiene) in IL media such $BMIMSbF_6$ or $BMIMPF_6$.[30]

In order to study this system but to avoid any anion exchange between IL and the catalyst, the synthesis of $[Rh(COD)(PPh_3)_2]NTf_2$ (COD = 1,5-cyclooctadiene) has been developed from a similar procedure. This original rhodium complex has been fully characterized by ^{1}H, ^{31}P, ^{13}C NMR, mass spectrometry and UV-Vis spectroscopy.

1,3-cyclohexadiene is added to the yellow solution of $[Rh(COD)(PPh_3)_2]NTf_2$ dissolved in $BMIMNTf_2$ or $BMMIMNTf_2$ to reach a molar ratio of R=0.5. The resulting red solution is stirred under 1.2bar of hydrogen at 30°C. To avoid any problem and particularly the

appearance of second phase during the reaction, the conversion has been determined by GC-analyses of the entire reaction system by dissolving it in CH_3CN/To 99:1. As a result, each point corresponds to one experiment and this studies have been performed in a carrousel apparatus.

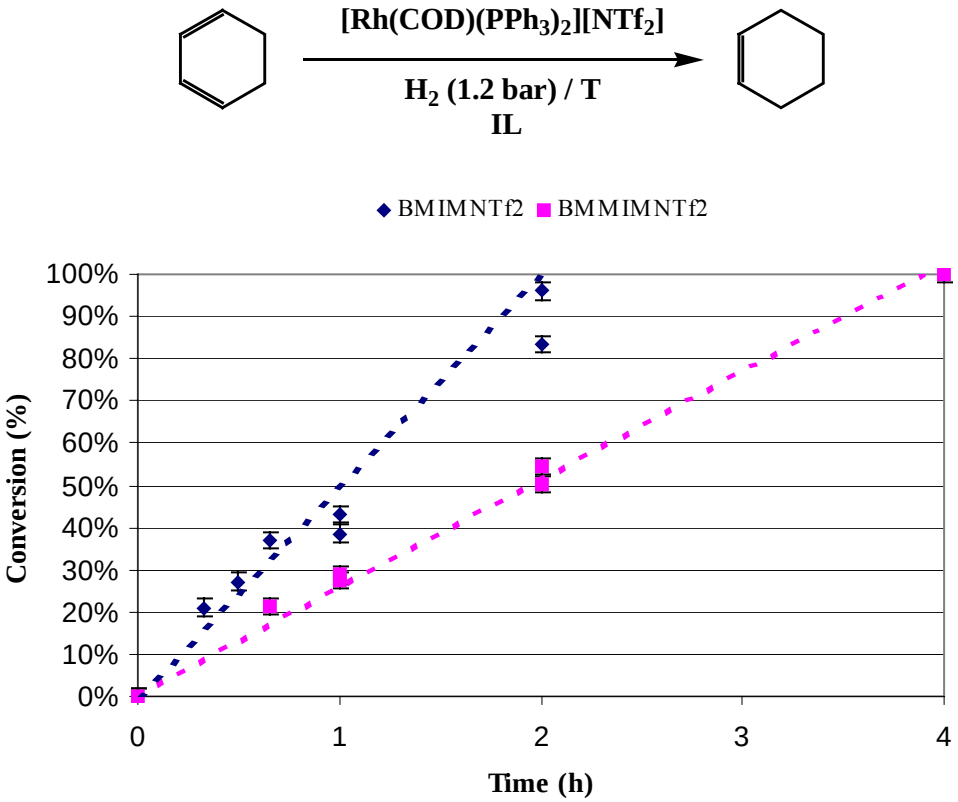

Figure 19. Hydrogenation of 1,3-cyclohexadiene in $BMIMNTf_2$ and $BMMIMNTf_2$ at 30°C under 1.2atm H_2 (R=0.5 and r = n(CYD)/n(Rh) =500)

The hydrogenation of 1,3-cyclohexadiene under 1.2bar H_2 by $[Rh(COD)(PPh_3)_2]NTf_2$ in both IL leads quantitatively and selectively to cyclohexene. In all cases, no significant amount (less than 2% at high or complete conversion) of cyclohexane have been detected by GC. As described in the literature, the rate of 1,3-cyclohexadiene reduction is constant till near the endpoint (l mol of H_2 absorbed) and cyclohexene is produced essentially quantitatively before it is hydrogenated to cyclohexane.[51]

In $BMIMNTf_2$, the conversion is complete in 2hrs. This result is similar to that observed in organic solvent[51] and IL : $BMIMPF_6$ or $BMIMSbF_6$. [30] In $BMMIMNTf_2$, only 50% conversion is obtained after 2hrs and the initial rate is halved.

In organic solvent, the first step of the hydrogenation reaction is (1) :

$$[Rh(COD)(PPh_3)_2]^+ + H_2 \longrightarrow [Rh(PPh_3)_2S_x]^+ + COA \qquad (1)$$

As IL are non-coordinating solvent and that the solubility of hydrogen is very low, the first step of the hydrogenation could be either the hydrogenation of $[Rh(COD)(PPh_3)_2]NTf_2$ or the ligand exchange between COD and CYD resulting in $[Rh(CYD)(PPh_3)_2]NTf_2$.

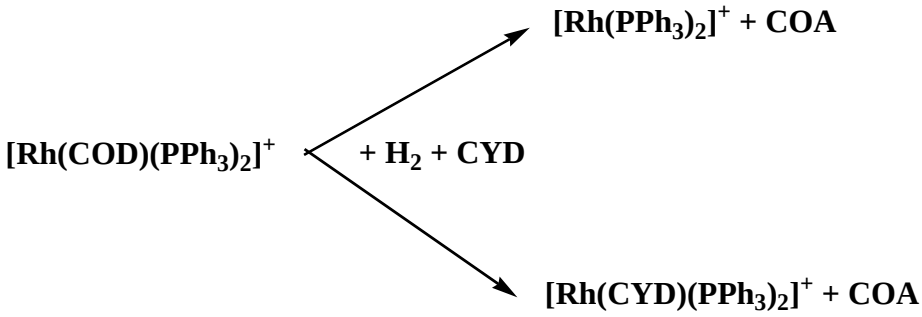

Consequently the ligand exchange reaction has been studied by performing this exchange reaction in both IL. The rhodium complex $[Rh(COD)(PPh_3)_2]NTf_2$ affords $[Rh(CYD)(PPh_3)_2]NTf_2$ in presence of 1,3-cyclohexadiene. These two complexes have been fully characterized by ^1H, ^{31}P, ^{13}C NMR, mass spectrometry and UV-Vis spectroscopy :

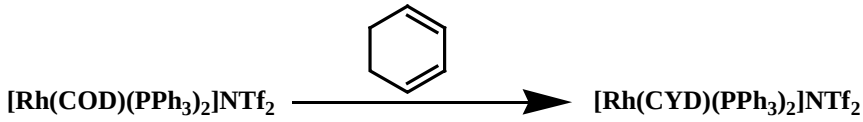

mass spectrometry	**mass spectrometry**
m/z = 735=> $Rh(COD)(PPh_3)_2^+$	m/z = 707=> $Rh(CYD)(PPh_3)_2^+$
m/z= 627,0 => $Rh(PPh_3)_2^+$	m/z= 627,0 => $Rh(PPh_3)_2^+$
m/z= 473,1 => $Rh(COD)(PPh_3)^+$	
NMR (CD_2Cl_2)	**NMR (CD_2Cl_2)**
^1H : 2,2 (8H, m) ; 4,6(4H, s) et 7,5ppm (32H, m)	^1H : 4,3 (2H, d) ; 5.99 (2H, dt) ; 8.80 (36H, m)
^{31}P : 26,5ppm with $^1J(^{103}Rh\text{-}^{31}P)$=145Hz	^{31}P : 25,2ppm with $^1J(^{103}Rh\text{-}^{31}P)$=177Hz
^{103}Rh : -80 ppm with $^1J(^{103}Rh\text{-}^{31}P)$=145Hz	
UV-Visible spectrophotometry	**UV-Visible spectrophotometry**
λ=450nm	λ=500nm

As $[Rh(COD)(PPh_3)_2]NTf_2$ is yellow (λmax=450nm) and $[Rh(CYD)(PPh_3)_2]NTf_2$ red (λmax=500nm), the ligand exchange reaction has been monitored by UV-Vis spectroscopy at λ=500nm. The UV-Vis spectra were recorded every second from the addition of the amount of 1,3-cyclohexadiene corresponding to molar ratio R=0.5 in stirred UV cells (Figure 20).

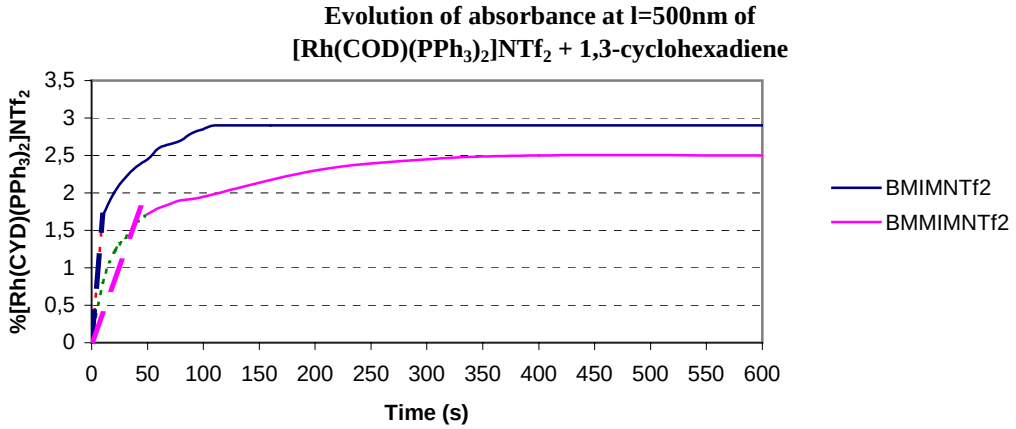

Figure 20. *Formation of [Rh(CYD)(PPh$_3$)$_2$]NTf$_2$ followed at λ=500nm from the complex [Rh(COD)(PPh$_3$)$_2$]NTf$_2$ in IL in presence of 1,3-cyclohexadiene (R=0.5) in function of time.*

The ligand exchange CYD/COD in rhodium complex : [Rh(COD)(PPh$_3$)$_2$]NTf$_2$ is much slower in BMMIMNTf$_2$ than in BMIMNTf$_2$.

Moreover the red complex [Rh(CYD)(PPh$_3$)$_2$]NTf$_2$ becomes colourless in presence of hydrogen. The conversions during the hydrogenation of 1,3-cyclohexadiene using modified complex [Rh(CYD)(PPh$_3$)$_2$]NTf$_2$ instead of [Rh(COD)(PPh$_3$)$_2$]NTf$_2$ have been monitored by UV-Vis spectroscopy in BMIMNTf$_2$ or BMMIMNTf$_2$ (Figure 21).

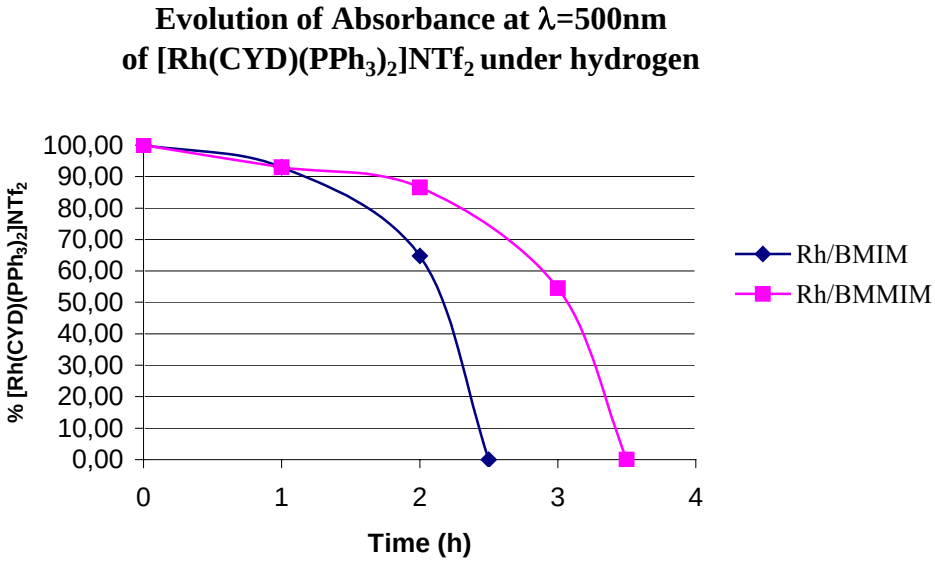

Figure 21. Evolution of the absorbance at λ=500nm of the complex [Rh(CYD)(PPh$_3$)$_2$]NTf$_2$ in presence of hydrogen in function of time.

In the same way, the discolouration of the catalytic system followed by UV-Visible is faster in $BMIMNTf_2$. This result confirm that the CYD is less reactive in $BMMIMNTf_2$ than in $BMIMNTf_2$ because it diffuses slower.

3.3 Hydrogenation of cyclohexene using ionic rhodium based catalyst

$[Rh(COD)(PPh_3)_2]NTf_2$ is also able to hydrogenate cyclohexene into cyclohexane in the same conditions as previously :

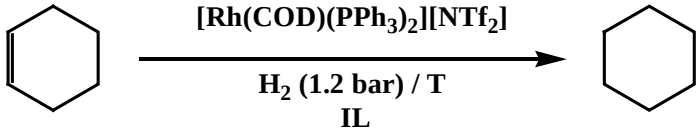

The hydrogenation of cyclohexene in both IL have been performed at 30°C. The reactions have been studied on saturated solutions of CYE/IL because the solubility of cyclohexene is about R=0.1.

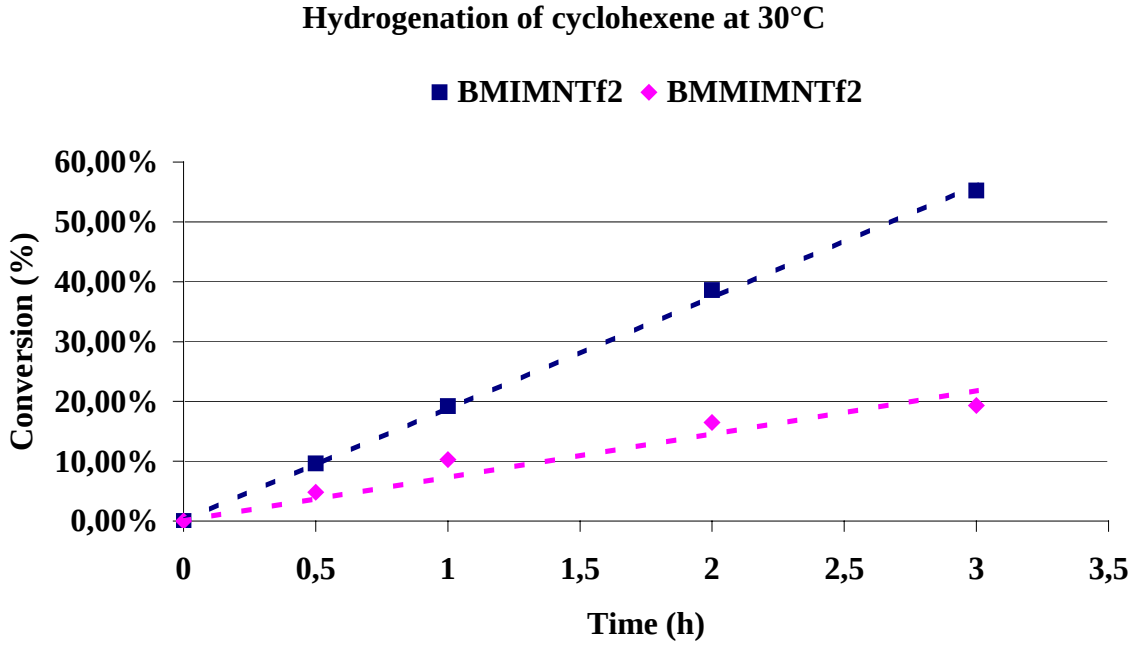

Figure 22. Hydrogenation of cyclohexene in $BMIMNTf_2$ and $BMMIMNTf_2$ at 30°C.

Cyclohexene is hydrogenated into cyclohexane in both catalytic systems but the reaction is slow compare to the hydrogenation of 1,3-cyclohexadiene in cyclohexene in the same conditions.

After 3h, the conversion is only 20% in $BMMIMNTf_2$ while it reaches 55% in $BMIMNTf_2$. For the same reason, the reaction is slower in BMMIM

To conclude, for all substrates, the hydrogenation with homogeneous or heterogeneous catalysts as well the reaction of ligand exchange between 1,3-cyclohexadiene and 1,5-cycloocatdiene are slower in $BMMIMNTf_2$ compare to $BMIMNTf_2$.

Conclusion

The role of π-cation interaction, crucial in biochemistry, has been reported in most of cases for the interaction of ammonium cation with aromatic ring. Although IL are only constituted by charges species, the presence and the influence of π-interaction have never been reported.

The aim of this chapter was to attempt to demonstrate an interaction between π-system of substrates and imidazolium ring of IL and to study their influence on the reactivity of unsaturated substrates in catalytic hydrogenation.

The selected model catalytic reactions are hydrogenation of benzene into cyclohexane using ruthenium nanoparticles and of 1,3-cyclohexadiene into cyclohexene in presence of $[Rh(COD)(PPh_3)_2]NTf_2$.

In order to favor π-interactions between these substrates and cation of IL, two aromatic and planar cations : BMIM and BMMIM have been chosen and associate to NTf_2 anion to generate hydrophobic IL liquid at room temperature.

Firstly the solubility of all substrates have been determined. For all IL, the solubility of hydrocarbons increases when the number of double bonds increases :

benzene ≥ toluene > 1,3-cyclohexadiene > cyclohexene > cyclohexane

The solubility of IL in hydrocarbons have been found relatively low but **not negligible** which can be a major inconvenience in biphasic catalysis .

Then NMR studies (chemical shift evolution, ROESY and DOSY experiments) have been carried out for substrates/IL mixtures at various molar ratio R.

NMR experiments have demonstrated that π-systems of toluene, benzene, 1,3-cyclohexadiene and even cyclohexene interact with the imidazolium cation of $BMMIMNTf_2$ but not in the case of $BMIMNTf_2$.

The molecular dynamics confirm that toluene is closer to the methyl group (H(9)) at the end of the butyl chain of $BMIMNTf_2$ while it is closer to carbon (C-Me) in position 2 of the imidazolium ring of $BMMIMNTf_2$ and in a parallel plane to BMMIM.

The difference of behaviour of toluene in these two system could only be attributed to the presence of H-bonding C2-H…anion in $BMIMNTf_2$ generating a stronger association ($>20kJ.mol^{-1}$) than in the case of $BMMIMNTf_2$. Toluene can not cleave this H-bond in $BMIMNTf_2$ which stay in large aggregates of ionic pairs. On the contrary, toluene can penetrate in less strongly bonded network of $BMMIMNTf_2$ and interact with BMMIM cations.

The hydrogenation of all substrates, with homogeneous or heterogeneous catalysts, are **slower** in $BMMIMNTf_2$ compare to $BMIMNTf_2$.

This general observation could be due to several factors :

a) solubility of the reactants (H_2, Aromatic)
b) difference of the nature of the catalyst
c) viscosity of the media
d) interaction with cation

The effects of the factors a) and b) have been reduced as much possible as explained above by choosing very precise experimental conditions such as low temperature, low concentration, low conversion and similar catalyst. Even if the influence of viscosity could not be totally excluded, the proximity and the π-interaction of all unsaturated studied substrates with BMMIM have a major effect on their reactivity. Their diffusion is slower, they are less accessible and consequently their reactivity decreases in catalytic hydrogenation compare to BMMIM.

Experimental Section

1-methylimidazole (>99%), 1,2-dimethylimidazole (>98%) (Aldrich) were distilled prior to use. Anhydrous toluene (99,8%), benzene (99%), 1,3-cyclohexadiene (97%), cyclohexene (>99%) and cyclohexane (99,5%) (Aldrich) are distilled and stored on zeolithe. 1,5-cyclooctadiene (Aldrich) was purified through an alumina column prior to use. Bis(trifluoromethanesuflonyl)imide lithium salt (>99%, Solvionic company), zinc powder (Merck) and $RuCl_3.xH_2O$ (Avogado) was dried under vacuum prior to use. Only $[Rh(COD)Cl]_2$ (>99%, Strem) were used as received.

GC Analyses

The products were quantitatively analysed by gas chromatography on a HP6890 chromatograph equipped with FID detector and a Al_2O_3/KCl column (L=50m, ϕ_{int}=0.32mm, film thickness = 5µm). Injector and detector temperature was 230°C and injection volume 1µL. The temperature was fixed at 190°C. From those relative response factors, the mass of each product can be determined by the general formula :

$$M(x) = K(x) \bullet \left(\frac{A(x)}{A(s)} \right) \bullet M(s)$$

With: M(x) = Mass of product x

K(x) = Relative response factor of product x

A(x) = GC area of product x

A(s) = GC area of standard (butylbenzene)

M(s) = Mass of standard in the sample

Data presentation : Conversion, yields and mass balance are defined by the following equations:

* Conversion of substrates was calculated from unreacted substrates remaining after reaction:

$$\text{Conv. substrate} = \frac{\text{moles of substrate introduced} - \text{moles of substrate final}}{\text{moles of substrate introduced}}$$

* Yield of product A:

$$\text{Yield A} = \frac{\text{moles of product A after reaction} - \text{moles of product A introduced}}{\text{moles of substrate introduced}}$$

* Mass balance:

$$\text{Mass balance} = \frac{\text{moles of product after reaction}}{\text{moles of substrate introduced}}$$

UV-Visible spectrometer

UV-Visible spectra were recorded on a Perkin-Elmer LAMBDA 950 Spectrophotometer. A stirred and closed UV cells has been used.

Mass spectrometry

All mass spectrometry were carried out using a LCQ Advantage HPLC/MS from ThermoFinningan. All solutions were directly introduced into the MS via a syringe pump (ESI as ionization method, sheet gas: nitrogen, flow:5-10, no auxiliary gas).

NMR

^{1}H, ^{13}C and ^{31}P NMR at liquid state data were collected at room temperature on a Bruker AC 300 MHz spectrometer with the resonance frequency at 300,130 MHz.

The solvents used (CD_2Cl_2, $CDCl_3$, C_6D_6) (SDS) were distilled and kept in a rotaflo and used as received. Chemicals shifts are expressed in ppm (singlet = s, doublet = d, doublet of doublet = dd, and multiplet = m) and were measured relative to residual proton of the solvent to $CHDCl_2$ for ^{1}H, to CD_2Cl_2 for ^{13}C and to H_3PO_4 for ^{31}P.

NMR Instrumentation

NMR ROESY and DOSY experiments were carried out on a Bruker DRX 500 instrument at 298 K (nominal) with a resonance frequency at 500,130 MHz.

ROESY(Rotational nuclear Overhauser Effect SpectroscopY)

Rotating-frame **O**verhauser **E**ffect **S**pectroscop**Y** is an experiment in which homonuclear NOE effects are measured under spin-locked conditions. ROESY is especially suited for molecules with motional correlation times (τ_c) such that $\omega\tau_c \sim 1$, where ω is the angular frequency $\omega = \gamma B$. In such cases the laboratory-frame NOE is nearly zero, but the rotating-frame NOE (or ROE) is always positive and increases monotonically for increasing values of τ_c. In ROESY the mixing time is the spin-lock period. During this time spin exchange occurs among spin-locked magnetization components of different nuclei (recall that spin exchange in NOESY occurs while magnetization is aligned along the z axis). Different spectral density functions are relevant for ROESY than for NOESY and these cause the ROE's to be positive for all values of τ_c. ROESY spectra can be obtained in 2D absorption mode. This is also useful for the identification of certain artifacts. Spurious cross peaks, both

COSY-type and TOCSY-type, can be observed due to coherence transfer between scalar coupled spins. COSY-type artifacts (anti-phase) arise when the mixing pulse transfers antiphase magnetization from one spin to another (the long spin-lock pulse acts like the mixing pulse in COSY). TOCSY-type artifacts (which have the same phase as the diagonal peaks, while ROESY cross peaks have the opposite phase) arise when the Hartmann-Hahn condition is met (e.g., when spins A and B have opposite but equal offsets from the transmitter frequency or when they have nearly identical chemical shifts). In general, to minimize these artifacts, it is suggested to limit the strength of the spin-locking field [52] or to apply a strong off resonance field.

The 2D sequence was built with the scheme proposed by Bodenhausen [53]. The mixing time (200ms) is split in 2 parts separated by a π-pulse. At each side of the spin lock the B1 field is ramped linearly (4,5ms) to insure adiabatic conditions for spinlock. During the first spinlock pulse, the frequency is shifted to O1 + Δf whereas the second pulse frequency is set to O1 - Δf, where O1 is the offset frequency and Δf set to give a B1 field at the magic angle. On this way, the ROESY response is roughly constant upon the spectra width of interest.

For 1D sequence, PFGSE (Pulse Field Gradient Spin Echo for Selective Excitation) have been used and spinlock followed the same scheme as previously.

ROESY pulse sequences.

Notice that the pulse **p1** must be set to the appropriate 90° time obtained after pulse calibration. The pulse **p17** is the cw spinlock pulse, during which ROE buildup occurs.

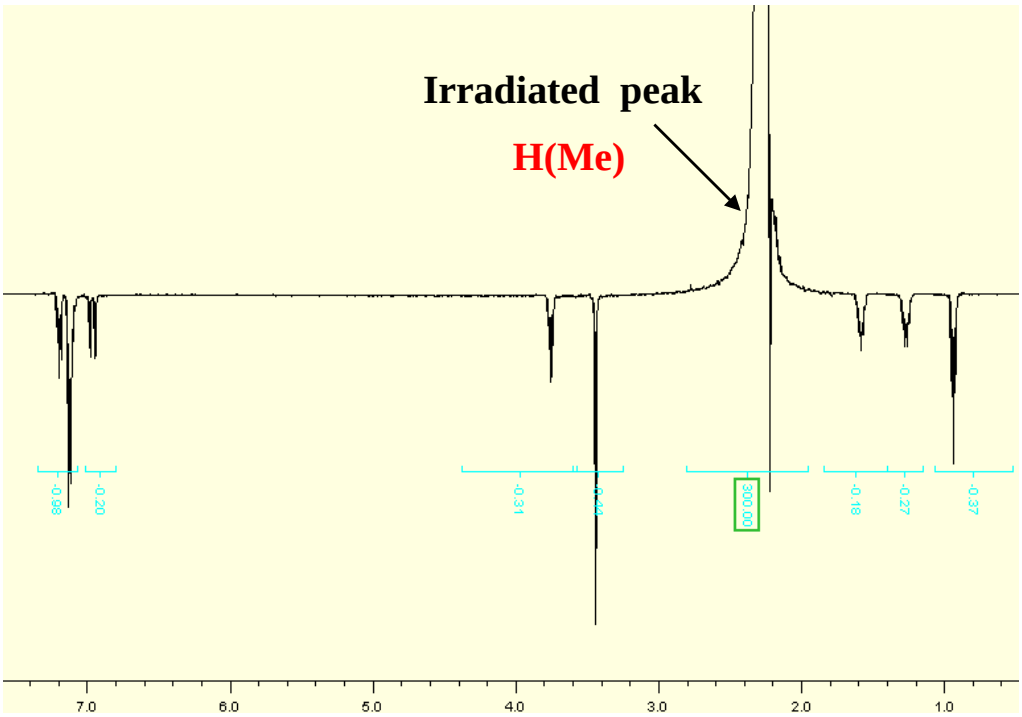

ROESY Spectrum of To/BMMIMNTf$_2$ at molar ratio 0.5

DOSY (Diffusion Order SpectroscopY)

Molecules in liquid or solution state move. This translational motion is, in contrast to rotational motion, known as Brownian molecular motion and is often simply called diffusion or self-diffusion. It depends on a lot of physical parameters like size and shape of the molecule, temperature, and viscosity. Assuming a spherical size of the molecule the diffusion coefficient ***D*** is described by the Stokes-Einstein equation:

$$D = \frac{kT}{6\pi\eta r_s}$$

k : Boltzman constant

T : temperature

η : viscosity of the liquid

r_s : (hydrodynamic) radius of the molecule.

Pulsed field gradient NMR spectroscopy can be used to measure translational diffusion of molecules and is sometimes referred to as q-space imaging. By use of a gradient, molecules can be spatially labelled, i.e. marked depending on their position in the sample tube. If they move after this encoding during the following diffusion time Δ, their new position can be decoded by a second gradient. The measured signal is the integral over the

whole sample volume and the NMR signal intensity is attenuated depending on the diffusion time **Δ** and the gradient parameters (**g**, **δ**). This intensity change is described by

$$I = I_0 \, e^{-D\gamma^2 g^2 \delta^2 (\Delta - \delta/3)}$$

I : the observed intensity

I₀ : reference intensity (unattenuated signal intensity)

D : diffusion coefficient

γ the gyromagnetic ratio of the observed nucleus

g the gradient strength

δ the length of the gradient

Δ the diffusion time.

To simplify this equation some parameters are often combined

$$I = I_0 \, e^{-Dq^2 (\Delta - \delta/3)} \quad \text{or} \quad I = I_0 \, e^{-DQ}$$

to emphasize the exponential decay behaviour. If bipolar gradients are used for dephasing and rephasing a correction for the time τ between those bipolar gradients has to be applied :

$$I = I_0 \, e^{-D\gamma^2 g^2 \delta^2 (\Delta - \delta/3 - \tau/2)}$$

2D DOSY experiments used a slightly modified Bruker experiment ledbpgp2s to improve lineshape and trapezoidal gradients where implemented for shorter pulses gradients. The diffusion evolution time was set to 100ms, the constant amplitude part of the gradient was set to 3ms, and the cosine raising and falling part of gradient where set to 150µs. The diffusion space where sampled by 32 linearly spaced gradients.

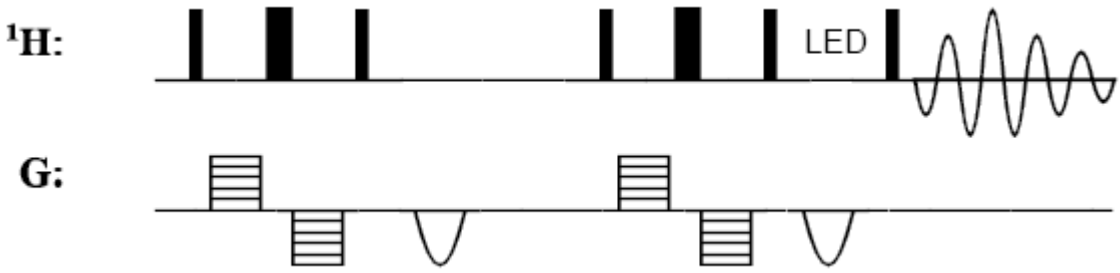

DOSY pulse sequences.

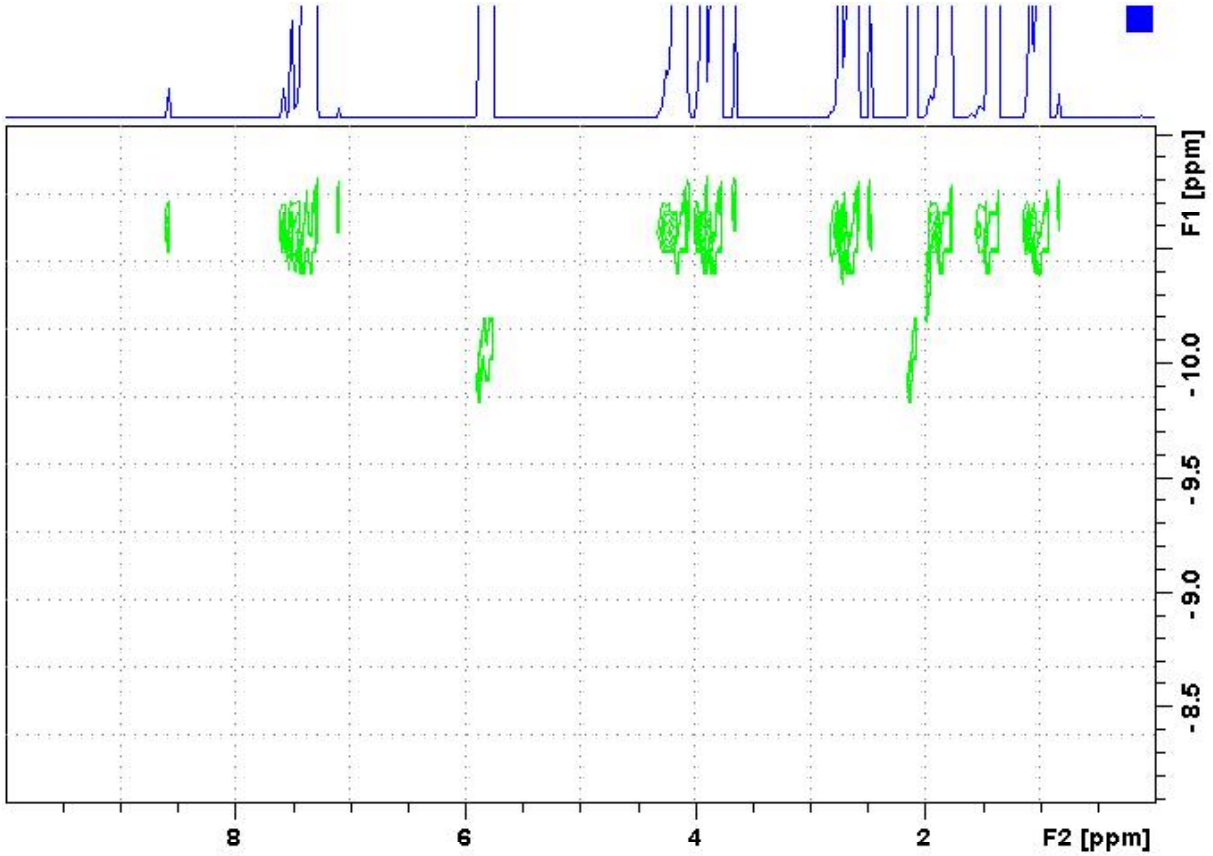

Figure. DOSY spectrum of CYD/BMMIMNTf$_2$ at molar ratio R=0.5.

Modelisation using SYBYL software.

Molecular dynamics have been performed using SYBYL software (version 7.0, Tripos Inc.1699 South Hanley Rd., St.Louis, Missouri, 63144, USA) according the TRIPOS force field developed by Clark *et al.*[48] Intermolecular distances have been fixed using results from NMR ROESY experiments and the energy of systems : CYD/BMIM and CYD/BMMIM have been minimized.

Ionic liquids were prepared according to the known method, dried overnight under high vacuum and stored in a glovebox (Jacomex) in order to guarantee rigorously anhydrous products.

Transmission electron microscopy analyses

Samples for TEM observations were prepared by placing a thin film of the ruthenium nanoparticles dispersed in ionic liquids in a holed carbon grid. The size distribution of the metal particles was determined from the measurement of ≈200 particle, assuming spherical shape, found inside five superstructures.

Determination of solubility of compounds in ionic liquid.

In a glove box, 2mL of toluene, benzene, 1,3-cyclohexadiene, cyclohexene and cyclohexane were added to 1mL of each ionic liquids. The resulting systems were stirred during 24h at 30°C and leads to biphasic system. 0.1mL of the lower phases (IL rich phases) were dissolved in 0.9mL of acetonitrile in presence of an internal standard (toluene or benzene).

Hydrogenations of benzene.

The hydrogenation was carried out either under 1.2atm of H_2 in a Schlenk tube or at 4atm in a glass autoclave.

In usual run, benzene (0.15mL, 1,6mmol) was added to a solution of ruthenium nanoparticles in ionic liquid (1mL) under hydrogen. After 4h of reaction, 4mL of acetonitrile/toluene 99/1 was added to the catalytic solution and the conversion was determined by GC analyses in the same conditions as the determination of solubilities.

Preparation of $[Rh(COD)(PPh_3)_2]NTf_2$: The procedure adapted from the literature.[51]

A system of 100mg of $[Rh(COD)Cl]_2$ (0,2mmol) dissolved in 2mL of dichloromethane and 107mg of $LiNTf_2$ (0,37mmol) dissolved in 2mL of water was stirred vigorously while 405mg of triphenylphosphine was added. After 2h, the dichloromethane layer was removed, washed three times with 2mL of water and dried with Na_2SO_4. Ethanol (1mL) and diethyl ether (2mL) were slowly added to complete crystallization. The orange crystals were filtered off and dried under reduced pressure.Yield : 200mg (99%). ^{1}H-NMR (CD_2Cl_2) : δ (ppm) : 2,2 (m, 8H) ; 4,6 (s, 4H) ; 7,5 (m, 30H) ; ^{31}P-NMR (CD_2Cl_2) : δ (ppm) : 23,6pm with J_{Rh-P}=147Hz

; ^{103}Rh-NMR (CD_2Cl_2) : δ (ppm) : -80ppm with J_{Rh-P}=147Hz ; Mass spectrometry ESI : positive mode : 473, 627 ; negative mode : 280 ; UV-Vis Spectroscopy : λ_{max}=450nm

Hydrogenation of 1,3-cyclohexadiene and cyclohexene

The hydrogenation of 1,3-cyclohexadiene and cyclohexene were carried out at 1.2atm of H_2 and 30°C.

1,3-cyclohexadiene (0.15mL, 1.6mmol) was dissolved in a system of 3.2mg of $[Rh(COD)(PPh_3)_2]NTf_2$ (3.2µmol) of in one of ionic liquids $BMIMNTf_2$ or $BMMIMNTf_2$ (1mL) under argon resulting in red homogeneous solutions.

The same procedure as for the hydrogenation of 1,3-cyclohexadiene has been used for this study. (3.2mg of $[Rh(COD)(PPh_3)_2]NTf_2$ of 1mL of IL, 0.06mL of cyclohexene)

The reaction mixture is kept under hydrogen atmosphere (1.2 atm, constant pressure). At desired time, 4mL of acetonitrile was added to the catalytic solution and the conversion was determined by GC analyses in presence of an internal standard (toluene).

Preparation of $[Rh(CYD)(PPh_3)_2]NTf_2$:

100mg of $[Rh(COD)(PPh_3)_2]NTf_2$ was dissolved in 1mL of 1,3-cyclohexadiene. After 10min, the excess of solvent was removed under reduced pressure. Yield : 100mg (99%). ^{1}H-NMR (CD_2Cl_2) : δ (ppm) : 2,1 (s, 2H) ; 5,3 (s, 2H) ; 7,5 (m, 30H) ; ^{31}P-NMR (CD_2Cl_2) : δ (ppm) : 25,2pm with J_{Rh-P}=17Hz ; Mass spectrometry ESI : positive mode : 627, 707 ; negative mode : 280 ; UV-Vis Spectroscopy : λ_{max}=500nm

UV-Visible Study :

6.6mg of $[Rh(COD)(PPh_3)_2]NTf_2$ is dissolved in 2mL of one of ionic liquids $BMIMNTf_2$ or $BMMIMNTf_2$. The UV-visible spectrum was record : λ_{max}=450nm.

6.6mg of $[Rh(CYD)(PPh_3)_2]NTf_2$ is dissolved in 2mL of one of ionic liquids $BMIMNTf_2$ or $BMMIMNTf_2$. The UV-visible spectrum was record : λ_{max}=500nm.

0.15mL of 1,3-cyclohexadiene (1.6mmol) was added to a system of 1,6mg of $[Rh(COD)(PPh_3)_2]NTf_2$ (1.6µmol) of in one of ionic liquids $BMIMNTf_2$ or $BMMIMNTf_2$ (1mL). The UV-visible spectra were recorded at λ_{max}=500nm every 1s.

8mg of $[Rh(CYD)(PPh_3)_2]NTf_2$ is dissolved in 5mL of one of ionic liquids $BMIMNTf_2$ or $BMMIMNTf_2$ and pressurized at 1.2bar of dihydrogen. The UV-visible spectra of 1mL of the solution were recorded at λ_{max}=500nm at desired time.

Bibliography

(1) Olivier-Bourbigou, H.; Vallee, C. In *Multiphase Homogeneous Catalysis*; Wiley-VCH: Weinheim, 2005; Vol. 2, pp 413-431.
(2) Wasserscheid, P.; Welton, T. *Ionic Liquids in Synthesis*; Wiley-VCH: Weinheim, 2003.
(3) Bonhote, P.; Dias, A.-P.; Papageorgiou, N.; Kalyanasundaram, K.; Graetzel, M. *Inorg. Chem.* **1996**, *35*, 1168-1178.
(4) Mele, A.; Romano, G.; Giannone, M.; Ragg, E.; Fronza, G.; Raos, G.; Marcon, V. *Angew. Chem. Int. Ed.* **2006**, *45*, 1123-1126.
(5) Dupont, J.; Suarez, P. A. Z.; De Souza, R. F.; Burrow, R. A.; Kintzinger, J.-P. *Chem. Eur. J.* **2000**, *6*, 2377-2381.
(6) Hanke, C. G.; Johansson, A.; Harper, J. B.; Lynden-Bell, R. M. *Chem. Phys. Lett.* **2003**, *374*, 85-90.
(7) Holbrey, J. D.; Reichert, W. M.; Nieuwenhuyzen, M.; Sheppard, O.; Hardacre, C.; Rogers, R. D. *Chem. Comm.* **2003**, 476-477.
(8) Deetlefs, M.; Hardacre, C.; Nieuwenhuyzen, M.; Sheppard, O.; Soper, A. K. *J. Phys. Chem. B* **2005**, *109*, 1593-1598.
(9) Harper, J. B.; Lynden-Bell, R. M. In *Mol. Phys.*, 2004; Vol. 102, pp 85-94.
(10) Ma, J. C.; Dougherty, D. A. *Chem. Rev.* **1997**, *97*, 1303-1324.
(11) Reddy, A. S.; Sastry, G. N. *J. Phys. Chem. B* **2005**, *109*, 8893-8903.
(12) Yamada, S.; Saitoh, M.; Misono, T. *Tetrahedron Lett.* **2002**, *43*, 5853-5857.
(13) Hunter, C. A.; Low, C. M. R.; Rotger, C.; Vinter, J. G.; Zonta, C. *Proc. Natl. Acad. Sci.* **2002**, *99*, 4873-4876.
(14) Deakyne, C. A.; Meot-Ner, M. *J. Am. Chem. Soc.* **1985**, *107*, 469-474.
(15) Meot-Ner, M.; Deakyne, C. A. *J. Am. Chem. Soc.* **1985**, *107*, 474-479.
(16) France, M. R.; Pullins, S. H.; Duncan, M. A. *J. Chem. Phys.* **1998**, *109*, 8842-8850.
(17) Inokuchi, F.; Miyahara, Y.; Inazu, T.; Shinkai, S. *Angew. Chem. Int. Ed.* **1995**, *34*, 1364-1366.
(18) Garel, L.; Lozach, B.; Dutasta, J. P.; Collet, A. *J. Am. Chem. Soc.* **1993**, *115*, 11652-11653.
(19) Masci, B. *Tetrahedron* **1995**, *51*, 5459-5464.
(20) Stepnowski, P.; Nichthauser, J.; Mrozik, W.; Buszewski, B. *Anal. Bioanal. Chem.* **2006**, *385*, 1483-1491.
(21) Holbrey, J. D.; Reichert, W. M.; Rogers, R. D. *Dalton Trans.* **2004**, 2267-2271.
(22) Koelle, P.; Dronskowski, R. *Inorg. Chem.* **2004**, *43*, 2803-2809.
(23) Welton, T. *Chem. Rev.* **1999**, *99*, 2071-2083.
(24) Welton, T. *Coord. Chem. Rev.* **2004**, *248*, 2459-2477.
(25) Hunt, P. A. *J. Phys. Chem. B* **2007**, *111*, 4844-4853.
(26) Magna, L.; Chauvin, Y.; Niccolai, G. P.; Basset, J.-M. *Organometallics* **2003**, *22*, 4418-4425.
(27) Billard, I.; Moutiers, G.; Labet, A.; El Azzi, A.; Gaillard, C.; Mariet, C.; Luetzenkirchen, K. *Inorg. Chem.* **2003**, *42*, 1726-1733.
(28) Dyson, P. J.; Geldbach, T. J. *Metal Catalysed Reactions in ionic liquid* Dordrecht, 2005; Vol. 29.
(29) Fonseca, G. S.; Domingos, J. B.; Nome, F.; Dupont, J. *J. Mol. Catal. A* **2006**, *248*, 10-16.
(30) Chauvin, Y.; Mussmann, L.; Olivier, H. *Angew. Chem. Int. Ed.* **1996**, *34*, 2698-2700.
(31) Blanchard, L. A.; Brennecke, J. F. *Ind. Eng. Chem. Res.* **2001**, *40*, 287-292.

(32) Cornils, B.; Herrmann, W. A.; Horvath, I. T.; Leitner, W.; Mecking, S.; Olivier-Bourbigou, H.; Vogt, D. *Multiphase Homogeneous Catalysis, Volume 2*; Wiley-VCH: Weinheim, 2005.
(33) Domanska, U.; Marciniak, A. *J. Chem. Eng. Data* **2003**, *48*, 451-456.
(34) Su, B.-M.; Zhang, S.; Zhang, Z. C. *J. Phys. Chem. B* **2004**, *108*, 19510-19517.
(35) Haigh, C. W.; Mallion, R. B. *Organic Magnetic Resonance* **1972**, *4*, 203-228.
(36) Avent, A. G.; Chaloner, P. A.; Day, M. P.; Seddon, K. R.; Welton, T. *Dalton Trans.* **1994**, 3405-3413.
(37) Zhai, C.; Wang, J.; Zhao, Y.; Tang, J.; Wang, H. *Z. Phys. Chem.* **2006**, *220*, 775-785.
(38) Ämmälahti, E. B., M., Molko, D. Cadet, J. *J. Magn. Reson.* **1996**, *122*, 230-232.
(39) Comminges, C.; Barhdadi, R.; Laurent, M.; Troupel, M. *J. Chem. Eng. Data* **2006**, *51*, 680-685.
(40) Seddon, K. R.; Stark, A.; Torres, M.-J. *Pure Appl. Chem.* **2000**, *72*, 2275-2287.
(41) Francois, Y.; Zhang, K.; Varenne, A.; Gareil, P. *Anal. Chim. Acta* **2006**, *562*, 164-170.
(42) Dzyuba, S. V.; Bartsch Richard, A. *Chem. Phys. Phys. Chem* **2002**, *3*, 161-166.
(43) Canongia Lopes, J. N.; Costa Gomes, M. F.; Padua, A. A. H. *J. Phys. Chem. B* **2006**, *110*, 16816-16818.
(44) Canongia Lopes, J. N. A.; Padua, A. A. H. *J. Phys. Chem. B* **2006**, *110*, 3330-3335.
(45) Padua, A. A. H., 2007.
(46) Katsyuba, S. A.; Dyson, P. J.; Vandyukova, E. E.; Chernova, A. V.; Vidis, A. *Helv. Chim. Acta* **2004**, *87*, 2556-2565.
(47) Lachwa, J.; Bento, I.; Duarte, M. T.; Lopes, J. N. C.; Rebelo, L. P. N. *Chem. Comm.* **2006**, 2445-2447.
(48) Clark, M.; Cramer, R. D., III; Van Opdenbosch, N. *J. Comp. Chem.* **1989**, *10*, 982-1012.
(49) Dyson, P. J.; Laurenczy, G.; Ohlin, C. A.; Vallance, J.; Welton, T. *Chem. Comm.* **2003**, 2418-2419.
(50) Dupont, J.; Fonseca, G. S.; Umpierre, A. P.; Fichtner, P. F. P.; Teixeira, S. R. *J. Am. Chem. Soc.* **2002**, *124*, 4228-4229.
(51) Schrock, R. R.; Osborn, J. A. *J. Am. Chem. Soc.* **1976**, *98*, 4450-4455.
(52) Bax, A.; Davis, D. G. *J. Magn. Reson.* **1985**, *63*, 207-213.
(53) Cutting, B.; Ghose, R.; Bodenhausen, G. *J. Magn. Reson.* **1999**, *138*, 326-329.

Chapter IV : Consequences of the self-organization of ionic liquids on the synthesis of ruthenium nanoparticles.

Introduction

The use of ionic liquids (IL) as solvents for organic or inorganic synthesis and catalysis has been largely reported.[1-3]

Recently imidazolium based IL have been used as media for the synthesis of a plethora of stable transition-metal nanoparticles (MNP) with small size and narrow size distributions.[4-15] These particles immobilized in IL constitute highly active multiphase catalytic systems for various reactions. But most reports using the combination of IL with MNP have been concentrated on their morphology and catalytic activity. However, the factors which govern the formation, the size and the stabilization of MNP in IL have been much less examined.[16]

After a short bibliographic review about the synthesis of MNP in IL, we have listed herein the most significant factors involved in the stabilization and in the control of size of MNP generated in organic solvent, in water and in IL.

Then our results dealing with the synthesis of ruthenium nanoparticles (RuNP) in imidazolium based IL have been described and the parameters involved in their stabilization by IL has been studied.

Eventually we have attempted to establish a relationship between the 3D organization of IL and the control of the size of RuNP.

1 Metal nanoparticles

The use of MNP is a new and very promising field for catalysis as their small sizes lead to high surface/volume ratios and may result in a continuous variation of surface metallic atoms possibly located in different crystallographic positions (corners, edges, faces). The properties of metal colloids are related to i) particle size and distribution and ii) their structure and surface environment. Controlling the size of MNP and consequently the resulting number of "active sites" is still a challenge whatever solvent is used (organic, aqueous).[17-23]

1.1 Organic solvent and aqueous media.

Synthesis of MNP

Two efficient and convenient chemical routes in MNP synthesis (Scheme 1) have been reported according to the nature of the precursor namely, (i) mild chemical reduction of transition metal salt solutions (Pathway B), (ii) metal atom extrusion starting from

organometallic compounds able to decompose in solution under mild conditions (Pathway A). Nevertheless in chemical reduction process, salts, water and by-products often remain in contact with the surface of the particles, thus passivating them and potentially modifying their reactivity in catalysis leading to the production of halides, oxides or hydroxides. For this reason, the bibliography will be focused on the latter approach (Pathway A).[23]

Scheme 1. *Usual synthetic methods for MNP synthesis*[23]

The precursors preferably carrying purely olefinic complexes : Ru(COD)(COT), Rh(η^3-$C_3H_5)_3$, $Ni(COD)_2$ (COD : 1,5-cyclooctadiene ; COT : 1,3,5-cyclooctatriene)… are decomposed in solution in the presence of a reactive gas and under mild conditions (CO or H_2, temperature 20–80°C, pressure 1–3 bar) and they give rise to alkanes which are inert towards the surface of particles under these conditions.[23]

The usual characterization methods of materials science have been used, such as transmission electron microscopy and low and high resolutions (TEM, HRTEM), wide-angle X-ray scattering (WAXS), dust X-ray diffraction (DRX), elemental analysis, infrared spectroscopy (IR), etc… From these data, it is possible to determine the number of atoms contained in MNP from their size and their crystal structure. For instance, in the case of RuNP which can be considered as cuboctahedral structures with n edges, the two parameters : size (d) and dispersion (D) can be correlated (Figure 1).[17]

$$D = \frac{\text{number of surface atoms}}{\text{total number of atoms}}$$

$$\text{d(nm)} = 2\left(\frac{3MN_t}{4\pi N_A \rho}\right)^{1/3}$$

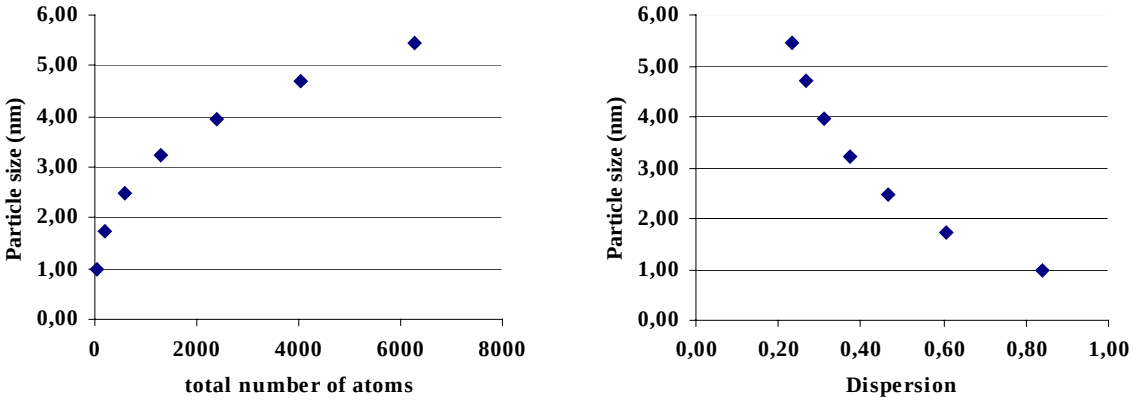

Figure 1. *Total number of atoms and dispersion (D) in function of the size of RuNP (d). M=molecular weight ; N_t = total number of atoms ; ρ=density*

RuNP in IL is a good catalyst system for the hydrogenation of carbon-carbon double bonds[7,14,24-26] and its activity in hydrogenation of benzene has already been reported in chapter III. For this reason, this bibliographic part has been restricted to the synthesis of RuNP and to the stabilizing factors involved in organic solvents, in water and in IL.

General procedure for the synthesis of RuNP from Ru(COD)(COT)

Ru(COD)(COT) reacts rapidly with dihydrogen to give RuNP and cyclooctane (COA). The resulting particles size, size distribution and shape are strongly dependent on the nature of the reaction medium.[23]

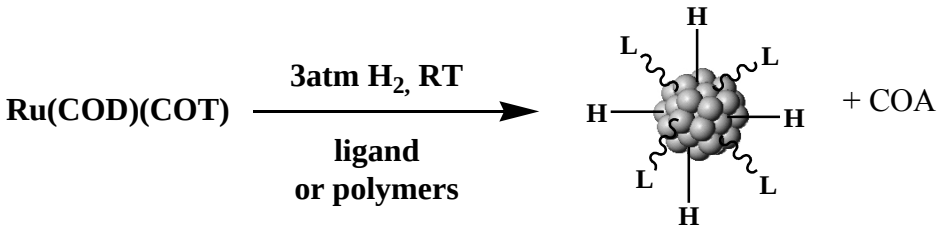

To control the size and to avoid the aggregation of RuNP, several approaches have been developed :

- *Synthesis of RuNP embedded in polymers or dendrimers*

Polymers by bonding to MNP surface atoms, physically occupying space around the MNP and dendrimers as structurally well-defined steric stabilizers offer the opportunity, by isolating the nuclei, to control the size and distribution of the MNP.[4,27] For instance in presence of polyvinylpyrrolidone (PVP) or cellulose acetate (CA), the reaction produces monodisperse ruthenium particles of 1 to 1.7 nm mean size.[28]

Scheme 2. *Representation of RuNP embedded in a polymer (left) and in a dendrimer (right)*[29-31]

- *Synthesis of RuNP dispersed in Solid Supports (Oxide and carbon supports)*

The use of an oxide or carbon support could disperse and prevent aggregation of MNP. By this procedure, RuNP included in silica,[32,33] in alumina membranes[34] or dispersed on γ-alumina[35] have been prepared.[36,37]

Scheme 3. *Representation of a section of alumina membrane loaded with MNP*[36,37]

- *Synthesis of RuNP using phase segregation*

Micelles, microemulsions and surfactants could be used as a « nanoreactor » but to our knowledge, no synthesis of RuNP from Ru(COD)(COT) has been performed using micellar processes.

Scheme 4. *Schematic representation of MNP in water-in-oil microemulsion*[38]

- *Synthesis of RuNP in weakly coordinating solvents*

The introduction of ligands as MNP stabilizers is of special interest, because it focuses on the precise molecular definition of the catalytic materials. This strategy potentially allows optimization of the parameters that govern the efficiency in catalytic reactions. Alkanethiols, long-chain amines, phosphines[23] and silane $RSiH_3$[39] provide examples of ligand-stabilization of MNP. RuNP displaying a low size dispersity and a mean size of 2–3 nm are obtained. However, these stabilizers do not avoid the formation of "superstructures" of colloids which are shown by TEM micrographs.

Scheme 5. Representation of the synthesis of ligand-protected MNP[23]

To sum up, when a polymer or an organic ligand is added to the medium, the MNP are stabilized and protected against agglomeration. This method is efficient, reproducible and can be adopted for the synthesis of various transition-metal nanoparticles (Pt, Pd, Rh, Ru, …) as well as for the preparation of bi-metallic particles (Pt/Ru, Pd/Cu, …). Size, shape and surface of the particles could be determined by the choice of stabilizing agent (alcohol, amine, thiol, phosphine, mixture of ligands, …). Particular interest is paid to the characterization of the objects that are produced, with the aim of establishing structure/property relationships.[40-44]

1.2 Ionic liquids

IL are generally reported as good media for the preparation of MNP of various metals like Ir, Ru, Pt, Rh and Pd. In this part, this work has been described for RuNP.[45]

Note that the syntheses of RuNP in IL have already been reported by the decomposition of Ru(COD)(COT) dispersed in 1-butyl-3-methylimidazolium hexafluorophosphate

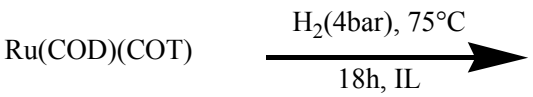

Ionic liquid	size (nm)
$BMIMPF_6$	2.6+/-0.4
$BMIMBF_4$	2.5+/-0.4
BMIMOTf	1.9+/-0.6

($BMIMPF_6$), tetrafluoroborate ($BMIMBF_4$) and trifluoromethanesulfonate (BMIMOTf). These syntheses have been carried out with vigorous stirring under 4 bar of molecular hydrogen during 18h at 75°C. Sizes of RuNP determined by TEM analyses are reported below.[14] Moreover TEM observations show the formation of spherical superstructures of Ru particles with a regular size of 57±8nm.[14]

Note that X-ray photoelectron spectroscopy (XPS) of RuNP shows oxidized ruthenium and oxygen peaks that indicate the presence of a passivated surface layer. It is worth mentioning that the purity, in particular the water and halide contents,[46] of the imidazolium IL plays an important role in the MNP chemistry, since these impurities may influence the stability and catalytic properties of the material. For instance iridium nanocluster of about 300 atoms prepared in a medium containing about 200ppm of Cl^- leads to approximately 12 Cl^- atoms per surface metal atom.[19]

From the literature, it appears that three main effects can intervene in the stabilization of MNP : i) electrostatic (also known as electronic, or DLVO-type stabilization named after its proponents Derjaugin, Landau, Verwey and Overbeek),[47,48] ii) ligand stabilization (steric) and iii) “electrosteric” stabilization (a combination of electrostatic and steric factors).

As IL are complex media, many sources of stabilization can be identified and all their contributions must be carefully considered. Consequently the precise composition of the medium must be known in order to consider all the possible alternative hypotheses for the true stabilizer in the system.[19]

Electrostatic/DLVO-type stabilization

The classic theory of electrostatic colloidal stabilization was developed in the 1940s by Derjaugin, Landau, Verwey, and Overbeek, and is commonly referred to DLVO theory. DLVO theory predicts that MNP stabilization is based on a delicate balance in interparticle forces between repulsive Coulombic forces opposing attractive van der Waals forces. [48]

Ionic compounds such as halides, carboxylates, or polyoxoanions, dissolved in (generally aqueous) solution can generate an electrostatic stabilization. The adsorption of these compounds and their related counterions at the metallic surface generates an electrical double-layer around the particles (scheme 7). This results in a Coulombic repulsion between the particles. If the electric potential associated with the double layer is high enough, then the electrostatic repulsion will prevent particle aggregation.[19]

Scheme 6. *Pictorial representation of electrostatic/DLVO-type stabilized MNP*[19]

The intrinsic high charge of imidazolium salts, which creates an electrostatic colloid type protection (DLVO-type stabilization)[47] for the MNP similar for those proposed to quaternary ammonium salts,[49,50] may be, as a first approximation,[19] adequate for the description of the stabilizing effect because it is noticeable that the anions and cations form aggregates of the type $[(BMIM)_x(X)_{x-n})]^{n+}[(BMIM)_{x-n}(X)_x)]^{n-}$ where BMIM is the 1-*n*-butyl-3-methylimidazolium cation and X is the anion. Therefore, it is quite probable that the coordination of anion to the MNP surface in imidazolium IL occurs via anionic aggregates of the type $[(BMIM)_{x-n}(X)_x)]^{n-}$ rather than isolated X anions. Therefore the DLVO model is not totally correct in these systems since it was not designed to account for counterions with multiple charges.[51,52]

Scheme 7. *Schematic illustration of MNP surrounding by* $[(BMIM)_x(X)_{x-n})]^{n+}[(BMIM)_{x-n}(X)_x)]^{n-}$ *aggregates*[9,10]

Ligand stabilization

IL can act as “surface ligand” as described in the previous part providing a protective shell for MNP. These alternative source(s) of high stabilization have been formulated :

1) Some functionalized IL have been designed to stabilize MNP. These include thiol- or nitrile-functionalized imidazolium cations.[53,54]

2) C-H oxidative addition of the acidic C-H bond (aqueous pKa ≈ 21-24) in the H(2) of the imidazolium ring, resulting in N-heterocyclic carbene formation on the RuNP surface.[55] Indeed, the formation of such intermediates has already been detected using Ni or Pd complexes.[56]

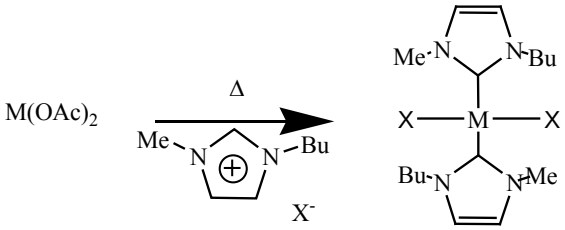

M=Pd or Ni ; X=Br or I

This reaction is also possible with H(4) and H(5) of the imidazolium ring but less probable.[57] H/D and D/H labeling experiments during the formation of iridium nanoparticles (IrNP) have been recently observed using either D_2 or deuteriated imidazolium IL indicating the intervention of N-heterocyclic carbenes at the metal surface, at least as transition species.[55]

3) H-bonding of H(2) but also H(4) and H(5) of imidazolium ring at RuNP surface.

4) η^5-coordination of the imidazolium cation to the electron deficient metal(0) surface.

These two last possibilities have never been experimentally demonstrated.

5) Coordination of anions to nanocluster surfaces. For instance, it has been reported that ytterbium is coordinated through oxygen atoms of bis(trifluoromethylsulfonyl)imide (NTf_2) in $Yb(NTf_2)_4$ complexes.[58] XPS analyses also suggested the coordination of hexafluorophosphate anion (PF_6) at IrNP surface in IL (Scheme 8).[9] However in this last example, the highly hydrolysable nature of PF_6 could induce side-reaction such the production of HF.

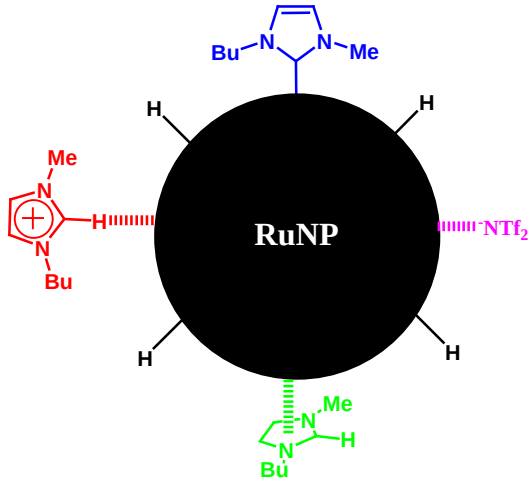

Scheme 8. *Representation of $BMIMPF_6$ ions surrounding MNP*[9]

Scheme 9. *Possible coordination modes of IL on RuNP surface*

Electrosteric stabilization

The electrostatic and ligand stabilizations can be combined to maintain MNP stable in solution. This kind of stabilization is generally provided by means of ionic surfactants. These compounds bear a polar headgroup able to generate an electric double layer and a lypophilic side chain able to provide steric repulsion. The electrosteric stabilization can be obtained from polyoxoanions such as the couple ammonium (Bu_4N)/polyoxoanion ($P_2W_{15}Nb_3O_{629}$), scheme 11) for IrNP. The significant steric repulsion of the associated bulky Bu_4N^+ countercations associated with the highly charged polyoxoanion (Coulombic repulsion) provide an efficient electrosterical stability toward agglomeration in solution of the resulting nanoclusters.[19]

Scheme 10. *Representation of the barrier created by the combined, high charge 'inorganic' : $P_2W_{15}Nb_3O_{629}$ electrostatic and steric 'organic' : Bu_4N colloid-type stabilization of transition metal nanoclusters provided by the polyoxoanion component and its associated Bu_4N cations.*[59]

To conclude, it has been highlighted that the stabilization of MNP in water, organic solvents and IL is due to the presence of a electronic protective shell (electrostatic stabilization) or of a "surface ligand". To our knowledge, only these factors have been reported for the stabilization of MNP in IL whereas these media offer another factor of stabilization : their high organization.

2 Structural aspect of IL

IL could act as a stabilizing medium but the most important advantage is their high self-organization at the molecular scale (see chapter I). IL form extended hydrogen-bond network in the liquid state and they are per-definition "supramolecular" fluids. This structural organization of IL can be used as "entropic drivers" for spontaneous, well-defined, and extended ordering of nanoscale structures.[60] Indeed IL have already been used as media for the synthesis of some zeolite-related, microporous aluminophosphates or ordered mesoporous materials in which IL serve both as solvent and as structure-directing agents.[61]

In addition to this H-bond network, a computer simulation study has recently reported side-chain aggregation while the cation head-groups and the anions show homogeneous distributions. These authors observed tail aggregation for systems $RMIMPF_6$ corresponding to the range of R : C_nH_{2n+1} with n= 4 to 8 but no aggregation for shorter chains. These authors suggested that the aggregation of tail groups should clearly exist in most organic IL systems.[62]

That is in agreement with the fact that the distribution of the charged domains is not homogeneous, but instead, it has the form of a continuous tridimensional network of ionic channels, coexisting with the nonpolar domains which form, in some cases, dispersed microphases (n=2) or, in others, continuous ones (n=12).[63]

a **b** **c** **d**

Figure 2. *Snapshots of simulation boxes containing 700 ions of hexafluorophosphate (a) 1-ethyl-3-methylimidazolium, (b) 1-butyl-3-methylimidazolium, (c) 1-hexyl-3-methylimidazolium and (d) 1-octyl-3-methylimidazolium. The application of a coloring code enables clear identification of the charged and nonpolar domains that form in ionic liquids with red/green (charged/nonpolar) coloring.*

IL	peak wavenumber (A^{-1})	length scale (A)
EMIMPF6	0.56	11
BMIMPF6	0.52	12
HMIMPF6	0.50	13
OMIMPF6	0.43	15

Table 1. The length scales of the polar/nonpolar domains obtained from analysis of the static structure factors, in IL with increasing alkyl-chain length.

Recently, the existence of nanoscale heterogeneities in neat liquid and supercooled IL have been experimentally supported by X-ray diffraction (DRX) studies on chloride based IL: RMIMCl with R : C_nH_{2n+1} with n= 3 to 10.[64] The size of these nonpolar domains is found to linearly scale with the alkyl chain length (R) and evolve from 13 to 27 Å when the alkyl chain increase : R=C_nH_{2n+1} with n= 3 to 10.[64] However, the nonpolar domains size have been underestimated by calculations and they have been experimentally found larger than expected.[64]

Figure 3. *X-ray diffraction patterns from the series of supercooled liquid IL: RMIMCl with R=C_nH_{2n+1} : n= 3, 4, 6, 8, 10, at 25 °C. In the inset the spatial correlation L =$2\pi Q_{MAX}$, Q_{MAX} being the interference peak position, is plotted (circles) as a function of n, the alkyl chain length, for n ≥ 4. The corresponding data are also reported for the cases n = 6 and 8 for $RMIMBF_4$ (squares).*[64]

The reported straight line correspond to a linear fit which nicely describes the growth of the spatial correlation upon increasing the alkyl chain length, with increasing of 2.1 Å per –CH_2- units. These authors confirm that nonpolar domains size are similar in chloride based IL comared to those in BF_4 and PF_6 based IL.[64,65] The realization that pure room-temperature IL can be understood as nanostructured fluids could lead to new insights on the many unique properties of these materials.[63]

The segregation of polar and nonpolar domains in imidazolium-based IL with alkyl side chains of intermediate length changes the way in which solvation can be understood in these liquids and can be correlated with their ability to interact with different species in diverse and complex ways. Indeed, polar substrates will be preferentially dissolved in polar domains and apolar compounds in nonpolar ones. For instance, radial distributions of n-hexane (mole fraction x=0.1), acetonitrile, methanol, and water (all with x=0.2) in 1-butyl-3-methylimidazolium hexafluorophosphate clearly show that the substrates are located on different regions of the IL : hexane (C_3H is a methyl carbon atom) is close to the end carbon of the alkyl side chain (C_{4c}) and is found in the nonpolar region while water molecules (O is the oxygen atoms) are connected to the imidazolium ring in the position between the nitrogen atoms (H(2)) which belongs to the charged part of the cation and to the anion (P is the central part of the anion). Methanol (O is the oxygen atom) and acetonitrile (CN is a nitrile carbon atom) molecules are intermediate with a polar part and a nonpolar one.[65]

Figure 4. *Solute-solvent radial distribution functions showing the position of the solutes relative to the different domains of IL. The insets indicate schematically the preference of each solute for the nonpolar (green) or charged (red) domains*[65]

To conclude, IL should be good media for the synthesis of RuNP because :

1. IL present the possibility of stabilizing MNP *via* ligand and/or electrostatic effects.
2. IL possess 3D-organization which is maintained in the presence of apolar substrates (hexane) or polar ones (acetonitrile or water).
3. IL present an organization in microdomains of polar and nonpolar nature. The nature of the solute (polar or nonpolar) will determine the domains in which it will be dissolved.(nonpolar or polar microdomains)

The stabilization of RuNP by IL has already been reported in the literature[14] but to our knowledge, the control of the size of RuNP has never been correlated either to the 3D organization or to the presence and the size of polar and apolar domains. But in function of the polar or apolar nature of substrates, the solvation will not take place in the same part. Consequently the distribution of substrates will not be homogeneous in the media resulting in high local concentration in specific domains. Even if IL as a stabilizer (as ionic or neutral ligand of MNPs) has been well documented, to our knowledge, no direct correlation between the self-organization of IL and the resulting size of the MNP generated *in situ* have been

reported in the literature. The aim of this work is to attempt to establish these two relationships.

RESULTS

1 Choice of IL

The goal of this work is to study the influence of the organization of imidazolium based IL on the synthesis of RuNP. Bis(trifluoromethylsulfonyl)imide ($N(SO_2CF_3)_2$ = NTf_2) anion which afford hydrophobic and low melting point IL have been chosen.

Moreover it has been previously demonstrated that the organization of IL is strongly dependent on :

- the presence of hydrogen bond in position 2 which determine the type of IL structure. A 1,3-dialkylated cations : 1-butyl-3-methylimidazolium (BMIM) but also an 1,2,3-trialkylimidazolium based IL : 1-butyl-2,3-dimethylimidazolium (BMMIM) have been chosen in order to study the influence of the alkyl group in position 2 and of the difference of structure (A or B, see details in chapter I).
- the alkyl chain length which governs the size of nonpolar domains. In order to study the influence of the size of these microdomains, a series of symetrical or unsymetrical imidazolium based cation with various alkyl chain length has been studied : 1-ethyl-3-methylimidazolium (EMIM), 1-butyl-3-methylimidazolium (BMIM), 1-hexyl-3-methlimidazolium (HMIM), 1-methyl-3-octylimidazolium (OMIM), 1-decyl-3-methlimidazolium (DMIM) and 1,3-dibutylimidazolium (BBIM).

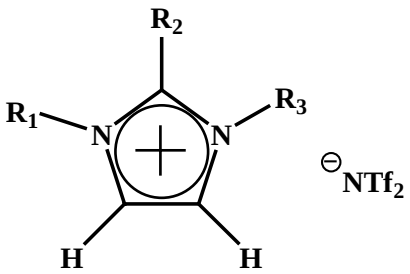

IL	R_1	R_2	R_3
$EMIMNTf_2$	CH_3	H	C_2H_5
$BMIMNTf_2$	CH_3	H	C_4H_9
$HMIMNTf_2$	CH_3	H	C_6H_{13}
$OMIMNTf_2$	CH_3	H	C_8H_{17}
$DMIMNTf_2$	CH_3	H	$C_{10}H_{21}$
$BBIMNTf_2$	C_4H_9	H	C_4H_9
$BMMIMNTf_2$	CH_3	CH_3	C_4H_9

2 Synthesis of RuNP in $BMIMNTf_2$

2.1 General procedure for the preparation of RuNP in IL

Synthesis of (η^4-1,5-cyclooctadiene)(η^6-1,3,5-cyclooctatriene)Ru(0)

(η^4-1,5-cyclooctadiene)(η^6-1,3,5-cyclooctatriene)Ru(0) (Ru(COD)(COT)) is obtained by direct reaction of 1,5-cyclooctadiene (COD) with hydrated ruthenium trichloride in presence of metallic zinc :[66-69] This complex has been fully characterized by ^1H and ^{13}C NMR.

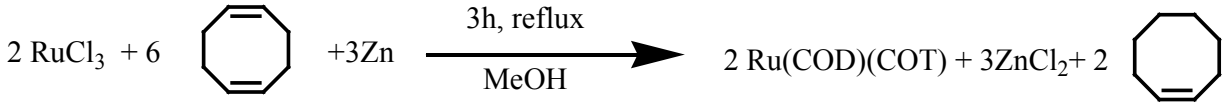

Synthesis of RuNP from Ru(COD)(COT)

In a glove box, IL (10mL, IL=$EMIMNTf_2$, $BMIMNTf_2$, $HMIMNTf_2$, $OMIMNTf_2$, $DMIMNTf_2$, $BBIMNTf_2$ and $BMMIMNTf_{2)}$) is introduced in a 500mL glass autoclave, then Ru(COD)(COT) (135mg, 0,43mmol) is dissolved at room temperature under vigorous stirring during 1h resulting in an homogenous yellow solution. The autoclave is located in a regulated temperature bath (25°C or 0°C). In all experiments, no precipitation of Ru(COD)(COT) was observed. After evacuation of argon atmosphere under vacuum, the autoclave was pressurized with 4bar of dihydrogen, during 18h for reactions performed at 25°C and at 0°C under stirring, and 3 days at 0°C without stirring.

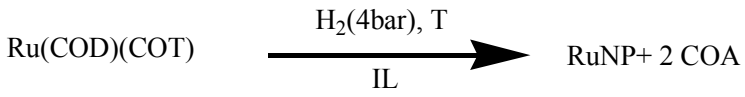

After evacuation of COA under vacuum, a black colloidal suspension of RuNP is obtained which is stable for several months under argon atmosphere at room temperature. In contrast to previously described RuNP synthesis,[14] the separation of nanoparticles from IL was not possible either by centrifugation or by addition of several types of solvents (pentane, toluene). Consequently, transmission electronic microscopy (TEM) experiments were performed directly in the IL media.

Note that whatever the experimental conditions, the diffusion of dihydrogen in IL takes place. Attempts to form RuNP from Ru(COD)(COT) in $BMIMNTf_2$ without dihydrogen failed even under heating up to 150 °C.

In order to measure their size and to determine their form, each solutions of nanoparticles in IL was analyzed *in situ* in TEM by depositing a droplet on holey carbon film supported by a copper grid. The mean size of RuNP was estimated from ensembles of 200 particles found in arbitrary chosen areas of the enlarged micrographs. The obtained size distribution is presented and can be fitted reasonably well to a Gaussian curve.

2.2 Results obtained in the case of $BMIMNTf_2$ at room temperature under stirring

The decomposition of Ru(COD)(COT) by dihydrogen in $BMIMNTf_2$ under stirring at room temperature (RT) leads to RuNP of 2.4+/-0.3nm size. According to the relationship between the mean size (d) and the dispersion (D) (see details p3), it can be evaluated that the dispersion of RuNP in $BMIMNTf_2$ is about 45%. This value will be used in order to estimate the amount of surface Ru atoms in the following part.

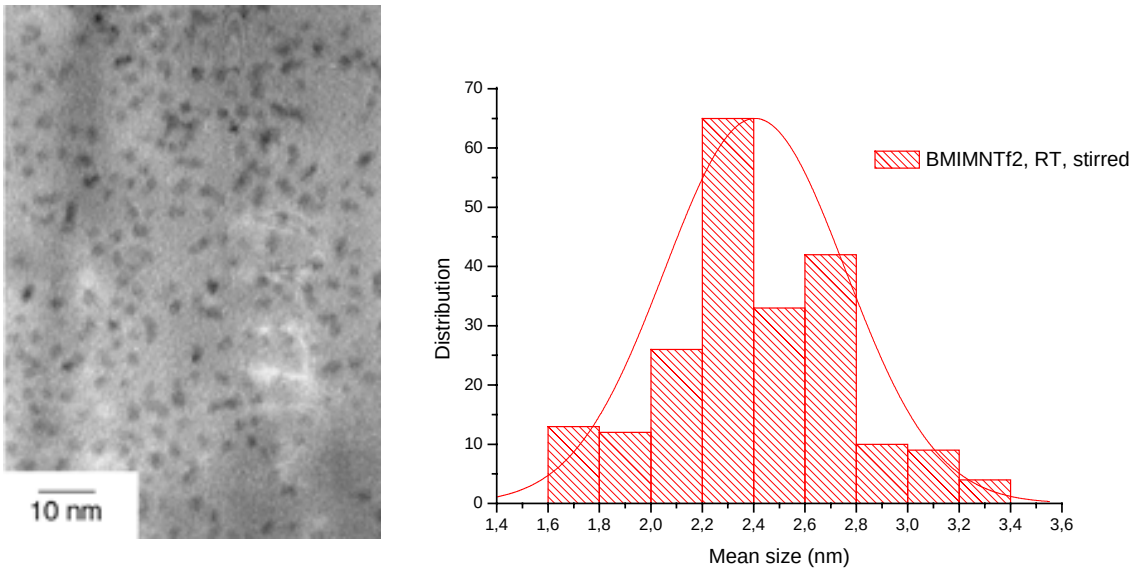

Figure 5. TEM pictures and histograms of RuNP/$BMIMNTf_2$ prepared at room temperature under stirring.

By comparison of our results with those of the literature, we observed that the size of RuNP synthesized in IL at 25°C and at 75°C are similar. These results confirm that IL limits the crystal growth of RuNP probably due to stabilizing factors (electrostatic or steric) as already reported.[4,6,9,10,17,45,55]

We have then investigated by organometallic chemistry techniques which factors stabilize RuNP in particular if there are some ligands at the surface of RuNP and what is their nature.

2.3 Attempts to determine the stabilizing factors

In the literature, several surface ligands have been proposed to stabilize MNP in imidazolium based IL by coordination of the anion or of the cation (N-heterocyclic carbene formation, η^5-coordination or H-bonding of imidazolium ring).[55]

By analogy with organic solvents, surface hydrides should also be present on RuNP surface in IL.[44]

As RuNP is a good catalyst for hydrogenation, the presence of surface hydride has been tested by the reactivity of RuNP toward ethylene.

Hydrogenation of ethylene

Ru(COD)(COT) (135mg, 0,43mmol) has been dissolved in $BMIMNTf_2$ (10mL) at room temperature under vigorous stirring resulting in an homogenous yellow solution. After evacuation of argon atmosphere under vacuum, the autoclave has been pressurized with 4bar of dihydrogen during 18h for reactions. Black colloidal suspension of RuNP (2mL containing $n(Ru)=8.6x10^{-5}$mol) were treated overnight under argon in order to remove dihydrogen dissolved in IL. Samples have been stirred under ethylene atmosphere (105.5mbar) and the conversion to ethane present in the gas phase have been determined by GC analyses.

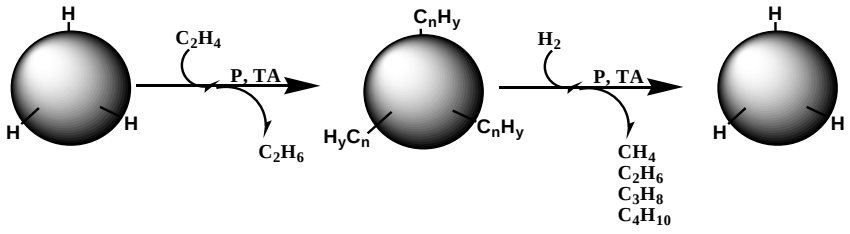

As it has been previously reported, the mean size of RuNP is d=2.4nm which correspond to a dispersion of D=0.45. Consequently surface ruthenium atoms (Ru_S) in this sample is about : $n(Ru_S) \approx 3.9x10^{-5}$mol in 2mL of $BMIMNTf_2$.

After 3h reaction, 10µmol of ethane are obtained e.g. 10µmol of dihydrogen are consumed. Therefore, there is n(H)=20µmoles for $n(Ru_S)\approx 3.9x10^{-5}$mol in 2mL of $BMIMNTf_2$ which correspond to 0.51 H per surface ruthenium atoms.

At this step, RuNP after treatment under vacuum, has been exposed under dihydrogen and a small amount of methane (0.6µmol), ethane (5.6µmol) , propane (0.1µmol) and butane (0.1µmol) have been released in the gas phase (about 0.16H per surface RuNP). This phenomenon, known as homologation of olefins, has been already reported for RuNP included in silica.[70,71]

Note that if RuNP is treated overnight under high vacuum (10^{-6}mbar) during 12h at room temperature (25°C) instead of under argon atmosphere, the reaction of ethylene leads to a very low amount of ethane compared to what is expected and correspond to $52x10^{-3}$ H atoms per surface ruthenium atom.

To conclude, these result suggest the presence of surface hydride on RuNP which can be almost completely desorbed under high vacuum.

Secondly, we have attempted to displace surface ligand of RuNP/IL with carbon monoxide.[72]

Ligand exchange by carbon monoxide

Firstly, the adsorption of carbon monoxide in IL without RuNP at room temperature has enabled to determine that $n(CO)_{diss}$=1.4µmol of CO are dissolved in 2mL of $BMIMNTf_2$.

Freshly prepared RuNP/$BMIMNTf_2$ (2mL containing n(Ru) =$8.6x10^{-5}$mol) have been treated overnight under high vacuum (10^{-6}mbar) during 12h at room temperature (25°C). Then samples have been exposed to CO atmosphere (116.65mbar). The pressure was 111.65mbar after 7hrs (no more pressure variation was detected). As in the case of ethylene, due to our pre-treatment under high vacuum, only a small amount of dihydrogen is detected in the gas phase corresponding to $14x10^{-3}$ H atoms per surface ruthenium atom.

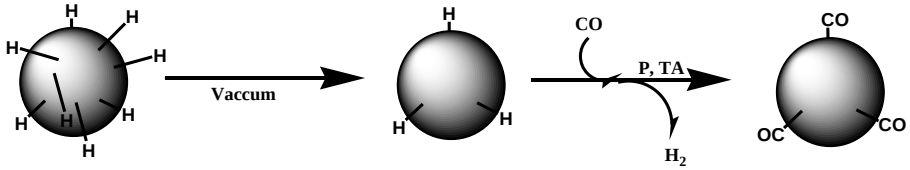

The consumed amount of CO is $n(CO)_{cons}$=20µmol in 2mL of Ru/$BMIMNTf_2$

Consequently the amount of CO adsorbed on RuNP sufarce in 2mL of Ru/$BMIMNTf_2$ correspond to : $n(CO)_{ads} = n(CO)_{cons} - n(CO)_{diss}$ =18.6 µmol.

Therefore there is $n(CO)_{ads}$=18µmoles for $n(Ru_S) \approx 3.9x10^{-5}$mol in 2mL of $BMIMNTf_2$ which correspond to 0.48 CO adsorbed per surface Ru atoms. Note that RuNP treated under CO are inactive in hydrogenation and showed rapid aggregation.

It appears that the amount of adsorbed CO per surface Ru atoms (0.48) is comparable to the amount of hydrogenated ethylene per surface Ru atoms (0.51).

Even if the dispersion of RuNP is evaluated from their mean size and could be misestimated, the ratio CO/Ru_S and H/Ru_S are about 0.5 which is low in comparison with literature values.[72] These results could indicate the presence of a strongly linked surface ligand such as N-heterocyclic carbene (NHC). It has been proposed in the literature that the formation under D_2 of imidazolium ring mainly deuteriated at the position C2 demonstrated the presence of NHC linked to iridium nanoparticles.[55]

In order to investigate this hypothesis, this experiment has been reproduced.

Addition of deuterium

A solution of RuNP/$BMIMNTf_2$ has been exposed to deuterium atmosphere for 3h at room temperature.

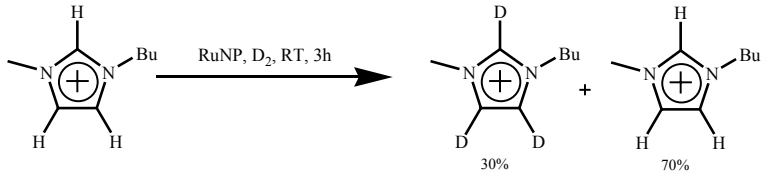

The ^{1}H NMR of the solution proves that imidazolium ring protons are partially deuteriated (30%). The integration of H(2) and H(4)/H(5) protons signals shows that these positions have been deuteriated in the same proportion in contrast with what is observed in the literature.[55]

Moreover the reaction with iodoalkane at 100 or 150°C, which could generate 1,2,3-trialkylimidazolium cation by nucleophilic substitution do not allow confirmation of the presence of NHC.

To conclude, these partial and preliminary results have only demonstrated the presence of surface hydride. No other ligands has been detected but even if their presence can not be excluded, our experimental results suggested that there is no ligand on the RuNP surface in $BMIMNTf_2$.

Although these parameters of stabilization need further investigation, another factor could be proposed : the isolation of RuNP due to the self-organization of IL (as it reported in polymers or dendrimers).[29]

In order to study the effect of the high organization of IL on the synthesis of RuNP, the influence of the substitution of the imidazolium cation, temperature and stirring have been studied because these parameters will modify or perturb the self-organization of the media.

3 Influence of the 3D-organization of IL

Firstly we have investigated the influence of the presence of H-bond in position 2 by comparing $BMIMNTf_2$ and $BMMIMNTf_2$.

3.1 Influence of H-bonding in position 2

The organization of imidazolium based IL is governed by the strong H(2)-bond interaction between C2-H of cation and anion. The alkylation of this position induces a strong change in the organization of IL as shown by DRX studies (Figure 6).

Figure 6. *DRX structures of $MMIMNTf_2$ (left) and $EEEIMNTf_2$ (right)*[73]

Note that the possible formation of a strong surface ligand, known as N-heterocyclic carbene, from 1,3-dialkylimidazolium is less favorable but could also be occur in case of 1,2,3-trialkylimidazolium in position 4 and 5.[57]

To study the influence of these factors, the synthesis of RuNP from Ru(COD)(COT) with stirring at room temperature has been performed under identical experimental conditions in $BMIMNTf_2$ and $BMMIMNTf_2$.

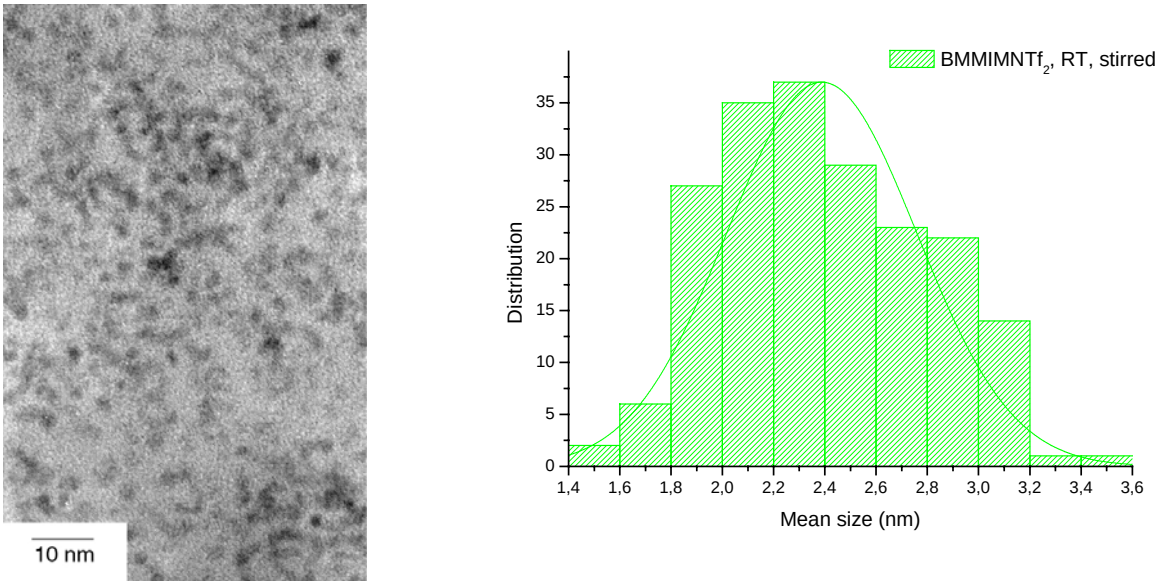

Figure 7. *TEM pictures and histograms of RuNP/BMMIMNTf$_2$ prepared at room temperature with stirring.*

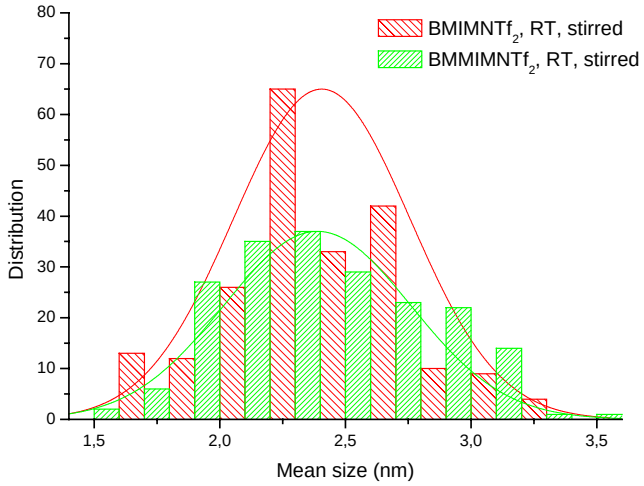

Figure 8. *Comparative histograms of RuNP prepared in BMIMNTf$_2$ and in BMMIMNTf$_2$ showing the particle size distribution of Ru(NP) at room temperature under stirring.*

The size of RuNP synthesized in $BMIMNTf_2$ and in $BMMIMNTf_2$ are 2.4+/-0.3 and 2.3+/-0.4nm respectively.

The presence of hydrogen in position 2 of the imidazolium ring appears to have **no particular consequences** on the mean size of RuNP. However it appears that RuNP are more homogeneously distributed in dialkylated cation than in trialkylated ones.

3.2 The influence of the temperature

It has been found that between 25 and 75°C, the size of RuNP are similar. As the structure of IL have been determined by the shock induced crystallization of the supercooled IL,[74] the resulting structure corresponds to the organization at 0°C. Consequently the synthesis of RuNP should be done at this temperature in order to reveal the true organization of the media.

The formation of RuNP has been performed in $BMIMNTf_2$ with stirring at room

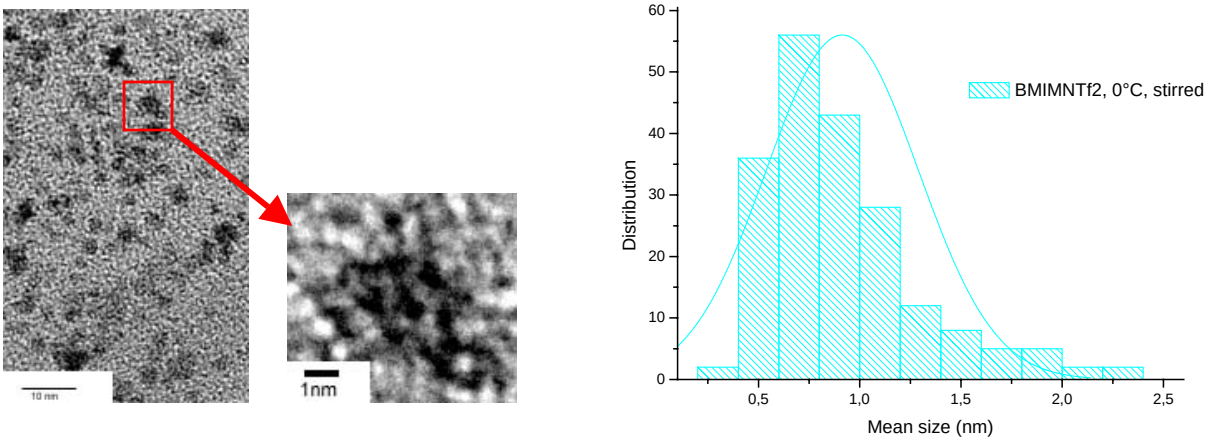

temperature and 0°C.

Figure 9. TEM pictures and histograms of RuNP/$BMIMNTf_2$ prepared at 0°C under stirring.

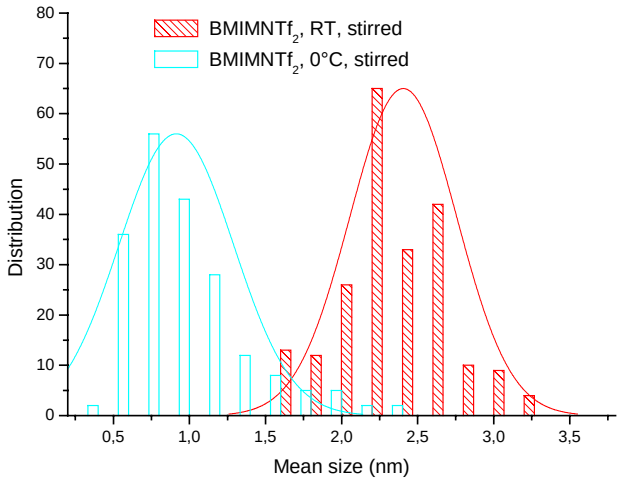

Figure 10. Comparative histograms of RuNP prepared in $BMIMNTf_2$ showing the particle size distribution of Ru(NP) at 0°C (left) and at room temperature (right).

RuNP prepared at room temperature (2.4+/-0.3nm) are larger than at 0°C (0.9+/-0.4nm).

This result is particular to this medium because some previous studies in organic solvent show that generally speaking, the size of nanoparticles increases when the temperature decreases. Indeed the effect of the temperature on the size of RuNP is the inverse in IL to that observed in THF/MeOH mixture. In this latter media, it is suggested that the COA pockets generated *in situ* during the decomposition of Ru(COD)(COT) have a size which decreases as the temperature increases. The segregation of Ru° nuclei occurs exclusively inside these pockets. Therefore the higher the temperature is, the smaller the size of the particles are. To sum up, in THF/MeOH, the presence of small and well separated pockets leads to small and homogenous RuNP at higher temperature.[75]

In contrast to THF–methanol, the size of the RuNP in IL decreases with the temperature. This effect suggests that the nanoparticle precursors and/or Ru nuclei in $BMIMNTf_2$ are better isolated at 0°C than at 25°C. The organization of IL should be better maintained at low temperatures, the confinement of nuclei in nonpolar microdomains should be more efficient and afford smaller particles

However, at 0°C, the particles are agglomerated in a kind of big cluster of 2-3 nm.

3.3 The influence of the stirring

The stirring effect have been studied by comparing the synthesis of RuNP prepared at 0°C with or without stirring.

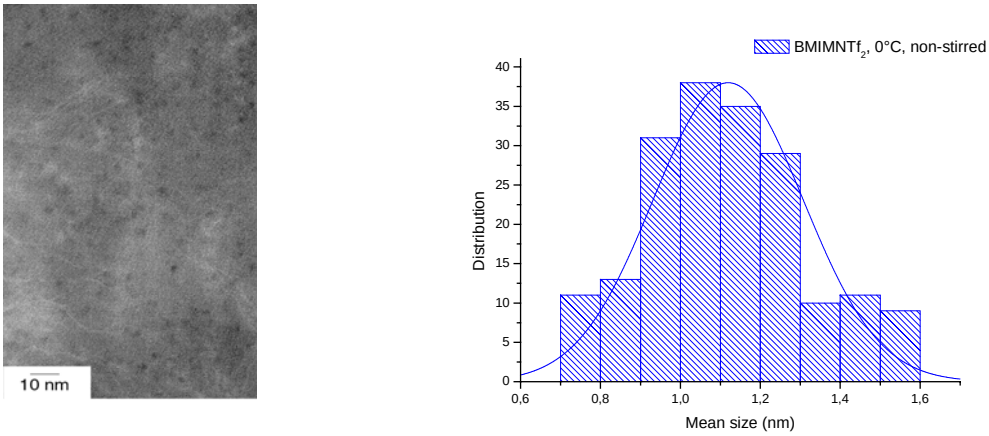

Figure 11. TEM pictures and histograms of RuNP/$BMIMNTf_2$ prepared at 0°C without stirring.

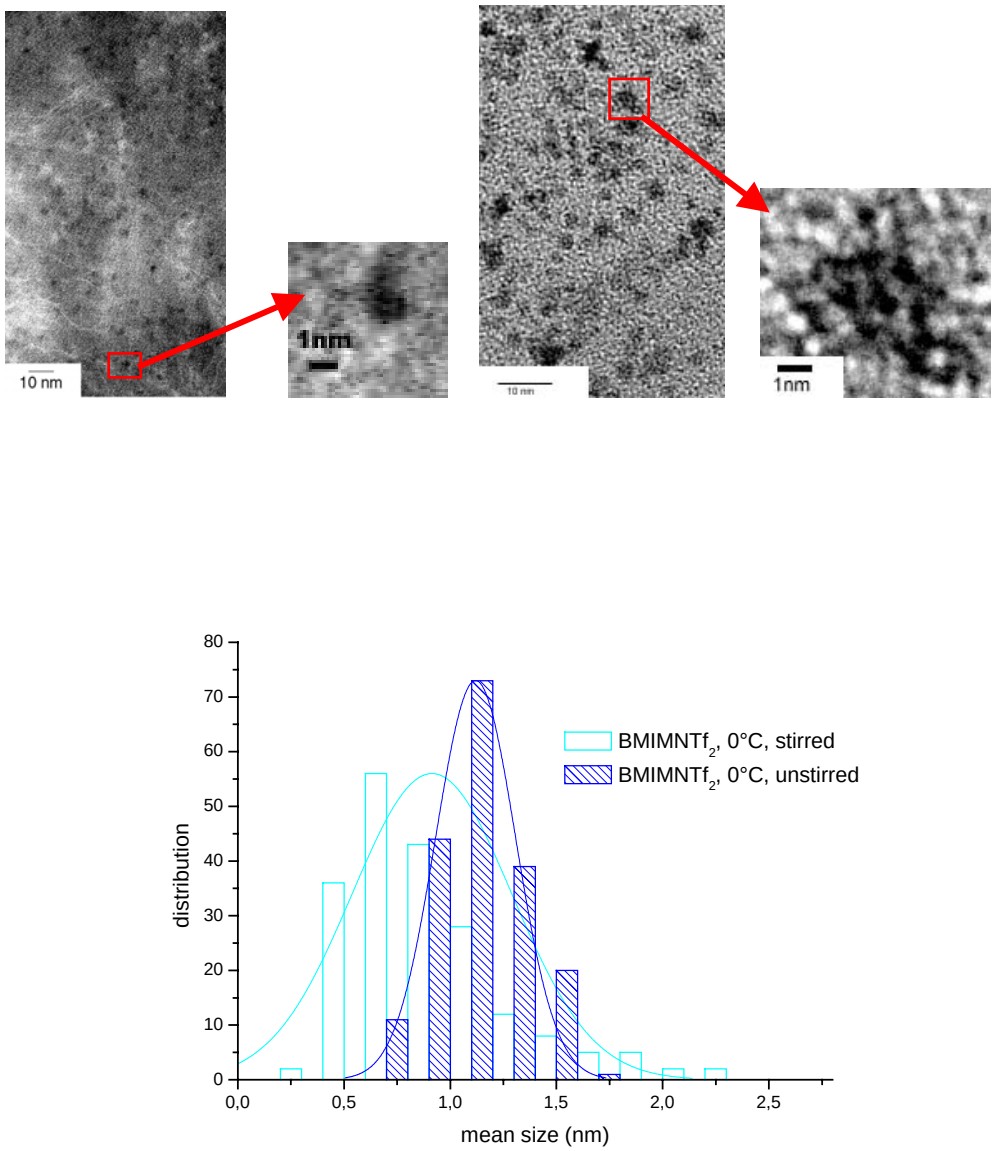

Figure 12. *Comparative TEM pictures and histograms showing the particle size distribution of Ru(NP) in BMIMNTf$_2$ at 0°C under stirring (right) or without stirring (left).*

The synthesis of RuNP at 0°C with and without stirring in BMIMNTf$_2$ leads to particle sizes of 0.9+/-0.4 and 1.1+/-0.2nm respectively. The stirring seems to have no significant effect on the mean size of nanoparticles. But under stirring, most of the particles display a sponge-like character (TEM pictures) which may result from the initial aggregation of individual crystallites. The presence of stirring can obviously favor the contact of growing particles and therefore the formation of superstructures. Inside these superstructures of 2-3nm, the particles appear homogeneous in size. On the contrary, at 0°C without stirring, there is a very narrow size distribution particle. The presence of stirring in IL at 0°C perturbs the 3D organization and leads to partial agglomeration of the small size nanoparticles into larger

aggregates. On the contrary, at 0°C without stirring, the 3D organization is maintained and RuNP are small, identical in size and homogeneously dispersed.

Once again, in THF/MeOH 90/10, the influence of the stirring is totally inverse because the presence of the stirring leads to the formation of rigid porous particles of homogenous size and of loose superstructures of various size containing independent particles in unstirred solutions.[75]

In summary these experiments show that IL media enable the formation of very well-defined nanoparticles of very small size, generally difficult to control in other media. Moreover it show that nanoparticle synthesis under mild conditions may be used to reveal the fine structures of complex media such as IL.

4 Influence of the size of microdomains

Recently, a new approach of the description of IL media by a microphase segregation between polar and nonpolar domains offer a novel way of understanding their solvent properties and their ability to interact with different species.

The nature of the solute (apolar or polar) determines the domains in which it will be dissolved. For instance, the apolar solute such n-hexane in $BMIMPF_6$ (molar fraction x=0.1) systems is concentrated in the nonpolar domain of IL and the solubility of hexane increase with the side alkyl chain length. That means that hexane is located in nonpolar domains and its local concentration increases with the length of the alkyl chain.

In the case of apolar Ru(COD)(COT), could the size of apolar domains control the preloading of Ru and consequently could IL act as supramolecular matrices for RuNP syntheses ?

4.1 Choice of IL

The molecular dynamics of IL derived from imidazolium cations and NTf_2 anions have been provided by Dr Padua. These calculations have been performed under the same conditions as previously described for imidazolium based IL with PF_6 anions.[63]

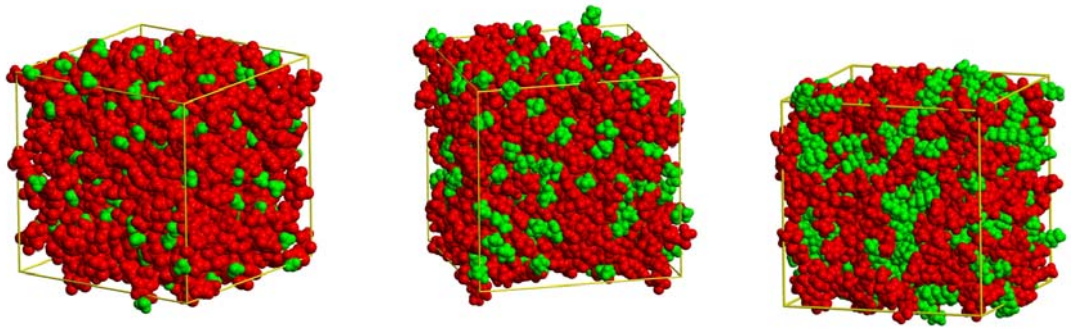

a **b** **c**

Figure 13. *Snapshots of simulation boxes containing 700 ions of $EMIMNTf_2$ (a), $BMIMNTf_2$ (b) and $OMIMNTf_2$ (c). The application of a coloring code enables clear identification of the charged (red) and nonpolar (green) domains that form in IL.*

It appears that the apolar domains grow when the alkyl chain length increases : $OMIMNTf_2$ presents large apolar domains which size decreases in $BMIMNTf_2$. The ethyl group of $EMIMNTf_2$ seems to be too short to generate significant apolar domains and can be considered as a polar medium. These molecular dynamics show clearly the formation of apolar domains which become significant from $HMIMNTf_2$ while it was already present from $BMIMPF_6$.

As it has been previously reported, the size of nonpolar microdomains increases in the range : $EMIMNTf_2 < BMIMNTf_2 < HMIMNTf_2 < BBIMNTf_2 < OMIMNTf_2 < DMIMNTf_2$

4.2 Influence of the nature of IL on the RuNP size

In order to determine if there is a relationship between the resulting size of RuNP and those of nonpolar domains of IL, their syntheses have been performed from Ru(COD)(COT) under 4bar of dihydrogen in IL : $RMIMNTf_2$: $R=C_nH_{2n+1}$ with n=2 ; 4 ; 6 ; 8 and 10, at room temperature under stirring and at 0°C without stirring.

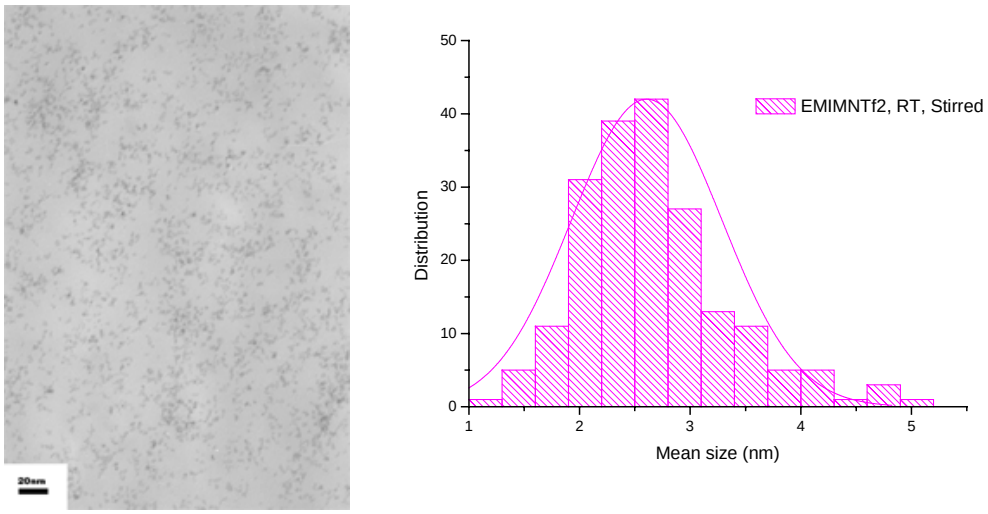

Figure 14. RuNP prepared under stirring at room temperature in $EMIMNTf_2$

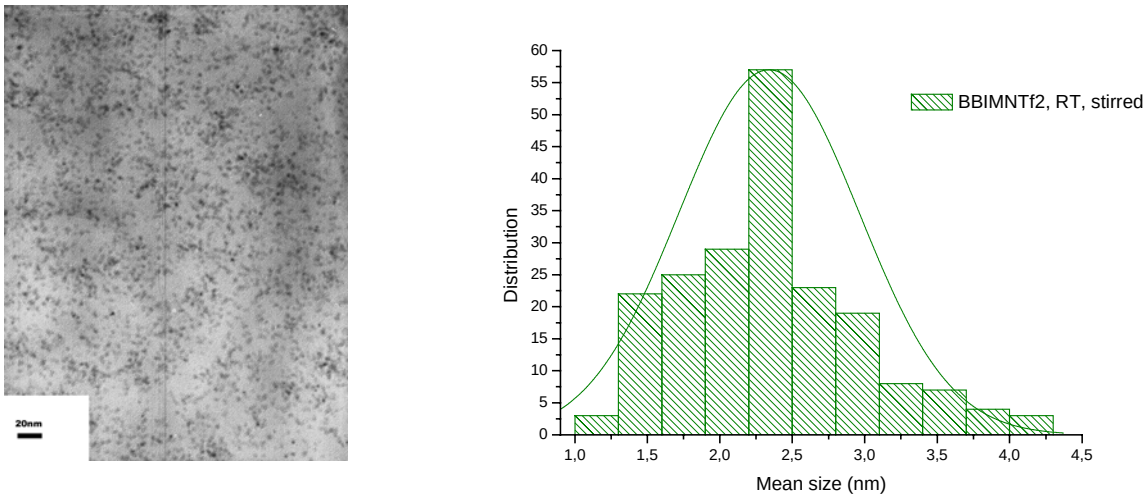

Figure 15. RuNP prepared under stirring at room temperature in $BBIMNTf_2$

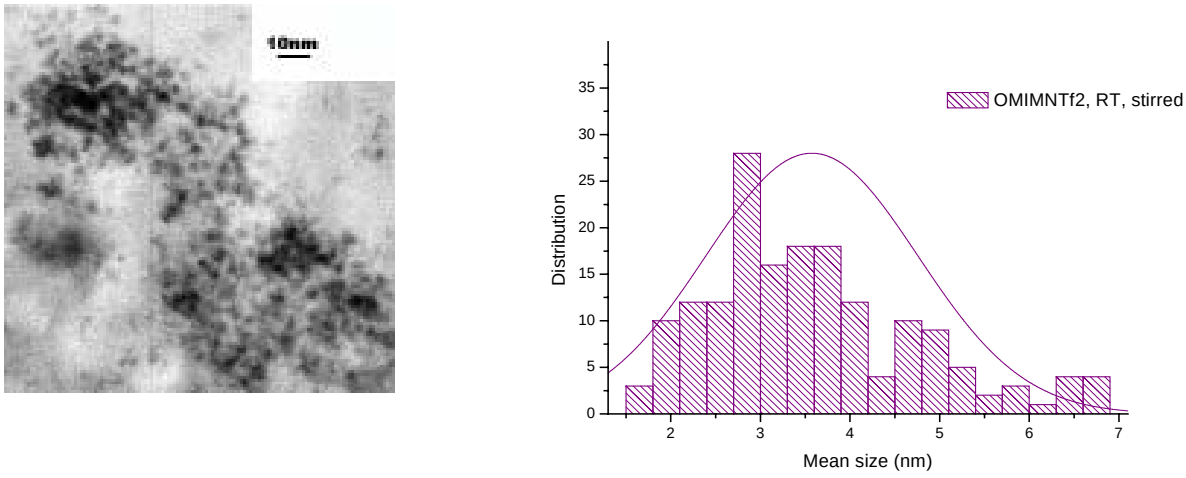

Figure 16. *RuNP prepared under stirring at room temperature in $OMIMNTf_2$*

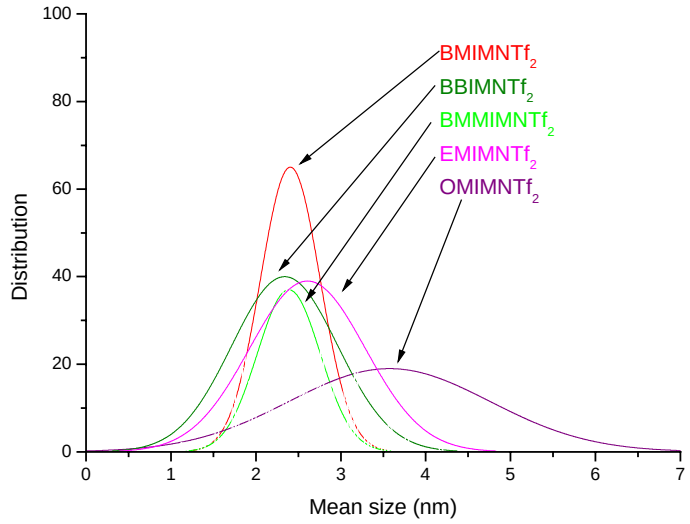

Nature of IL	25°C
$EMIMNTf_2$	2.6+/-0.7
$BMIMNTf_2$	2.4 +/- 0.3
$BMMIMNTf_2$	2.4 +/- 0.4
$HMIMNTf_2$	n.d.
$BBIMNTf_2$	2.3 +/- 0.6
$OMIMNTf_2$	3.6 +/- 1.2

Figure 17. *Comparative Gaussian curves of RuNP prepared at room temperature under stirring in $BMIMNTf_2$ (red), $BBIMNTf_2$ (Olive), $EMIMNTf_2$ (Magenta) and $OMIMNTf_2$ (purple).*

At room temperature under stirring, the size of RuNP increase as the length of the side alkyl chain : in $OMIMNTf_2$ (3.6+/-1.6nm), RuNP are larger than those prepared in $BMIMNTf_2$ (2.4+/-0.3nm at RT) or $BBIMNTf_2$ (2.3+/-0.6nm).

Moreover the TEM pictures shows the presence of large aggregates (20-30nm) constituted by small particles in $OMIMNTf_2$. Even if the size of RuNP are similar in $BMIMNTf_2$ and $BBIMNTf_2$, it appears that RuNP are more homogeneously dispersed in the first case. (Δ= +/-0.3 and +/-0.6nm respectively). Are these results related to the size of nonpolar microdomains ?

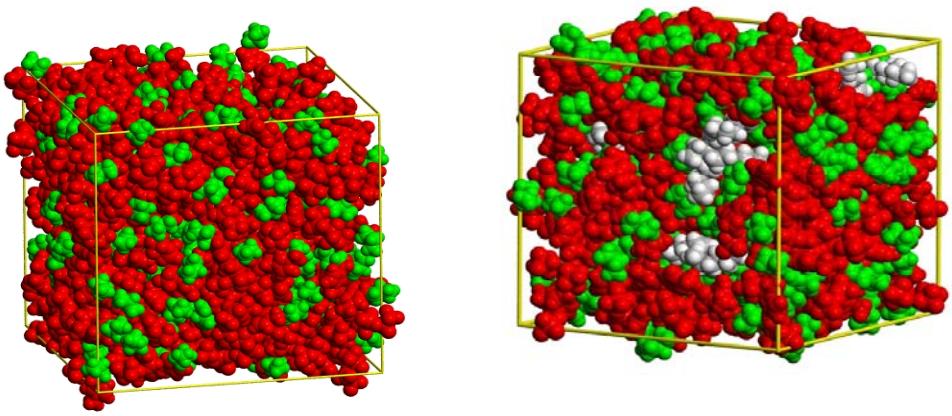

Figure 18. *Snapshots of simulation boxes containing 700 ions of $BMIMPF_6$ with (right, molar fraction : x=0.1) and without hexane(left). The application of a coloring code enables clear identification of hexane molecules (grey), the charged (red) and nonpolar (green) domains that form in IL.*[65]

As when n-hexane is dissolved in $BMIMPF_6$ (molar fraction x=0.1), it is concentrated in the nonpolar domain of IL and the size of the nonpolar domains increases (Figure 19). The synthesis of RuNP in $BMIMNTf_2$ has been performed in the same experimental conditions but in presence of one equivalent of cyclooctane per mole of ruthenium in order to increase the size of the apolar domains.

In these conditions, RuNP are larger (5.6=/0.9nm instead of 2.4+/-0.3nm without COA) and presents some agglomerations in a large clusters.

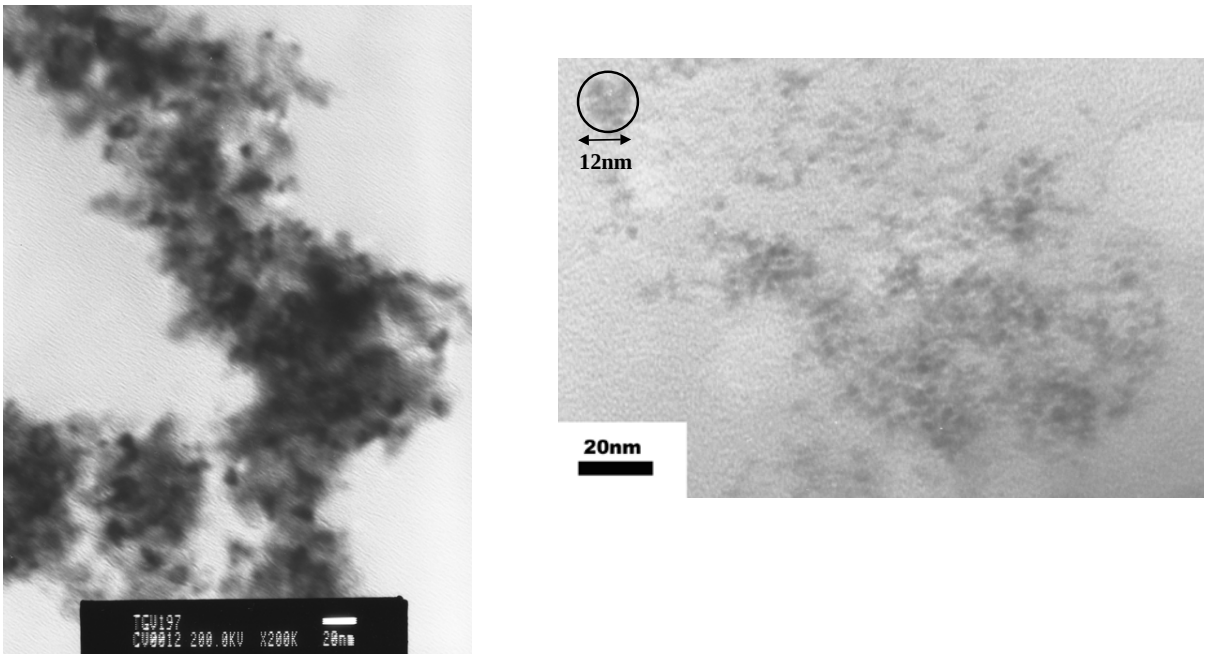

Figure 19. *TEM pictures of RuNP synthesized in $BMIMNTf_2$ at room temperature in presence of 1 equivalent of cyclooctane.*

Note that in case of THF/MeOH, the addition of cyclooctane before the decomposition of Ru(COD)(COT) induce an increase of apolar pocket size and also leads to larger RuNP.[75]

Consequently it clearly appears that there is a relationship between the size of nonpolar domains and those of RuNP.

Previous studies show that the influence of the organization of IL is more important at 0°C and that the structure is perturbed by the presence of stirring. Therefore, the comparative study of all IL systems have also been performed at 0°C without stirring.

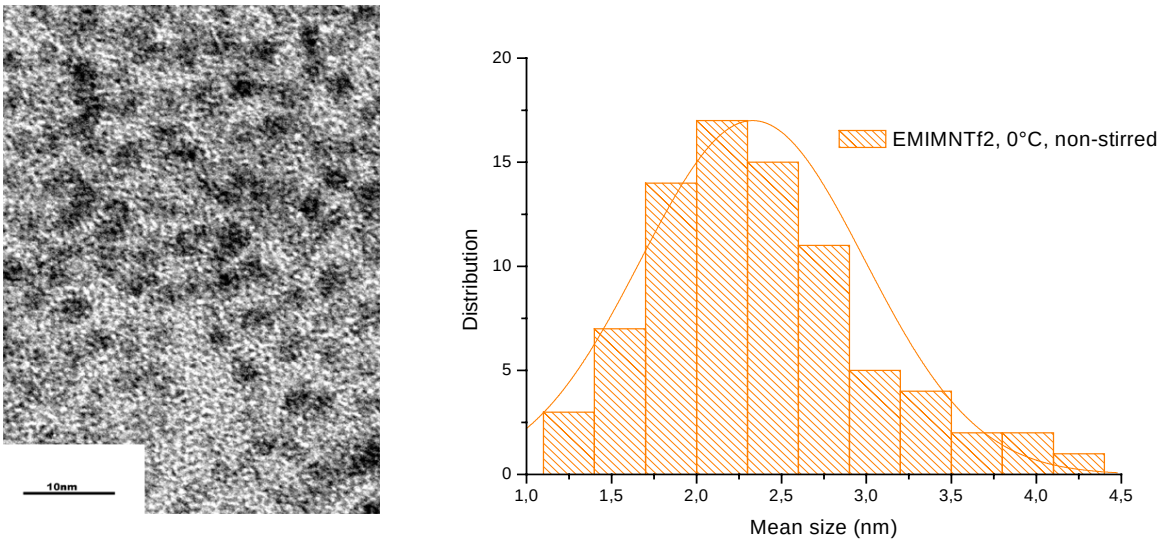

Figure 20. *RuNP prepared without stirring at 0°C in EMIMNTf$_2$*

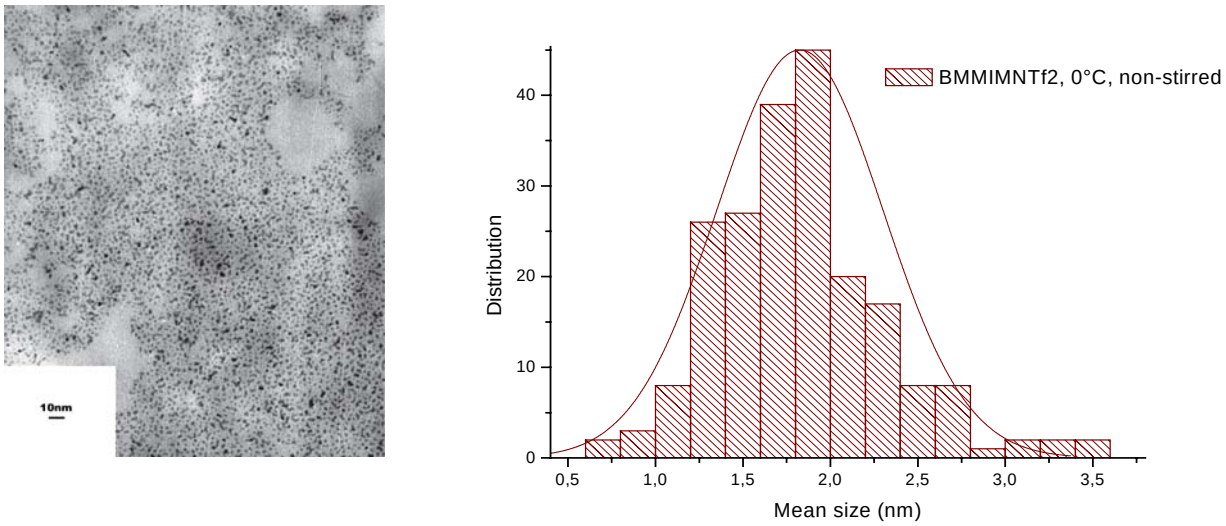

Figure 21. *RuNP prepared without stirring at 0°C in BMMIMNTf$_2$*

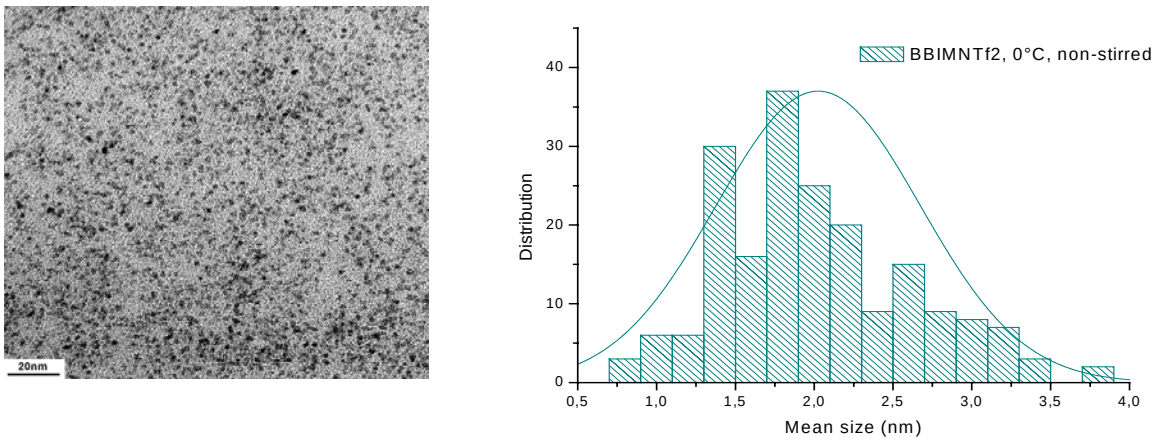

Figure 22. *RuNP prepared without stirring at 0°C in BBIMNTf$_2$*

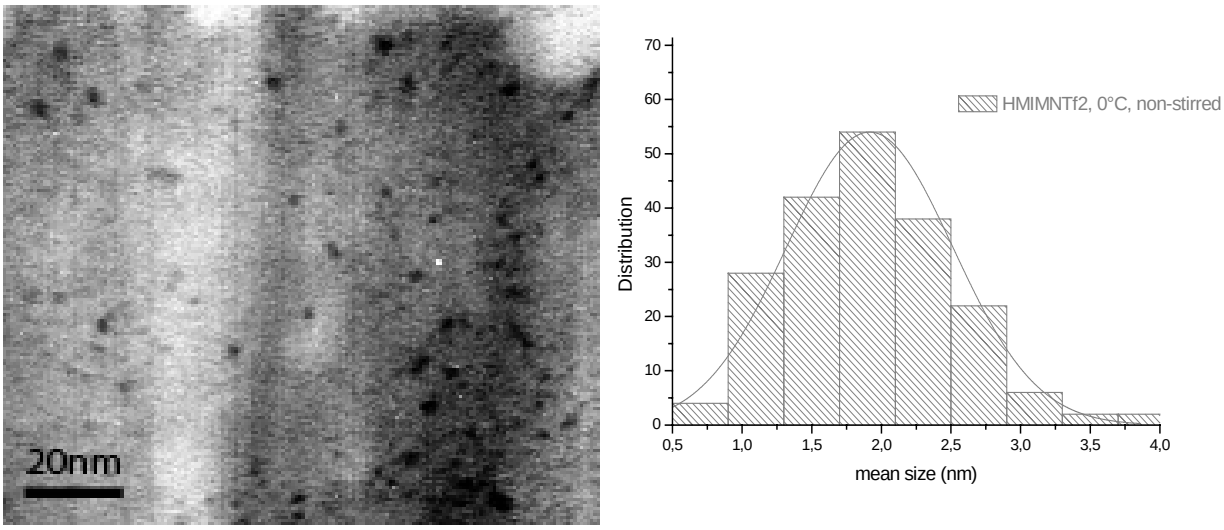

Figure 23. *RuNP prepared without stirring at 0°C in HMIMNTf₂*

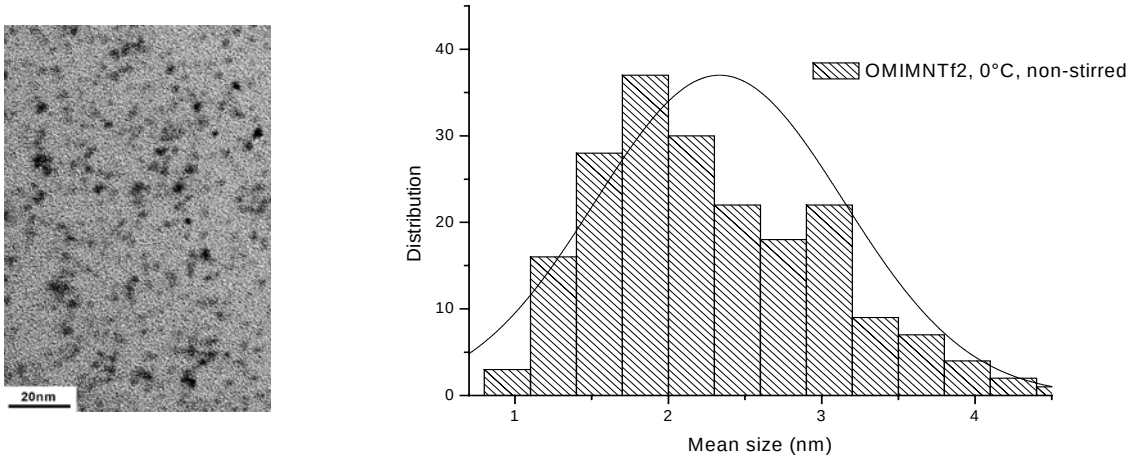

Figure 24. *RuNP prepared without stirring at 0°C in OMIMNTf₂*

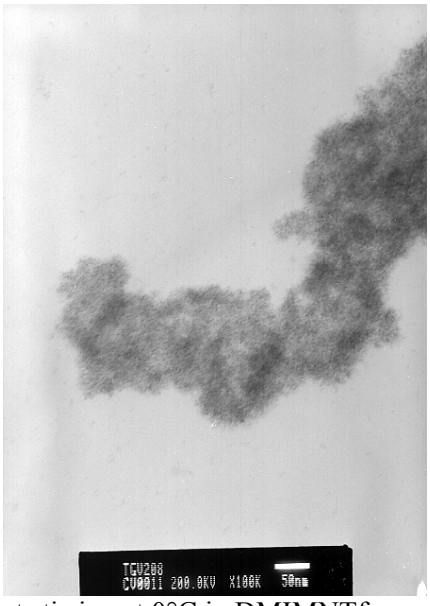

Figure 25. RuNP prepared without stirring at 0°C in $DMIMNTf_2$

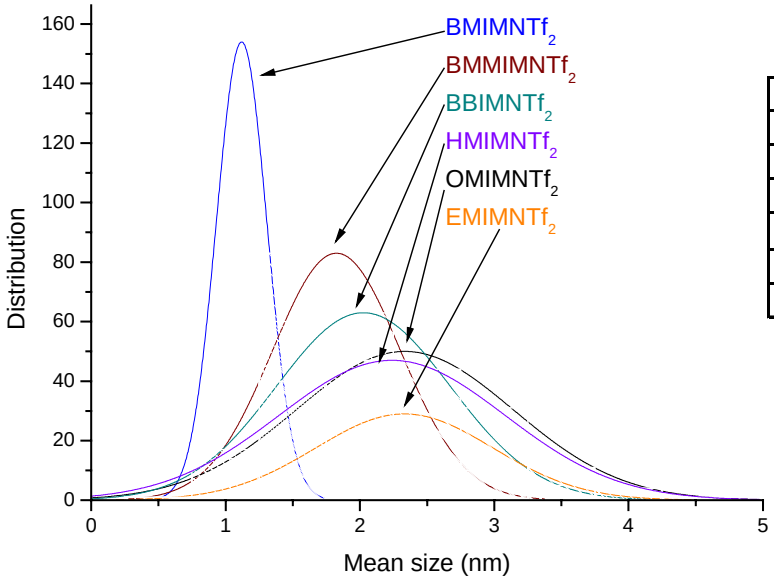

Nature of IL	0°C
$EMIMNTf_2$	2.3 +/-0.6
$BMIMNTf_2$	1.1 +/- 0.2
$BMMIMNTf_2$	1.8 +/- 0.5
$HMIMNTf_2$	1.9 +/-0.6
$BBIMNTf_2$	2.0 +/- 0.6
$OMIMNTf_2$	2.3 +/- 0.8

Figure 26. *Comparative histograms of RuNP prepared without stirring at 0°C in $EMIMNTf_2$ (orange), $BMIMNTf_2$ (blue), $BMMIMNTf_2$ (wine), $BBIMNTf_2$ (dark cyan) and $OMIMNTf_2$ (black).*

For all IL, the RuNP size are smaller at 0°C than at 25°C.

In both conditions (25°C under stirring or 0°C without stirring), the size of RuNP increases in the range :

$BMIMNTf_2 < BMMIMNTf_2 < BBIMNTf_2 < OMIMNTf_2 \approx EMIMNTf_2 < DMIMNTf_2$

At 0°C without stirring, no aggregation in 3D clusters is observed except for $DMIMNTf_2$. This aggregation is also observed in the case of $BMIMNTf_2$ at 0°C in presence of stirring and at 25°C in the presence of additional cyclooctane and in the case of $OMIMNTf_2$ at 25°C. It could be explained by a diffusive process which strongly affects the morphology of the apolar microdomains by interconnexion in nonpolar domains.

Besides $EMIMNTf_2$, the size of RuNP is related to the alkyl chain length of $RMIMNTf_2$: $R=C_nH_{2n+1}$ with n=2 ; 4 ; 6 ; 8 and 10 :

$BMIMNTf_2 < BMMIMNTf_2 < BBIMNTf_2 < OMIMNTf_2 \approx EMIMNTf_2 < DMIMNTf_2$

Surprisingly, the size of RuNP prepared in $EMIMNTf_2$ are larger than expected. This could be explained either by strong ion pairing or by the fact that ethyl chains do not generate significant apolar zones and $EMIMNTf_2$ so correspond to a polar medium. Indeed, it has been observed that RuNP generated in THF/MeOH mixture leads to larger particles when the content of methanol increases because the polarity of the medium increases.[75]

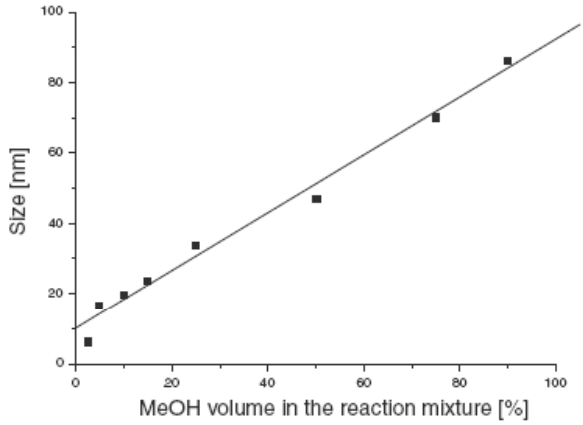

Figure 27. *Linear correlation between the THF/methanol volume ratio and the particle size.*[75]

It is worth to note that at 0°C without stirring, the size of RuNP is found linearly scale with the alkyl chain length C_nH_{2n+1} for $4 \leq n \leq 8$.

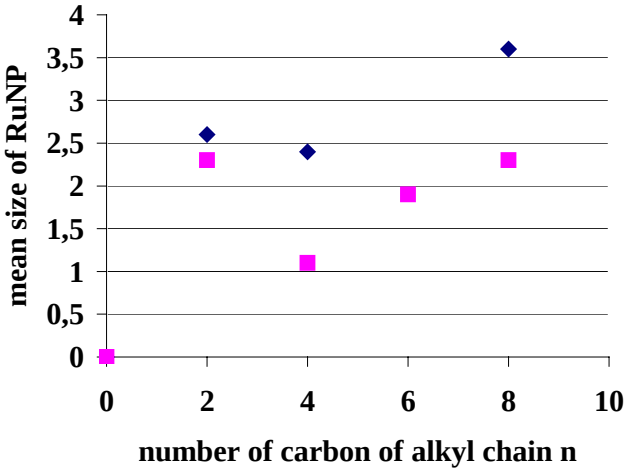

◆ **Room temperature, stirred**

■ **0°C, non-stirred**

Nature of IL	25°C	0°C
$EMIMNTf_2$	2.6+/-0.7	2.3 +/-0.6
$BMIMNTf_2$	2.4 +/- 0.3	1.1 +/- 0.2
$BMMIMNTf_2$	2.4 +/- 0.4	1.8 +/- 0.5
$HMIMNTf_2$	n.d.	1.9 +/-0.6
$BBIMNTf_2$	2.3 +/- 0.6	2.0 +/- 0.6
$OMIMNTf_2$	3.6 +/- 1.2	2.3 +/- 0.8

Figure 28. *Correlation of RuNP size with the number of carbon of alkyl chain C_nH_{2n+1}*

It has been already demonstrated by molecular dynamics and DRX studies that there is a segregation of polar and nonpolar domains in imidazolium based IL with an alkyl side chain of intermediate length. As the variation in the range : $BMIMNTf_2$; $HMIMNTf_2$; $BBIMNTf_2$; $OMIMNTf_2$; $DMIMNTf_2$ is only the length of side alkyl chain length, this difference in the stabilizing effect and in the resulting size of RuNP can only be attributed to an increase of the size of the apolar domains.

As reported for n-hexane, Ru(COD)(COT) and/or Ru nuclei can be considered as apolar substrates, they should be preferentially dissolved in the nonpolar parts of this kind of IL and should be more soluble in $RMIMNTf_2$ ($R=C_nH_{2n+1}$) when n increases.

Consequently, the local concentration of Ru(COD)(COT) should be higher in apolar domains and the resulting Ru nuclei should be located in the apolar part. When n increases, the number of Ru(COD)(COT) in apolar pocket is higher because the apolar domain is larger. As a result, the number of RuNP generated under dihydrogen in the apolar pocket is higher and their aggregation affords larger RuNP.

The same phenomenon is also suggested in case of THF/MeOH, the control of the size of RuNP is related to the segregation of cyclooctane resulting from hydrogenation of the ruthenium precursor from the rest of the solvent (Scheme 41).[75]

Scheme 11. *Hypothetical segregation in the solution allowing the size control of RuNP depending upon the reaction medium composition.*[75]

From these results, we proposed that two factors can limit the crystal growth of Ru nuclei and/or agglomeration of RuNP :

1. The local concentration of Ru(COD)(COT) and of the resulting number of available nuclei in each apolar pockets is related to their sizes. RuNP should correspond to the aggregation of a restricted amount of Ru atoms and as a result, to RuNP of a limited size.
2. the crystal growth should take place in the restricted volume defined by this apolar pocket which can limit the aggregation of Ru nuclei.

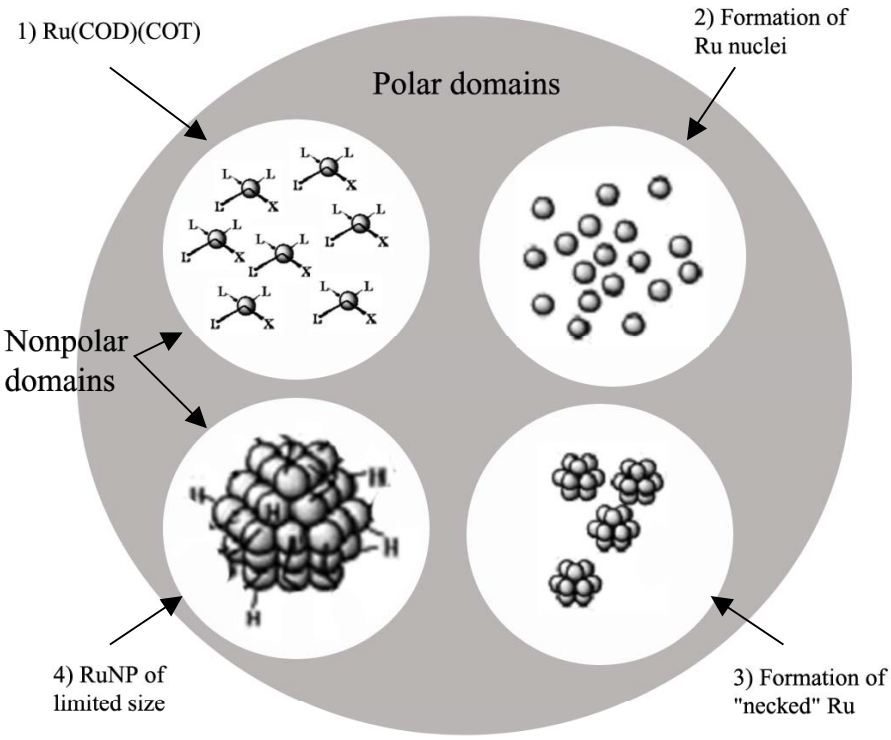

Scheme 12. *Proposed mechanism for generation of RuNP in IL.*

Conclusion

After a short bibliographic review, the synthesis of RuNP from Ru(COD)(COT) under 4bar of dihydrogen has been carried out in different IL in various conditions (0°C or room temperature, under or without stirring). This work confirms that IL are very good media for preparation and stabilization of ruthenium nanoparticles.

In a first part, the parameters involved in the stabilization of RuNP in IL have been investigated. No particular ligand has been found except the presence of **surface hydride**.

Secondly, it appears that in the case of $BMIMNTf_2$, the size of RuNP prepared under stirring was similar at 75 and 25°C but decreases strongly in size and size distribution at 0°C. Moreover the presence of stirring seems to perturb the crystal growth and lead to partial agglomeration of RuNP while they are better dispersed without stirring at 0°C. We demonstrated that there exists a relationship between the self-organization and the control of the size RuNP.

The relationship between the presence and the size of apolar microdomains and the resulting size of RuNP was experimentally established in $RMIMNTf_2$: $R=C_nH_{2n+1}$ with n=2 to 10 : in $RMIMNTf_2$. The longer R is, the larger RuNP are.

The microphase segregation between polar and nonpolar domains in IL is a novel way of understanding their solvent properties and their ability to interact with different species. In particular, IL could act as supramolecular matrices, whose size will be dictated by the design of the cation/anion combinations.

IL acts simultaneously as a nanoreactor that controls the size of RuNP and as a stabilizer that prevents aggregation but at the same time, the accessibily of the metal surface by reactants is still possible.

These experiments also show that nanoparticle synthesis in mild conditions may be used to reveal the fine structures of complex media such as IL. Indeed, the size and the nature of apolar pocket could be tune by modifying the nature of alkyl chain or by functionalized them.

This work open a novel way to design ruthenium nanoparticles but more generally metal nanoparticles because it enables an understanding of the mechanism of crystal growth in IL media.

Experimental section

General

1-methylimidazole (>99%), 1,2-dimethylimidazole (>98%), 1-butylimidazole (98%) (Aldrich) were distilled prior to use. Anhydrous 1-Chlorobutane (>99.5%), 1-bromohexane (98%), 1-chlorooctane (99%), 1-bromodecane (97%) (Aldrich) were used without further purification. Anhydrous benzene (99%) (Aldrich) are distilled and stored on zeolithe. 1,5-cyclooctadiene (Aldrich) was purified through an alumina column prior to use. Bis(trifluoromethanesuflonyl)imide lithium salt (>99%, Solvionic company), zinc powder (Merck) and $RuCl_3.xH_2O$ (Avogado) was dried under vacuum prior to use. Bis(trifluoromethanesuflonyl)imide 1-ethyl-3-methylimidazolium was provided by Rhodia company.

Liquid state NMR

^{1}H and ^{13}C NMR at liquid state data were collected at room temperature on a Bruker AC 300 MHz spectrometer with the resonance frequency at 300,130 MHz.

The solvents used (CD_2Cl_2, $CDCl_3$, C_6D_6) were purchased from SDS and used as received. Chemicals shifts are expressed in ppm (singlet = s, doublet = d, doublet of doublet =

dd, and multiplet = m) and were measured relative to residual proton of the solvent to $CHDCl_2$ for ^1H, to CD_2Cl_2 for ^{13}C.

Transmission electron microscopy

TEM analysis was carried out in Transmission Electron Microscope JEM 2010 operated at 200 kV with point resolution 2.3Å or Philips CM200 TEM operated at 200 kV with point resolution 1.9Å.

Ionic liquids were prepared according to the known method, dried overnight under high vacuum and stored in a glovebox (Jacomex) in order to guarantee rigorously anhydrous products.

1-hexyl-3-methylimidazolium bromide HMIMBr

1-bromohexane (56.4mL; 0.4mol) was added to 1-methylimidazole (20mL, 0.25mol) freshly distilled. The mixture was stirred for 48h at 65°C. The hot solution was then transferred to a dropping funnel and the lower phase was added dropwise under vigorous stirring to toluene (200mL). The white precipitate formed was filtered and then washed repeatedly with toluene (3*200mL) and dried overnight under vacuum, giving white powder (61.05g, 99 %). ^1H-NMR (CD_2Cl_2) : δ (ppm) : 10.52 (s, 1H) ; 7.33 (d, 2H) ; 4.30 (t, 2H) ; 4.00 (s, 3H) ; 1.98 (m, 2H) ; 1.31 (m, 6H) ; 0.87 (t, 3H) ; $^{13}C\{^1H\}$-NMR (CD_2Cl_2) : δ (ppm) : 124.6 (CH) ; 123.1 (CH) ;121.6 (CH) ; 50.1 (NCH_2) ; 36.5 (NCH_3) ; 30.1 (CH_2); 31.1(CH_2) ; 25.8 (CH_2) ; 22.4 (CH_2) ; 13.7 (CH_3)

1-octyl-3-methylimidazolium chloride OMIMCl

The procedure previously described for BMIMCl was used. From 15mL (0.18 mol) of 1-methylimidazole and 50mL g (0.29 mol) of 1-chlorooctane there were obtained 20.7g (50 %) of OMIMCl as a colourless liquid. ^1H-NMR (CD_2Cl_2) : δ (ppm) : 10.3 (s, 1H) ; 7.64 (d, 1H) ; 7.48 (d, 1H) ; 4.28 (t, 2H) ; 4.03 (s, 3H) ; 1.84 (qt, 2H) ; 1.23 (st, 10H) ; 0.88 (t, 3H) ; $^{13}C\{^1H\}$-NMR (CD_2Cl_2) : δ (ppm) : 137.5 (CH) ; 122.8 (CH) ;121.2 (CH) ; 49.2 (NCH_2) ; 35.6 (NCH_3) ; 31.0 (CH_2) ; 29.6 (CH_2) ; 28.3 (CH_2) ; 25.5 (CH_2) ; 21.9 (CH_2) ; 13.2 (CH_3)

1-decyl-3-methylimidazolium bromide DMIMBr :

The procedure previously described for HMIMBr was used. From 20.6g (0.25 mol) of 1-methylimidazole and 88.5g (0.4 mol) of 1-bromodecane there were obtained 76.01 g (99%) of DMIMBr as a colourless liquid. ^{1}H-NMR (CD_2Cl_2) : δ (ppm) : 10.64 (s, 1H) ; 7.29 (d, 2H) ; 4.31 (t, 2H) ; 4.07 (s, 3H) ; 1.88 (m, 2H) ; 1.34 (m, 16H) ; 0.85 (t, 3H) ; ^{13}C{^{1}H}-NMR (CD_2Cl_2) : δ (ppm) : 138.5 (CH) ; 128.5 (CH) ; 123.4 (CH) ; 50.5 (NCH_2) ; 32.2 (NCH_3) ; 30.5 (CH_2) ; 29.9-29.3 (CH_2) ; 26.6 (CH2) ; 23.0 (CH_2) ; 14.2 (CH_3)

1,3-dibutylimidazolium chloride [BBIMCl]

The procedure previously described for BMIMCl was used. From 40mL (0.31 mol) of 1-butylimidazole and 51mL (0.49 mol) of 1-chlorobutane, there were obtained 56.4g (84 %) of BBIMCl as an hygroscopic white solid. ^{1}H-NMR (CD_2Cl_2) : δ (ppm) : 10.96 (s, 1H) ; 7.38 (d, 2H) ; 4.26 (t, 4H) ; 1.83 (qt, 4H) ; 1.37 (st, 4H) ; 1.01 (t, 6H) ; ^{13}C{^{1}H}-NMR (CD_2Cl_2) : δ (ppm) : 138.6 (CH) ; 121.9 (CH) ; 49.9 (NCH_2) ; 32.4 (CH_2) ; 19.8 (CH_2) ; 13.6 (CH_3)

1-hexyl-3-methylimidazolium bis(trifluoromethylsulfonyl)imide [HMIMNTf$_2$] :

The procedure previously described for BMIMNTf$_2$ was used. From 43.2g (0.17mol) of HMIMBr and 50g (0.17mol) of LiNTf$_2$, there were obtained 62.8g (80.5 %) of HMIMNTf$_2$ as a colourless viscous liquid. ^{1}H-NMR (CD_2Cl_2) : δ (ppm) : 8.62 (s, 1H) ;; 7.34 (d, 2H) ; 4.13 (t, 2H) ; 3.91 (s, 3H) ; 1.90 (qt, 2H) ; 1.34 (st, 6H) ; 0.89 (t, 3H) ; ^{13}C{^{1}H}-NMR (CD_2Cl_2) : δ (ppm) : 136.8 (CH) ; 124.1 (CH) ; 122.4 (CH) ; 118.0 (CF_3) ; 50.3 (NCH_2) ; 36.2 (NCH_3) ; 30.9 (CH_2); 30.1(CH_2) ; 25.3 (CH_2) ; 22.1 (CH_2) ; 13.8 (CH_3)

1-octyl-3-methylimidazolium bis(trifluoromethylsulfonyl)imide OMIMNTf$_2$:

The procedure previously described for BMIMNTf$_2$ was used. From 11.4mL (0.05 mol) of OMIMCl and 14.4g (0.05 mol) of LiNTf$_2$ there were obtained 4.56 g (20 %) of OMIMNTf$_2$ as a colourless liquid. ^{1}H-NMR (CD_2Cl_2) : δ (ppm) : 8.64 (s, 1H) ; 7.33(d,1H) ; 7.26 (d, 2H) ; 4.06 (t, 2H) ; 3.93 (s, 3H) ; 1.86 (qt, 2H) ; 1.27-1.32 (m, 10H); 0.87 (t, 3H) ; ^{13}C{^{1}H}-NMR (CD_2Cl_2) : δ (ppm) : 136.3 (CCH_3) ; 123.9 (CF_3) ; 122.4 (CH) ; 50.7 (NCH_2) ; 36.8 (NCH_3) ; 31.9 (CH_2) ; 30.4 (CH_2) ; 29.3 (CH_2); 26.5 (CH_2) ; 22.9 (CH_2) ; 14.1 (CH_3)

1-decyl-3-methylimidazolium bis(trifluoromethylsulfonyl)imide DMIMNTf$_2$:

The procedure previously described for BMIMNTf$_2$ was used. From 52.8g (0.17 mol) of DMIMBr and 50 g (0.17 mol) of LiNTf$_2$ there were obtained 20.7g (23.7 %) of DMIMNTf$_2$ as a colourless liquid. ^{1}H-NMR (CD_2Cl_2) : δ (ppm) : 8.60 (s, 1H) ; 7.35(d,1H) ; 7.28 (d, 2H) (d,1H); 4.13 (t, 2H) ; 3.91 (s, 3H) ; 1.83 (qt, 2H) ; 1.30 (m, 14H) ; 0.86 (t, 3H) ; ^{13}C{^{1}H}-NMR (CD_2Cl_2) : δ (ppm) : 136.1 (CH) ; 124.1 (CH) ; 122.8 (CH) ; 118.2 (CF_3) ; 50.6 (NCH_2) ; 36.7 (NCH_3) ; 32.2 (CH_2) ; 30.4 (CH_2) ; 29.6 (CH_2); 26.4 (CH_2) ; 22.9 (CH_2) ; 14.1 (CH_3)

1,3-dibutylimidazolium bis(trifluoromethylsulfonyl)imide [BBIMNTf$_2$] :

The procedure previously described for BMIMNTf$_2$ was used. From 39.4 g (0.18 mol) of BBIMCl and 52.3g (0.18 mol) of LiNTf$_2$ there were obtained 71.2g (96 %) of BBIMNTf$_2$ as a colourless liquid. ^{1}H-NMR (CD_2Cl_2) : δ (ppm) : 8.65 (s, 1H) ; 7.28 (d, 2H) ; 7.36 (d, 1H) ; 4.17 (t, 4H) ; 1.83 (qt, 4H) ; 1.35 (st, 4H) ; 0.89 (t, 6H) ; ^{13}C{^{1}H}-NMR (CD_2Cl_2) : δ (ppm) : 135.0 (CH) ; 135.0 (CF_3) ; 119.8 (NCH_2) ; 49.9 (NCH_3) ; 32.0 (CH_2) ; 19.2 (CH_2) ; 13.1 (CH_3)

(1,3,5-cyclooctatriene)(1,5-cyclooctadiene)ruthenium [Ru(COD)(COT)]

Cycloocta-1,5-diene (60mL, 489mmol) and zinc dust (5.08g, 77.7mmol) were added to a solution of 3.07g (14.8mmol) of $RuCl_3 \cdot 3H_2O$ in 30 mL of methanol. The mixture was heated under reflux with magnetic stirring for 3 h. The resulting brown solution is filtered and the residue is washed with toluene (3 x 30mL). The filtrate is evaporated to dryness under reduced pressure at room temperature and the solid residue obtained extracted with pentane (5 x 50mL). The yellow pentane solution is concentrated and chromatographed with pentane on an alumina column. The yellow pentane solution is concentrated and cooled to –40°C giving yellow crystals. The yield, based on $RuCl_3.3H_2O$ is 32% (1,49g). ^{1}H NMR : (300 MHz, C_6D_6) δ = 5.19ppm (dd, 2H), 4.70 (m, 2H), 3.77 (m, 2H), 2.92 (m, 4H), 2.25 (m, 8H), 1.68 (m, 2H), 0.83 (m, 2H) ; ^{13}C NMR (75 MHz, C_6D_6) δ = 101.5ppm (CH), 99.4 (CH), 76.6 (CH), 65-75 (large) (CH), 37.0 (CH_2), 31.7 (CH_2)

Ruthenium nanoparticles.

In a Fischer-Porter bottle, Ru(COD)(COT) (0.43 mmol, 133 mg) was dissolved in one of the ionic liquids (10 mL) under vacuum during 1h at room temperature.

- *Room temperature synthesis :* the resulting solution was pressurized under vigorous stirring with 4 bar of dihydrogen at room temperature for 18h.
- *Low temperature synthesis :* the mixture was cooled at 0°C and then pressurized at 4bar of hydrogen. The reaction was performed either under stirring during 18h or without stirring for 4days.

In all cases, it afforded a black solution stable for several month under argon at room temperature.

TEM(Transmission Electronic Microscopy) analyses

Samples for TEM observations were prepared by depositing a thin film of the ruthenium nanoparticles dispersed in ionic liquids on holey carbon film supported by a copper grid. The size distribution of the metal particles was determined from the measurement of ≈200 particle, assuming spherical shape.

Hydrogenation of ethylene by RuNP in $BMIMNTf_2$

2mL of Ru/$BMIMNTf_2$ (containing n(Ru)=$8.6x10^{-5}$mol) was introduced in a Schlenk. After a overnight treatment under argon, the reaction mixture was exposed under stirring to ethylene (105.5mbar). The drop of the internal pressure was followed. GC analyses of gas phase have been performed after 2h (no more evolution of pressure was observed).

Adsorption of carbon monoxide

2mL of Ru/$BMIMNTf_2$ (containing n(Ru)=$8.6x10^{-5}$mol) was introduced in a Schlenk. After a overnight treatment under high vacuum, the reaction mixture was exposed under stirring to CO (116.65mbar). The drop of the internal pressure was followed and GC analyses of gas phase have been performed after 7h (no more evolution of pressure was observed).
The solubility of carbon monoxide in IL have been evaluated due to the difference of pressure in the gas phase.

Adsorption of deuterium

1mL of Ru/IL was introduced in a Schlenk. After a overnight treatment under high vacuum, the reaction mixture was exposed under stirring to D_2. No drop of the internal pressure is observed. The resulting mixture was analysed in ^1H NMR at solid and liquid state.

Reactivity with iodoalkanes

1mL of Ru/IL was introduced in a Schlenk. After a overnight treatment under high vacuum, iodomethane (0.1mL, 1.7mmol) was added and the system was heated at 100°C under stirring during 4h. The resulting mixture was analysed by ^{1}H NMR. The same procedure is used with iodobutane (0.19mL, 1.7 mmol) but the system was heated at 150°C.

Bibliography

(1) Wasserscheid, P.; Welton, T. *Ionic Liquids in Synthesis*; Wiley-VCH: Weinheim, 2003.
(2) Welton, T. *Coord. Chem. Rev.* **2004**, *248*, 2459-2477.
(3) Olivier-Bourbigou, H.; Vallee, C. In *Multiphase Homogeneous Catalysis*; Wiley-VCH: Weinheim, 2005; Vol. 2, pp 413-431.
(4) Astruc, D.; Lu, F.; Aranzaes, J. R. *Angew. Chem. Int. Ed.* **2005**, *44*, 7852-7872.
(5) Fonseca, G. S.; Scholten, J. D.; Dupont, J. *Synlett* **2004**, 1525-1528.
(6) Fonseca, G. S.; Umpierre, A. P.; Fichtner, P. F. P.; Teixeira, S. R.; Dupont, J. *Chem. Eur. J.* **2003**, *9*, 3263-3269.
(7) Fonseca, G. S.; Silveira, E. T.; Gelesky, M. A.; Dupont, J. *Adv. Synth. Catal.* **2005**, *347*, 847-853.
(8) Fonseca, G. S.; Domingos, J. B.; Nome, F.; Dupont, J. *J. Mol. Catal. A* **2006**, *248*, 10-16.
(9) Fonseca, G. S.; Machado, G.; Teixeira, S. R.; Fecher, G. H.; Morais, J.; Alves, M. C. M.; Dupont, J. *J. Colloid Interface Sci.* **2006**, *301*, 193-204.
(10) Migowski, P.; Dupont, J. *Chem. Eur. J.* **2006**, *13*, 32-39.
(11) Migowski, P.; Teixeira, S. R.; Machado, G.; Alves, M. C. M.; Geshev, J.; Dupont, J. *J. Electron Spectrosc.* **2007**, *156-158*, 195-199.
(12) Scheeren, C. W.; Machado, G.; Teixeira, S. R.; Morais, J.; Domingos, J. B.; Dupont, J. *J. Phys. Chem. B* **2006**, *110*, 13011-13020.
(13) Umpierre, A. P.; Machado, G.; Fecher, G. H.; Morais, J.; Dupont, J. *Adv. Synth. Catal.* **2005**, *347*, 1404-1412.
(14) Silveira, E. T.; Umpierre, A. P.; Rossi, L. M.; Machado, G.; Morais, J.; Soares, G. V.; Baumvol, I. J. R.; Teixeira, S. R.; Fichtner, P. F. P.; Dupont, J. *Chem. Eur. J.* **2004**, *10*, 3734-3740.
(15) Zhao, D.; Fei, Z.; Geldbach, T. J.; Scopelliti, R.; Dyson, P. J. *J. Am. Chem. Soc.* **2004**, *126*, 15876-15882.
(16) Parvulescu, V. I.; Hardacre, C. *Chem. Rev.* **2007**, *107*, 2615-2665.
(17) Schmid, G. *Nanoparticles: From Theory to Application*; Wiley-VCH: Weinheim, 2004.
(18) Ott, L. S.; Finke, R. G. *Inorg. Chem.* **2006**, *45*, 8382-8393.
(19) Ott, L. S.; Finke, R. G. *Coord. Chem. Rev.* **2007**, *251*, 1075-1100.
(20) Aiken, J. D., III; Finke, R. G. *J. Mol. Catal. A* **1999**, *145*, 1-44.
(21) Boennemann, H.; Nagabhushana, K. S. *Colloidal nanoparticles in catalysis*; CRC PressLLC: Mullheim an der Ruhr, 2006.
(22) Chaudret, B. *Topics in Organometallic Chemistry* **2005**, *16*, 233-259.
(23) Philippot, K.; Chaudret, B. *C. R. Chimie* **2003**, *6*, 1019-1034.

(24) Huang, J.; Jiang, T.; Han, B.; Wu, W.; Liu, Z.; Xie, Z.; Zhang, J. *Catal. Lett.* **2005**, *103*, 59-62.
(25) Miao, S.; Liu, Z.; Han, B.; Huang, J.; Sun, Z.; Zhang, J.; Jiang, T. *Angew. Chem. Int. Ed.* **2006**, *45*, 266-269.
(26) Rossi, L. M.; Machado, G.; Fichtner, P. F. P.; Teixeira, S. R.; Dupont, J. *Catal. Lett.* **2004**, *92*, 149-155.
(27) Fu, X.; Wayland, B. B. *J. Am. Chem. Soc.* **2005**, *127*, 16460-16467.
(28) Duteil, A.; Queau, R.; Chaudret, B.; Mazel, R.; Roucau, C.; Bradley, J. S. *Chem. Mat.* **1993**, *5*, 341-347.
(29) Andres, R.; de Jesus, E.; Flores, J. C. *New J. Chem.* **2007**, *31*, 1161-1191.
(30) Chung, Y.-M.; Rhee, H.-K. *J. Mol. Catal. A* **2003**, *206*, 291-298.
(31) Toshima, N.; Shiraishi, Y.; Teranishi, T.; Miyake, M.; Tominaga, T.; Watanabe, H.; Brijoux, W.; Bonnemann, H.; Schmid, G. *Appl. Organomet. Chem.* **2001**, *15*, 178-196.
(32) Kitajima, N.; Kono, A.; Ueda, W.; Morooka, Y.; Ikawa, T. *Chem. Comm.* **1986**, 674-675.
(33) Hulea, V.; Brunel, D.; Galarneau, A.; Philippot, K.; Chaudret, B.; Kooyman, P. J.; Fajula, F. *Micro. Meso. Mat.* **2005**, *79*, 185-194.
(34) Pelzer, K.; Philippot, K.; Chaudret, B.; Meyer-Zaika, W.; Schmid, G. *Z. Anorg. Allg. Chem.* **2003**, *629*, 1217-1222.
(35) Marconi, G.; Pertici, P.; Evangelisti, C.; Caporusso, A. M.; Vitulli, G.; Capannelli, G.; Hoang, M.; Turney, T. W. *J. Organomet. Chem.* **2004**, *689*, 639-646.
(36) Huang, J.; Jiang, T.; Gao, H.; Han, B.; Liu, Z.; Wu, W.; Chang, Y.; Zhao, G. *Angew. Chem. Int. Ed.* **2004**, *43*, 1397-1399.
(37) Kormann, H.-P.; Schmid, G.; Pelzer, K.; Philippot, K.; Chaudret, B. *Z. Anorg. Allg. Chem.* **2004**, *630*, 1913-1918.
(38) Yoon, B.; Kim, H.; Wai, C. M. *Chem. Comm.* **2003**, 1040-1041.
(39) Pelzer, K.; Laleu, B.; Lefebvre, F.; Philippot, K.; Chaudret, B.; Candy, J. P.; Basset, J. M. *Chem. Mat.* **2004**, *16*, 4937-4941.
(40) Rodriguez, A.; Amiens, C.; Chaudret, B.; Casanove, M.-J.; Lecante, P.; Bradley, J. S. *Chem. Mat.* **1996**, *8*, 1978-1986.
(41) Ramirez, E.; Jansat, S.; Philippot, K.; Lecante, P.; Gomez, M.; Masdeu-Bulto, A. M.; Chaudret, B. *J. Organomet. Chem.* **2004**, *689*, 4601-4610.
(42) Gomez, M.; Philippot, K.; Colliere, V.; Lecante, P.; Muller, G.; Chaudret, B. *New J. Chem.* **2003**, *27*, 114-120.
(43) Pan, C.; Pelzer, K.; Philippot, K.; Chaudret, B.; Dassenoy, F.; Lecante, P.; Casanove, M.-J. *J. Am. Chem. Soc.* **2001**, *123*, 7584-7593.
(44) Pery, T.; Pelzer, K.; Buntkowsky, G.; Philippot, K.; Limbach, H.-H.; Chaudret, B. *Eur. J. Chem. Phys. Phys. Chem.* **2005**, *6*, 605-607.
(45) Dupont, J.; Fonseca, G. S.; Umpierre, A. P.; Fichtner, P. F. P.; Teixeira, S. R. *J. Am. Chem. Soc.* **2002**, *124*, 4228-4229.
(46) Seddon, K. R.; Stark, A.; Torres, M.-J. *Pure Appl. Chem.* **2000**, *72*, 2275-2287.
(47) Verwey, E. J. W.; Overbeek, J. T. G. *Theory of the Stability of Lyophobic Colloids. The Interaction of Sol Particles Having an Electric Double Layer*, 1962.
(48) Verwey, E. J. W.; Overbeek, J. T. G. *Theory of the stability of lyophobic colloids*, 1999.
(49) Bucher, S.; Hormes, J.; Modrow, H.; Brinkmann, R.; Waldofner, N.; Bonnemann, H.; Beuermann, L.; Krischok, S.; Maus-Friedrichs, W.; Kempter, V. *Surface Sci.* **2002**, *497*, 321-332.
(50) Modrow, H.; Bucher, S.; Hormes, J.; Brinkmann, R.; Boennemann, H. *J. phys. Chem. B* **2003**, *107*, 3684-3689.

(51) Ninham, B. W. *Adv. Colloid Interfac.* **1999**, *83*, 1-17.
(52) Bostrom, M.; Williams, D. R. M.; Ninham, B. W. *Phys. Rev. Lett.* **2001**, *87*, 168103/168101-168103/168104.
(53) Fei, Z.; Geldbach, T. J.; Zhao, D.; Dyson, P. J. *Chem. Eur. J.* **2006**, *12*, 2122-2130.
(54) Fei, Z.; Zhao, D.; Pieraccini, D.; Ang, W. H.; Geldbach, T. J.; Scopelliti, R.; Chiappe, C.; Dyson, P. J. *Organometallics* **2007**, ACS ASAP.
(55) Ott, L. S.; Cline, M. L.; Deetlefs, M.; Seddon, K. R.; Finke, R. G. *J. Am. Chem. Soc.* **2005**, *127*, 5758-5759.
(56) Crudden, C. M.; Allen, D. P. *Coord. Chem. Rev.* **2004**, *248*, 2247-2273.
(57) Gruendemann, S.; Kovacevic, A.; Albrecht, M.; Faller Robert, J. W.; Crabtree, H. *Chem. Comm.* **2001**, 2274-2275.
(58) Mudring, A.-V.; Babai, A.; Arenz, S.; Giernoth, R. *Angew. Chem. Int. Ed.* **2005**, *44*, 5485-5488.
(59) Aiken, J. D., III; Finke, R. G. *Chem. Mat.* **1999**, *11*, 1035-1047.
(60) Antonietti, M.; Kuang, D.; Smarsly, B.; Zhou, Y. *Angew. Chem. Int. Ed.* **2004**, *43*, 4988-4992.
(61) Cooper, E. R.; Andrews, C. D.; Wheatley, P. S.; Webb, P. B.; Wormald, P.; Morris, R. E. *Nature* **2004**, *430*, 1012-1016.
(62) Wang, Y.; Voth, G. A. *J. Am. Chem. Soc.* **2005**, *127*, 12192-12193.
(63) Canongia Lopes, J. N. A.; Padua, A. A. H. *J. Phys. Chem. B* **2006**, *110*, 3330-3335.
(64) Triolo, A.; Russina, O.; Bleif, H.-J.; Di Cola, E. *J. Phys. Chem. B* **2007**, *111*, 4641-4644.
(65) Canongia Lopes, J. N.; Costa Gomes, M. F.; Padua, A. A. H. *J. Phys. Chem. B* **2006**, *110*, 16816-16818.
(66) Pertici, P.; Simonelli, G.; Vitulli, G.; Deganello, G.; Sandrini, P.; Mantovani, A. *Chem. Comm.* **1977**, 132-133.
(67) Pertici, P.; Vitulli, G.; Paci, M.; Porri, L. *Dalton Trans.* **1980**, 1961-1964.
(68) Pertici, P.; Vitulli, G. *Inorg. Syn.* **1983**, *22*, 176-181.
(69) Pertici, P.; Vitulli, G.; Porzio, W.; Zocchi, M.; Barili, P. L.; Deganello, G. *Dalton Trans.* **1983**, 1553-1555.
(70) Leconte, M.; Theolier, A.; Basset, J. M. *J. Mol. Catal. A* **1985**, *28*, 217-231.
(71) Leconte, M.; Theolier, A.; Rojas, D.; Basset, J. M. *J. Am. Chem. Soc.* **1984**, *106*, 1141-1142.
(72) Bradley, J. S.; Millar, J. M.; Hill, E. W.; Behal, S.; Chaudret, B.; Duteil, A. *Faraday Discussions* **1992**, *92*, 255-268.
(73) Holbrey, J. D.; Reichert, W. M.; Rogers, R. D. *Dalton Trans.* **2004**, 2267-2271.
(74) Dibrov, S. M.; Kochi, J. K. *Acta Cryst. C* **2006**, *62*, 19-21.
(75) Pelzer, K.; Vidoni, O.; Philippot, K.; Chaudret, B.; Collière, V. *Adv. Funct. Mater.* **2003**, *13*, 118-126.

Conclusion Générale

Mon travail de thèse concernait l'étude du rôle spécifique des liquides ioniques (LI) comme solvants de réaction catalytique. En effet, il ressort des différentes réactions catalytiques étudiées soit au laboratoire LCOMS soit dans la littérature, que les LI sont des solvants « non-innocents », pouvant intervenir comme ligands, co-catalyseurs ou catalyseurs. Cependant, l'interprétation des différences de réactivité des systèmes catalytiques utilisant soit des LI soit des solvants organiques est rarement corrélée à leur nature chimique, or les LI sont avant tout une association cations/anions.

Dans ce travail de thèse, nous avons développé une approche originale des propriétés de solvant des LI en tenant compte de leur nature chimique. Nous avons démontré que cette association cations/anions confère des propriétés spécifiques aux LI telle que la spéciation des ligands ioniques et la présence d'interaction π-cation avec les substrats insaturés, et étudié les conséquences de ces deux facteurs sur les résultats catalytiques.

Il est généralement admis que l'immobilisation de catalyseurs dans les LI nécessite qu'ils soient ioniques et de nombreux systèmes, en particulier utilisant un ligand chargé, ont été développés pour répondre à cette exigence. Mais la présence de paires d'ions dans les LI implique des possibilités d'évolution de la nature des entités chargées dissoutes dans ces solvants. Ces phénomènes de spéciation ont été mis en évidence dans le chapitre II et nous ont permis de d'expliquer le fait que l'isomérisation catalytique du 2M3BN en 3PN (1) était dépendante de la nature du LI.

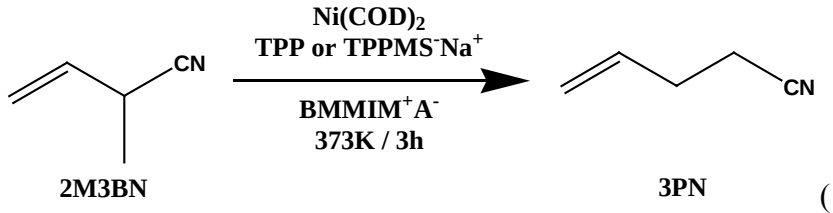

(1)

En effet, nous avons démontré par RMN solide ^{23}Na que la réaction d'échange des ions du LI avec le sel (m-sulfophenyl)diphenylphosphine de sodium : $TPPMS^-Na^+$ (2) comme dans le cas de nombreux autres sels inorganiques C^+A^-, est gouvernée par la théorie HSAB. Cet échange conduit à la formation *in situ* du ligand $TPPMS^-BMMIM^+$ dont les interactions intermoléculaires avec le LI inhibent la réaction (1).

$$TPPMS^-Na^+ + BMMIM^+A^- \rightarrow TPPMS^-BMMIM^+ + Na^+A^- \quad (2)$$

D'autre part, lorsque les réactions catalytiques font intervenir des substrats insaturés, les cations du LI peuvent donner lieu à des interactions particulières : des interactions π-cations.

Dans le chapitre III, des études RMN (évolution des déplacements chimiques, RMN ROESY et DOSY) sur des mélanges substrats insaturés/LI dans diverses proportions ont mis en évidence la présence de ce type d'interactions avec les systèmes π du toluène, du 1,3-cyclohexadiène et du cyclohexène avec les LI. Il apparaît que la structuration de $BMMIMNTf_2$ est propice à la formation d'interaction π-cation avec ces substrats alors qu'elles ne sont pas présentes avec $BMIMNTf_2$.

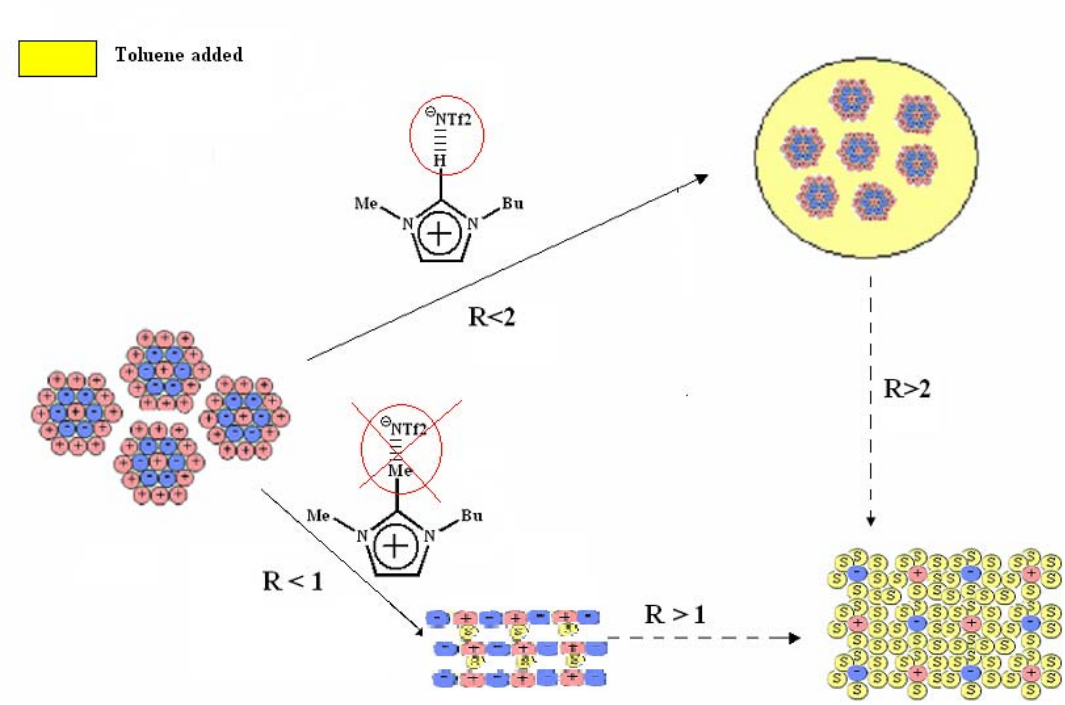

Figure 1. *Représentation de l'évolution de la structure de $BMIMNTf_2$ et $BMMIMNTf_2$ en présence de quantité croissante de toluène*

Ces résultats ont été corroborés par des études en dynamique moléculaire. Les différences apparaissant entre les LI dialkylés et trialkylés ont été attribuées à des différences de structures, de pouvoir ionique et de force de liaison hydrogène. Il ressort également que la présence d'interaction π-cations avec $BMMIMNTf_2$ diminue la réactivité en hydrogénation catalytique des substrats insaturés par rapport aux réactions conduites dans $BMIMNTf_2$.

Enfin les ions constituants les LI sont des molécules organiques. Ceci implique que les LI présente une auto-organisation liée à leur caractère ionique et une structuration hétérogène en microdomaines polaires et apolaires générés par les chaînes alkyles des cations. Dans le chapitre IV, cette nouvelle approche des LI a permis d'envisager la solubilisation préférentielle d'entités polaires ou apolaires dans des domaines spécifiques. Ces domaines peuvent être considérés comme des « nanoréacteurs » dont les propriétés seraient ajustables

par variation de la nature des ions du LI. Une relation entre la taille des domaines apolaires et celles des nanoparticules de ruthénium générées *in situ* a été établie.

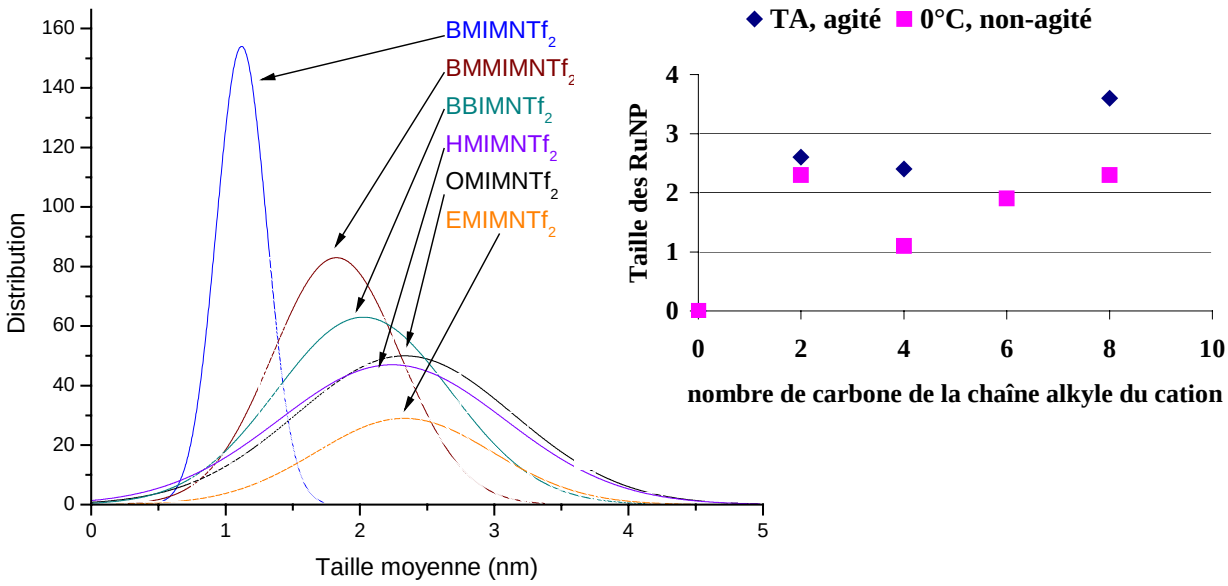

Figure 2. *histogrammes de tailles des RuNP en fonction de la nature du LI et corrélation avec le nombre de carbones de la chaîne alkyle du cation.*

Les LI joue ainsi le rôle de moule supramoléculaire lors de la synthèse de nanoparticules de ruthénium.

Dans ce travail, nous avons donc établi un relation entre la structure des LI et la réactivité des systèmes catalytiques dans ces milieux en nous appuyant sur les phénomènes de solvatation spécifiques des LI en particulier l'influence de trois facteurs :

- l'association anions/cations
- l'auto-organisation des LI
- la présence de microdomaines polaires et apolaires

La prise en compte de ces aspects particuliers nous a ainsi permis d'identifier les facteurs influant l'activité catalytique dans les LI mais également de concevoir une approche nouvelle de la croissance cristalline contrôlée de nanoparticules métalliques sans addition de ligands.

Les liquides ioniques, leur utilisation et leur rôle comme solvants de réaction catalytique

Les liquides ioniques, associations de cations organiques et d'anions, sont des milieux structurés sur plusieurs nanomètres et présentent une ségrégation en domaines polaires et apolaires. Utilisés comme solvants de réactions catalytiques, ils peuvent de ce fait engendrer des phénomènes de solvatation spécifique. Ainsi des réactions d'échange d'ions dans certains systèmes catalytiques et des interactions de type π-cation avec les hydrocarbures insaturés ont été mises en évidence par RMN. Les conséquences de ces solvatations spécifiques sur des réactions d'hydrogénation ont été étudiées. Il ressort que plus l'interaction entre les liquides ioniques et les réactifs est grande, plus les réactions sont lentes.

Enfin la présence de microdomaines polaires et apolaires conduit à une solubilisation préférentielle des complexes organométalliques dans les poches apolaires ce qui permet d'utiliser ces milieux comme moules supramoléculaires et de contrôler la croissance cristalline des nanoparticules de ruthénium générées *in situ* en fonction de la longueur de la chaîne alkyl et de la température.

Ionic liquids, use and specific task as solvents in catalytic reaction

Ionic liquids, associations of organic cations and anions, are media organized over several nanometers and present a segregation in polar and nonpolar microdomains. As they are used as solvents for catalytic reactions, they can induce specific solvation phenomena. For instance, ion exchange reactions in some catalytic systems and some π-cation interactions with unsaturated hydrocarbons have been observed by NMR. The consequences of the specific solvation on hydrogenation reactions have been studied. It appears that the stronger the interactions between IL and reactants are, the slower the reactions are.

The presence of nonpolar and polar microdomains leads to a preferential solvation of organometallic complexes in apolar pockets that enable the use of these media as supramolecular matrices and to control the crystal growth of metal nanoparticles generated *in situ* according to the alkyl chain length and the temperature.

DISCIPLINES : Chimie

MOTS-CLES : Liquides ioniques, Echange d'ions, hydrocarbures insaturés, Interaction π-Cation, Hydrogénation, Ruthénium, Nanoparticules, RMN ROESY et DOSY

Université Lyon 1, C2P2, Laboratoire de Chimie Organométallique de Surface (LCOMS), UMR 5265, CNRS-CPE Lyon, 43 Bd du 11 novembre 1918, 69616 Villeurbanne Cedex, France.